Development of lung and muscle factories to deliver therapeutic monoclonal antibodies

Thesis submitted in partial fulfilment of the requirements for the degree of

Doctor of Philosophy

Agata Antepowicz

Gene Medicine Research Group

Radcliffe Department of Medicine

St Peter's College

University of Oxford

Supervisors: Prof. Deborah R. Gill and Prof. Stephen C. Hyde

Trinity Term 2018

Development of lung and muscle factories to deliver therapeutic monoclonal antibodies

Agata Antepowicz

Radcliffe Department of Medicine and St Peter's College, University of Oxford

Thesis submitted for the degree of Doctor of Philosophy, Trinity Term 2018

Abstract

Monoclonal antibodies (mAbs), which represent the largest market of any protein therapeutic, are used in the treatment of conditions such as cancer and autoimmune diseases, and prophylaxis of infections. The complexity of manufacture of mAbs translates to a high cost compared with small-molecule drugs, and their use may be restricted as a result. Gene transfer for direct production of mAbs *in vivo* could offer an alternative to parenteral administration, with the added benefit of easing patient burden caused by repeated injections or infusions. Studies presented in this thesis investigated the possibility of using gene transfer agents for expression of mAbs in the lung lumen and circulation. Using the secreted reporter protein *Gaussia* luciferase, delivery of the lentiviral vector recombinant simian immunodeficiency virus, pseudotyped with F and HN proteins from Sendai virus (rSIV.F/HN) for targeting of pulmonary epithelium, was identified as an efficient means of gene transfer to the murine lung, with transgene

expression in the lung lumen lasting for at least 12 months in BALB/c mice. The recombinant adeno-associated viral vector serotype 8 (rAAV2/8) injected into the muscle directed robust expression of the reporter protein into the circulation and lung lumen of mice for at least 12 months. Two model applications were used to assess the effectiveness of these vectors for mAb gene transfer: respiratory syncytial virus (RSV) infection and rheumatoid arthritis. Both rSIV.F/HN and rAAV2/8 vectors expressing the anti-RSV mAb palivizumab protected mice from weight loss upon RSV infection. Recombinant AAV2/8 delivered intramuscularly was also used to express the anti-tumour necrosis factor alpha (TNFα) biologics infliximab and etanercept for at least 6 months and 56 days, respectively. Due to the immunosuppressive nature of TNFα antagonists, constitutive expression is undesirable and small molecule-assisted shutoff (SMASh) was investigated as a possible method of regulation of etanercept production. In conclusion, viral vector-mediated mAb gene transfer to the muscle and lung could be a feasible alternative to parenteral administration provided that an effective method of regulation of expression following vector delivery can be developed.

Acknowledgements

First and foremost, I would like to thank my supervisors Prof. Deborah Gill and Prof. Steve Hyde for their support, direction, encouragement and the (in)famous annual BBQs. Under your supervision, I have developed not only professionally but also personally and I am immensely grateful for your help during my DPhil journey.

I would like to thank Dr Cecilia Johansson and Freja Kirsebom for their help with RSV challenge experiments and making me feel so welcome in their lab in London.

I would also like to thank present and past members of the Gene Medicine Research Group: Dr Ian Pringle, Dr Lee Davies, Dr Cathy Oliveira, Dr Jean-François Gélinas, Dr Natasha Davie, Dr Jack Tan, Joost van Haasteren, Rosie Munday, Helena Meyer-Berg, Omar Habib, Rachel Ashworth, Eoin Mac Réamoinn, Toby Gamlen, Mariana Viegas, Tina Garland and Charlotte Rush for their advice, technical help, laughs, gossip, potluck dinners, nights out, special Lab Data Day tray bakes and making the lab such a brilliant place to work.

Big thanks to my parents and sister for the surprise birthday visits, numerous holidays to the Canaries and their love and support. Also many thanks to my friend Steffi for her moral support (not just with the DPhil) and always being there for me. Last but not least, I would like to thank my partner Taz. Your unfailing belief in me, copious amounts of chocolate and wine and the loving home you have provided me with have kept me going through this DPhil.

Declaration

This thesis has been composed by myself and has not been used in any previous application for a degree. The results presented were obtained by myself and contributions made by others have been acknowledged within the text. All sources of published or unpublished information have been specifically acknowledged by means of a reference or personal communication notation, respectively.

List of abbreviations

AAV	adeno-associated virus
AAVS1	adeno-associated virus integration site 1
ADA	anti-drug antibodies
ALL	acute lymphoblastic leukaemia
ASV	asunaprevir
BAL	broncho-alveolar lavage
BALF	broncho-alveolar lavage fluid
BLI	bioluminescence imaging
BMA	British Medical Association
BSA	bovine serum albumin
CAR	chimeric antigen receptor
CASI	CMV enhancer, chicken β-actin promoter and ubiquitin enhancer
CDC	Center for Disease Control and Prevention
cDNA	complementary DNA
CF	cystic fibrosis
CFTR	cystic fibrosis transmembrane conductance regulator
CHO	Chinese hamster ovary
CIA	collagen-induced arthritis
CMV	cytomegalovirus
COPD	chronic obstructive pulmonary disease
CTL	cytotoxic T lymphocyte
DAPI	4′,6-diamidino-2-phenylindole
DC	Detergent-Compatible
DMEM	Dulbecco's Modified Eagle's Medium
DMSO	dimethyl sulfoxide
DOPE	1,2-dioleoyl-sn-glycero-3-phosphoethanolamine
EC_{50}	half maximal effective concentration
EFI	CpG-free version of the elongation factor 1 alpha (EF1α) promoter
EGFP	enhanced fluorescent green protein
EIAV	equine infectious anaemia virus
ELISA	enzyme-linked immunosorbent assay
EMA	European Medicines Agency
ER	endoplasmic reticulum
F	fusion protein
Fc	fragment crystallisable
FcRn	neonatal Fc receptor
FDA	Food and Drug Administration
ffu	focus-forming unit
FI	formalin-inactivated
FIV	feline immunodeficiency virus

G	attachment protein
GAPDH	glyceraldehyde 3-phosphate dehydrogenase
hC	CpG-free version of the human cytomegalovirus (CMV) enhancer
hCEFI	combination of the CpG-free version of the human cytomegalovirus (CMV) enhancer (hC) and the CpG-free version of the elongation factor 1 alpha (EF1α) promoter (EFI)
HCV	hepatitis C virus
HEK293T	human embryonic kidney cells containing the SV40 T-antigen
HER2	human epidermal growth factor receptor 2
HGF	hepatocyte growth factor
HIV	human immunodeficiency virus
HLA	human leukocyte antigen
HN	haemagglutinin-neuraminidase protein of Sendai virus
hPIV	human parainfluenza virus
HRP	horseradish peroxidase
ICAM-1	intercellular adhesion molecule-1
IgE	immunoglobulin E
IgG	immunoglobulin G
IL-1	interleukin-1
IL-5	interleukin-5
IL-6	interleukin-6
IL-8	interleukin-8
IM	intramuscular
IN	intranasal
ITR	inverted terminal repeat
IV	intravenous
L	large RNA polymerase
LOD	limit of detection
LTR	long terminal repeat
mAb	monoclonal antibody
MAPK	mitogen-activated protein kinase
MDCK	Madin-Darby canine kidney cells
MHC	major histocompatibility complex
MMP	matrix metalloprotease
mTNFα	membrane-bound tumour necrosis factor alpha
mRNA	messenger RNA
N	nucleocapsid protein
NFκB	nuclear factor kappa-light-chain-enhancer of activated B cells
NHP	non-human primate
NHS	National Health Service
NS3	non-structural protein 3
ORF	open reading frame
P	phosphoprotein

PBS	phosphate-buffered saline
PCR	polymerase chain reaction
pDNA	plasmid DNA
PEI	polyethylenimine
PFA	paraformaldehyde
RA	rheumatoid arthritis
rAAV	recombinant adeno-associated virus
RIPA	radioimmunoprecipitation assay
rLV	recombinant lentiviral vector
rSIV.F/HN	recombinant simian immunodeficiency virus pseudotyped with F and HN proteins of Sendai virus
RSV	respiratory syncytial virus
SDS-PAGE	sodium dodecyl sulphate polyacrylamide gel electrophoresis
SIN	self-inactivating
SIV	simian immunodeficiency virus
SMA	spinal muscular atrophy
S/MAR	scaffold/matrix attachment region
SMASh	small molecule-assisted shutoff
SMN	survival motor neuron
sTNFα	soluble tumour necrosis factor alpha
SV40	simian virus 40
TBS	Tris-buffered saline
TLR	Toll-like receptor
TM	transmembrane
TMB	3,3′,5,5′-tetramethylbenzidine
TNFα	tumour necrosis factor alpha
TNFR1	tumour necrosis factor alpha receptor 1
TNFR2	tumour necrosis factor alpha receptor 2
UK	The United Kingdom of Great Britain and Northern Ireland
USA	The United States of America
UTR	untranslated region
VSV-G	G protein from vesicular stomatitis virus
WFI	water for injection
WPRE	woodchuck hepatitis virus regulatory element

Table of Contents

List of Figures

List of Tables

Chapter 1: Introduction

1.1 Gene therapy as an alternative to passive monoclonal antibody administration

1.1.1 Monoclonal antibodies as therapeutics

Monoclonal antibodies (mAbs) represent the largest market of any protein therapeutic, with global sales revenue amounting to $75 billion in 2013, projected to rise to $125 billion by 2020 (Ecker et al., 2015). They are used for treatment of a number of diseases, including certain forms of cancer, immunological disorders such as multiple sclerosis and rheumatoid arthritis, and infections. The first mAb was approved by the United States (US) Food and Drug Administration (FDA) in 1986. Since then, many more antibodies have been developed and marketed for a wide variety of clinical applications, with 68 therapeutic mAbs approved by the FDA as of early January 2017 (listed in Hongrong Cai, 2017).

Large-scale production of mAbs occurs in bioreactors, typically using Chinese Hamster Ovary (CHO) cells or hybridoma technology. A multi-step purification process then removes potential contaminants such as DNA or endogenous viruses. This usually involves capture using protein A or G affinity chromatography, ion exchange chromatography, and ultrafiltration or diafiltration, and is followed by extensive testing and characterisation to ensure the product meets stringent quality control requirements (Shukla and Thommes, 2010).

The complexity of large-scale production and purification of mAbs and the high doses required to achieve therapeutic efficacy translate to a substantial cost

burden for patients or the healthcare systems supporting them (Park et al., 2015), especially in lower-income economies (Jakovljevic et al., 2014). Anti-tumour necrosis factor alpha (TNFα) biologics, for instance, are one of the most expensive classes of drugs, with costs reaching $15,000-30,000 per patient per year in the USA (Bonafede et al., 2012, Schabert et al., 2013). It is estimated that biologic drugs command on average a two-fold higher price than small-molecule drugs, independent of disease prevalence (Isaacson, 2016).

The requirement for frequent injections or infusions is another source of patient burden. The half-life of therapeutic mAbs in the human serum varies from 3 days to a month (reviewed in Keizer et al., 2010), necessitating repeated administration to maintain efficacy. Additionally, the infusions are also administered slowly to minimise the risk of undesired reactions; for example, rituximab, which is used to treat lymphoma, needs to be infused for a minimum of 3 hours to minimise the risk of adverse events (Pritchard et al., 2014). In light of these issues, an alternative method of administering mAbs is desirable that would reduce costs and patient burden.

1.1.2 Rationale for using gene transfer agents for antibody delivery

Recombinant protein drugs, such as mAbs, can be synthesised *in vivo* and gene transfer could therefore be used to facilitate a patient to produce them. Such an approach could also reduce burden associated with frequent infusions and injections of the drug, as a single dose of the gene delivery vector could, in theory, offer sustained protein expression over a long period. This approach was first explored using adenovirus, which was delivered intraperitoneally to express a

single chain antibody against cancer-associated human epidermal growth factor receptor 2 (HER2) and was shown to successfully reduce tumour burden in a mouse model of ovarian cancer (Deshane et al., 1995). Since then, a number of other gene transfer agents, both viral and non-viral, have been investigated for *in vivo* mAb expression.

Skeletal muscle is the most commonly targeted organ (Hollevoet and Declerck, 2017) for a number of reasons. Firstly, skeletal muscle cells are relatively long-lived compared to other cell types in the body, with an average lifespan of 15 years (Spalding et al., 2005). Targeting this organ would therefore minimise dilution of the genetic payload delivered by a gene transfer vector through tissue proliferation and maximise duration of expression from a single administration. Secondly, muscle fibres are formed from multinucleated syncytia (Pavelka and Roth, 2010), which is expected to aid dispersion of the transgene upon transfer and thus increase production of the protein of interest. Thirdly, the high degree of vascularisation of skeletal muscle (Latroche et al., 2015) facilitates secretion of transgene protein into the blood. Lastly, skeletal muscle has already been demonstrated to efficiently express recombinant protein into systemic circulation in humans following gene transfer, for example following delivery of alipogene tiparvovec (Glybera) to treat the rare genetic disease lipoprotein lipase deficiency (Gaudet et al., 2013). Other target organs have also been explored, including the liver which is accessed through intravenous (IV) delivery route. Delivery of factor IX cDNA to the liver for secretion into circulation is being evaluated for treatment of haemophilia B, with promising results emerging from clinical trials with cDNA delivery mediated by recombinant adeno-associated viral vector (rAAV) (Nathwani et al., 2014).

The lung could also be a useful target organ for two reasons. Firstly, the large surface area and extensive vasculature could facilitate systemic expression. Efficient and sustained secretion of erythropoietin and factor IX into the circulation of mice was demonstrated following administration of an rAAV to the lung (Auricchio et al., 2002), providing proof-of-concept for targeting the lung to achieve systemic delivery of therapeutic proteins. Secondly, local antibody production into the lung lumen could be particularly advantageous for applications which require local presence of the mAb, such as protection against respiratory pathogens. Transfer of mAb genes to the lung was shown to provide protection against Ebola (Limberis et al., 2016) and influenza (Tutykhina et al., 2013) infections using intranasal (IN) delivery of rAAV and adenovirus, respectively, and against RSV using intrapleural administration of rAAV (Skaricic et al., 2008). Direct delivery of an adenoviral vector encoding an anti-vascular endothelial growth factor (VEGF) mAb to the mouse lung was also shown to reduce VEGF-induced pulmonary oedema (Watanabe et al., 2009). These studies demonstrated that expression of a mAb directly in the lung can be a useful strategy for certain indications.

The following subsections describe the various gene transfer agents that have been investigated or might be suitable for *in vivo* mAb expression. Attributes desirable of such agents are: (i) the ability to direct therapeutically relevant expression levels, (ii) the ability to direct sustained expression, or to be repeatedly administered for long-term expression, and (iii) safety.

1.1.3 Naked DNA

Non-viral gene delivery agents do not rely on packaging of the gene of interest into a recombinant viral vector, but rather utilise chemical or physical methods to facilitate transfection. They have several advantages over viral vectors: they do not stimulate adaptive immune responses as they contain no viral proteins, rendering them amenable to repeated administration; they are relatively straightforward and inexpensive to synthesise; and they can accommodate large genetic constructs. Compositionally, the simplest non-viral gene delivery method is the direct administration of naked DNA, usually in the form of an episomal plasmid grown in bacteria. Naked DNA could also take the form of minicircle DNA vectors, which, while similar to plasmids, are devoid of bacterial sequences for selection and replication (Darquet et al., 1997) that are unnecessary for mammalian transgene expression. A number of studies have demonstrated improved reporter gene expression from minicircles *in vivo*, compared to conventional plasmid DNA (Chen et al., 2003, Huang et al., 2009). The enhanced efficiency of transfection observed with minicircles was hypothesised to be a result of the smaller size of the vector, which could confer better bioavailability (Darquet et al., 1997), or of the lack of formation of repressive heterochromatin on the bacterial selection/replication sequences, which are absent in minicircles (Chen et al., 2008b). Subsequent *in vivo* studies in the mouse lung, however, found no improvement in reporter gene activity when using a minicircle compared to conventional plasmid vector when both constructs were devoid of CpG dinucleotides (Gill et al., 2016). This may suggest that minicircles are of limited utility where CpG removal from plasmid DNA is possible.

Naked DNA has limited intrinsic capacity to diffuse across the plasma membrane due to its hydrophilic, negatively charged phosphate groups. The existence of a specific DNA receptor on the surface of leukocytes has been suggested (Hefeneider et al., 1990), which is thought to function in scavenging of DNA for nucleotide salvage (Bennett et al., 1985). Nucleolin was also shown to bind DNA nanoparticles at the surface of cells grown *in vitro* (Chen et al., 2008a), although the relevance of this mechanism in gene transfer *in vivo* has not been explored. To enhance the efficiency of naked DNA uptake, physical methods are often employed.

The most widely used physical method of enhancing transfer of naked DNA is electroporation, which applies pulses of an electric field following an injection of plasmid to increase plasma membrane permeability and facilitate nucleic acid uptake into cells (Neumann et al., 1982). Electroporation was shown to enhance transfection efficiency in the mouse lung (Dean et al., 2003, Pringle et al., 2007) and muscle (Aihara and Miyazaki, 1998), compared to naked DNA administration. This strategy was also investigated for mAb gene transfer in the muscle in a number of studies. Expression of an anti-HER2 mAb could be sustained for up to 9 months using this approach in immunocompromised mice, although expression was limited to 2 weeks in immunocompetent mice due to anti-drug responses (Hollevoet et al., 2018). Electroporation was also used to deliver anti-Ebola and anti-influenza mAb cDNAs to muscle to confer protection against Ebola and influenza infections in mice, although expression declined to levels below 1 μg/ml by 9 months after administration of vector, despite optimising the gene cassettes, vector backbones and electroporation regimen (Andrews et al., 2017). Overall, the levels of mAb expression obtained in serum using electroporation were in the range

of a few hundred ng/ml (Perez et al., 2004) to single-digit µg/ml (Andrews et al., 2017, Hollevoet et al., 2018) in mice, and up to 50 ng/ml in sheep (Tjelle et al., 2004). This is likely too low to provide a therapeutic effect in humans, which might require as much as tens of micrograms per ml, depending on the mAb (Sections 4.1 and 5.1). Additionally, expression was transient and only sustained for a few months.

Hydrodynamic delivery (reviewed in Suda and Liu, 2007) is also used to enhance uptake of naked DNA into cells. It involves rapid IV injection of a large volume of DNA (Budker et al., 1998) and is especially effective at transfecting hepatocytes when performed systemically (Liu et al., 1999). This method was used to deliver minicircles encoding tocilizumab (an anti-interleukin 6 receptor mAb) and etanercept (an anti-TNFα biologic) to mouse liver and was effective at ameliorating arthritis, but expression of the biologics was short-lived and declined within 30 days (Yi et al., 2014). Overall, the limited duration of expression achieved with naked DNA delivery suggests that repeated administration would be necessary for treatment of chronic conditions or for prophylaxis of recurrent infections.

1.1.4 Polyplexes and lipoplexes

The most common chemical methods of gene transfer involve complexing DNA with cationic polymers or lipids to form polyplexes or lipoplexes, respectively. This results in plasmid compaction and facilitates uptake into cells. Polyethylenimine (PEI) is amongst the most commonly used cationic polymers. It is available in a range of molecular weights and branched or linear form, and is an efficient gene

transfer agent *in vitro* and *in vivo* (Boussif et al., 1995). Polyethylenimine has received notable interest for airway gene transfer, particularly for the treatment of the genetic disease cystic fibrosis (CF), for which the linear form of 22 kDa was first investigated (Ferrari et al., 1999). This form of PEI was also used for systemic delivery through IV injection in mice, although the use of sufficient doses of the polyplexes to mediate efficient lung delivery was associated with liver toxicity and death (Chollet et al., 2002), indicating a suboptimal relationship between efficacy and safety of this gene transfer agent *in vivo*. Whilst direct airway delivery by instillation results in acute inflammation (Davies et al., 2008), aerosol inhalation is an effective means of gene transfer in the lung and results in sustained expression in the absence of pathology (Davies et al., 2012), indicating that toxic effects are dependent on polyplex formulation and route of administration. Nonetheless, concerns remain about the toxicity of PEI and the route of degradation and excretion from the body (Taranejoo et al., 2015), and biologically degradable derivatives are being explored as a safer alternative (Jere et al., 2009).

The second class of chemical gene transfer agents are lipoplexes, which consist of a liposome complexed with plasmid DNA. The liposomes are typically made of an amphiphilic cationic lipid and a neutral co-lipid such as cholesterol or DOPE (1,2-dioleoyl-sn-glycero-3-phosphoethanolamine), addition of which is thought to increase transfection efficiency by enhancing complex uptake into the cell, entry of DNA into the cytoplasm, and its release from the lipid complex (Fasbender et al., 1997). This method of gene delivery has been extensively explored in the context of airway gene transfer. Of particular interest is the lipid mixture GL67A, comprising Genzyme Lipid 67 (GL67; Cholest-5-en-3-ol (3P)-,3-[(3-aminopropyl)[4-[(3-aminopropyl)amino]butyl] carbamate]), DOPE and the polyethylene glycol-

containing lipid DMPE-PEG5000 (1,2-Dimyristoyl-sn-Glycero-3-Phosphoethanolamine–N-[methoxy (Polythene glycol) 5000]) (Eastman et al., 1997), which has been investigated for treatment of CF lung disease (Alton et al., 1999). In a recent phase II clinical trial, aerosol administration of GL67A lipoplexes to the lung was found to be a safe and effective method of gene delivery to this organ (Alton et al., 2015). Instillation of GL67A lipoplexes into the lung resulted in significant expression of a secretory protein in the serum of mice (Griesenbach et al., 2011), indicating that this might be a potentially useful gene transfer agent for facilitating secretory protein production in the lung.

1.1.5 Adeno-associated virus

1.1.5.1 Adeno-associated virus biology

Adeno-associated viruses (AAV) are non-enveloped single-stranded DNA viruses belonging to the family *Parvoviridae*, first discovered in 1965 as a contaminant of adenovirus preparations (Atchison et al., 1965). They are not known to cause disease in humans (with the exception of isolated reports, discussed in Section 1.1.5.3), and are unable to replicate in the absence of co-infection with a helper virus such as adenovirus, herpes virus or bocavirus (Schlehofer et al., 1986, Wang et al., 2017).

The AAV genome and its products are shown in Figure 1.1. The genome is either positive or negative sense; a virus population will contain an equal mixture of both (Berns and Rose, 1970). The viral genome contains two genes: *rep* and *cap*, which are flanked by inverted terminal repeats (ITRs) on each end. These are 145-base

(b) palindromic sequences folded into T-shaped hairpins which function in genome replication and packaging of viral DNA into the AAV capsid (Koczot et al., 1973, Srivastava et al., 1983). Through the use of two promoters (p5 and p19) and alternative splicing, *rep* encodes four proteins involved in integration and replication of the genome: Rep40, Rep52, Rep68 and Rep78. The *cap* gene is transcribed from a single promoter p40 and through alternative splicing and use of a non-canonical start codon gives rise to the three capsid monomers: VP1, VP2 and VP3. Through an alternative reading frame, *cap* also encodes the assembly-activating protein (AAP).

A number of AAV serotypes exist, classified on the basis of cross-neutralisation by antibodies specific against one group. Twelve human serotypes and over 100 serotypes from other hosts have been identified (Daya and Berns, 2008), which use a variety of different receptors to bind to and enter target cells. The most well-characterised serotype is 2, which uses heparan sulphate proteoglycan as its receptor (Summerford and Samulski, 1998). Novel AAV serotypes with altered tropism are being continuously developed using combinatorial and rational approaches (reviewed in Kotterman and Schaffer, 2014). Directed evolution of AAV using libraries generated through shuffling or error-prone PCR led to generation of enhanced serotypes for gene transfer in a variety of organs including the nervous system (Tervo et al., 2016), eye (Dalkara et al., 2013), liver (Paulk et al., 2018b) and skeletal muscle (Paulk et al., 2018a).

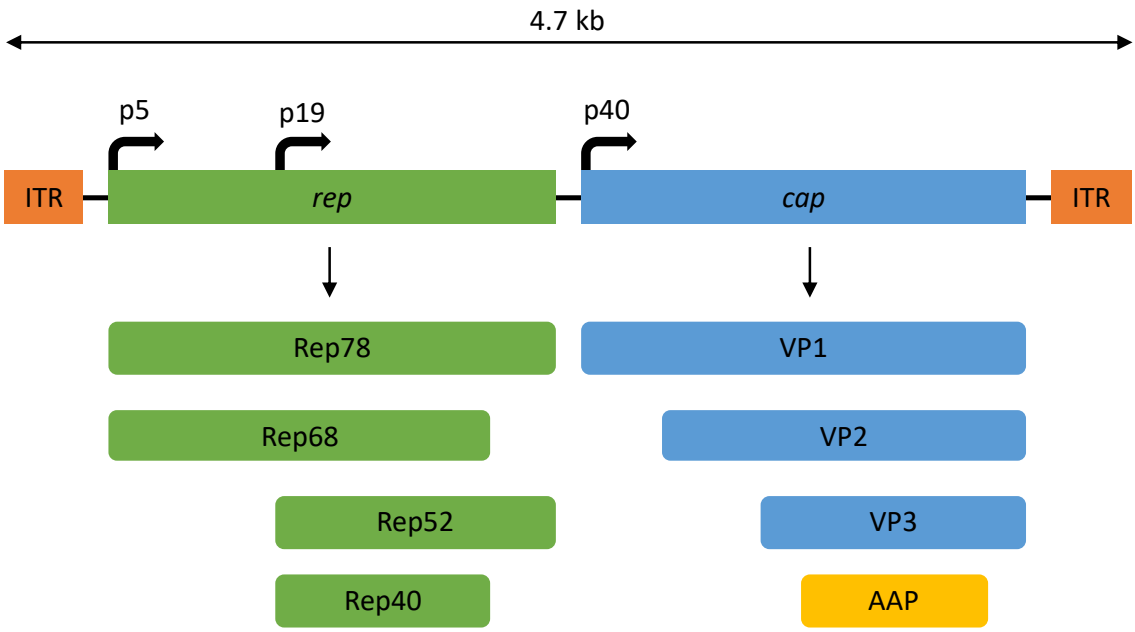

Figure 1.1. Schematic of adeno-associated virus genome.

The genome is 4.7 kb in length (Srivastava et al., 1983) and contains two genes: *rep* and *cap*. These are flanked by a pair of inverted terminal repeats (ITRs), which have promoter activity and function in genome replication, transcription and packaging (Carter et al., 1976). The *rep* gene is transcribed from two promoters (p5 and p19) and encodes four proteins involved in genome replication and integration: Rep78, Rep68, Rep52 and Rep40, called thus on the basis of their molecular weight. *Cap* has a single promoter p40 and encodes three monomeric capsid units in one reading frame: VP1, VP2 and VP3, which assemble to form the viral capsid at a molar ratio of 1:1:10 (Johnson et al., 1971); and the assembly-activating protein (AAP), which facilitates capsid assembly (Earley et al., 2017), in an alternative reading frame.

The mechanism for internalisation of AAV is not completely understood, but it is believed to involve clathrin-mediated endocytosis, at least for serotype 2 (Duan et al., 1999). The decreasing pH in the endosome leads to escape of the virion, which moves to the nucleus and enters it prior to uncoating (Bartlett et al., 2000). Once in the nucleus, the virus may follow the lytic or lysogenic pathway. The former requires co-infection with a helper virus and involves genome replication and production of virions. The adenoviral factors important for AAV replication have been identified and include E1a, E1b, E2a and E4 proteins, and VA RNA (Ferrari et al., 1996). The lysogenic pathway occurs in the absence of a helper virus which would allow replication, and establishes latent infection by means of integration of the genome into a specific site on chromosome 19 called adeno-associated virus integration site 1 (*AAVS1*) (Kotin et al., 1991), encoding the gene *PPP1R12C* (Tan et al., 2001). This locus is known as a "safe harbour" site, as integration of an exogenous sequence in this location does not appear to have pathogenic effects and the integrated transgenes have uniform expression in many cell types. Thus, *AAVS1* is often used as a genomic target for 'knock-in' studies (DeKelver et al., 2010). The Rep78 and Rep68 proteins interact with Rep-binding elements (RBE) in the viral ITR and the *AAVS1* locus and mediate site-specific integration (Surosky et al., 1997) through the non-homologous end-joining pathway of DNA repair (Daya et al., 2009). The integrated provirus can be rescued from latency by infection with adenovirus (Cheung et al., 1980), or treatment of host cell with genotoxic agents such as chemical carcinogens, ultraviolet light, heat shock, and metabolic inhibitors of DNA replication or protein synthesis (Yalkinoglu et al., 1988)

1.1.5.2 Recombinant adeno-associated viral vector

For use as a gene transfer agent, AAV was modified to create a “gutless” replication-deficient vector by replacing the *rep* and *cap* genes with the genetic payload of interest. As Rep proteins are also necessary for integration, the recombinant AAV vector (rAAV) genome tends to remain in nuclei of transduced cells as monomeric or concatameric episomal circles (Duan et al., 1998), though integration at *AAVS1* and other genomic loci has been observed at low frequency (Deyle and Russell, 2009). The episomal form of the genome is stable and long-lived (Afione et al., 1996), particularly in non-dividing tissues such as muscle (Penaud-Budloo et al., 2008), which results in long-term gene expression. For rAAV production, *rep* and *cap* genes are supplied in *trans*, along with adenoviral helper genes required for encapsidation of the genome. Originally, production involved co-infection with adenovirus, which required removal from the final product by chromatography, heat inactivation or other methods. Cloning of the helper genes into a plasmid removed the need for adenovirus infection and further improved the safety of the vector (Xiao et al., 1998). The transient transfection system for rAAV production is outlined in Figure 1.2.

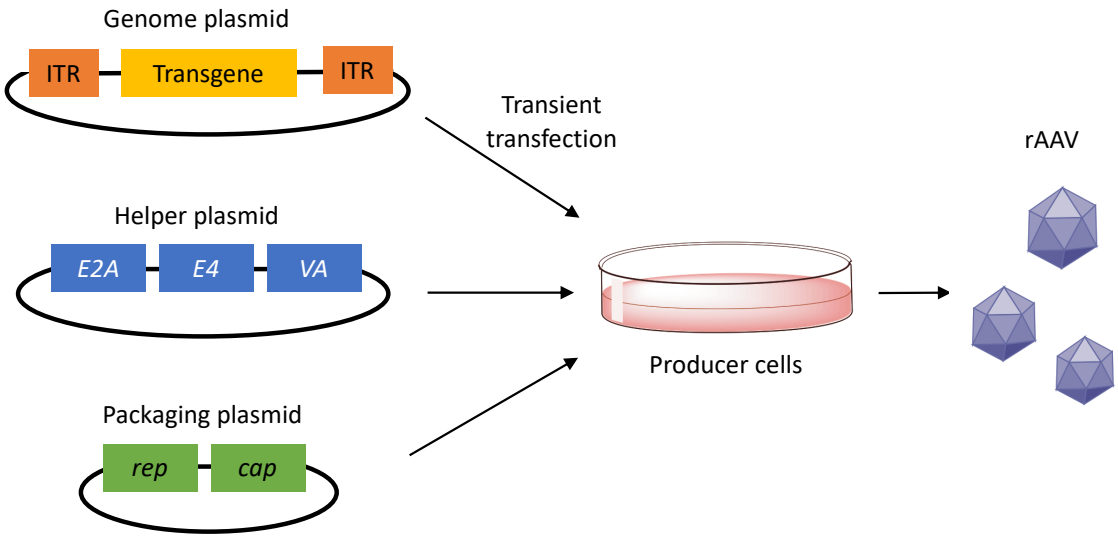

Figure 1.2. Schematic of recombinant AAV production.

The vector is usually produced using a three-plasmid transient transfection. The genome plasmid typically contains a transgene of interest, flanked by a pair of inverted terminal repeat sequences (ITR) to facilitate packaging of the vector genome. The helper plasmid supplies adenoviral genes necessary for virion production: *E2A, E4 and VA*. *E1* is also necessary, and is typically already present in producer cells. The packaging plasmid encodes Rep and Cap proteins required for production and encapsidation of the vector genome. Following transfection of the plasmids, the vector is harvested and purified.

Gene transfer with rAAV was first demonstrated in 1984 (Tratschin et al., 1984) and the vector has seen extensive use in gene therapy research since. The first clinical trial with rAAV was carried out in CF patients, where a single dose of vector encoding *CFTR* gene delivered to the nose and single lung lobe was found to be well-tolerated, although efficiency of gene transfer and efficacy of the treatment were not evaluated (Flotte et al., 1996). The vector has since been demonstrated to be an efficient and safe gene transfer vehicle in a number of clinical trials for various applications (some of which are reviewed in Samulski and Muzyczka, 2014), culminating in the first ever approval of a gene therapy drug by the European Medicines Agency (EMA) in 2012 (Ylä-Herttuala, 2012). Glybera (alipogene tiparvovec) is based on rAAV2 genome with Cap protein from serotype 1 (rAAV2/1) and is licensed for treatment of an ultra-rare inherited disorder lipoprotein lipase deficiency. This serotype was selected due to its ability to efficiently transduce skeletal muscle in animal models (Arruda et al., 2004, Chao et al., 2000, Xiao et al., 1999). Another rAAV-based drug, Luxturna (oretigene neparvovec-rzyl), is licensed in the USA for treatment of vision loss associated with inherited retinal disease (Nature Biotechnology News, 2018).

1.1.5.3 Limitations to gene therapy using recombinant adeno-associated virus

Due to the perceived non-pathogenicity of wild-type AAV and the lack of adverse effects in clinical trials using rAAV, the vector has been widely regarded as having an excellent safety profile. Some concerns about safety of rAAV-based gene therapy in humans emerged when integrated copies of wild-type AAV genome were found in tumour samples from hepatocellular carcinoma patients (Nault et al.,

2015). However, the relevance of these findings to rAAV vectors has been called into question (Berns et al., 2015). Further concerns about potential toxicity of the vector were raised when it was reported that primates and piglets receiving high IV doses of rAAV9 encoding human survival motor neuron (SMN) protein experienced severe, life-threatening side effects (Hinderer et al., 2018). This is at odds with the findings from a clinical trial investigating a similar rAAV9 vector for the treatment of spinal muscular atrophy (SMA), in which the vector appeared safe and effective (Mendell et al., 2017). The potential toxicity of rAAV in humans continues to be investigated.

There are other limitations associated with the use of rAAV in gene therapy. Firstly, the vector has a restricted packaging capacity. Whilst some have reported successful packaging of genomes as large as 8.9 kb (Allocca et al., 2008), efficiency of expression following transduction decreases substantially for constructs >5 kb (Wu et al., 2010); thus, the limited packaging capacity of rAAV remains a challenge for certain applications. Secondly, the vector stimulates a neutralising antibody response which abolishes transduction upon subsequent re-administration of the same serotype (Xiao et al., 1999). Formation of this adaptive immunity can be prevented with transient immunosuppression during the initial exposure (Halbert et al., 1998, Meliani et al., 2016). However, this approach might be undesirable in certain circumstances (e.g. cancer or CF patients), and re-administration of rAAV remains a challenge.

1.1.5.4 In vivo expression of antibodies using rAAV

Despite the limitations outlined in Section 1.1.5.3, rAAV remains a promising candidate for *in vivo* mAb expression. Lewis et al. reported the first use of this vector in the successful delivery of a broadly neutralising mAb b12 against human immunodeficiency virus (HIV) to mice (Lewis et al., 2002). Since then, expression of >1 mg/ml of mAbs in serum has been achieved with rAAV (Fang et al., 2005), and the vector was further investigated for applications including Ebola infection (Robert et al., 2017) and contraception (Li et al., 2015). Prophylaxis against HIV has been the most extensively studied application (reviewed in Brady et al., 2017). Following successful protection from HIV and simian immunodeficiency virus (SIV) challenge in mouse (Balazs et al., 2011, Balazs et al., 2014) and non-human primate (NHP) models (Gardner et al., 2015, Saunders et al., 2015), two phase I clinical trials are underway to assess the safety of rAAV expressing anti-HIV mAbs. If successful, these will set precedent for rAAV-mediated mAb gene delivery in humans.

1.1.6 Lentivirus

1.1.6.1 Lentivirus biology

Lentiviruses are a member of the *Retroviridae* family and, as such, are enveloped RNA viruses with a life cycle involving reverse transcription of the genome into DNA and integration thereof into the host genome. Lentiviruses were one of the first viruses discovered, with equine infectious anaemia virus (EIAV) identified as a “filterable agent” in 1904 (Craigo and Montelaro, 2011). Other well-known examples include HIV type 1 and 2 (HIV-1 and HIV-2), SIV and feline

immunodeficiency virus (FIV). Lentiviruses are characterised by a long incubation period and slowly progressing disease, from which they derive their name. The lentiviral genome is typically 9-11 kb long and contains a number of overlapping genes flanked by long terminal repeats (LTRs) which function in viral replication, integration, and expression (Figure 1.3). The structure of a lentivirus particle is shown in Figure 1.4.

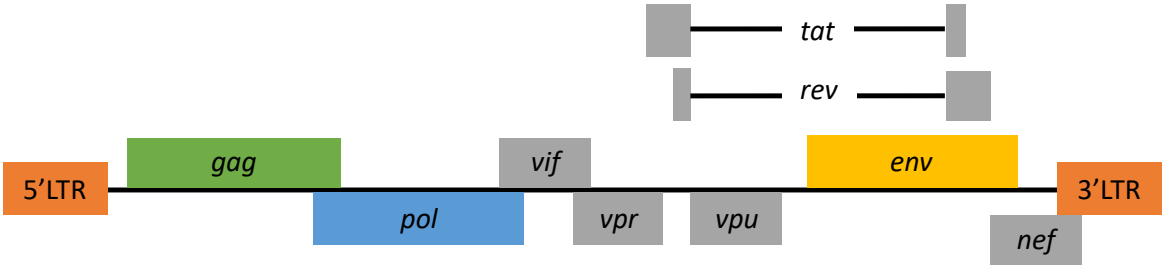

Figure 1.3. Schematic of the lentivirus genome (HIV-1).

The genome contains genes in three different reading frames flanked by two long terminal repeats (LTR) required for virus replication, integration, and expression. *Gag* encodes proteins that constitute the internal structure of the virus, including the nucleocapsid, capsid and matrix proteins. *Pol* encodes the enzymes reverse transcriptase, integrase and protease, which are important in various steps of the lentiviral life cycle. Components of the surface envelope protein are encoded by *env*. The HIV-1 genome also encodes additional regulatory and accessory proteins: Nef, Rev, Tat, Vif, Vpr and Vpu.

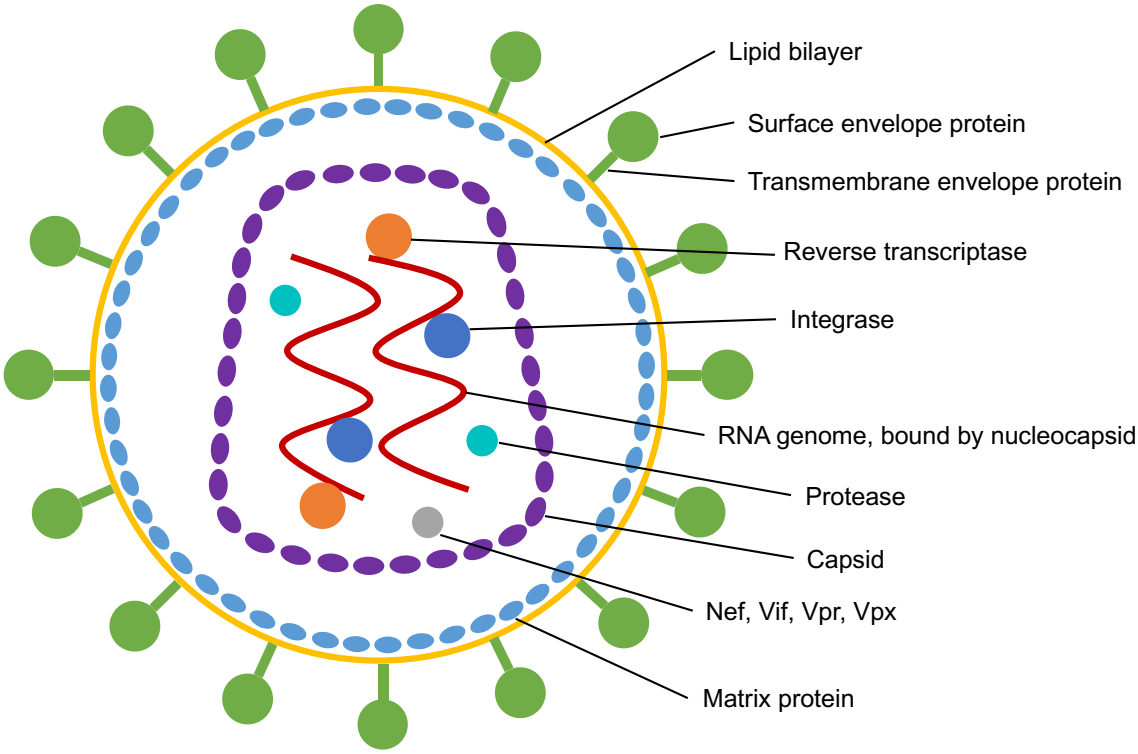

Figure 1.4. Structure of a lentivirus particle.

Two copies of the positive sense RNA genome, bound by nucleocapsid, are enclosed in a capsid together with the enzymes reverse transcriptase, integrase and protease, and the accessory proteins (in HIV-1, these are Nef, Vif, Vpr and Vpx). The capsid is further surrounded by a lipid bilayer originating from the membrane of the host cell from which the virion had budded. The envelope protein on the surface of the virus mediates attachment to a receptor and fusion with the target membrane.

1.1.6.2 Recombinant lentiviral vectors

The ability to infect both dividing and non-dividing cells (Lewis et al., 1992) combined with long-term expression due to integration into host genome has made lentiviruses attractive candidates for gene transfer vectors. Recombinant lentiviral vectors (rLV) were first developed in 1996 using a three-plasmid packaging system to reduce the chance of generating a replication-competent virus by recombination (Naldini et al., 1996). Further improvements led to the development of third generation rLV (Dull et al., 1998), which are produced using a four-plasmid packaging system (Figure 1.5), further reducing the chance of recombination. Genes encoding the accessory proteins Nef, Vif, Vpr and Vpx have been removed, as in the second generation system (Zufferey et al., 1997). Crucially, third generation rLV are also self-inactivating (SIN) by virtue of a deletion in the promoter-enhancer region U3 in the 3'LTR (ΔU3) (Figure 1.6). During the reverse transcription phase of cellular transduction, the 5'LTR is copied from the 3'LTR, leading to elimination of promoter activity of the 5'LTR U3 in the provirus and preventing generation of full-length viral RNA. Downstream transcription from the ΔU3 3'LTR is also blocked, preventing read-through into potentially oncogenic genomic regions (Herman and Coffin, 1987).

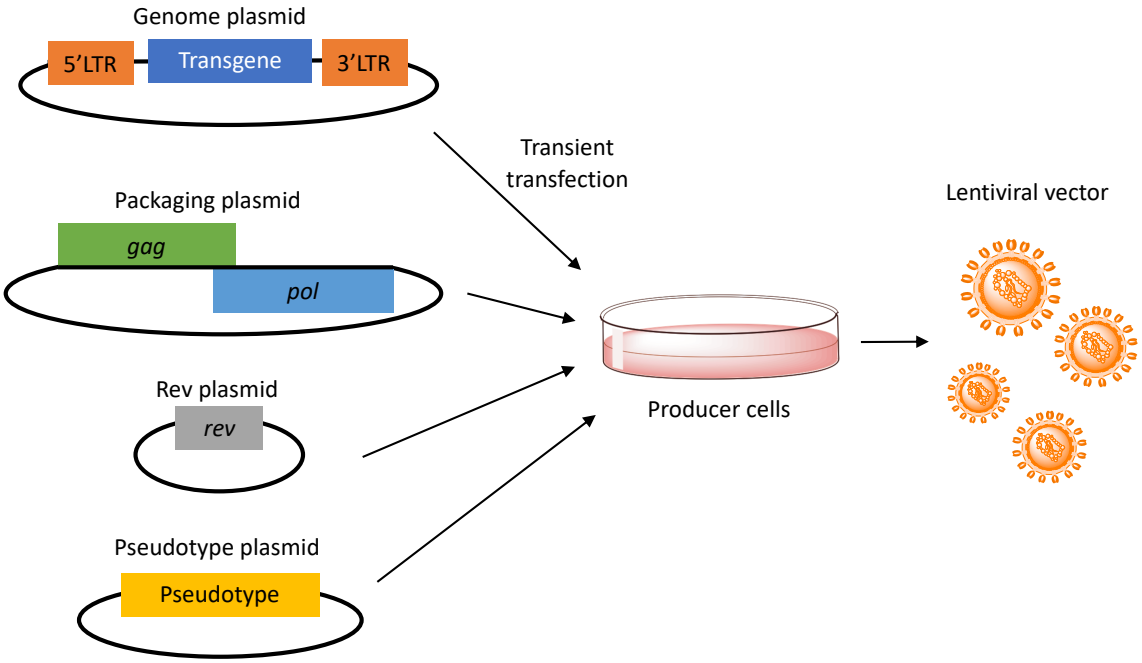

Figure 1.5. Third generation recombinant lentiviral vector packaging system. The packaging system comprises four plasmid components. The genome plasmid encodes the transgene of interest, transcribed from a heterologous promoter, flanked by long terminal repeats (LTRs). The packaging plasmid provides the products of *gag* and *pol* genes, whilst *rev* is encoded on another plasmid. The fourth plasmid provides the envelope protein of choice with which to pseudotype the vector.

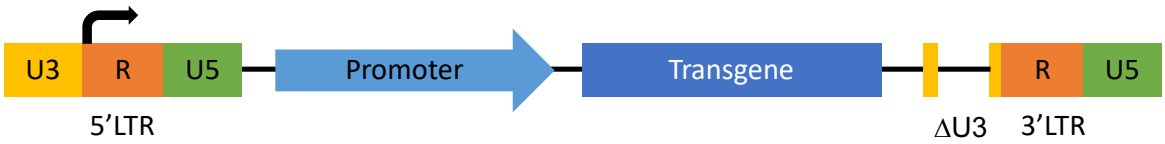

Figure 1.6. Organisation of self-inactivating lentiviral vector genome.

The U3 region of the 5' long terminal repeat (5'LTR) has promoter-enhancer activity (black arrow) when integrated as a provirus. To generate self-inactivating (SIN) vector, the U3 region of the 3'LTR is partially deleted (ΔU3). During reverse transcription, the 5'LTR is copied from the 3'LTR, introducing ΔU3 into the 5'LTR. This abolishes transcription of the full-length viral RNA from the 5'LTR in the provirus. Transcription of the transgene of interest is driven by a heterologous promoter of choice.

To redirect or broaden the tropism of rLV, the vector is typically pseudotyped, such that the original envelope protein (Env for HIV) is replaced with that of another virus with a more desirable cell transduction profile. The most commonly used pseudotype is the G glycoprotein from vesicular stomatitis virus (VSV-G) which confers broad tropism and improves stability of the vector, allowing concentration to high titres to facilitate gene transfer applications (Burns et al., 1993). Whilst VSV-G-pseudotyped rLV exhibits wide tropism, it fails to transduce certain tissues such as the apical surface of the airway epithelia in the lung (Johnson et al., 2000). Consequently, rLV has also been pseudotyped with other proteins, including those of Ebola virus (Chan et al., 2000, Kobinger et al., 2001), rabies virus (Mochizuki et al., 1998), baculovirus (Kumar et al., 2003), Sendai virus (Kobayashi et al., 2003), and influenza virus (Patel et al., 2013).

Recombinant LV vectors have several desirable features as gene transfer agents that could make them useful for *in vivo* mAb expression. Firstly, due to integration of the viral genome into the host DNA, expression of transgenes is anticipated to be long-lived, especially in terminally differentiated or slowly dividing tissues. Delivery of a single dose of an SIV-based vector pseudotyped with the fusion (F) and haemagglutinin-neuraminidase (HN) glycoproteins from Sendai virus (rSIV.F/HN) to mouse lung, for instance, results in expression for the lifetime of the animal (Griesenbach et al., 2012). Secondly, in contrast to other viral gene transfer agents, successful repeat administration of rLV can be achieved without loss of activity (Alton et al., 2017, Sinn et al., 2008). This is especially pertinent to applications requiring long-term expression of the therapeutic transgene. Thirdly, lentiviral vectors are not associated with oncogenic genotoxicity as, unlike gamma-

retroviral vectors (Hacein-Bey-Abina et al., 2003, Howe et al., 2008), they do not preferentially integrate near oncogenic loci (Alton et al., 2017, Montini et al., 2006).

One application for which rLV is utilised is *ex vivo* gene transfer in haematopoietic cells, particularly the preparation of chimeric antigen receptor (CAR) T-cells for treatment of leukaemia. Kymriah (tisagenlecleucel), indicated for treatment of B-cell precursor acute lymphoblastic leukaemia (ALL), uses recombinant HIV and is the first gene therapy drug to be approved by the FDA (Bach et al., 2017). *Ex vivo* gene transfer using rLV has also been studied for mAb production. This was first investigated for engineered myoblasts expressing Tg10, an anti-human thyroglobulin mouse mAb, which were grafted into mouse muscle and shown to secrete antibody into circulation (Noel et al., 1997). Customised therapy involving isolation of and *ex vivo* gene transfer in autologous cells is, however, a costly and labour-intensive process compared to *in vivo* delivery of an off-the-shelf vector, and is therefore not a feasible approach for antibody delivery for most applications. Recombinant LV has been used for *in vivo* transfer of mAb genes in a small number of studies as a potential cancer treatment. Intravenous (IV) and intramuscular (IM) injection of a VSV-G-pseudotyped HIV vector expressing anti-tumour mAbs was found to have a therapeutic effect in mouse models (Li et al., 2012, Vigna et al., 2008).

The rSIV.F/HN vector, originally developed by the UK Cystic Fibrosis Gene Therapy Consortium (UKCFGTC) for treatment of CF, is an efficient gene transfer agent in the murine lung, transducing at least 14% of airways epithelial cells (Alton et al., 2017). A single dose of the vector was shown to direct sustained expression of the secreted proteins factor VIII and α1-anti-trypsin to the circulation and lung

lumen of mice for at least 19 months (Paul-Smith et al., 2018), indicating that this platform could be useful to direct long-term expression of mAbs in those compartments.

1.1.7 Model applications to evaluate strategies for antibody gene transfer

To evaluate the feasibility of using a gene transfer platform to deliver therapeutic mAbs, it is necessary to demonstrate its efficacy in a model application, as biological activity of an antibody produced *in vivo* might not be equivalent to the commercially available drug. Two model diseases were selected for evaluation of antibody gene transfer approaches in this thesis: one which requires delivery of mAb to the circulation and one which requires mAb in the lung. Selection of applications in which to appraise gene transfer agents was based on (i) the prevalence of the condition and wide-spread use of the relevant mAb and (ii) the relevance and applicability to other diseases.

Delivery to the serum was investigated because mAbs in clinical use are typically administered systemically through IV, IM or subcutaneous injections and infusions, with the exception of ranibizumab, which is used in treatment of age-related macular degeneration and is administered intravitreally (Figurska and Stankiewicz, 2011). For systemic delivery, anti-TNFα biologics were investigated for treatment of rheumatoid arthritis; these studies are presented in Chapter 5. Delivery to the lung lumen was also investigated, as presence of mAbs in this compartment could be useful in prevention or treatment of respiratory infections, such as influenza (Shriver et al., 2015), or pulmonary diseases such as asthma (Desoubeaux et al.,

2016). For delivery to the lung, as well as the circulation, the anti-respiratory syncytial virus (RSV) mAb palivizumab was investigated, and the results are presented in Chapter 4. In the following sections, the two applications and the biologics selected for delivery using gene transfer agents are described.

1.2 Model disease: respiratory syncytial virus infection

Infection with RSV imposes a significant burden on the global economy and affects virtually all children. An effective means of prophylaxis through a mAb is available, but cost considerations dictate that its use is limited. The following sections describe the pathophysiology of the disease, virology of the pathogen, strategies used to prevent infection, and the rationale for investigating antibody gene transfer for RSV prophylaxis.

1.2.1 Epidemiology and pathophysiology of RSV infection

Human respiratory syncytial virus (RSV) is the most common cause of lower respiratory tract infections in young children. Globally, the number of incidents of acute lower respiratory infections in children younger than 5 years due to RSV was estimated at 33.8 million in 2005, of which about 10% required hospitalisations (Nair et al., 2010). By 2 years of age, nearly all children will have been infected with RSV at least once (Henderson et al., 1979), and although only a small proportion of cases (0.7%) require hospitalisation (Jepsen et al., 2018), the

pathogen nonetheless imposes a heavy burden on health services; between 1997 and 2000, RSV-related hospital charges in the USA exceeded 2.6 billion dollars (Leader and Kohlhase, 2003). Mortality rates amongst infants are low in the western world (three or four deaths per 10,000 admissions) (Byington et al., 2015), with the vast majority of deaths (99%) occurring in developing countries (Nair et al., 2010). Underlying cardiac or pulmonary disease significantly increases the risk of death (Navas et al., 1992). The virus is also a substantial burden in the elderly, with mortality rates reaching 6-8% (Colosia et al., 2017) and accounting for 78% of all RSV-related deaths (Thompson et al., 2003).

In temperate climates, peak RSV activity typically occurs during the winter (Gilchrist et al., 1994). The virus is transmitted through direct inoculation of the nose or eye (Hall et al., 1981) with virion-laden droplets spread by sneezing and coughing, or by self-inoculation after touching contaminated surfaces (Hall and Douglas, 1981). Infants are typically infected by an older sibling or a parent (Heikkinen et al., 2015). The incubation period is usually 3-5 days and viral shedding lasts for up to 8 days, though young children and immunocompromised patients may shed virus for as long as 3 weeks (Eiland, 2009). Following an initial inoculation, the virus starts replicating in the nasopharynx, causing nasal discharge. From there, it spreads to the bronchi and bronchioles, causing wheezing, increased breathing rate and rattling on inhalation. If the virus spreads further to the alveoli, pneumonia and severe respiratory distress may occur (Nye et al., 2016). RSV is also associated with long-term complications, as children who have been infected have an increased risk of developing recurrent wheezing (Fauroux et al., 2017), asthma (Wu et al., 2008) and allergic sensitisation (Schauer et al., 2002), rendering the virus a serious burden in the paediatric population.

1.2.2 RSV virology

RSV is an enveloped virus belonging to the *Pneumoviridae* family (Afonso et al., 2016). Its negative sense RNA genome (Huang and Wertz, 1982) is 15.2 kb long and contains 10 genes (Collins et al., 1986) coding for 11 proteins. A schematic representation of an RSV virion and the proteins encoded by its genome are shown in Figure 1.7.

The life cycle of RSV, outlined in Figure 1.8, begins with attachment of the virion to the target cell surface. This is thought to be mediated by G protein (Bourgeois et al., 1998), although viral entry is still observed in its absence, suggesting it is not essential but rather an accessory protein (Karron et al., 1997, Teng and Collins, 1998). The F protein, on the other hand, is strictly required for viral entry and replication. It is a trimeric glycosylated transmembrane protein, synthesised as an inactive precursor (F_0) and processed by a host protease into two fragments, F_1 and F_2, which come together in the mature, active form (Collins and Mottet, 1991). It is highly conserved amongst RSV strains, with protein sequence identity of 91% (Johnson and Collins, 1988). A number of putative receptors have been proposed for F protein, including intercellular adhesion molecule-1 (ICAM-1) (Behera et al., 2001), annexin II (Malhotra et al., 2003), nucleolin (Tayyari et al., 2011) and CX3CR1 (Johnson et al., 2015). Following attachment of the virion to the target cell surface, F binds to one of its putative receptors and mediates fusion by undergoing a dramatic conformational change which brings the viral and host membranes together (Zhao et al., 2000). The presence of F protein on the surface of infected cells causes fusion with adjacent cells and formation of syncytia, from which the virus derives its name. This allows RSV to spread from cell to cell without

having to emerge into the extracellular milieu (Shigeta et al., 1968), and constitutes an alternative mechanism for viral spread. The prefusion form of F protein is most effective in stimulating optimally neutralising antibodies (McLellan et al., 2013b) and is an important target in RSV vaccine development (McLellan et al., 2013a, Steff et al., 2017).

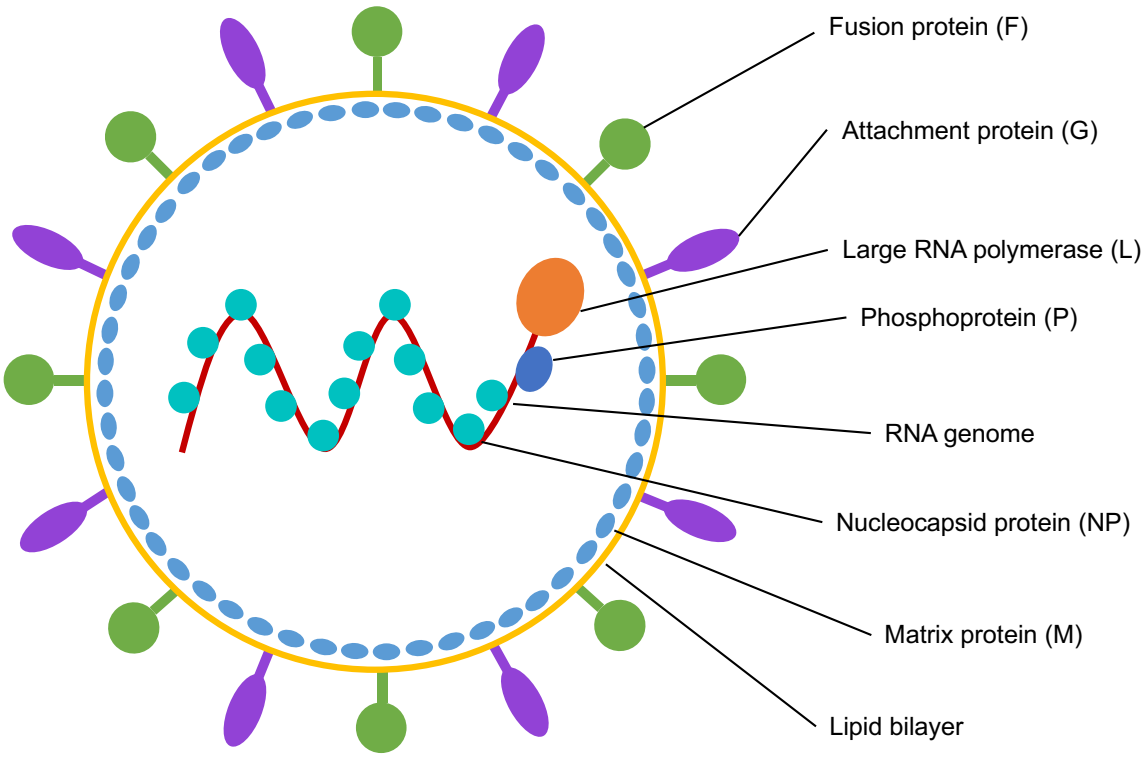

Figure 1.7. Structure of a respiratory syncytial virus (RSV) particle.

The negative sense RNA genome is bound by the nucleocapsid protein (NP) and associated with phosphoprotein (P) and large RNA polymerase (L), which are important in viral genome transcription and replication. This ribonucleoprotein complex is surrounded by the matrix, made up of matrix (M) protein, and further enveloped by a lipid bilayer of host origin. The fusion (F) and attachment (G) proteins are found on the surface of the virion and function in attachment to, and fusion with, the target cell membrane. Whilst a spherical form is shown, the virus may also assume filamentous shape.

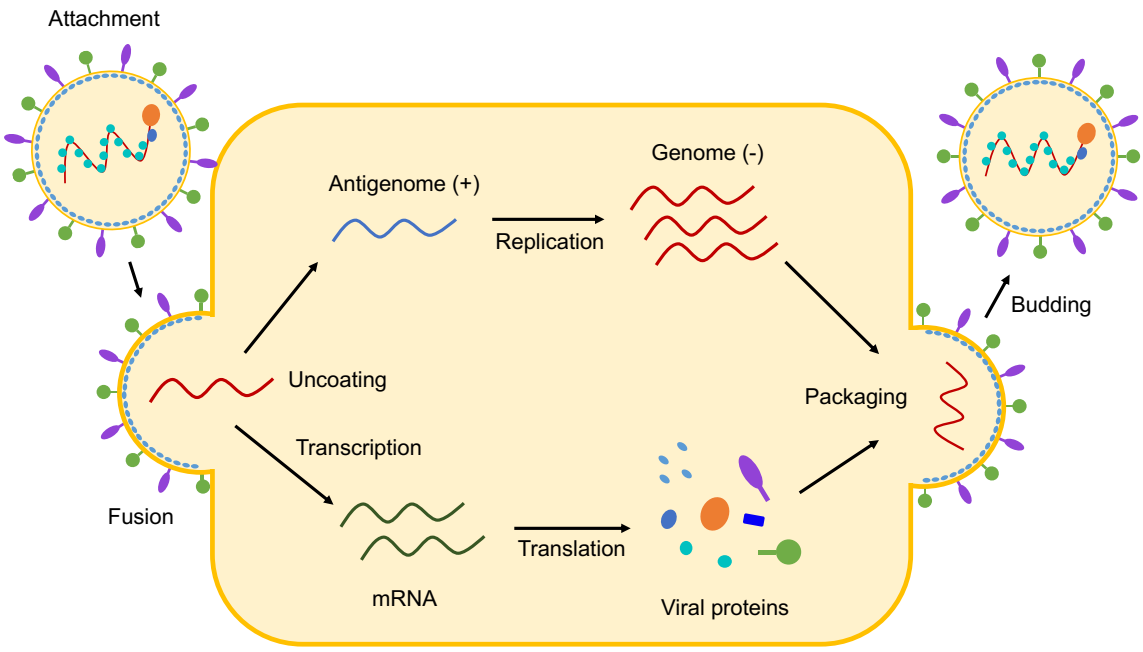

Figure 1.8. Respiratory syncytial virus life cycle.

The attachment (G) protein facilitates attachment of the virus to the host cell membrane and fusion (F) protein mediates subsequent fusion between the viral envelope and host membranes. This allows uncoating and release of the genome. The nucleocapsid (NP), phosphoprotein (P) and large RNA polymerase (L) proteins present in the virion come together to form the RNA-dependent RNA polymerase complex and transcribe the 10 viral genes into mRNA and replicate the genome through an antigenome intermediate (Huang et al., 1993). Following protein and genome synthesis, viral components are packaged and the progeny virion is released from the cell membrane by budding.

1.2.3 Prophylaxis of RSV infection

1.2.3.1 Strategies for prophylaxis of RSV infection

Treatment of patients presenting with RSV-induced lower respiratory tract infection consists primarily of supportive care such as oxygen therapy and fluid replacement to maintain hydration (Mejias and Ramilo, 2015). An antiviral drug ribavirin is available, although the evidence of its clinical benefit is limited (Ohmit et al., 1996, Ventre and Randolph, 2007) and it is not commonly used. There is no vaccine currently licensed for RSV. A formalin inactivated (FI) vaccine was investigated in clinical trials in the 1960s, but it was found to be non-protective and predisposed children to developing severe RSV disease upon infection with naturally circulating virus (Kapikian et al., 1969), with two participants dying as a result (Kim et al., 1969). The non-protective and disease-enhancing effects of the vaccine are thought to be caused by the induction of carbonyl groups on antigens by formalin treatment (Moghaddam et al., 2006) or stimulation of a non-neutralising antibody response due to the lack of affinity maturation as a result of deficient Toll-like receptor (TLR) activation in B cells (Delgado et al., 2009). The failure of the FI-RSV vaccine hampered further development for many years, however, a number of new RSV vaccines are now in the pipeline, including live-attenuated viruses, particle- and subunit-based formulations and gene-based vector approaches (reviewed in Neuzil, 2016). The furthest in clinical development is Novavax's formulation for maternal immunisation, based on F protein with alum adjuvant (August et al., 2017). It is currently being evaluated in a phase III clinical trial, with a readout of the study's primary endpoint expected in early 2019.

In the absence of a licensed vaccine, prophylaxis is instead achieved with passive immunisation. The first of such prophylactic interventions for RSV infection to be developed was respiratory syncytial virus immune globulin intravenous (RSV-IGIV, trade name RespiGam). The RSV-IGIV is prepared from donor sera screened for neutralising activity against the virus (Siber et al., 1992), and reduces risk of hospitalisation due to RSV infection by 41% (Connor et al., 1997). Its use has several disadvantages, however, including the requirement for IV cannulation and infusion over several hours and possibility of transmission of blood-borne infections from donors. Furthermore, it was deemed to not be cost-effective when used according to the approved indications (Barton et al., 2001), and has since been superseded by palivizumab, a potent anti-RSV mAb (Section 1.2.3.2).

1.2.3.2 Palivizumab and its use for prophylaxis of RSV infection

Palivizumab is a humanised mAb developed by MedImmune (Gaithersburg, Maryland, USA). When screening for an RSV-neutralising antibody, the F protein was selected as a target, as it is essential for RSV replication and highly conserved among RSV isolates (Young, 2002). The murine candidate MAb 1129 was isolated, which recognises antigenic site A, present on both the pre- and postfusion conformation of the F glycoprotein (Beeler and Coelingh, 1989). The mAb 1129 was humanised by replacing all sequences save the complementarity-determining regions (CDRs) with those of human IgG to prevent an anti-mouse response on administration to patients. The resulting product, designated MEDI-493 and later named palivizumab, was found to reduce RSV replication in a cotton rat model of infection by >99%, with corresponding serum concentrations of 25-30 μg/ml

(Johnson et al., 1997). In subsequent clinical trials, administration of the mAb was shown to reduce the rate of RSV-related hospitalisations by 45-55% (Feltes et al., 2003, Null et al., 1998). The mechanism of action was later shown to be mediated by blocking the F protein from fusing the viral and host membranes (Huang et al., 2010). Palivizumab was licensed in the USA in 1998 and in Europe in 1999 and is sold under the brand name Synagis.

The mAb is used during the RSV season, which typically lasts from November to March in the Northern Hemisphere (Pavilack et al., 2017). It is administered through IM injection, which can be done in an outpatient setting. Patients usually receive up to five monthly doses of 15 mg of palivizumab per kg of body weight (American Academy of Pediatrics Committee on Infectious and American Academy of Pediatrics Bronchiolitis Guidelines, 2014), resulting in trough serum concentrations of 37-72 μg/ml between subsequent doses (Null et al., 1998).

Prophylaxis of RSV infection using palivizumab is expensive. In the UK, a full course of palivizumab costs the National Health Service (NHS) £2,544-4,236 for a child weighing 3-6 kg (Simpson and Burls, 2001). Due to the cost, use of the drug has been limited to select, vulnerable infant populations including preterm neonates (Farber et al., 2016) and children with congenital heart or chronic lung disease (American Academy of Pediatrics Committee on Infectious and American Academy of Pediatrics Bronchiolitis Guidelines, 2014). Nevertheless, the cost-effectiveness of palivizumab is under continuous debate (Smart et al., 2010).

A more potent variant of palivizumab was developed by MedImmune, called motavizumab. The mAb was generated using affinity maturation, resulting in a 20-fold increase in virus neutralisation rates (Wu et al., 2007) and superior protection

from RSV infection relative to palivizumab in two clinical trials (Carbonell-Estrany et al., 2010, Feltes et al., 2011). Unfortunately, motavizumab was associated with an increased risk of serious allergic reactions (O'Brien et al., 2015), and failed to secure approval from the FDA. Other potent anti-RSV mAbs are being developed, such as MEDI8897 (Griffin et al., 2017), which was shown to be safe and effective in a recent phase 1b/2a clinical trial (Domachowske et al., 2018). However, at present, palivizumab remains the only licensed prophylaxis strategy against RSV.

1.2.4 Antibody gene transfer for prophylaxis of RSV infection

The limitations imposed on the use of palivizumab due to the cost of therapy with the mAb, discussed in Section 1.2.3.2, combined with the continued absence of a licensed vaccine (Section 1.2.3.1) necessitate development of novel, cost-effective solutions for prophylaxis of RSV infection which would be more widely accessible in the paediatric population. Transfer of palivizumab cDNA using one of the gene therapy vectors described in Section 1.1 for secretion into the circulation or lung lumen could offer an alternative to passive administration of the mAb. This application was therefore selected for study in this thesis.

1.3 Model disease: rheumatoid arthritis

Rheumatoid arthritis (RA) was selected for study as a model application for delivery of mAbs to the circulation. This disease was selected for several reasons: (i) it is common, affecting approximately 1% of the population (Gabriel et al., 1999, Symmons et al., 2002), (ii) the biologics used for its treatment are costly, leading to inequities in access to therapy (Putrik et al., 2014), and (iii) anti-TNFα is used for treatment of other autoimmune diseases such as psoriasis and Crohn's disease (Li et al., 2017b), meaning the benefits of establishing robust and sustained expression of these agents *in vivo* could be extended to further patient populations. The following sections describe the pathoaetiology of RA and the role of TNFα therein, treatment of the disease using TNFα antagonists, and the considerations associated with anti-TNFα gene transfer.

1.3.1 Epidemiology, symptoms and pathoaetiology of rheumatoid arthritis

Rheumatoid arthritis is a systemic autoimmune disease characterised by inflammation of the synovial joints. It affects an estimated 400,000 adults in the UK (Symmons et al., 2002), costing the economy nearly £8 billion a year, as reported by the National Rheumatoid Arthritis Society in 2010 (NRAS, 2010). The disease can present at almost any age, with median age of onset being 58 (Innala et al., 2014). Heritability contributes a small but significant risk to developing RA, with over 101 genes identified as relevant (Okada et al., 2014). Of those, the MHC class II locus is of particular importance, and people with the HLA-DR4 and DR1 variants are more likely to develop RA (Stastny, 1978). Environmental conditions are also

important, with smoking a well-known risk factor (Chang et al., 2014). Symptoms of RA include pain, swelling and stiffness of the joints, typically starting in the hands and wrists and spreading to other parts of the body, causing progressive loss of function. Patients often develop complications such as cardiovascular disease; these contribute to the elevated risk of mortality in RA patients, which is over 50% higher than in the general population (Avina-Zubieta et al., 2008).

The first line of treatment for RA are disease-modifying drugs, chiefly methotrexate. This folate antagonist is an immunosuppressant and, at higher doses, a chemotherapeutic agent (Huennekens, 1994). The mechanism of methotrexate's immunosuppressive properties is unclear, but it is thought to involve deletion of activated T-cells (Genestier et al., 1998). Therapy with the drug is moderately effective, though 16% of patients discontinue treatment due to adverse effects (Lopez-Olivo et al., 2014).

Although pathoaetiology of RA is not completely understood, research into the underlying processes has established the general mechanism, offering new targets for more effective treatments. The key features of the currently presumed mechanism of pathogenesis of RA are presented in Figure 1.9.

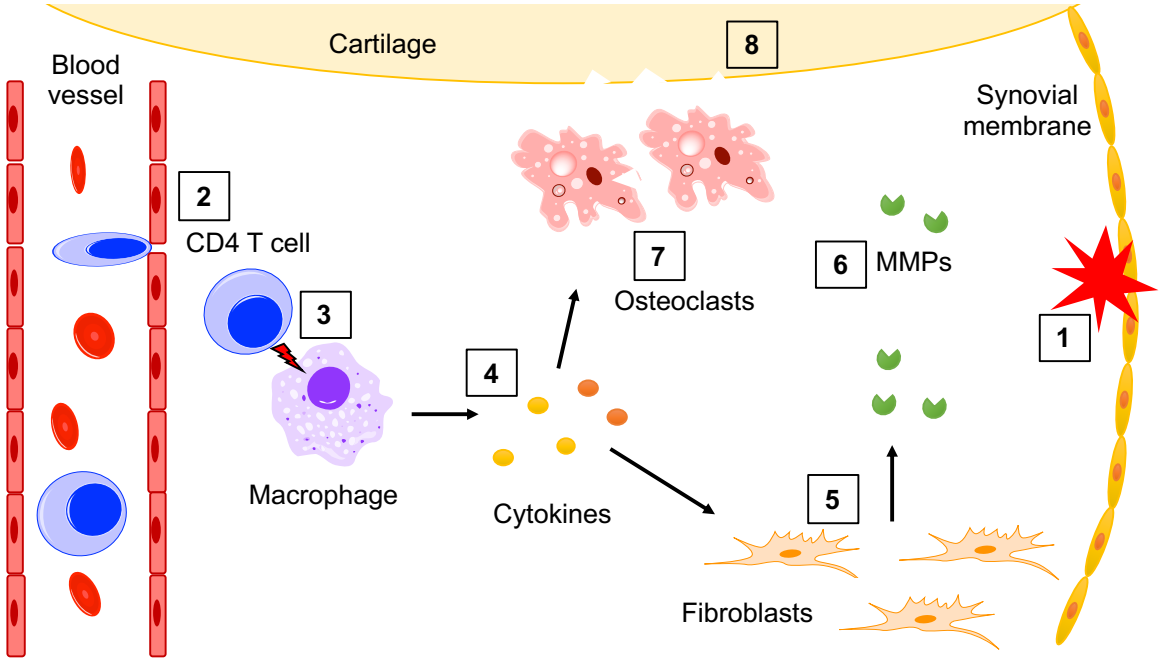

Figure 1.9. Mechanism of pathogenesis in rheumatoid arthritis joint.

An unknown trigger sets up an initial focus of inflammation in the synovial membrane lining the joint cavity (1). The inflammatory environment attracts various leukocytes, including autoreactive CD4 helper T cells which extravasate into the joint space (2) (Vanboxel and Paget, 1975). These CD4 cells activate macrophages (3) which secrete pro-inflammatory cytokines such as tumour necrosis factor alpha (TNFα), interleukin-1 (IL-1) and interleukin-6 (IL-6) (4) (McInnes et al., 2000). These in turn activate fibroblasts (5) to start producing matrix metalloproteases (MMPs) (6) which degrade the extracellular matrix (Burrage et al., 2006). The cytokines also activate osteoclasts (7) – bone-resorbing cells, which start degrading the cartilage (8), resulting in progressive damage to the joint (Schett, 2007). Continued inflammation leads to eventual loss of function.

1.3.2 Role of TNF-α in rheumatoid arthritis

The cytokine TNFα plays a pivotal role in the pathogenesis of RA (Vasanthi et al., 2007) and is a key target for treatment. It is produced by macrophages and is a major initiator of acute inflammation in normal immune responses. It is a trimeric protein and can be found in two forms: soluble (sTNFα) and membrane-bound (mTNFα). The soluble form is cleaved from the membrane-bound form by TNFα converting enzyme (TACE). The ligand has two receptors: TNF receptor 1 (TNFR1, also known as p55), which is expressed on all cell types in the body, and TNF receptor 2 (TNFR2, also called p75), which is only expressed in a subset of cells, including T-regulatory cells (Ware et al., 1991) and a type of neuron (Yang et al., 2002). The two receptors act through distinct signalling pathways, but there is a substantial overlap which includes nuclear factor kappa-light-chain-enhancer of activated B cells (NFκB) and mitogen-activated protein kinase (MAPK) pathways. As a general rule, signalling through TNFR1 is associated with cell death, while TNFR2 promotes cell survival (Faustman and Davis, 2013). Signalling of TNFα through its receptors is described in Figure 1.10.

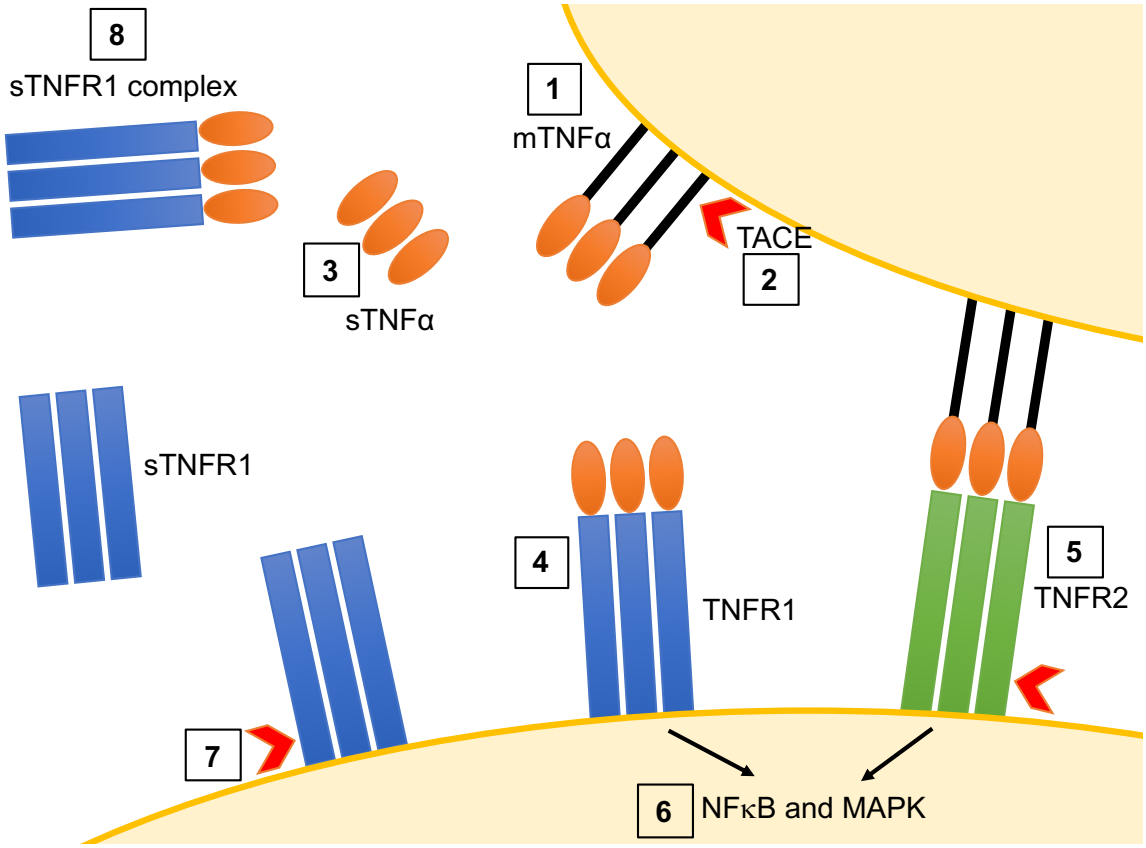

Figure 1.10. Tumour necrosis factor alpha and its receptors.

Tumour necrosis factor alpha (TNFα) is produced as a trimeric transmembrane form (mTNFα) (1), which is cleaved by TNFα converting enzyme (TACE) (2) and released as the 17 kDa soluble TNFα (sTNFα) (3). Both forms can bind to either of two receptors: TNFα receptor 1 or 2 (TNFR1 and 2, respectively) (4 and 5). TNFR1 is expressed on all cells in the body, while TNFR2 is only expressed in a specific subset, including certain immune cells. Signalling through both receptors involves the NFκB and MAPK pathways (6), but results in different effects: TNFR1 triggers inflammation, cytokine production, angiogenesis and cell death, while TNFR2 signals cell survival. Both receptors can be released from cell membrane through proteolytic cleavage of the extracellular domain by TACE (7). Such soluble forms, sTNFR1 and sTNFR2, can bind sTNFα and sequester it (8), thus acting as TNFα antagonists.

The involvement of TNFα in pathogenesis of RA was first suspected when elevated levels of the cytokine were found in the synovial fluid and serum of RA patients (Saxne et al., 1988). The role of the cytokine was further confirmed in a transgenic mouse model overexpressing human TNFα, which spontaneously developed RA-like symptoms (Keffer et al., 1991). Further evidence came from the discovery that addition of anti-TNFα antibody to rheumatoid synovial primary cultures inhibited production of other pro-inflammatory cytokines (Brennan et al., 1989, Haworth et al., 1991). Anti-TNFα antibodies were then shown to ameliorate disease in a mouse model of RA (Piguet et al., 1992, Williams et al., 1992, Wooley et al., 1993), setting precedent for targeting the cytokine in treatment of RA.

1.3.3 Anti-TNFα biologics for treatment of rheumatoid arthritis

A number of anti-TNFα biologics have been developed and marketed: infliximab (Remicade; Johnson & Johnson, NJ, USA), adalimumab (Humira; AbbVie, Chicago, IL, USA) and certolizumab pegol (Cimzia; UCB, Brussels, Belgium), which are mAbs or fragments thereof, and etanercept (Enbrel; Amgen, Thousand Oaks, CA, USA), which is a TNF receptor/IgG fusion protein. These are summarised in Table 1.2. Since TNFα is important in a number of autoimmune diseases, most of these drugs also have other indications, such as inflammatory bowel disease, psoriasis or ankylosing spondylitis. Biologic drugs against other cytokines and molecules are also available for treatment of RA, such as rituximab (anti-CD20 mAb), abatacept (CTLA4–Ig fusion protein) and tocilizumab (anti-IL-6R mAb). Treatment of RA with biologic drugs has increased from 3 to 26% of patients between 1999 and 2006 (Yazici et al., 2008) and is now standard of care and

second line of treatment for patients who don't respond to synthetic disease-modifying anti-rheumatic drugs such as methotrexate (Monaco et al., 2015).

Infliximab was the first anti-TNFα agent to be used in the clinic (Elliott et al., 1993). It is a chimeric mAb (Figure 1.11), containing variable antigen-binding regions from the original mouse antibody and constant regions from human IgG1 to reduce its potential to cause immune reactions in patients (Knight et al., 1993). Infliximab was demonstrated to be an effective treatment for RA in a number of clinical trials (Maini et al., 1999, Maini et al., 1998). It was approved by the FDA in 1999, and is now sold under trade name Remicade. The drug is administered through an IV infusion; the standard dose is 3 mg per kg of body weight, repeated 2 and 6 weeks later and every 8 weeks thereafter, according to British National Formulary from British Medical Association (BMA). With this dose, the median trough levels of serum infliximab between subsequent infusions have been measured as 22.3 μg/ml after 2 weeks, 14.6 μg/ml after a 4-week interval and 2.8 μg/ml after a further 8 weeks (Wolbink et al., 2005). After 14 weeks of treatment, patients who responded to treatment with the drug had an average trough serum level of 3.6 μg/ml (Wolbink et al., 2005).

Another TNFα antagonist commonly prescribed for treatment of RA is etanercept, which is a fusion protein comprising the Fc portion of human IgG1 and the extracellular portion of human TNFR2 (Figure 1.11) (Mohler et al., 1993). In preclinical studies, its efficacy was evaluated in the collagen-induced arthritis (CIA) mouse model, where administration of the drug 2-4 weeks after collagen immunisation or up to 2 weeks after disease onset was found to reduce incidence by two-thirds (Wooley et al., 1993). It was subsequently demonstrated to improve

disease outcomes in RA patients (Weinblatt et al., 1999), and was the first TNFα antagonist to be licensed for treatment of the disease by the FDA. Etanercept is administered through subcutaneous injection at a dose of 25 mg/kg body weight twice weekly or 50 mg/kg once weekly (Keystone et al., 2004). Frequent dosing is necessitated by its relatively short half-life of 3-4 days (Korth-Bradley et al., 2000), compared to mAbs such as infliximab which has a half-life of 9.5-14 days (Cornillie et al., 2001, Fasanmade et al., 2009). Average trough serum levels of etanercept prior to subsequent doses have been measured as 1.8 μg/ml (Moots et al., 2017), with 1.2 μg/ml identified as an optimal cut-off level for a good therapeutic response (Sanmarti et al., 2015).

Table 1.2. Anti-tumour necrosis factor alpha biologic drugs used for treatment of rheumatoid arthritis.

Name	Trade name	Company	Type	Origin	Year licensed
infliximab	Remicade	Johnson & Johnson (New Jersey, NJ, USA)	mAb	chimeric (mouse)	1999
etanercept	Enbrel	Amgen (Thousand Oaks, CA, USA)	Receptor/IgG fusion protein	human	1998
adalimumab	Humira	AbbVie (Chicago, IL, USA)	mAb	human	2002
golimumab	Simponi	Janssen (Horsham, PA, USA)	mAb	human	2009
certolizumab pegol	Cimzia	UCB (Brussels, Belgium)	Fab' fragment	humanised	2009

mAb: full length monoclonal antibody; Fab' fragment: fragment antigen-binding, composed of one constant and one variable domain of each of the heavy and the light chain. Structure of chimeric and humanized antibodies and fusion proteins is shown in Figure 1.11.

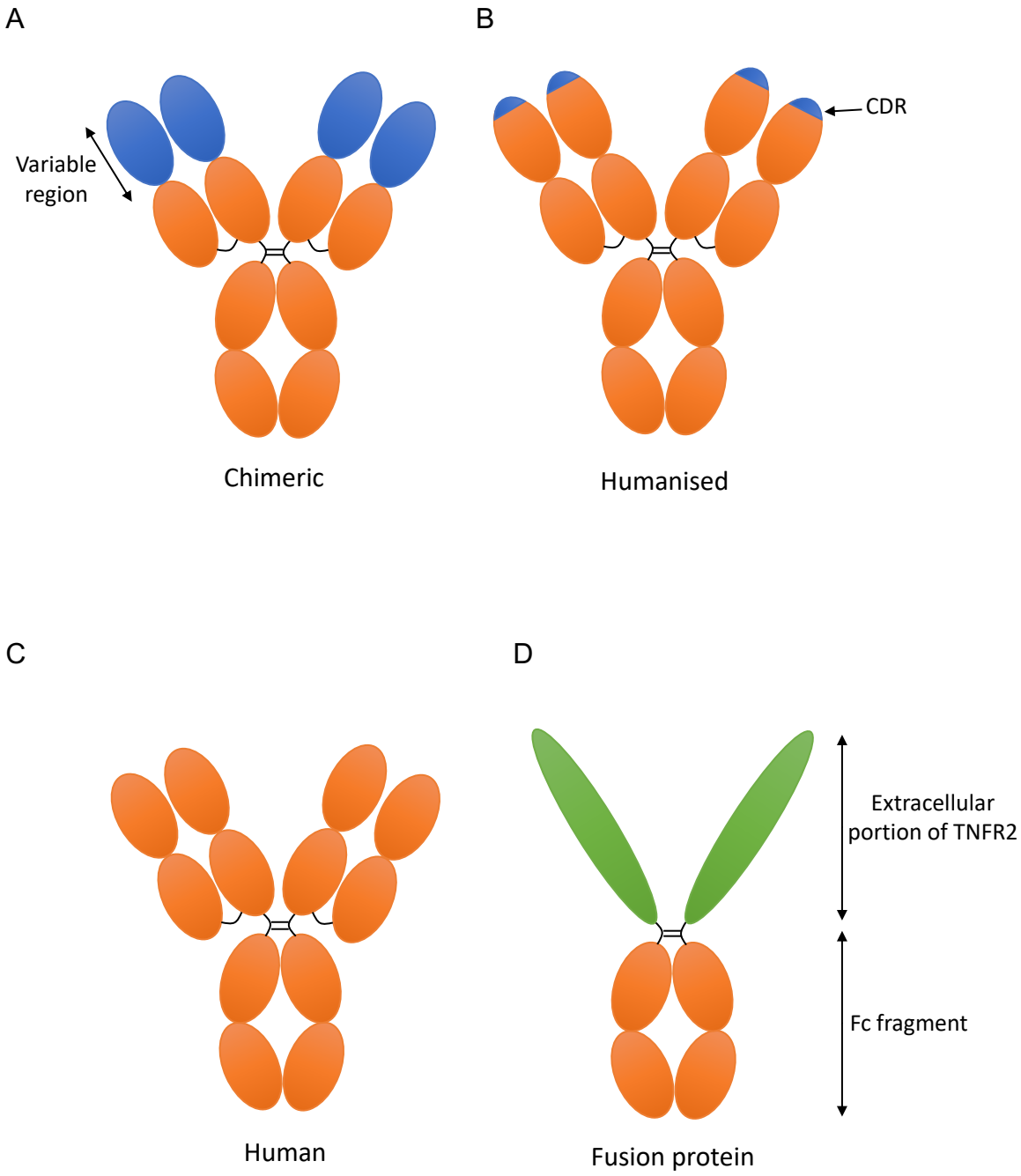
A
Variable region
Chimeric
B
CDR
Humanised
C
Human
D
Extracellular portion of TNFR2
Fc fragment
Fusion protein

Figure 1.11. Schematic of the composition of chimeric, humanised and human antibodies, and fusion proteins.

To reduce immune responses to sequences from the host in which the antibody was raised (blue), various portions are replaced with those of human origin (orange). In chimeric antibodies (A), all sequences except the variable regions have been replaced with human. Humanised antibodies (B) only contain the complementarity-determining regions (CDRs) of the original animal-derived antibody. Fully human antibodies (C) do not contain any sequences of animal origin and are typically generated in mice transgenic for human immunoglobulin genes or isolated from human donors. Receptor/IgG fusion proteins (D) combine an antibody fragment (usually Fc) with a portion of another protein (green), such as TNFα receptor 2 (TNFR2) in the case of etanercept.

1.3.4 Concerns associated with biologic TNFα antagonists

Anti-TNFα biologics have revolutionised treatment of RA but there are some problems associated with their use. Firstly, they are an expensive class of drugs, with an estimated cost of $18,000 and $27,000 per patient per year for etanercept and infliximab, respectively (Bonafede et al., 2014). This constitutes a substantial burden for healthcare systems and individual patients and prompts many to question the cost-effectiveness of this treatment (Nair et al., 2013, Wailoo et al., 2008). With the expiry of patents protecting some of the oldest TNFα antagonists, biosimilars are now entering the market. Three biosimilar versions of infliximab are now available in the UK: Inflectra (Pfizer; New York City, NY, USA); Remsima (Celltrion; Incheon, South Korea), approved by the European Medicines Agency (EMA) in 2013 (Mellstedt, 2013); and Flixabi (Samsung Bioepis, Incheon, South Korea), available since 2016. An etanercept biosimilar is also available, called Benepali (Samsung Bioepis), which was approved in the UK in 2016 (Erhorn, 2016). Availability of biosimilars is expected to lower the cost of therapy with these antibodies and offer substantial savings to healthcare systems and patients (Hawkes, 2015). Whilst there is extensive evidence confirming bioequivalence of anti-TNFα biosimilars (Chingcuanco et al., 2016), some studies have found structural differences between biosimilar drugs and their predecessors, cautioning against characterising biosimilars as “generic” versions of the innovator drugs (Grampp and Ramanan, 2015). Additionally, due to the extensive testing required to demonstrate the bioequivalence of generic biologics to the drugs they reference, biosimilars command 65-90% of the market price of the original product (Farfan-Portet et al., 2014), reflecting limited savings.

Another important issue with TNFα blockers relates to safety. Although anti-TNFα biologics have been found to be generally well-tolerated in clinical trials, concerns have emerged regarding a potential for increased risk of malignancies and serious infections amongst patients receiving the drugs due to their strongly immunosuppressive nature. Whilst anti-TNFα biologics do increase the risk of contracting serious bacterial infections two-fold (Curtis et al., 2007), their association with carcinogenesis and tumour progression is in dispute (Rosenblum and Amital, 2011). Nonetheless, cessation of therapy might be necessary in such cases.

1.3.5 Antibody gene transfer for treatment of rheumatoid arthritis

Due to the high cost of TNFα antagonists, discussed in Section 1.3.4, more competitively priced alternatives are desirable, rendering these biologics an attractive target for gene transfer. Reliable and well-researched animal models of rheumatoid arthritis exist, described in Section 5.3.2, which would enable evaluation of efficacy of anti-TNFα gene transfer approaches *in vivo*. For these reasons, delivery of mAb to the circulation was studied in this thesis in the context of treatment of RA.

1.4 Aims

In vivo antibody gene transfer is an attractive alternative to passive delivery of mAbs (Section 1.1.2). Various gene transfer agents, such as naked DNA electroporation and rAAV, are being investigated for this purpose by several research groups. Differences in vector design, antibody-specific expression levels and observed pharmacokinetics in a variety of animal disease models make it difficult to compare efficacy between methods. The main aim of this thesis is to investigate a number of available gene transfer agents as potential tools to establish *in vivo* mAb expression, using RSV infection and rheumatoid arthritis as model applications. In Chapter 3, selected viral and non-viral gene transfer systems are explored for effective *in vivo* expression of a secretory reporter protein. Chapter 4 investigates the use of rLV and rAAV vectors for expression of the anti-RSV mAb palivizumab, while Chapter 5 focuses on expression of TNFα antagonists as a method of treatment of RA. Together, these studies provide a basis for comparison of various methods for antibody gene transfer and demonstrate utility of a subset for the two model diseases.

Chapter 2: Materials and methods

2.1 Reagents and solutions

All solutions were prepared with Milli-Q reverse osmosis ultrapure water (Merck, Feltham, UK), nuclease-free water (Promega, Southampton, UK), endotoxin-free water for injection (WFI) (B. Brain Medical Ltd., Sheffield, UK) or absolute ethanol (VWR, Lutterworth, UK). Phosphate-buffered saline (PBS) was prepared from tablets (Sigma-Aldrich, St. Louis, MO, USA) for a final concentration of 140 mM NaCl, 10 mM phosphate buffer, and 3 mM KCl. Sterilisation of solutions was achieved by autoclaving for 15 to 30 minutes at 121ºC, or by filtration through a 0.22 µm surfactant-free cellulose acetate filter (Thermo Fisher Scientific, Cramlington, UK). Solutions were stored at room temperature (RT; 20-25ºC) unless otherwise stated. Where concentrations of solutions are indicated by percentages, they refer to weight:volume (w/v) ratios for solids at RT and volume:volume (v/v) ratios for liquids at RT.

2.2 Centrifugation

Centrifugation was carried out using the Micro Star 17 microcentrifuge with the Ch.500034PP rotor (VWR) or 5415D microcentrifuge with the F45-36-8 rotor (Eppendorf, Westbury, New York, USA) for microtubes (Corning, Flintshire, UK), the J2-HS centrifuge with the JA-10 or JA-20 rotor (Beckman Coulter, High Wycombe, UK) for centrifuge tubes (Starstedt, Leicester, UK) and pots (Beckman Coulter), the Sorvall Legend RT (Thermo Fisher Scientific) with swing bucket for

conical tubes (Corning), and the Optima XPN with Ti70 rotor (Beckman Coulter) for ultracentrifugation. Centrifugation using the J2-HS centrifuge was performed at 4ºC while other centrifugations were performed at RT.

2.3 Molecular cloning and amplification of plasmids

2.3.1 Plasmids used in the studies

The plasmids used in this study are summarised in Table 2.1. They can be broadly divided into general expression plasmids, rSIV vector genome and accessory plasmids, and rAAV vector genome and accessory plasmids. Unless otherwise indicated, the plasmids were specifically constructed for this study.

Table 2.1. List of plasmids used in this study.

Plasmid	Enhancer/promoter	Transgene	Source	Laboratory reference
Expression plasmids				
pG4.hCEFI.soLux	hCEFI	soLux	Hyde et al., 2008	pGM144
pG4.hCEFI.soGLux	hCEFI	soGLux	Gift of Ian Pringle	pGM206
pG6.93.soLux	93 bp minimal hC enhancer and EFI promoter	soLux	Oliveira, 2015	pGM365
pG6.2x93.soLux	Dual tandem 93 bp minimal hC enhancer and EFI promoter	soLux	Oliveira, 2015	pGM441
pG6.3x93.soLux	Triple tandem 93 bp minimal hC enhancer and EFI promoter	soLux	This study	pGM464
pG6.4x93.soLux	Quadruple tandem 93 bp minimal hC enhancer and EFI promoter	soLux	This study	pGM465
pG6.hCEFI.SMASh	hCEFI	SMASh	Gift of Ian Pringle	pGM506
pG6.hCEFI.Lux-SMASh	hCEFI	Lux fused to SMASh	Gift of Ian Pringle	pGM501
pG6.hCEFI.soGLux-SMASh	hCEFI	soGLux fused to SMASh	This study	pGM540

pG6.hCEFI.etanercept	hCEFI	etanercept	This study	pGM563
pG6.hCEFI.etanercept-SMASh	hCEFI	etanercept fused to SMASh	This study	pGM538
pG6.hCEFI.etanercept-NS3	hCEFI	etanercept fused to NS3 protease	This study	pGM593
pEGFP-N1	CMV	EGFP	Clontech	-
pCIKsoGLux	CMV	soGLux	Gift of Ian Pringle	-
Genome plasmids for rSIV.F/HN production				
pSIV.hCEF.palivizumab	hCEF	Single-ORF palivizumab	This study	pGM463
Accessory plasmids for rSIV.F/HN production				
pCMV.SIV.GagPol	CMV	*Gag* and *pol* genes from SIV	Addgene (Cambridge, MA, US)	pGM297
pRSV.Rev	RSV	*Rev* gene from SIV	Addgene	pGM299
pCAG.SeV.Fct4	CAG	Gene for Sendai virus F envelope protein	Gift of Lee Davies	pGM301
pCAG.SeV.EnvctHN	CAG	Gene for Sendai virus HN envelope protein	Gift of Lee Davies	pGM303

Genome plasmids for rAAV production				
pAAV2.hCEFI.soGLux	hCEFI	soGLux	Tan, 2017	pGM495
pAAV2.CASI.palivizumab	CASI	palivizumab	This study	pGM459
pAAV2.CASI.infliximab	CASI	infliximab	This study	pGM458
pAAV2.CASI.hGH-etanercept	CASI	etanercept	This study	pGM521
pAAV2.CASI.TNFR2-etanercept	CASI	etanercept	This study	pGM537
Accessory plasmids for rAAV production				
pAAV2/8	p5	*Rep* gene from AAV serotype 2 and *Cap* gene from AAV serotype 8	Penn Vector Core	-
pAAV2/9	p5	*Rep* gene from AAV serotype 2 and *Cap* gene from AAV serotype 9	Penn Vector Core	-
pAdDeltaF6		*E2a, E4* and *VARNA* genes from adenovirus	Penn Vector Core	-

The expression plasmids were named according to the backbone (i.e. pG4 = fourth generation, pG6 = sixth generation).

AAV: adeno-associated virus; CAG: modified chicken β-actin promoter with human cytomegalovirus immediate early enhancer (Junichi et al., 1989); CASI: a combination of the CMV enhancer, chicken β-actin promoter and ubiquitin enhancer (Balazs et al., 2013); EGFP: enhanced fluorescent green protein; EGFPLux: EGFP fused to firefly luciferase (cDNA obtained from pEGFP-Luc, Promega); hCEF: a combination of synthetic, CpG-free human CMV enhancer and synthetic, CpG-free human elongation factor 1 α promoter (Hyde et al., 2008); hCEFI: hCEF with a synthetic, CpG-free intron; CMV: cytomegalovirus enhancer/promoter (Boshart et al., 1985); hGH: signal sequence from human growth hormone (Balazs et al., 2013); NS3: non-structural protein 3 from hepatitis C virus; rAAV: recombinant adeno-associated virus; SIV: simian immunodeficiency virus (Fukasawa et al., 1988); soGLux: codon-optimised CpG-depleted *Gaussia* luciferase (Griesenbach et al., 2011); SMASh: small molecule-assisted shutoff tag (Figure 5.1); TNFR2: signal sequence from tumour necrosis factor receptor 2 (Osslund, 2003).

2.3.2 Molecular cloning techniques

2.3.2.1 Polymerase chain reaction

Amplification of plasmid sequences was performed by preparing individual reactions containing ~100 ng/µl of the pDNA template, Phusion Buffer (Thermo Fisher Scientific), 10 mM dNTPs (NEB, Hitchin, UK), 10 µM forward primer, 10 µM reverse primer, 2 units of Phusion Hot Start II DNA polymerase (Thermo Fisher Scientific) and nuclease-free water to a total volume of 50 µl. The components were added to thin-walled 0.2 ml tubes (Corning), briefly centrifuged and placed in a GeneAmp PCR system 2700 thermal cycler (Thermo Fisher Scientific). Cycling conditions were: 5 minutes at 98°C, followed by 30 1-minute cycles at 98°C, varying annealing temperatures based on optimal annealing temperature calculated by MacVector software v15 (MacVector, Cary, NC, USA) for 1 minute, and 2 minutes at 72°C, with a final extension step of 72°C for 7 minutes.

2.3.2.2 Gel electrophoresis

DNA was size-fractionated by agarose gel electrophoresis. Gels typically consisted of 0.7% agarose (Thermo Fisher Scientific) in Tris-acetate-EDTA (TAE) buffer (40 mM Tris(hydroxylmethyl)aminomethane (Tris)-acetate and 1 mM ethylenediaminetetraacetic acid (EDTA), pH 8.3). Agarose was heated in a microwave oven for approximately 2 minutes to dissolve and allowed to cool before adding SYBR Safe DNA Gel stain (Thermo Fisher Scientific; 7 µl per 100 ml) and pouring into a mould. Prior to electrophoresis, DNA samples were mixed with Gel Loading Dye (NEB) in a final volume of 5 to 30 µl, then electrophoresed at 10-15

V/cm until sufficiently resolved (typically 1 to 2 hours). To allow DNA fragment size estimation, 10 µl of 100 bp DNA ladder, 1 kb DNA ladder or supercoiled DNA ladder (NEB) were included on each gel. Following electrophoresis, DNA bands were visualised under UV light (312 nm wavelength) using GeneFlash Gel Documentation System (Syngene, Cambridge, UK).

2.3.2.3 Restriction enzyme digestion

All restriction enzyme digests were performed using enzymes purchased from NEB, according to the manufacturer's instructions. Typically, a 20-30 µl reaction volume containing between 500 ng and 5 µg pDNA was incubated for 1-2.5 hours at the temperature recommended by the supplier.

2.3.2.4 Gel extraction and purification of DNA fragments

Typically, 30 µl of restriction enzyme digestion reaction (Section 2.3.2.4) containing 5 µg of DNA was electrophoresed as described in Section 2.3.2.2. Bands were visualised with long-wavelength UV light (366 nm), using a UVL-56 hand-held gel illuminator (UVP Inc., CA, USA). The QIAquick Gel Extraction Kit (Qiagen, Hilden, Germany) was used for fragment purification according to the manufacturer's instructions. The purified DNA fragments were eluted into 30 µl nuclease-free water and stored at -20°C.

2.3.2.5 Ligation of DNA fragments

Purified DNA fragments were ligated using T4 DNA ligase and associated buffers (NEB) according to manufacturer's instructions. Generally, 1 µl of T4 DNA ligase (400 U) was mixed with ~100 ng vector DNA and ~700 ng insert DNA in a final volume of 10 µl and incubated for 1-2 hours at 18°C. The ligated samples were stored at -20°C if not used immediately for bacterial transformation.

2.3.2.6 Quantification of DNA in solution

DNA concentration was measured spectrophotometrically using a NanoDrop Spectrophotometer 2000 (Thermo Fisher Scientific), using the relationship between the absorption of UV light by DNA at 260 nm and the DNA concentration, with an optical density at 260 nm (OD_{260}) of 1.0 for a 50 µg/ml solution of double-stranded DNA. Each 2 µl sample was read in duplicate or triplicate, and the average was used to determine the final concentration. The purity of the preparation was measured by calculation of the OD_{260}/OD_{280} ratio, with values of <1.8 indicating protein contamination.

2.3.3 Amplification of plasmid DNA in bacterial culture

2.3.3.1 Preparation of selective Luria Bertani broth and plates

Luria Bertani (LB) broth was prepared using 1% Tryptone (Ameresco, Solon, OH, US), 1% NaCl (Sigma-Aldrich) and 0.5% granulated yeast extract (Merck) in Milli-Q water. LB agar was prepared by addition of 1.5% of Select Agar (Thermo Fisher

Scientific) to LB broth. Both LB broth and LB agar solutions were sterilised by autoclaving (Section 2.1). Kanamycin or ampicillin (Sigma-Aldrich), which had been sterilised by filtering (Section 2.1) and stored at 4ºC, were added to a final concentration of 50 µg/ml or 100 µg/ml, respectively, before use. For preparation of LB agar plates, LB agar was microwaved until molten and allowed to cool to 50ºC in a water bath. Approximately 25 ml of the molten agar was poured into 9 cm petri dishes (Sterilin, Newport, UK), allowed to set and stored at 4ºC. Before use, the plates were dried for at least 1 hour at 42ºC.

2.3.3.2 Bacterial transformation of plasmid DNA

All pDNA constructs were grown in *Escherichia coli* One Shot Stbl3, TOP10 (Thermo Fisher Scientific) or GT115 (InvivoGen, Toulouse, France) chemically competent cells. Cells were transformed according to the manufacturer's instructions. At least two dilutions of transformed cells were spread on LB agar plates (Section 2.3.3.1) containing the appropriate antibiotic and incubated for 12-16 hours at 37ºC. Single colonies were isolated for amplification.

2.3.3.3 Bacterial inoculation of growth media

A single transformed *E. coli* colony, grown overnight on selective LB agar plates (Section 2.3.3.2), was inoculated into either 5 ml or 400 ml LB broth (Section 2.3.3.1) containing 50 µg/ml kanamycin or 100 µg/ml ampicillin. Cultures were incubated overnight at 37ºC in an orbital shaking incubator with a diameter of 2.54 cm (Innova 4300, New Brunswick Scientific, Edison, NJ, USA) rotating at 175 rpm.

2.3.3.4 Extraction and purification of plasmid DNA from bacterial culture

Plasmid DNA from 5 ml cultures (Section 2.3.3.3) was purified using the Wizard Plus SV MiniPrep DNA Purification System (Promega), according to manufacturer's instructions. The DNA was eluted in 100 µl nuclease-free water and stored at -20 ºC. Large-scale preparations of plasmid DNA (yielding approximately 1-2 mg) were purified from 400 ml cultures using the EndoFree Plasmid Mega Kit (Qiagen) according to manufacturer's instructions. Final plasmid DNA pellets were typically resuspended in 500 µl of WFI and stored at -20ºC.

2.3.4 Construction of tandem minimal hC enhancer-containing plasmids

The plasmids pG6.3x93.soLux and pG6.4x93.soLux (Table 2.1), containing triple and quadruple 93 bp minimal enhancers, respectively, were constructed for and used in studies in Chapter 3 (Section 3.2.1). For construction of these plasmids, the fragment for insertion was generated by PCR amplification (Section 2.3.2.1) of the 93 bp minimal enhancer region, with addition of a *Bam*HI restriction site using the reverse primer. The PCR product was sub-cloned using the Zero Blunt TOPO PCR Cloning Kit (Thermo Fisher Scientific) according to the manufacturer's instructions. The resulting intermediate plasmid was digested with *Bam*HI and *Eco*RV restriction endonucleases (Section 2.3.2.3), subjected to agarose gel electrophoresis (Section 2.3.2.2) and the desired insert extracted (Section 2.3.2.4). For construction of pG6.3x93.soLux, the backbone was prepared by digestion of pG6.2x93.soLux (Table 2.1) with *Eco*RV and *Bgl*II (the overhang generated by this enzyme is compatible with that of *Bam*HI) (Section 2.3.2.3). The insert and backbone were ligated (Section 2.3.2.5) and used to transform *E. coli* GT115 cells

(Section 2.3.3.2). Several colonies were used to inoculate small scale cultures (5 ml; Section 2.3.3.3), from which pDNA was purified (Section 2.3.3.4). Prior to large-scale (400 ml; Section 2.3.3.3) endotoxin-free plasmid production (Section 2.3.3.4), the identity of the pDNA construct was confirmed by restriction enzyme digests (Section 2.3.2.3) followed by gel electrophoresis (Section 2.3.2.2). For construction of pG6.4x93.soLux (Table 2.1), the insert generated previously was ligated to the backbone produced by digestion of pG6.3x93.soLux (Table 2.1) with *Bgl*II and *Hind*III. The resulting plasmid was then amplified as described above.

2.3.5 Construction of rSIV and rAAV genome plasmids encoding palivizumab and infliximab

The single-ORF cDNAs of palivizumab (Section 4.2.1) and infliximab (Section 5.2.1) were extracted from the plasmids supplied by GeneArt (Thermo Fisher Scientific) by digestion with *Nhe*I and *Psp*OMI restriction endonucleases (Section 2.3.2.3) and purified (Section 2.3.2.4). The rSIV and rAAV genome plasmid backbones were prepared by digestion of pSIV.hCEF.soGLux and pAAV2.CASI.soGLux, respectively (Table 2.1), with *Nhe*I and *Psp*OMI (Section 2.3.2.3), followed by gel electrophoresis to size-fractionate the fragments (Section 2.3.2.2) and subsequent extraction and purification from the gel (Section 2.3.3.4). Palivizumab-containing insert was ligated to rSIV and rAAV plasmid backbones (Section 2.3.2.5) and used to transform *E. coli* Stbl3 cells (Section 2.3.3.2). Colonies formed by the transformed bacteria were used to inoculate small scale cultures (5 ml; Section 2.3.3.3), from which pDNA was purified (Section 2.3.3.4). Prior to large-scale (400 ml; Section 2.3.3.3) endotoxin-free plasmid production

(Section 2.3.3.4), the identity of the pDNA construct was confirmed by restriction enzyme digests (Section 2.3.2.3) followed by gel electrophoresis (Section 2.3.2.2). The resulting plasmids were termed pSIV.hCEF.palivizumab and pAAV2.CASI.palivizumab (Table 2.1). Infliximab-containing insert was ligated with rAAV genome plasmid backbone to generate pAAV.CASI.infliximab (Table 2.1), which was amplified as described above.

2.3.6 Construction of rAAV genome plasmids encoding etanercept

A construct containing TNFR2 signal sequence and hGH-etanercept cDNA was synthesised by GeneArt (Thermo Fisher Scientific). The hGH-etanercept cDNA was removed from the supplied plasmid by digestion with *Nhe*I and *Psp*OMI restriction endonucleases (Section 2.3.2.3) and purified (Section 2.3.3.4). The rAAV plasmid backbone was prepared by digestion of pAAV2.CASI.soGLux (Table 2.1) with *Nhe*I and *Psp*OMI (Section 2.3.2.3), followed by gel electrophoresis to size-fractionate the fragments (Section 2.3.2.2) and subsequent extraction and purification from the gel (Section 2.3.3.4). Etanercept-containing insert was ligated to the obtained rAAV plasmid backbone (Section 2.3.2.5) and used to transform *E. coli* Stbl3 cells (Section 2.3.3.2). Colonies formed by the transformed bacteria were used to inoculate small scale cultures (5 ml; Section 2.3.3.3), from which pDNA was purified (Section 2.3.3.4). Prior to large-scale (400 ml; Section 2.3.3.3) endotoxin-free plasmid production (Section 2.3.3.4), the identity of the pDNA construct was confirmed by restriction enzyme digests (Section 2.3.2.3) followed by gel electrophoresis (Section 2.3.2.2). The resulting plasmid was termed

pAAV2.CASI.hGH-etanercept (Table 2.1). The insert containing the TNFR2 signal sequence was released from the plasmid supplied by GeneArt by digestion with *Afe*I and *Sph*I restriction endonucleases (Section 2.3.2.3) and purified (Section 2.3.2.4). The backbone was generated by digestion of pAAV2.CASI.hGH-etanercept with the same enzymes, ligated with the insert (Section 2.3.2.5) and the resulting plasmid pAAV2.CASI.TNFR2-etanercept (Table 2.1) was amplified as described above.

2.3.7 Construction of plasmids containing SMASh tag and NS3 protease

Incorporation of SMASh sequence into cDNA was achieved using a seamless cloning strategy involving *Fau*I, a restriction endonuclease which recognises an asymmetric DNA sequence and cleaves outside of its recognition sequence (Ian Pringle, personal communication), and a SMASh "acceptor" plasmid pG6.hCEF.SMASh (Table 2.1; gift of Ian Pringle). The GLux and etanercept-containing fragments for insertion were generated by PCR amplification (Section 2.3.2.1) of the desired sequence. The reverse primer for the reaction was designed such that it would omit the STOP codon at the end of the cDNA and instead incorporate a *Fau*I recognition site. The PCR product was sub-cloned using the Zero Blunt TOPO PCR Cloning Kit (Thermo Fisher Scientific) according to the manufacturer's instructions. The resulting intermediate plasmid was digested with *Nhe*I and *Fau*I restriction endonucleases (Section 2.3.2.3), subjected to agarose gel electrophoresis (Section 2.3.2.2) and the desired insert extracted (Section 2.3.3.4). The extracted fragment was then ligated (Section 2.3.2.5) with the backbone, which was generated by digestion of pG6.hCEFI.SMASh (Table 2.1)

with *Nhe*I and *Fau*I (Section 2.3.2.3), and the resulting plasmid used to transform *E. coli* GT115 cells (Section 2.3.3.2). Colonies formed by the transformed bacteria were used to inoculate small scale cultures (5 ml; Section 2.3.3.3), from which pDNA was purified (Section 2.3.3.4). Prior to large-scale (400 ml; Section 2.3.3.3) endotoxin-free plasmid production (Section 2.3.3.4), the identity of the pDNA construct was confirmed by restriction enzyme digests (Section 2.3.2.3) followed by gel electrophoresis (Section 2.3.2.2). The resulting plasmids were termed pG6.hCEFI.soGLux-SMASh and pG6.hCEFI.etanercept-SMASh (Table 2.1).

To generate plasmid pG6.hCEFI.etanercept-NS3 (Table 2.1), encoding etanercept fused to NS3 protease (Section 5.2.3), the etanercept-containing fragment for insertion was generated by PCR amplification (Section 2.3.2.1) of the desired sequence. The reverse primer for the reaction was designed such that it would introduce a STOP codon immediately after the NS3 protease sequence (Figure 5.12), and a *Psp*OMI recognition sequence. The PCR product was sub-cloned using the Zero Blunt TOPO PCR Cloning Kit (Thermo Fisher Scientific) according to the manufacturer's instructions. The resulting intermediate plasmid was digested with *Nhe*I and *Psp*OMI restriction endonucleases (Section 2.3.2.3), subjected to agarose gel electrophoresis (Section 2.3.2.2) and the desired insert extracted (Section 2.3.3.4). The extracted fragment was then ligated (Section 2.3.2.5) with the backbone, which was generated by digestion of pG6.hCEFI.etanercept-SMASh (Table 2.1) (Section 2.3.2.3), and the resulting plasmid used to transform *E. coli* GT115 cells (Section 2.3.3.2). Colonies formed by the transformed bacteria were used to inoculate small scale cultures (5 ml; Section 2.3.3.3), from which pDNA was purified (Section 2.3.3.4). Prior to large-scale (400 ml; Section 2.3.3.3) endotoxin-free plasmid production (Section 2.3.3.4), the identity of the pDNA

construct was confirmed by restriction enzyme digests (Section 2.3.2.3) followed by gel electrophoresis (Section 2.3.2.2). The resulting plasmid was termed pG6.hCEFI.etanercept-NS3 (Table 2.1).

2.4 Cell culture

2.4.1 Cells and culture conditions

Adherent human embryonic kidney 293T (HEK293T) cells (Graham et al., 1977) were used for plasmid transfections (Section 2.4.2), rAAV vector production (Section 2.5.4) and rSIV and rAAV transduction. Cells of the human epithelial type 2 (HEp-2) line (ATCC; Moore et al., 1955) were used for RSV plaque reduction assay (Section 2.4.4). Cells of the Madin-Darby Canine Kidney (MDCK) line overexpressing human alpha-2,6 sialic acid via stable transfection with the cDNA of human alpha2,6-sialytransferase 1 (SIAT1) (Matrosovich et al., 2003) were used for transfections with SMASh-encoding plasmids (Section 5.2.3). All of the above cells were maintained in Dulbecco's Modified Eagle's Medium (DMEM) (Life Technologies) supplemented with 10% foetal bovine serum (FBS; Sigma-Aldrich), 100 U/ml of penicillin and 100 mg/ml of streptomycin (Sigma-Aldrich) and 2 mM L-glutamine (Sigma-Aldrich), in a 5% CO_2 humidified incubator at 37ºC.

HEK293T cells previously adapted to suspension growth using sequential serum reduction (gift of Lee Davies) were used for lentiviral vector production (Section 2.5.2), while HEK293F cells (Thermo Fisher Scientific) were used for lentiviral vector titration (Section 2.5.3). They were maintained in an 8% CO_2 humidified

agitating incubator (135 rpm) (Thermo Fisher Scientific) at 37ºC in FreeStyle 293 Expression medium (Thermo Fisher Scientific) without serum or antibiotics.

2.4.2 Transient transfection of cultured cells with plasmid DNA

Adherent HEK293T cells were seeded in six- or 12-well plates at 10^6 or 5 x 10^5 cells per well, respectively. MDCK cells were seeded in 12-well plates at 2 x 10^4 cells per well. Twenty-four hours after seeding, cells were transfected with the appropriate plasmid using Lipofectamine 2000 (Thermo Fisher Scientific). For six-well plates, 1.6 µg of DNA and 4 µl of Lipofectamine 2000 were complexed in a total volume of 500 µl per well. For 12-well plates, 4 µg of DNA and 10 µl of Lipofectamine 2000 were complexed in a total volume of 200 µl per well.

2.4.3 Preparation of cell lysates for luciferase assay

Cell growth medium was aspirated and the cell monolayer rinsed twice in ice-cold PBS. Cells were lysed by 15-minute incubation with Reporter Lysis Buffer (RLB; Promega). The lysate was scraped from the well, transferred to a 1.7 ml microcentrifuge tube (Corning) and frozen at -80°C for ≥15 minutes. After thawing, the lysate was centrifuged at 13,000 rcf for 20 minutes to pellet cell debris. The cleared supernatant was used for measurement of luciferase activity (Section 2.7.2) and protein content (Section 2.7.1), or stored at -80°C.

2.4.4 Plaque reduction assay

Plaque reduction assay was used to assess the RSV-neutralising capacity of palivizumab-containing serum and BALF. Flat-bottomed 96-well plates (Corning) were seeded with HEp-2 cells at 2.5 x 10^4 cells/well and incubated for approximately 24 hours until confluent. When the cell monolayers were ready, various dilutions of mouse serum and BALF samples (Sections 2.6.6.1 and 2.6.6.2) were prepared. Serially diluted samples were mixed with an equal volume of RSV, previously diluted to give 200 focus-forming units (ffu) per 25 µl. The sample/virus mixtures were incubated at 37°C and 5% CO_2 for 1 hour. Media was then aspirated from the previously seeded cells, which were subsequently washed with PBS. A 50 µl volume of the sample/virus mixture was added per well in duplicate and incubated at 37°C and 5% CO_2 for 2 hours. Then, 150 µl of pyruvate-free DMEM with 2% FBS were added to each well and the plate was further incubated for 16-20 hours. Media was then aspirated and the cells were fixed in methanol with 2% hydrogen peroxide for 20 minutes at RT. Cells were then washed with 1% bovine serum albumin (BSA) in PBS (PBS/BSA) and 100 µl of biotinylated anti-RSV antibody (AbD serotec, Kidlington, UK), diluted 1:500 in PBS/BSA, was added to each well and incubated for 1 hour at RT. After washing twice with PBS/BSA, 100 µl of ExtrAvidin-peroxidase, diluted 1:500 in PBS/BSA (Sigma-Aldrich), was added per well and incubated for 30 min in the dark at RT. Cells were then washed three times with PBS/BSA and 50 µl of 3,3'-diaminobenzidine (DAB) substrate was applied (Sigma-Aldrich). The plate was incubated in the dark until the plaques acquired the desired colouration (5-10 minutes). The reaction was stopped by washing the plate with PBS and the number of immunoplaques in each well was quantified by manual counting under a light microscope.

2.5 Viral vector production

2.5.1 Viral vectors used in this study

The viral vectors used in this study are summarised in Table 2.2.

2.5.2 Lentiviral vector production

Lentiviral vector production was performed by Ian Pringle, Lee Davies, Steve Hyde and Rachel Ashworth. Recombinant SIV vectors were produced by transient transfection of suspension-cultured HEK293T cells, according to previously established conditions (Steve Hyde, personal communication) using a mixture of five producer plasmids at a total of 0.33 µg pDNA per 10^6 cells using PEIpro (Polyplus-transfection, Illkirch, France) at a volume:mass ratio of 2:1. Recombinant SIV-based lentiviral vectors were produced using the respective genome plasmid and four accessory plasmids (Table 2.1) at a mass ratio of genome plasmid: pCMV.SIV.GagPol: pRSV.Rev: pCAG.SeV.Fct4: pCAG.SeV.EnvctHN of 20:9:6:6:6.

Table 2.2. Viral gene transfer vectors used in this study.

Vector	Pseudotype/serotype	Promoter	Transgene	Genome plasmid	Source	Laboratory reference
rSIV vectors						
rSIV.F/HN hCEF soGLux	F/HN	hCEF	soGLux	pSIV.hCEF.soGLux (pGM352)	Gift of Ian Pringle	vGM124
rSIV.F/HN hCEF EGFP	F/HN	hCEF	EGFP	pSIV.hCEF.EGFP (pGM357)	Gift of Ian Pringle	vGM107
rSIV.F/HN hCEF palivizumab	F/HN	hCEF	palivizumab	pSIV.hCEF.palivizumab (pGM463)	This study	vGM160
rAAV vectors						
rAAV2/8 CASI soGLux	8	CASI	soGLux	pAAV2.CASI.soGLux (pGM453)	Gift of Jack Tan	-
rAAV2/8 CASI EGFPLux	8	CASI	EGFPLux	pAAV2.CASI.EGFPLux (pGM452)	Gift of Jack Tan	-
rAAV2/9 hCEFI soGLux	9	hCEFI	soGLux	pAAV2.hCEFI.soGLux (pGM495)	Gift of Jack Tan	-

rAAV2/9 CASI soGLux	9	CASI	soGLux	pAAV2.CASI.soGLux (pGM453)	This study	-
rAAV2/8 CASI palivizumab	8	CASI	palivizumab	pAAV2.CASI.palivizumab (pGM459)	This study	-
rAAV2/8 CASI infliximab	8	CASI	infliximab	pAAV2.CASI.infliximab (pGM458)	This study	-
rAAV2/8 CASI hGH-etanercept	8	CASI	etanercept with SS from hGH	pAAV2.CASI.hGH-etanercept (pGM521)	This study	-
rAAV2/8 CASI TNFR2-etanercept	8	CASI	etanercept with SS from TNFR2	pAAV2.CASI.TNFR2-etanercept (pGM537)	This study	-

CASI: a combination of the CMV enhancer, chicken β-actin promoter and ubiquitin enhancer (Balazs et al., 2013); EGFP – enhanced fluorescent green protein; EGFPLux: EGFP fused to firefly luciferase (cDNA obtained from pEGFP-Luc, Promega); F/HN: modified forms of fusion (F) and haemagglutinin-neuraminidase (HN) glycoproteins from Sendai virus (Kobayashi et al., 2003); hCEF: a combination of synthetic, CpG-free human CMV enhancer and synthetic, CpG-free human elongation factor 1 α promoter (Hyde et al., 2008); hCEFI: hCEF with synthetic, CpG-free intron; hGH: signal sequence from human growth hormone (Balazs et al., 2013); TNFR2: signal sequence from tumour necrosis factor receptor 2 (Osslund, 2003); SIV: simian immunodeficiency virus (Fukasawa et al., 1988); soGLux: codon-optimised, CpG-depleted *Gaussia* luciferase (Griesenbach et al., 2011); SS: signal sequence.

The HEK293T cells were cultured in single-use 10 l (5 l working volume) WAVE Cellbag bioreactors (GE Healthcare, Amersham, UK) mounted on a WAVE 20/50 rocking platform (GE Healthcare). The Cellbag was inflated with 5% CO_2, primed with 2 l FreeStyle 293 Expression medium (Thermo Fisher Scientific) containing 2.5 ml/l 10% Pluronic F-68 (Thermo Fisher Scientific), seeded with HEK293T cells to 8 x 10^5 cells/ml and incubated at 37°C, rocking at 20 rpm at an 8° rocking angle for 48 hours. pH of the growth media was automatically maintained via a WAVEPODII controller (GE Healthcare) at 7.2 by controlling the concentration of CO_2 in the headspace and/or injection of 7% sodium bicarbonate (Sigma-Aldrich). Cells were transfected using PEIpro (Polyplus-transfection) complexed with the appropriate five-plasmid mixture described above, with the required amount of transfection mix determined by the number of cells present in the Cellbag at the time of transfection. At approximately 18 hours after transfection, 3 l of media, 7.5 ml of 10% Pluronic F-68 (Thermo Fisher Scientific) and sodium butyrate (Sigma-Aldrich) to a final concentration of 5 mM were added.

Cells were also supplemented with 5 ml/l of 45% glucose (Sigma-Aldrich) immediately prior to and 48 hours after transfection. Two separate additions of benzonase (5 U/l) (Merck) were performed to reduce nucleic acid contaminant burden: 48 hours post-transfection and again 1 hour before harvest. Magnesium chloride was added to 1 mM final concentration 1 hour before harvest. At 72 hours after transfection, the cell supernatant was filtered through a series of filters comprising GE Ultra 5 µm filter (GE Healthcare) and AcroPak 0.8/0.45 µm filter (Pall, Portsmouth, UK). The filtrate was stored at -80°C.

The filtered supernatant was thawed and the Sendai F protein activated by incubation (30 min, 37ºC) with 0.05x TrypLEselect recombinant trypsin analogue (Thermo Fisher Scientific). Activated vector was then cooled to 4ºC and concentrated/purified using a combination of anion exchange chromatography (AEX) and tangential flow filtration (TFF). Initial virus capture was performed using an AKTA Pure 150L chromatography station (GE Healthcare) in conjunction with 5 ml Mustang Q XT5 quaternary ammonium AEX membrane (Pall). Viral supernatant was loaded onto the membrane at a flow rate of 25 ml/min, washed with low-salt buffer (150 mM NaCl, 25 mM HEPES, pH 7.5) and eluted in high salt buffer (1 M NaCl, 25 mM HEPES, pH 7.5). Vector-containing fractions were identified by UV absorbance peaks, diluted to a final volume of 100 ml in media and kept at 4ºC to maintain vector viability. Isolated vector was then concentrated and purified via TFF using a KRIIi TFF system (Spectrum Europe, Breda, The Netherlands). Initially, 100 ml of vector was concentrated via ultrafiltration to 10 ml using a C02-E500-05N MicroKros TFF module (Spectrum Europe) consisting of a 20 cm^2 surface area modified polyethylsulfone membrane with a 500 kDa molecular weight cut-off. Concentrated virus was then diafiltered against 10 diavolumes (100 ml) of Freestyle 293 Expression media (Thermo Fisher Scientific) or TSSM buffer (20 mM tromethamine, 100 mM NaCl, 10 mg/ml sucrose, 10 mg/ml mannitol) before a final ultrafiltration volume reduction step yielding approximately 5 ml of final viral product. Purified vector was divided into 100 µl aliquots and stored at -80ºC.

2.5.3 Determination of lentiviral vector titre

Lentiviral vector quantification was performed with the assistance of Ian Pringle and Eoin Mac Réamoinn. The titre of lentiviral vectors was determined by qPCR using the Applied Biosystems 7900HT Fast Real-Time PCR system (Thermo Fisher Scientific) based on the genomic integration of WPRE DNA sequence. HEK293F suspension cells were transduced with dilutions of purified lentiviral vectors in the presence of 8 µg/ml of polybrene (Sigma-Aldrich). Cells were incubated for 72 hours before genomic DNA was extracted using the QIAamp DNA Mini kit (Qiagen). The integrated WPRE DNA was quantified against a standard curve of DNA mimics containing the WPRE sequence (gift of Stephanie Sumner-Jones) using the following primers: forward: TGGCGTGGTGTGCACTGT; reverse: CCCGGAAAGGAGCTGACA; probe: FAM-TTGCTGACGCAACCCCCACTGG-TAMRA in triplicate using TaqMan FAST Universal PCR Master Mix (Thermo Fisher Scientific), normalised against total DNA determined using Nanodrop (Section 2.3.2.6). The PCR profile used was as following: 50ºC for 2 minutes, 95ºC for 10 minutes followed by 40 cycles of 95ºC for 15 s and 60ºC for 1 minute. "TaqMan transducing units" per ml of vector preparation (TTU/ml) were determined from the slope of a linear regression line generated from the dilution series using Prism software v7.0 for Mac (GraphPad Software, La Jolla, CA, USA).

2.5.4 Production of recombinant adeno-associated viral vector

The production of rAAV was performed as previously described (de Silva et al., 2015). Briefly, 3.4 x 10^8 HEK293T cells were seeded in a 175 cm^2 tissue culture

flask (Corning). After 72 hours, the flask was used to seed one 1,720 cm^2 surface area HYPERFlask (Corning); between two and four HYPERFlasks were used for each rAAV preparation. The cells were transfected with 500 µg of the genome plasmid, pAdDeltaF6 and pAAV2/8 or pAAV2/9 (Table 2.1; calculation of plasmid ratio is described in Table 2.3) using 25 kDa linear PEI (Polysciences Inc, Hirschberg an der Bergstrasse, Germany) in reduced-serum media (4.5 g/l glucose, 2 mM L-glutamine, 2% FBS, 100 U/ml penicillin and 100 µg/ml streptomycin). After 72 hours, cells were pelleted by centrifugation at 1,400 rcf for 10 minutes. Individual cell pellets were resuspended in 15 ml lysis buffer (1 M Tris(hydroxymethyl)aminomethane, 150 mM NaCl). EDTA-free cOmplete Mini protease inhibitor cocktail (Roche, Welwyn Garden City, UK) was added to the manufacturer's recommended final concentration. The resuspended pellets were then subjected to four freeze-thaw cycles (freeze for 1 hour at -80˚C and thaw at 37˚C for 15 minutes). Benzonase (Merck) was added to the cell lysates for a final concentration of 50 U/ml followed by a 45-minute incubation at 37˚C. The lysates were then centrifuged at 3,700 rcf for 20 minutes to pellet cell debris.

Vector was purified by iodixanol gradient ultracentrifugation. Iodixanol step-gradient solutions were prepared according to the recipe in Table 2.4 with 60% iodixanol (OptiPrep, Sigma-Aldrich), 5 x PBS-MK (5 x PBS, 12.5 mM $MgCl_2$, 12.5 mM KCl), 5 M NaCl, Milli-Q water and 0.5% phenol red (Sigma-Aldrich). The 15%, 25%, 40% and 60% iodixanol solutions were layered in 32.4 ml OptiSeal tubes (Beckman Coulter) using a Pasteur pipette (Appleton Woods Ltd, Birmingham, UK). First, 7.2 ml of 15% was pipetted directly into the bottom of the tube, followed by laying of 4.8 ml of 25% iodixanol fraction below the 15% fraction, 4 ml of 40% below the 25% fraction and finally 4 ml of 60% below the 40% fraction. The

benzonase-treated and cleared cell lysate was then layered on top of the 15% fraction by drop-wise application. The gradients were centrifuged at 59,000 rpm (256,146 rcf) for 1.5 hours in the Optima XPN-80 Ultracentrifuge (Beckman Coulter) with the 70Ti rotor (Beckman Coulter). Following centrifugation, the tube was punctured at the junction between the 40% and 60% iodixanol fractions using an 18G needle (Becton Dickinson, Plymouth, UK). The 40% fraction was collected using a 5 ml syringe (Becton Dickinson) and subsequently concentrated and dialysed into PBS using Amicon Ultra-15 100K MWCO centrifugal devices (Merck). Purified vector was divided into 40 µl aliquots and stored at -80ºC.

2.5.5 Determination of recombinant adeno-associated viral vector titre

The number of DNase-resistant genome copies per ml (DRGC/ml) was determined by qPCR using the Applied Biosystems 7900HT Fast Real-Time PCR system (Thermo Fisher Scientific). Purified rAAV was diluted 1:10 in Milli-Q water and treated with 2 U of DNAse I (Thermo Fisher Scientific) in a final volume of 10 µl for 20 minutes at 37°C to remove any residual pDNA or unpackaged viral DNA. Samples were then incubated at 100°C for 10 minutes to denature the viral capsids and release the genome. Various dilutions were prepared and the viral DNA was quantified in triplicate using TaqMan Fast Universal PCR Master Mix (Thermo Fisher Scientific) against a standard curve of DNA mimics containing the WPRE sequence (gift of Stephanie Sumner-Jones). The primers used were as follows: forward: TGGCGTGGTGTGCACTGT; reverse: CCCGGAAAGGAGCTGACA; probe: FAM-TTGCTGACGCAACCCCCACTGG-TAMRA. The qPCR was

performed according to the following conditions: 50°C for 2 minutes followed by 40 cycles of 95°C for 10 s and 60°C for 1 minute.

2.6 Animal studies

2.6.1 Mouse strains

Specific pathogen-free female BALB/c mice were purchased from Envigo (Bicester, UK) and were used for all experiments.

2.6.2 General conditions

All procedures involving laboratory mice were carried out under United Kingdom Home Office-approved project and personal licenses for performing experiments on animals under the terms of the Animals (Scientific Procedures) Act 1986. Mice were housed in accordance with the United Kingdom Home Office ethical and welfare guidelines and fed on standard chow and water *ad libitum.* All mice were aged 5-9 weeks at point of procedure initiation and had been allowed to acclimatise for at least seven days prior to procedures being performed. Euthanasia of animals was performed by cervical dislocation or intraperitoneal injection of 100 µl pentobarbitone (Centaur, Somerset, UK).

Table 2.3. Ratio of plasmids for rAAV production.

Plasmid	Size (kb)	Amount per transfection (µg)
pAdDeltaF6	15.4	15.4 x **R**
pAAV2/x	7.3	7.3 x **R**
pTransgene	T	T x **R**
Total	K	500 µg
Ratio (**R**) mass/kb	500/K	

rAAV: recombinant adeno-associated virus; pAdDeltaF6: helper plasmid containing the *E2a*, *E4*, and *VARNA* genes from adenovirus; pAAV2/8: plasmid containing the *Rep* gene from AAV serotype 2 and *Cap* gene from AAV serotype 8; pTransgene: rAAV genome plasmid, containing transgene flanked by AAV ITRs.

Table 2.4. Iodixanol solutions required for four gradients.

Step	60% iodixanol	5 M NaCl	5 x PBS-MK	H_2O	Phenol red
15%	8 ml	6.4 ml	6.4 ml	11.2 ml	-
25%	10 ml	-	4.8 ml	9.2 ml	40 µl
40%	13.4 ml	-	4 ml	2.6 ml	-
60%	20 ml	-	-	-	40 µl

2.6.3 Mouse anaesthesia

For nasal instillation (Section 2.6.5.1), intramuscular injection (Section 2.6.5.3) and *in vivo* bioluminescence imaging (Section 2.6.8), anaesthesia was induced using inhalation of 3-4.5% isoflurane (Abbott, Maidenhead, UK) and maintained with 2.5-3% isoflurane. Depth of anaesthesia was continuously monitored by observing the animal's breathing rate and testing reflex responses to the foot pad pinch.

2.6.4 Preparation of polyplexes and lipoplexes

2.6.4.1 Preparation of PEI polyplexes for aerosolisation

The PEI polyplexes were prepared for aerosolisation as previously described (Davies et al., 2008). A volume of 10 ml polyplex was formed at a PEI nitrogen:DNA phosphate (N:P) molar ratio of 1:10. Plasmid DNA was diluted to a concentration of 0.4 mg/ml in WFI and 25 kDa branched PEI (Sigma-Aldrich) was prepared at a concentration of 4.3 mg/ml in sterile water at pH 7.4 and filtered through a 0.22 μm filter. Polyplexes were prepared by mixing 5 ml pDNA solution with 5 ml PEI solution using continuous vortexing. Complexes were allowed to form for 20 minutes to 1 hour at RT. Approximately 10 ml of the final mixture containing 2 mg pDNA was aerosolised (Section 2.6.5.2).

2.6.4.2 Preparation of GL67A lipoplexes for instillation

Liposomes were generated by hydrating a vial of GL67A (Eastman et al., 1997) (1:2:0.05 molar ratio of GL67:DOPE:DMPE-PEG5000) (OctoPlus, Leiden,

Netherlands) to 1.2 mM with WFI and mixing until dissolved. The liposome solution was subsequently kept on ice for a maximum of 8 hours before being discarded. An 800 µl aliquot of the liposome solution was transferred to a 7 ml sterile polystyrene bijou tube (Sterilin) and incubated for 5 minutes at 30°C. A volume of 800 µl of pDNA at 1.6 mg/ml was added to the liposomes and the combined solution was incubated for a further 15 minutes at 30°C to allow complex formation. A 100 µl dose of the lipoplexes containing 80 µg pDNA, at a pDNA:GL67A mM ratio of 2.4:0.6, equivalent to a 1:0.25 ratio of lipid nitrogen (N):DNA phosphate (P), was delivered per mouse (Section 2.6.5.1).

2.6.4.3 Preparation of GL67A lipoplexes for aerosolisation

Lipoplexes for aerosolisation were prepared as previously described (Davies et al., 2010). A volume of 10 ml lipoplex was formed at a plasmid DNA:GL67A molar ratio of 8:6. Liposomes were generated by hydrating a vial containing GL67A (OctoPlus) to 12 mM with WFI and mixing until dissolved. The liposome solution was subsequently kept on ice for a maximum of 8 hours before being discarded. Plasmid DNA was diluted to a concentration of 5.28 mg/ml (16 mM). Lipoplexes were prepared by mixing 5 ml plasmid DNA solution (16 mM) with 5 ml liposome solution (12 mM). Complexes were allowed to form for 15 minutes to 1 hour at RT. Approximately 10 ml of the final mixture containing 25 mg plasmid DNA was aerosolised (Section 2.6.5.2).

2.6.5 Administration of substances

2.6.5.1 Nasal instillation

Nasal instillation was used to deliver GL67A lipoplexes (Section 2.6.4.2), D-luciferin (Section 2.6.8) and RSV to the mouse lung. Animals were anaesthetised (Section 2.6.3) and administered the appropriate dose of the substance diluted to a total volume of 100 µl by nasal sniffing as previously described (Xenariou et al., 2007). In brief, the anaesthetised mouse was held vertically and a continuous droplet was maintained during topical application of the substance to the nose.

2.6.5.2 Aerosol inhalation

Aerosol delivery of polyplexes (Section 2.6.4.1) and lipoplexes (Section 2.6.4.3) was performed using a continuous, unrestrained whole-body exposure system as previously described (Davies et al., 2008). Mice were placed in an 8 l Perspex chamber and exposed to aerosol, which was generated using an Aerotech II nebulizer (Biodex, Shirley, NY, USA), operating at 40 pound-force per square inch (psi).

2.6.5.3 Intramuscular injection

Animals were anaesthetised (Section 2.6.3), followed by optional fur removal from the site of injection. The appropriate dose of vector or vehicle diluted in a total volume of 40 µl was injected into the gastrocnemius or quadriceps muscle using a 500 µl insulin syringe with 29G needle (Braun, Sheffield, UK).

2.6.5.4 Intravenous injection

Lidocaine 4% cream was applied to the tails of animals 30 minutes before injection and the animals were placed at 37°C until procedure. The mice were then restrained and 100 µl of vector was injected into the tail vein using a 500 µl insulin syringe with 29G needle (Braun).

2.6.6 Collection of cells and tissues

2.6.6.1 Serum collection

Lidocaine 4% cream was applied to the tails of animals 30 minutes before blood sampling. Mice were kept at 37°C for 20 minutes before being restrained and blood was collected from the tail vein using Microvette CB 300 serum collection tubes (Sarstedt). Blood was stored overnight at 4°C and centrifuged at 10,000 rcf for 5 minutes to pellet the clot. Serum was collected and stored at -80^{o}C. Prior to use in ELISA (Section 2.7.4) and plaque reduction assay (Section 2.4.4), serum was heat-inactivated at 56°C for 30 minutes.

2.6.6.2 Broncho-alveolar lavage

Mice were euthanised and dissected to expose the trachea. A small tear was made in the trachea and a 0.75 mm cannula (Harvard Apparatus, Kent, UK) attached to a 21G needle (Becton Dickinson) was inserted. A syringe was used to infuse the lung with 1 ml BALF solution (PBS, 50 µM EDTA; 1% BSA was included except in studies involving RSV infection) and then collect the fluid by gentle aspiration.

Flushing the lung was performed three times using the same (for studies with mAbs) or fresh (for studies with GLux) BALF solution. Repeated washing with the same solution maximised concentration of mAbs and the chance of detecting them using ELISA (Section 2.7.4)

2.6.6.3 Harvest of lung tissue and preparation of lysates

Mice were euthanised by cervical dislocation and the lungs removed. The tissue was rinsed in PBS, immersed in 300 µl RLB (Promega) and placed on ice. Lungs were homogenised using Lysing Matrix D tubes (MP Biomedicals, Cambridge, UK) and processed using the FastPrep Instrument (MP Biomedicals) for 45 seconds at a speed setting of 4.0 m/s. The homogenates were subsequently frozen at -80°C for ≥15 minutes. Following thawing to RT, the homogenates were mixed by vortexing for 10 s, transferred to QIAshredder columns (Qiagen) and centrifuged at 9,300 rcf for 2 minutes. The lysates were frozen at -80°C for at least 30 minutes, then thawed to RT and centrifuged for 10 minutes at 9,300 rcf. The supernatant was transferred to a clean microcentrifuge tube and luciferase activity measured (Section 2.7.2) and total protein quantified (Section 2.7.1), or frozen at -80 °C for later analysis.

2.6.7 Total and differential BALF leukocyte quantification

Following collection of BALF (Section 2.6.6.2), the sample was centrifuged at 3,500 rcf and the supernatant removed and stored at -80°C. The resulting cell pellet was resuspended in 100 µl Ammonium-Chloride-Potassium buffer (150 mM NH_4Cl, 10

mM $KHCO_3$, 0.1 mM EDTA) to lyse red blood cells. After 2 minutes, 400 µl of DMEM was added and the samples were centrifuged at 3,500 rcf. The pellet was resuspended in 500 µl of DMEM. For total leukocyte quantification, an aliquot of the cell suspension was mixed with 0.1% trypan blue and the total number of cells manually counted using a haemocytometer. For differential leukocyte quantification, 100 µl of the cell suspension was transferred onto a glass slide (Tharmac, Waldsoms, Germany) using Cytospin III Cytocentrifuge (Thermo Fisher Scientific) and allowed to air-dry. The slides were fixed and stained using Reastain Quick-Diff Kit (Reagena, Toivala, Finland) according to the manufacturer's protocol. The slides were then visualised using a light microscope and at least 300 cells per slide were counted and differentiated into macrophages, lymphocytes and neutrophils based on their morphology.

2.6.8 *In vivo* bioluminescence imaging

Bioluminescence was measured in living mice using the IVIS100 imaging system (PerkinElmer, Waltham, United States) and the software programme Living Image v4.5 (PerkinElmer). For imaging of expression in the lung, mice were first anaesthetised (Section 2.6.3) and 100 µl of 15 mg/ml D-luciferin (Perkin Elmer) was delivered to the lungs by nasal instillation (Section 2.6.5.1). For imaging of expression in the liver and muscle, mice were injected intraperitoneally with 300 µl of 15 mg/ml D-luciferin (PerkinElmer) diluted in PBS (150 µl into each side) and then anaesthetised. Anaesthesia was maintained while the animals were visualised in the imaging system. The automated "wizard" setting was used to capture photon emission. Luciferase activity was measured by marking a

standardised area for quantification around an organ. Average luminescence in the region of interest was calculated and expressed as photons/sec/cm^2/sr.

2.6.9 Immunofluorescence studies of mouse lung sections

2.6.9.1 Preparation of formalin-fixed, paraffin embedded sections of mouse lung

Mice were euthanised and dissected to expose the trachea. A small tear was made in the trachea and a 0.75 mm cannula (Harvard Apparatus, Kent, UK) attached to a 21G (Becton Dickinson) was inserted. A 5 ml syringe (Becton Dickinson) was used to infuse the lung with 4% paraformaldehyde (PFA; Sigma-Aldrich), previously dissolved in PBS (Sigma-Aldrich), adjusted to pH 7 and stored at -20^{o}C. A suture (Johnson & Johnson, St-Stevens-Woluwe, Belgium) was tied around the trachea to prevent leakage of PFA. The inflated lung was left *in situ* for one hour at RT and then dissected out and submerged in 4% PFA for 48 hours at RT. The individual lobes were separated using a scalpel, placed in plastic histology cassettes (Simport, Quebec City, Canada) and processed overnight in the Tissue-Tek VIP 5 Jr. vacuum infiltration processor (Sakura, Alphen aan den Rijn, Netherlands). The lobes were then embedded in paraffin and the left lobe trimmed until large airways were exposed. A number of 4 µm sections were then cut, which were mounted onto Superfrost Plus glass slides (VWR, PA, USA) and allowed to dry at 37^{o}C. Paraffin-embedded blocks and tissue slides were stored at 4^{o}C if not used immediately after preparation.

2.6.9.2 Immunostaining of mouse lung sections

Slides were deparaffinised and rehydrated by submerging them in a series of solutions for 3 minutes each. Ethanol solutions were prepared with industrial methylated spirit (VWR). The order of solutions was as follows: Citroclear (TCS Biosciences, Botolph Claydon, UK) twice, 100% ethanol twice, 70% ethanol, 50% ethanol, and PBS twice. For antigen retrieval, slides were treated with pre-heated 1 mM EDTA (pH 8) for 10 minutes at 95-100°C. Briefly, a plastic coplin jar (Thermo Fisher Scientific) was filled with the buffer and placed in a water bath set to 95-100°C for approximately 30 minutes. Immediately following deparaffinisation and rehydration, slides were placed in the hot buffer and the jar placed back in the water bath for 10 minutes. The slides were then allowed to cool in the jar for 20 minutes at RT and washed three times in 0.1% Triton X-100 (Sigma-Aldrich) in PBS. A solution of 0.1% Triton X-100 (Sigma-Aldrich) in PBS was used for all dilutions and washing steps. EGFP and cell type-specific markers were detected by incubation with a combination of the appropriate antibodies, listed in Table 2.5. All antibody incubations were performed in the dark in a humid slide staining system (Simport) at RT. Following heat-induced antigen retrieval, a hydrophobic pen (Sigma-Aldrich) was used to demarcate a region around the tissue section. Approximately 25-50 µl of primary antibody mixture at 1:100 dilution was applied onto the tissue. Following the incubation, the slides were washed once and 25-50 µl of secondary antibodies diluted 1:500 applied. After the second incubation, slides were washed once, mounted with ProLong Gold Antifade medium with DAPI (Thermo Fisher Scientific) and incubated overnight in the dark at RT. If not subsequently imaged, the slides were stored at 4°C.

2.6.9.3 Imaging of sections using confocal microscopy

Images were captured using a Zeiss LSM-780 inverted confocal microscope (Zeiss, Jena, Germany) using 63x oil immersion objective. Alexa Fluor 594 was excited with the HeNe543 laser. The emission signal was filtered by a 595 nm long pass filter. Alexa Fluor 488 was excited with a 488 nm laser and detected with a 505-550 nm band pass filter. 4′,6-diamidino-2-phenylindole (DAPI) was excited with a 405 nm laser and the detection range was 420-490 nm. Ten images were acquired of each section. The area of the lung to be captured was determined by the cell type which was being visualised: for ATI and ATII cells, images of the alveolar regions were captured, whilst for the remaining cell types, images of the airways were captured. Regions of the airway which were captured were selected based on high density of cells positive for the respective cell-type-specific marker to avoid bias for highly transduced regions. Processing and analysis of the images was carried out using Fiji software (Schindelin et al., 2012). The cell type marker, EGFP and DAPI channels were merged. The total number of cells stained for the cell type-specific marker and the total number of cells stained with both the cell type-specific antibody and GFP antibody were manually counted for each image.

Table 2.5. List of antibodies used for immunostaining of mouse lung sections.

Target	Antibody	Supplier	Catalogue no.
GFP	Chicken anti-GFP	Abcam plc Cambridge, UK	Ab13970
GFP	Rabbit anti-GFP	Life Technology Eugene, OR, USA	A-11122
Ciliated cells	Mouse anti-β-tubulin	Chemicon Int, Temecula, Ca	MAB3408
Club cells	Rabbit anti-uteroglobin	Abcam plc	Ab40873
Goblet cells	Mouse anti-mucin 5Ac	Abcam plc	Ab212636
Basal cells	Rabbit anti-cytokeratin 5	Abcam plc	Ab52635
Type I alveolar cells (ATI)	Hamster anti-podoplanin	Santa Cruz Biotechnology, Inc Dallas, TX, USA	sc-53533
Type II alveolar cells (ATII)	Rabbit anti-surfactant protein C	Millipore, Temecula, CA, USA	AB3786
Secondary	Goat anti-chicken Alexa Fluor 488	Life Technology	A11039
Secondary	Goat anti-rabbit Alexa Fluor 488	Life Technology	A11008
Secondary	Goat anti-mouse Alexa Fluor 594	Life Technology	A11005
Secondary	Goat anti-rabbit Alexa Fluor 594	Life Technology	A11012
Secondary	Goat anti-hamster Alexa Fluor 594	Life Technology	A21113

2.7 Quantification of transgene activity

2.7.1 Quantification of protein in lysates

Total protein in cell culture lysates (Section 2.4.3) or mouse lung lysates (Section 2.6.6.3) was determined using the Detergent-Compatible (DC) protein assay kit (Bio-Rad, Hemel Hempstead, UK). Cell culture lysates were analysed neat or diluted by a factor of 2-5, while mouse lung lysates required a 40-fold dilution. A volume of 5 µl of lysate was transferred into a 96-well plate (Thermo Fisher Scientific) in triplicate. Lyophilised BSA (Bio-Rad) resuspended in Milli-Q water (5 mg/ml) was used to generate a 7-point standard curve (range 1.75 mg/ml to 0.25 mg/ml in 0.25 mg/ml increments). Each standard was analysed in triplicate on the same plate as the samples. Reagents of the DC protein assay kit were added according to the manufacturer's instructions and the plate was incubated for 15 minutes at RT to allow the colourimetric assay to develop. Absorbance at 750 nm was measured in SpectraMAX i3x microplate reader (Molecular Devices, Wokingham, UK) and SoftMax Pro software v7.0 (Molecular Devices) was used to quantify protein in samples by comparison to the BSA standard curve.

2.7.2 Firefly luciferase assay

The quantity of firefly luciferase activity in cell culture lysates (Section 2.4.3) or mouse lung lysates (Section 2.6.6.3) was determined using the Luciferase Assay Reagent System (Promega). A volume of 100 µl of Luciferase Assay Substrate, dissolved in the supplied buffer, was added to 20 µl of the sample to be assayed, previously transferred to 96-well white opaque polystyrene assay plates (Corning).

After 2 s, light output in arbitrary relative light units (RLU) was measured over 10 s in SpectraMAX i3x microplate reader (Molecular Devices). All samples were read in duplicate and luciferase activity was normalised to total protein in the same sample, as determined in Section 2.7.1.

2.7.3 *Gaussia* luciferase assay

The activity of *Gaussia* luciferase (GLux) in cell culture supernatant, mouse serum (Section 2.6.6.1) and BALF (Section 2.6.6.2) was determined by measuring the light produced by the reaction catalysed by GLux in the presence of coelenterazine (BioLux *Gaussia* Luciferase Assay Kit, NEB). Samples were analysed undiluted with the exception of serum, which was diluted in Tris-buffered saline (TBS; Sigma-Aldrich) by a factor of 10. A volume of 50 µl of GLux assay substrate, diluted in the supplied buffer, was added to 20 µl of sample. After 2 s, light output in arbitrary relative light units (RLU) was measured over 10 s in GloMax 20/20 luminometer (Promega) or SpectraMAX i3x microplate reader (Molecular Devices). All samples were measured in duplicate.

2.7.4 Enzyme-linked immunosorbent assay

Anti-human IgG Enzyme-Linked Immunosorbent Assay (ELISA) was performed using Human IgG ELISA kit (Bethyl, Cambridge, UK) according to the manufacturer's instructions. Briefly, flat-bottomed 96-well plates (Corning) were coated with goat anti-human IgG-Fc antibody (10 mg/ml, 100 µl per well) for 1 hour at RT. Plates were washed three times with TBS-T (50mM Tris-Cl, 150 mM NaCl,

0.05% Tween 20, pH 8.0) and incubated with blocking buffer (TBS, 1% BSA; 200 µl per well) overnight at 4°C. Samples and standards diluted in sample diluent (TBS, 0.1% BSA, 0.05% Tween 20; 100 µl per well) were added to the plates and incubated for 1 hour at RT. Plates were washed and 100 µl horseradish peroxidase (HRP)-conjugated goat anti-human IgG antibody (diluted 1:200,000 in sample diluent) was added to each well and incubated for 1 hour at RT. Plates were then washed with TBS-T and 50 µl 3,3′,5,5′-tetramethylbenzidine (TMB) substrate was added per well, followed by a 15-minute incubation in the dark. The colour reaction was stopped with the addition of 50 µl of 0.18 M H_2SO_4. Plates were read at 450 nm (OD_{450}) using SpectraMAX i3x microplate reader (Molecular Devices). The concentration of human IgG in the sample was determined by comparison with Human Reference Serum (Bethyl). The samples and standards were measured in duplicate.

2.7.5 Quantification of mRNA levels using relative expression qRT-PCR

Total RNA was extracted from cells using the RNeasy Mini kit (Qiagen) according to the manufacturer's instructions. Complete DNA removal from total RNA preparations was ensured by incubation with an excess of DNase (Thermo Fisher Scientific) during RNA extraction. Total RNA yield was determined using the Quant-IT Ribogreen assay kit (Thermo Fisher Scientific) according to the manufacturer's instructions. Messenger RNA (mRNA) copy number was determined using two-step TaqMan real-time qRT-PCR instrumentation and reagents (Thermo Fisher Scientific). The comparative ΔΔCT method (Schmittgen and Livak, 2008) was used to determine relative expression levels of the target

mRNA. Three independent replicates were carried out for each RNA sample for both the target mRNA (etanercept) and glyceraldehyde 3-phosphate dehydrogenase (GAPDH) mRNA which was used as normalising mRNA. Cycle thresholds (Ct) values were determined for both target and normalising mRNA and the difference between these values was used to calculate an RNA sample ΔCt value ($\Delta Ct = Ct_{normalising\ mRNA} - Ct_{target\ mRNA}$). One of the experimental samples was selected as a comparator. The difference in ΔCt values between the comparator and all remaining RNA samples was determined to calculate ΔΔCt values ($\Delta\Delta Ct = \Delta Ct_{comparator} - \Delta Ct_{RNA\ Sample}$). Mean ΔΔCt values for each RNA sample were calculated from three replicates and transformed into relative expression values using the formulae: relative expression = $2^{-\Delta\Delta Ct}$. Using this approach, the relative expression of the target mRNA for the comparator RNA sample was deemed to be one, and the relative expression of the target mRNA in each of the other RNA samples was expressed relative to this value. Complementary DNA (cDNA) synthesis reactions (10 µl final volume) included 10 ng of total RNA and were primed with 400 nM reverse primer. qPCR reactions (10 µl final volume) included 300 nM forward and reverse primer and 100 nM TaqMan probe. The primers used for etanercept were as follows: forward: AAGCTTCTGCCTTCTCCCTCC; reverse: TGGCCATGGTGGCTAGCAA; probe: FAM-TGAGTTTGGTTGGTGTACAGT-NFQ. The primers used for GAPDH were as follows: forward: CAAGGTCATCCATGACAACTTTG; reverse: GGGCCATCCACAGTCTTCTG; probe: VIC-ACCACAGTCCATGCCATCACTGCCA-TAMRA. All RNA samples were analysed with and without reverse transcriptase in the cDNA synthesis step to control for the possible contribution of contaminating DNA to the calculated relative expression value.

2.7.6 Immunoblotting for Flag tag

2.7.6.1 Preparation of cell lysates

Radioimmunoprecipitation assay (RIPA) buffer was prepared freshly from 10x stock solution (Merck). One tablet of cOmplete Mini protease inhibitor cocktail (Roche) was dissolved in 10 ml of RIPA buffer, and the solution was kept on ice. Media was aspirated from the six-well plates and the cells gently washed with ice-cold PBS. The RIPA buffer/protease inhibitor was added (200 µl per well) and the plates incubated for 10 minutes at RT. The plates were then placed on ice, the wells scraped and their contents transferred to a 1.7 ml microcentrifuge tube (Corning) and kept on ice. Subsequent shearing using a 21G needle (Becton Dickinson) was used to further break up the cells and DNA, retaining the intact proteins. Insoluble material was removed by centrifugation for 5 minutes at 13,000 rcf and the total protein remaining in the supernatant quantified (Section 2.7.1). Single-use aliquots of the protein solution were prepared to avoid protein degradation through repeated freezing and thawing and stored at -80^{o}C if not used immediately. An aliquot of the sample was optionally subjected to denaturation and deglycosylation using Protein Deglycosylation Mix II (NEB) according to the manufacturer's instructions.

2.7.6.2 Sodium dodecyl sulphate polyacrylamide gel electrophoresis (SDS-PAGE)

Protein for analysis (10 µg) was mixed with an equal volume of 2 x Laemmli Sample Buffer (Bio-Rad) and incubated at 100^{o}C for 8 minutes. Samples were loaded onto 4-12% or 10% Bolt Bis-Tris Plus polyacrylamide gels (Thermo Fisher Scientific)

and electrophoresed at 200 V for 35 minutes using Bolt MOPS SDS Running Buffer (Thermo Fisher Scientific). To allow protein size estimation, 10 µl of Precision Plus Protein Kaleidoscope Prestained Protein Standard (Bio-Rad) was included on each gel.

2.7.6.3 Western transfer

Once SDS-PAGE had completed, the polyacrylamide gel was removed and the proteins transferred onto a 0.45 µm nitrocellulose membrane (Bio-Rad). Electrotransfer took place in a Trans-Blot Cell (Bio-Rad) in Bolt Transfer Buffer (Thermo Fisher Scientific) with 10% methanol for 90 minutes at 200 mA.

2.7.6.4 Immunoblotting

All washing steps and incubations were carried out on a platform shaking at 50-60 rpm. Once electrotransfer was complete, the membrane was briefly (2-3 minutes) washed in Mili-Q water and incubated with blocker solution (3% blotting grade blocker (Bio-Rad), 50 mM Tris, 0.138 M NaCl, 2.7 mM KCl, pH 8.0) for 2 hours at RT to block non-specific binding sites. The membrane was then washed in TBS (Tris-buffered saline; 50 mM Tris, 0.138 M NaCl, 2.7 mM KCl, pH 8.0) and incubated with anti-Flag antibody (clone M2, Sigma-Aldrich) diluted to 0.1 µg/ml in blocker solution. The membrane was subsequently washed in TBS and primary antibody detected by incubation with goat anti-mouse HRP-conjugated antibody, diluted 1:10,000 in blocker solution, for 1 hour at RT. The membrane was then washed eight times in TBS-T (50 mM Tris, 0.138 M NaCl, 2.7 mM KCl, 0.05%

Tween-20, pH 8.0) for a total of 20 minutes at RT, and once in Mili-Q water. Protein bands were detected by incubation with Clarity Western ECL substrate (Bio-Rad) and visualised in the iBright FL1000 system (Thermo Fisher Scientific).

2.8 Statistical analyses

Statistical analysis was performed using Prism software v7.0 for Mac (GraphPad Software). Parametric tests were performed unless sample size was less than 4 or the data was discontinuous. If the distribution significantly deviated from normal, a logarithmic transformation was performed before statistical analysis. A calculated p-value of <0.05 was deemed a significant difference and indicated on figures where appropriate (*=$p<0.05$, **=$p<0.01$, ***=$p<0.001$ and ****=$p<0.0001$). Error bars in figures represent the standard error of the mean.

Chapter 3: Investigation into gene delivery for expression of secretory proteins *in vivo*

3.1 Introduction

Lung gene delivery has the potential to be useful for applications where the presence of a mAb is particularly beneficial in the lung lumen, such as those involving respiratory infections (Borrok et al., 2018). If efficient secretion of the mAb into circulation can be achieved, administration of a gene transfer agent to the lung could also be useful as a non-invasive means of systemic delivery. Non-viral gene transfer agents have many advantages, including the relative simplicity of manufacture and ability to repeatedly administer them due to the lack of adaptive immune responses (Section 1.1.4). Here, the possibility of using non-viral gene transfer vehicles to establish *in vivo* protein factories was investigated. A potential candidate is the widely used cationic polymer PEI. Aerosol administration of pDNA complexed with 25 kDa branched PEI to the mouse lung was shown to result in sustained transgene expression in the absence of toxic effects (Davies et al., 2012). However, in previous studies, administration of these polyplexes by aerosol did not direct detectable expression of the secretory reporter protein *Gaussia* luciferase (GLux) in the circulation (I. Pringle, personal communication). Attention was therefore also focused on the biodegradable and non-toxic cationic lipid formulation GL67A (Eastman et al., 1997), which has been investigated for treatment of CF lung disease (Alton et al., 1999) and is to date the only non-viral gene transfer agent to have been evaluated for lung delivery in the clinic. The utility of GL67A for directing secretion of protein from the lung to the circulation was previously investigated using a different formulation, which is instilled to the lung

rather than aerosolised. Griesenbach and colleagues found that instillation of GL67A lipoplexes into the lung resulted in detectable expression of GLux in the serum of mice and sheep 24 hours later (Griesenbach et al., 2011). The ability of GL67A lipoplexes to direct expression beyond 1 day was not explored, however. Furthermore, the instilled formulation examined in the study above is associated with the induction of an inflammatory response in mice, whilst administration of the aerosolised complexes does not result in inflammation (Eastman et al., 1997). This chapter therefore investigated the feasibility of using pDNA/GL67A aerosol formulation to direct sustained secretion of a reporter protein from the mouse lung.

The possibility of directing secreted protein expression using viral gene transfer vehicles was also studied. Recombinant AAV serotype 8 has been successfully used to express the HIV-neutralising mAbs b12 and VRC01, as well as a number of other mAbs, in the mouse muscle (Balazs et al., 2011) (Section 1.1.5.4). This vector was selected for evaluation in the model diseases RSV infection (Section 1.2) and rheumatoid arthritis (Section 1.3) because of its high muscle tropism (Louboutin et al., 2005), ability to direct abundant life-long transgene expression in mouse skeletal muscle (Balazs et al., 2013), and evidence of safety as evaluated in clinical trials (Nathwani et al., 2014). Serotype 9, which has been reported to direct anti-influenza mAb expression following administration to the mouse lung (Limberis et al., 2013), was also studied.

The second viral vector selected for study is rSIV.F/HN (section 1.1.6.2), currently undergoing preclinical evaluation for CF gene therapy. This vector achieved a transduction efficiency of about 15% in mouse lung epithelium (Alton et al., 2017) and directed sustained reporter gene expression in the respiratory epithelium lining

the murine nose for the lifetime of the animal following a single dose (Griesenbach et al., 2012, Mitomo et al., 2010). Delivery of the vector to the lung was also shown to result in expression of secretory proteins into the circulation and lung lumen of mice for at least 19 months (Paul-Smith et al., 2018). Importantly, this vector can be repeatedly administered in mice without loss of efficacy (Alton et al., 2017).

The aims of the work presented in this chapter included: (i) to investigate the use of non-viral gene transfer agents PEI and GL67A for expression of secretory protein from the lung, (ii) to investigate the use of rSIV.F/HN and rAAV for expression of secretory protein from the lung and muscle and (iii) to determine the optimal delivery method of selected vectors for secretion of protein into the circulation and lung lumen.

3.2 Results

3.2.1 Expression of secretory reporter protein following delivery of non-viral gene transfer agents to the lung

Transgene expression levels were determined following aerosol delivery to the lung of pDNA complexed with PEI or GL67A. Plasmid pG4.hCEFI.soLux (Table 2.1) was complexed with each of the two gene transfer agents and aerosolised to the lungs of mice according to well-established protocols (Sections 2.6.4.1 and 2.6.4.3). Luciferase activity in the lung was measured throughout the experiment using bioluminescence imaging (BLI) (Section 2.6.8), and at the end of the experiment using luminometry (Section 2.7.2) of homogenised lung tissue (Section

2.6.6.3). Figure 3.1 shows that aerosol delivery of both gene transfer formulations directed significant luciferase expression in the lung ($p<0.0001$ at 28 and 56 days post-delivery), and although levels were ~2-fold higher for PEI than GL67A at 28 days post-delivery when measured with BLI (Figure 3.1 B, $p<0.01$), there was no significant difference between the two treatment groups at 56 days when luminometry was used ($p>0.05$, Figure 3.1 A). It was therefore concluded that PEI and GL67A directed comparable levels of lung transgene expression when complexed with pDNA and aerosolised to mouse lung. Due to the concerns related to the non-biodegradable nature of PEI (Section 1.1.4), GL67A was selected for further evaluation in this study.

The secretory reporter gene, *Gaussia* luciferase (GLux), was used to detect expression in the serum and lung lumen of mice as it has previously been demonstrated to be a sensitive secreted reporter in airway gene transfer using non-viral formulations (Griesenbach et al., 2011). Plasmid pG4.hCEFI.soGLux (Table 2.1) encoding GLux reporter protein was complexed with GL67A for aerosol delivery (Section 2.6.4.3). A positive control group, in which mice were administered pG4.hCEFI.soGLux/GL67A by nasal instillation, was also included as this formulation and delivery route was previously shown to result in detectable GLux levels in the serum of treated mice 24 hours after administration (Griesenbach et al., 2011). As shown in Figure 3.2, and consistent with the previously published findings, significant expression of GLux in the serum and lung lumen was observed 24 hours after instillation of GL67A lipoplexes. Disappointingly, no significant GLux expression could be detected in the serum (Figure 3.2 A) or broncho-alveolar lavage fluid (BALF) (Figure 3.2 B) of mice 28 days after exposure to pG4.hCEFI.soGLux/GL67A aerosol ($p>0.05$), suggesting

that expression from this gene delivery system might be too low to be an effective method of directing secretion of protein from the lung.

Expression of GLux from plasmid pG4.hCEFI.soGLux (Table 2.1) is under the control of the hCEFI enhancer/promoter, which combines the CpG-free version of the human cytomegalovirus (CMV) enhancer (termed hC) with the CpG-free version of the human elongation factor 1 alpha (EF1α) promoter (termed EF) and a synthetic CpG-free intron (termed I), and directs persistent transgene expression in the mouse lung following a GL67A aerosol (Hyde et al., 2008). A previous study reported that, although a 93 bp region of the hC enhancer is necessary and sufficient to mediate the high-level activity observed in the mouse lung with the full-length 302 bp hC sequence, a plasmid containing two of these minimal enhancers in tandem (pG6.2x93.soLux; Table 2.1) directed seven-fold higher reporter expression levels than a single 93 bp enhancer (Oliveira, 2015). To increase the level of transgene expression in the lung following pDNA/GL67A aerosol delivery, an investigation was undertaken into alternative enhancer sequences. Plasmids containing three or four minimal enhancers in tandem (pG6.4x93.soLux and pG6.3x93.soLux respectively; Table 2.1) were constructed as described in Section 2.3.4. For practical reasons, a PEI aerosol, requiring lower amounts of plasmid DNA (2 mg compared with 26mg for the equivalent GL67A aerosol), was selected as the gene transfer agent for this experiment. Mice were administered pDNA/PEI formulations of plasmids containing the full-length hC enhancer, minimal 93 bp enhancer, 2x minimal enhancer, 3x minimal enhancer and 4x minimal enhancer (pG6.hCEFI.soLux, pG6.93.soLux, pG6.2x93.soLux, pG6.3x93.soLux and pG6.4x93.soLux, respectively; Table 2.1). Luciferase expression in the lung was measured using luminometry or BLI (Figure 3.3).

A

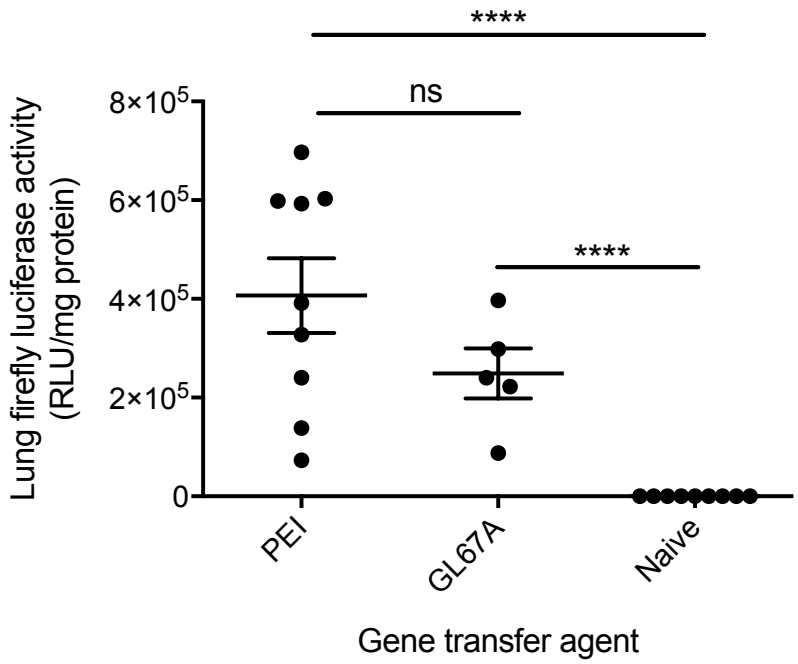
****
ns
****
8×10^5
6×10^5
4×10^5
2×10^5
0
Lung firefly luciferase activity
(RLU/mg protein)
PEI
GL67A
Naive
Gene transfer agent

B

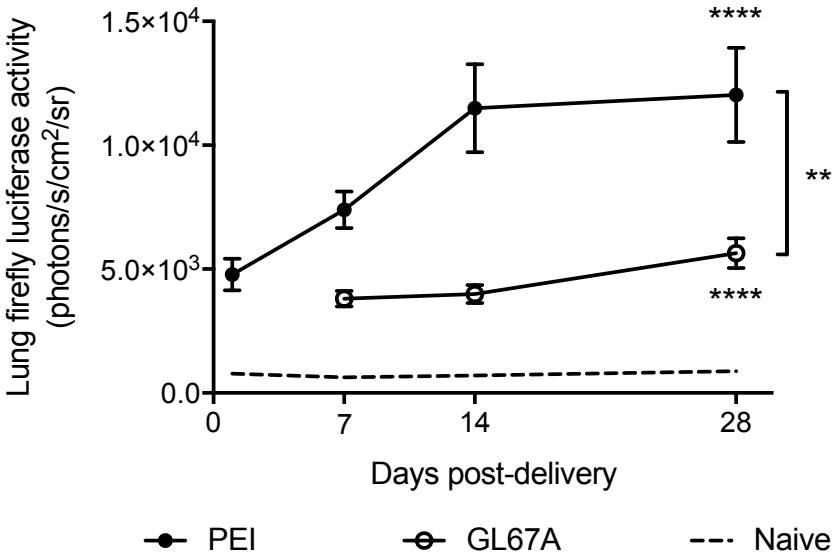
1.5×10^4
1.0×10^4
5.0×10^3
0.0
Lung firefly luciferase activity
(photons/s/cm²/sr)
****
**
****
0
7
14
28
Days post-delivery
PEI
GL67A
Naive

Figure 3.1. Comparison of luciferase activity in the lung after aerosol administration of pG4.hCEFI.soLux complexed with PEI or GL67A.

Female BALB/c mice were dosed with 10 mL PEI polyplexes (Section 2.6.4.1) or GL67A lipoplexes (Section 2.6.4.3) containing 2 mg or 26 mg pG4.hCEFI.soLux (Table 2.1), respectively, by aerosol delivery (Section 2.6.5.2). Lung firefly luciferase activity was measured using (A) luminometry (Section 2.7.2) of homogenised lung tissue (Section 2.6.6.3, n = 5-9) at 56 days post-delivery and (B) *in vivo* bioluminescence imaging (BLI) (Section 2.6.8, n = 4-10) for up to 28 days post-delivery. Data are shown as individual values and/or mean ± standard error of the mean. Statistical differences between groups were analysed by ANOVA on log-transformed data, with Tukey post hoc multiple comparison test. A calculated p value of >0.05 was deemed non-significant as indicated with ns on figures. Calculated p values of <0.01 or <0.0001 were deemed a significant difference as indicated with two stars (**) or four stars (****), respectively.

A

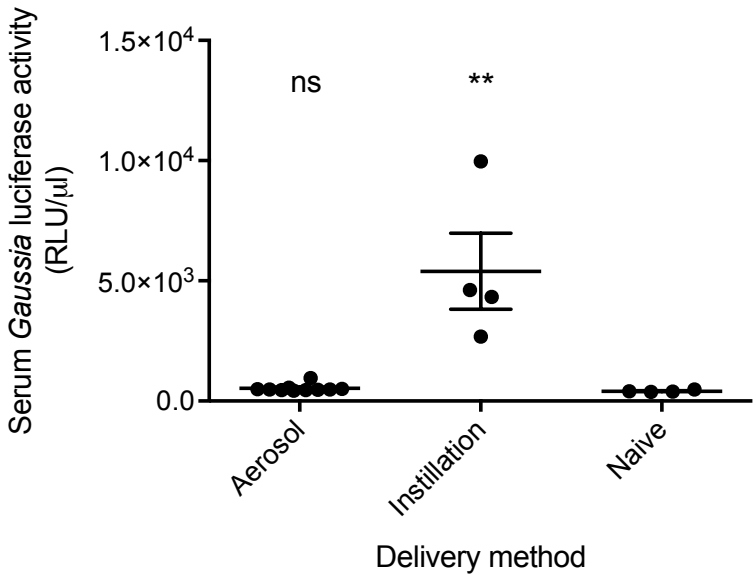
Serum Gaussia luciferase activity (RLU/μl)
1.5×10^4
1.0×10^4
5.0×10^3
0.0
ns
**
Aerosol
Instillation
Naive
Delivery method

B

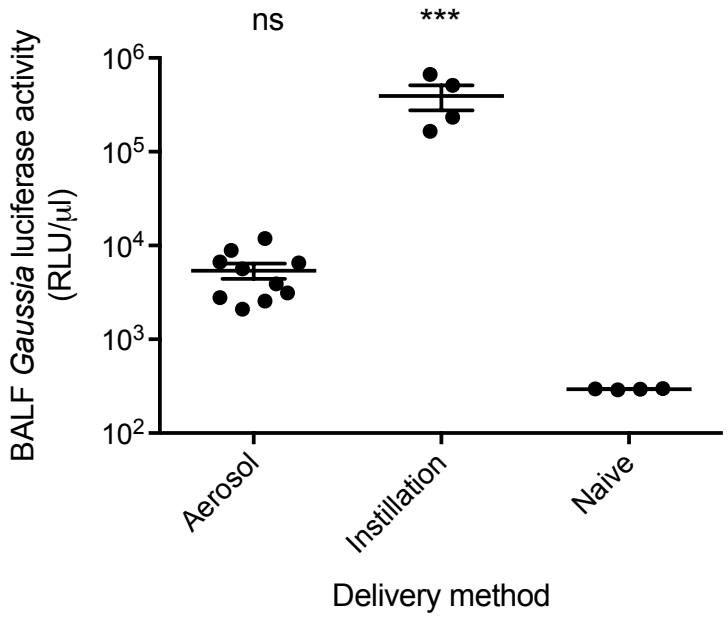
BALF Gaussia luciferase activity (RLU/μl)
10^6
10^5
10^4
10^3
10^2
ns
***
Aerosol
Instillation
Naive
Delivery method

Figure 3.2. *Gaussia* luciferase activity in the serum and broncho-alveolar lavage fluid after aerosol administration or instillation of pG4.hCEFI.soGLux complexed with GL67A.

Female BALB/c mice were dosed with pG4.hCEFI.soGLux (Table 2.1) by intranasal instillation (Section 2.6.5.1; n = 4) of 80 µg or aerosol delivery (Section 2.6.5.2) of 26 mg pDNA complexed with GL67A (Section 2.6.4.3, n = 10). *Gaussia* luciferase activity in (A) the serum (Section 2.6.6.1) and (B) broncho-alveolar lavage fluid (BALF) (Section 2.6.6.2) was measured using luminometry (Section 2.7.3). Data for aerosol and naïve groups were collected at day 56 post-delivery, while the instillation group was harvested and analysed 1 day post-delivery. Data are shown as individual values and mean ± standard error of the mean. Statistical differences between groups were analysed by Kruskal-Wallis test, with Dunn's post hoc test, compared with naïve values. A calculated p value of >0.05 was deemed non-significant as indicated with ns on figures. Calculated p values of <0.01 or <0.001 were deemed a significant difference as indicated with two stars (**) or three stars (***), respectively.

A

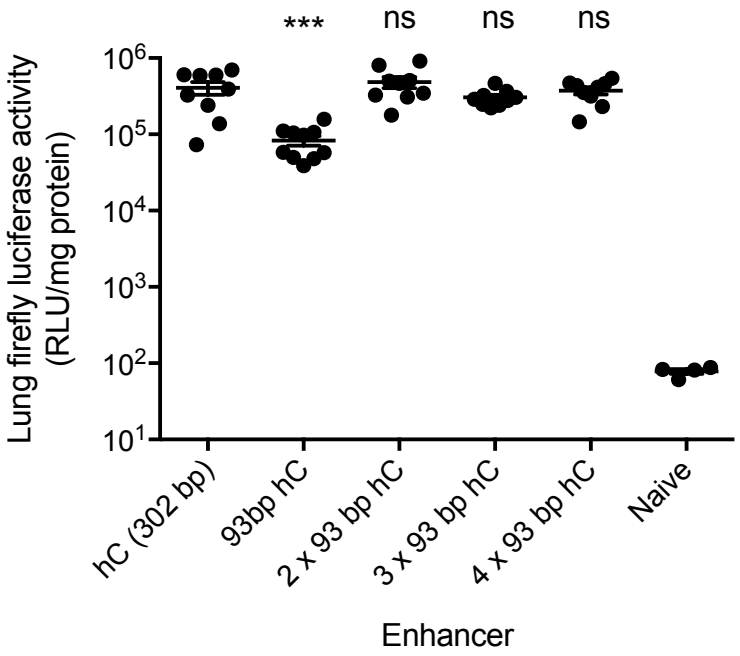
***
ns
ns
ns
Lung firefly luciferase activity
(RLU/mg protein)
10^6
10^5
10^4
10^3
10^2
10^1
hC (302 bp)
93bp hC
2 x 93 bp hC
3 x 93 bp hC
4 x 93 bp hC
Naive
Enhancer

B

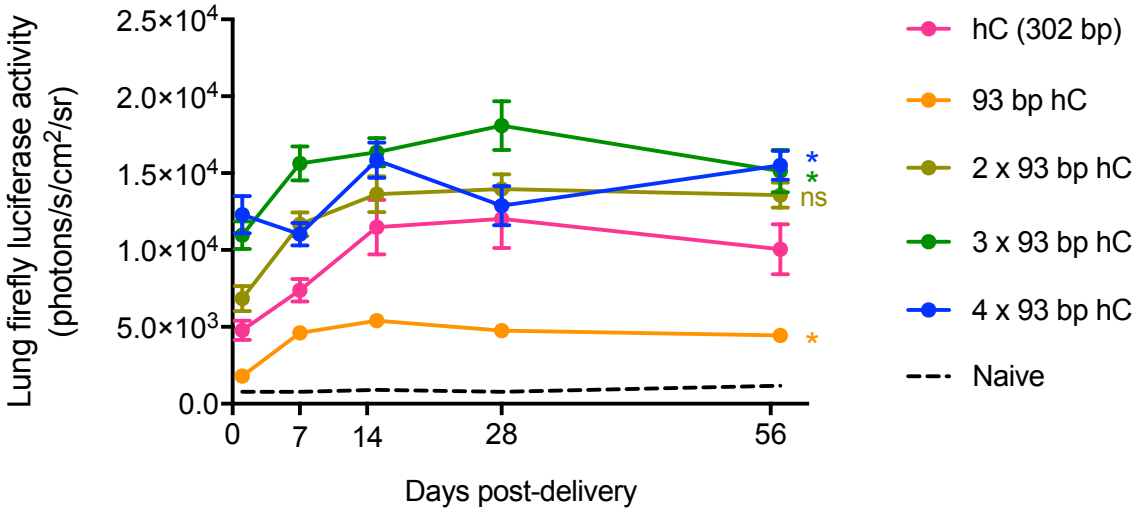
Lung firefly luciferase activity
(photons/s/cm2/sr)
2.5×10^4
2.0×10^4
1.5×10^4
1.0×10^4
5.0×10^3
0.0
0
7
14
28
56
Days post-delivery
*
*
ns
*
hC (302 bp)
93 bp hC
2 x 93 bp hC
3 x 93 bp hC
4 x 93 bp hC
Naive

Figure 3.3. Comparison of luciferase activity in the lung after PEI aerosol administration of plasmids containing multiple minimal hC enhancers.

Female BALB/c mice (n = 10) were exposed to 10 ml PEI aerosols (Section 2.6.5.2) complexed with 2 mg of plasmid (Section 2.6.4.1) containing either the full-length hC enhancer, or one, two, three or four copies of the minimal 93 bp enhancer (pG6.hCEFI.soLux, pG6.93.soLux, pG6.2x93.soLux, pG6.3x93.soLux and pG6.4x93.soLux, respectively; Table 2.1). Luciferase activity in the lung was measured using (A) luminometry at 57 days post-delivery (Section 2.7.2, n = 4-10) or (B) *in vivo* bioluminescence imaging (BLI) (Section 2.6.8, n = 4-10) at the indicated time-points. Data are shown as individual values and/or mean ± standard error of the mean. Statistical differences between groups were analysed by ANOVA on log-transformed data with Dunn's post hoc test compared with hC (302 bp). A calculated p value of >0.05 was deemed non-significant as indicated with ns on figures. Calculated p values of <0.05 or <0.001 were deemed a significant difference as indicated with one star (*) or three stars (***), respectively.

In contrast to previous observations (Oliveira, 2015), plasmid containing the 93 bp minimal enhancer directed significantly lower expression levels than the full-length hC enhancer in plasmid pG6.hCEFI.soLux ($p<0.001$ and $p<0.05$ when measured using luminometry and BLI, respectively). Although there appeared to be a modest increase in reporter gene expression from plasmids containing three or four tandem enhancers using BLI ($p<0.05$, Figure 3.3 B), this effect was not significant when measured using luminometry ($p>0.05$, Figure 3.2 A). In the absence of a substantial improvement in transgene activity in the mouse lung using the selected non-viral formulations, focus was turned to viral vectors as platforms for establishing secretory protein production in the lung.

3.2.2 Expression of secretory reporter protein *Gaussia* luciferase (GLux) following intranasal delivery of rSIV.F/HN in mice

The lentiviral vector rSIV.F/HN was identified as a promising vehicle with which to facilitate expression of secretory protein to the circulation and lung lumen (Section 1.1.6.2). Administration of the vector to the lungs of mice resulted in production of therapeutically relevant levels of human α1-anti-trypsin and factor VIII into the lung lumen and systemic circulation of mice for at least 19 months (Paul-Smith et al., 2018). To confirm and further evaluate the potential of this vector for sustained secretion after lung delivery, a time-course experiment was undertaken with the vector rSIV.F/HN hCEF soGLux (Table 2.2). Mice were administered 10^6, 10^7 or 10^8 TTU of rSIV.F/HN hCEF soGLux via nasal instillation and GLux activity (Section 2.7.3) in the serum (Section 2.6.6.1) and BALF (Section 2.6.6.2) measured (Figure 3.4). At early time-points, expression in the serum appeared to

be dose-related: at 28 days post-delivery, all groups were significantly different from each other ($p<0.0001$) and the high dose (10^8 TTU) group had 8- and 30-fold higher GLux levels in the serum than the medium and low dose groups (10^7 and 10^6 TTU/mouse), respectively ($p<0.001$). Expression of GLux was observed to peak approximately 1 month post-delivery and fall somewhat thereafter. This decline was only significant for the high dose (10^8 TTU) group in which reporter expression declined approximately 9-fold between 1 and 12 months ($p<0.0001$). By 12 months post-delivery, serum reporter activity in the low dose (10^6 TTU) group was not significantly different from naïve mice ($p>0.05$), while the high and medium doses (10^8 and 10^7 TTU/mouse, respectively) directed significant ($p<0.001$) but similar ($p>0.05$) levels of reporter activity in the serum. Significant dose-dependent expression in the BALF was observed for all three treatment groups at 12 months post-delivery (Figure 3.4 B). This study demonstrates that rSIV.F/HN instillation in the murine lung results in sustained expression of secretory protein into the circulation and lung lumen of mice for >12 months.

A

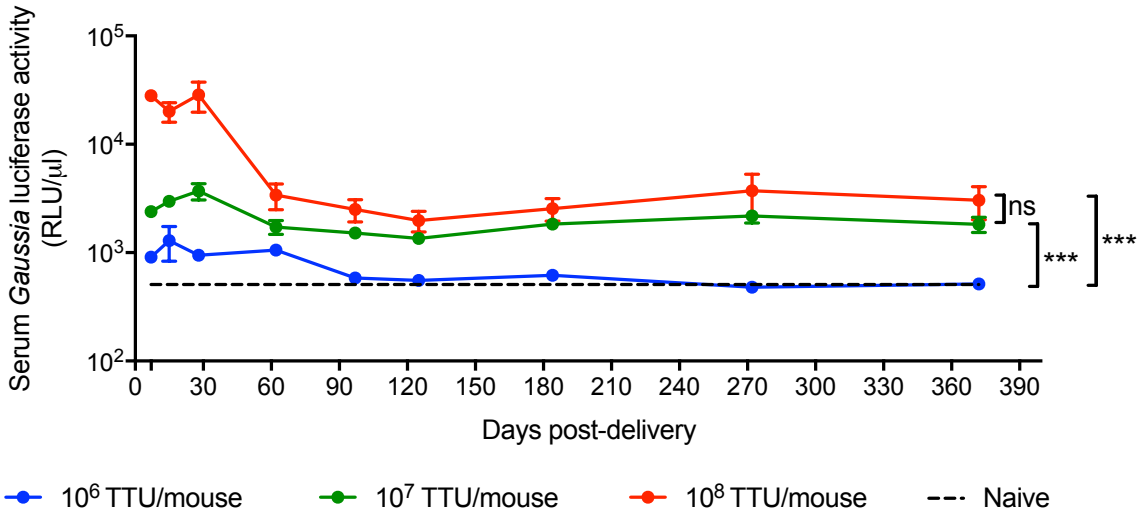
Serum Gaussia luciferase activity (RLU/μl)
10^5
10^4
10^3
10^2
0 30 60 90 120 150 180 210 240 270 300 330 360 390
Days post-delivery
ns
***
***
10^6 TTU/mouse
10^7 TTU/mouse
10^8 TTU/mouse
Naive

B

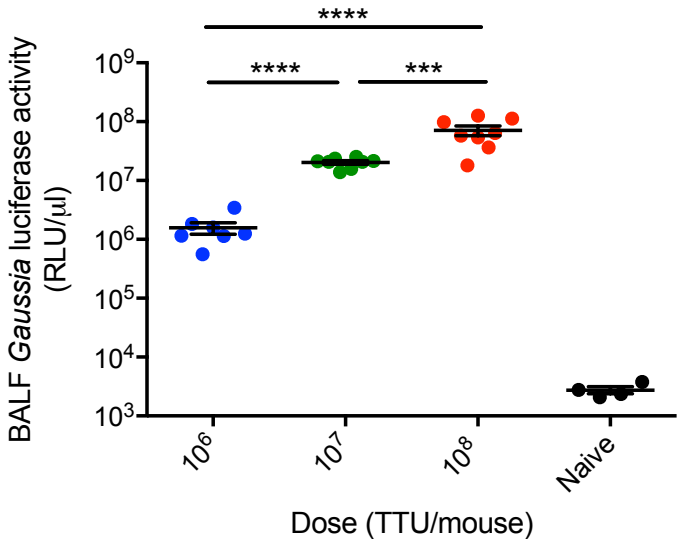
BALF Gaussia luciferase activity (RLU/μl)
****
****
***
10^9
10^8
10^7
10^6
10^5
10^4
10^3
10^6
10^7
10^8
Naive
Dose (TTU/mouse)

Figure 3.4. *Gaussia* luciferase activity in the serum and broncho-alveolar lavage fluid after intranasal instillation of rSIV.F/HN hCEF soGLux.

Female BALB/c mice (n = 11) were administered 10^6, 10^7 or 10^8 TTU of rSIV.F/HN hCEF soGLux by intranasal instillation (Section 2.6.5.1). *Gaussia* luciferase activity in (A) the serum (Section 2.6.6.1, n = 8-15) and (B) broncho-alveolar lavage fluid (BALF) (Section 2.6.6.2, n = 4-8) collected at 12 months was measured using luminometry (Section 2.7.3). Data are shown as individual values and/or mean ± standard error of the mean. Statistical differences between groups were analysed by ANOVA on log-transformed data, with (A) Tukey's or (B) Dunn's post hoc test. A calculated p value of >0.05 was deemed non-significant as indicated with ns on figures. Calculated p values of <0.001 or <0.0001 were deemed a significant difference as indicated with three stars (***) or four stars (****), respectively.

3.2.3 Identification of cell types transduced by rSIV.F/HN in the mouse lung

The lung is a complex organ consisting of a number of highly specialised cells and it is unclear which cell types are expressing reporter genes in the above experiments. The airways are mainly composed of ciliated cells, basal cells and secretory club cells, whilst the alveolar sacs are lined with large, squamous, gas exchanging type I alveolar cells (ATI), interspersed with surfactant-secreting type II alveolar cells (ATII). Basal cells function as progenitors which self-renew and give rise to other cell types (Rock et al., 2009). Club cells also have the ability to divide, and they differentiate into goblet and ciliated cells during homeostasis and tissue repair (Montoro et al., 2018, Plasschaert et al., 2018). The lentiviral vector rSIV.F/HN was previously reported to transduce all of the above cell types in the mouse lung (Alton et al., 2017), when examined 7 days after administration. An experiment was undertaken to confirm these results and to investigate the transduction profile of the vector at a later time-point following vector delivery. Mice were administered rSIV.F/HN hCEF EGFP (Table 2.2) and culled 7 days or 2 months later. Paraffin sections of the lungs were prepared (Section 2.6.9.1) and stained with antibodies against both EGFP and cell-type-specific markers for club cells (uteroglobin), ciliated cells (β-tubulin), goblet cells (mucin 5AC), basal cells (cytokeratin 5), type I alveolar cells (ATI; podoplanin) and type II alveolar cells (ATII; surfactant protein C) (Section 2.6.9.2; Table 2.5). Representative images of the sections (n = 3 animals per time-point) are shown in Figure 3.5 A. EGFP-positive cells of all types could be identified, except for basal cells (discussed in Section 3.3.2). The proportion of each cell type that was transduced with the vector, and therefore EGFP-positive, was quantified (Section 2.6.9.3) at the two time-points after delivery. The numbers of club and ciliated cells in the airways and ATII

cells in the parenchyma are reported in Figure 3.5 B. As shown in Figure 3.5 C, the proportion of EGFP-positive cells are similar for ATII and ciliated cells between 7 days and 2 months after vector administration. For club cells, the percentage of EGFP-positive cells tended to decrease from approximately 41% to 18%, although there was a considerable spread of the data within the 2-month group (Figure 3.5 C). A similar spread was also observed for the other analysed cell types (Figure 3.5 C), indicating higher overall transduction rates in one of the animals culled at that time-point, and potentially reflecting differences in efficiency of vector delivery. Goblet, basal and ATI cells were identified, but EGFP-positive cells could not be quantified for the following reasons: very few goblet cells were identifiable at 2 months, very few basal cells could be identified at 7 days, and very few transduced ATI cells were observed at either time-point (Figure 3.5 A). These observations are further discussed in Section 3.3.2.

A

7 days

2 months

Club

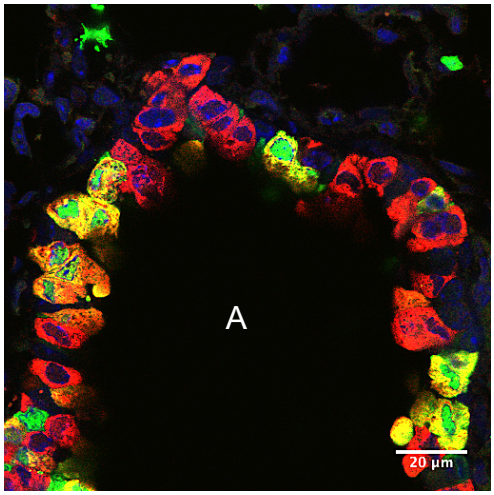

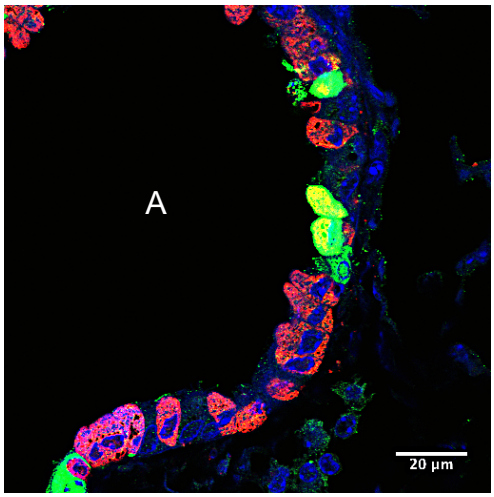

Ciliated

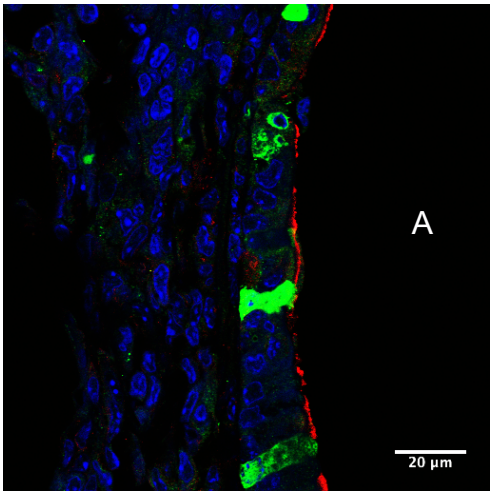

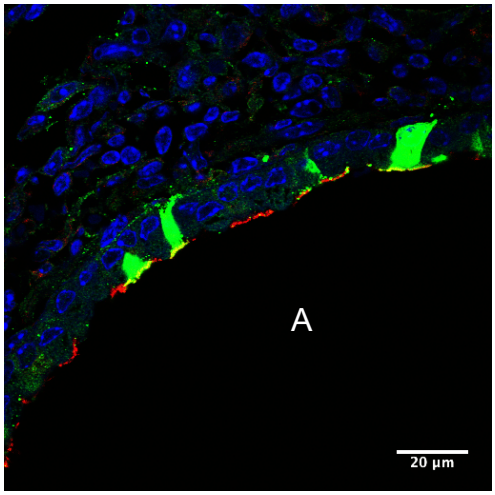

Goblet

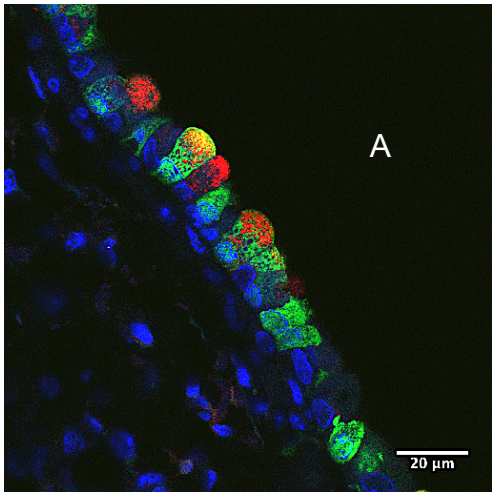

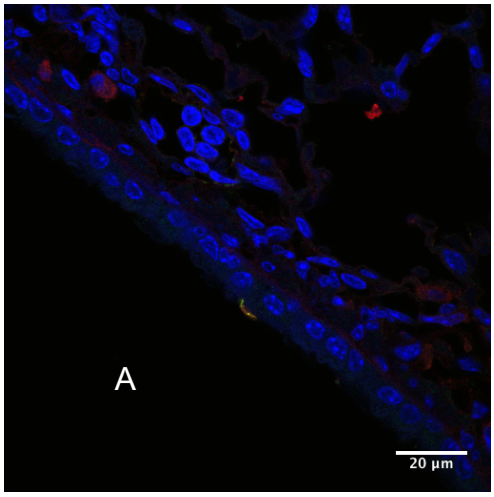

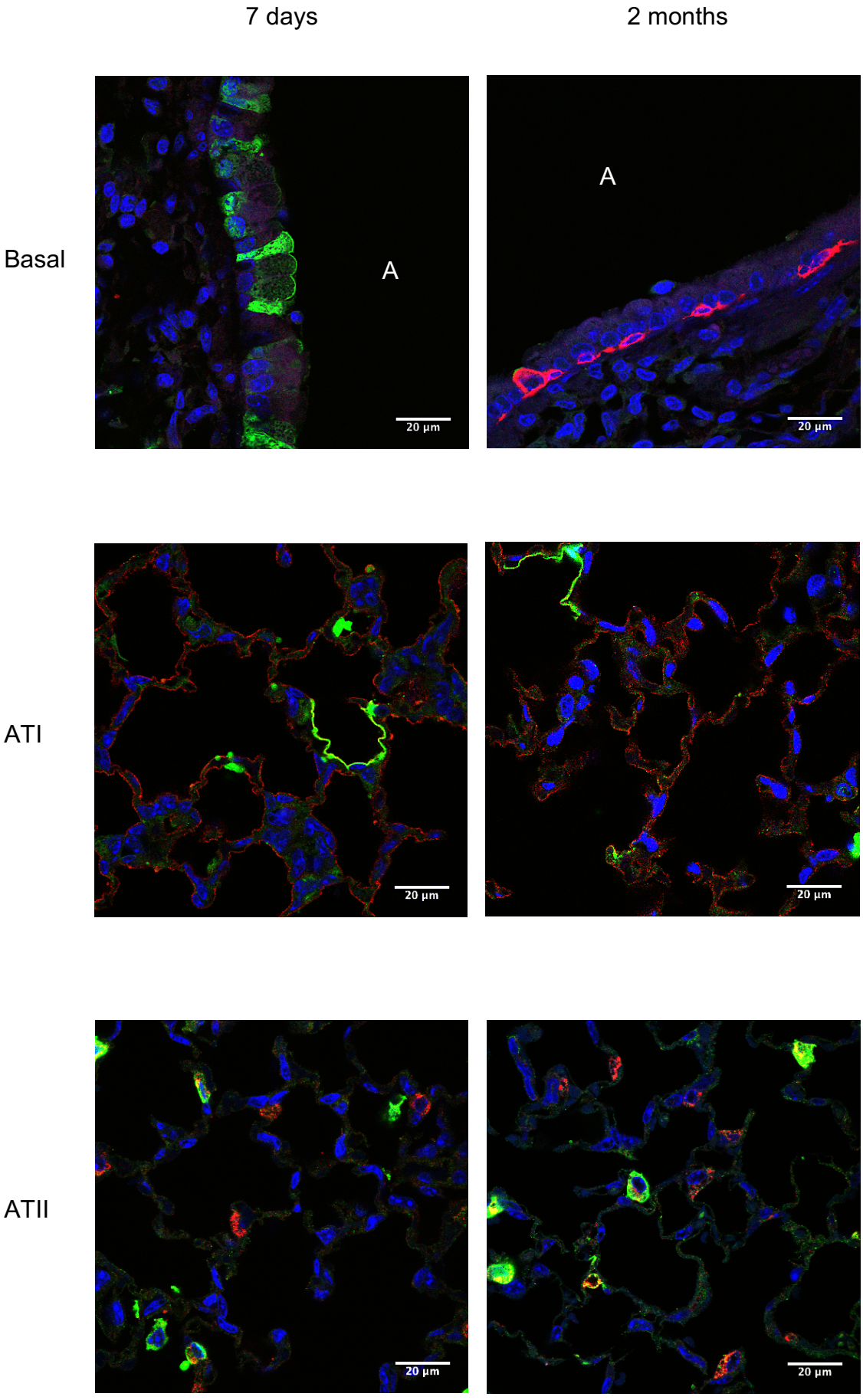
7 days
2 months
Basal
ATI
ATII
A
A
20 µm
20 µm
20 µm
20 µm
20 µm
20 µm

B

	7 days			2 months		
Cell type	Number of cells stained with cell-type marker	Number of cells stained with EGFP and cell-type marker	Proportion of cells stained with cell-type marker that are transduced	Number of cells stained with cell-type marker	Number of cells stained with EGFP and cell-type marker	Proportion of cells stained with cell-type marker that are transduced
Club	692	281	40.61%	665	117	17.59%
Ciliated	408	98	24.02%	501	114	22.75%
ATII	275	36	13.09%	224	27	12.05%

C

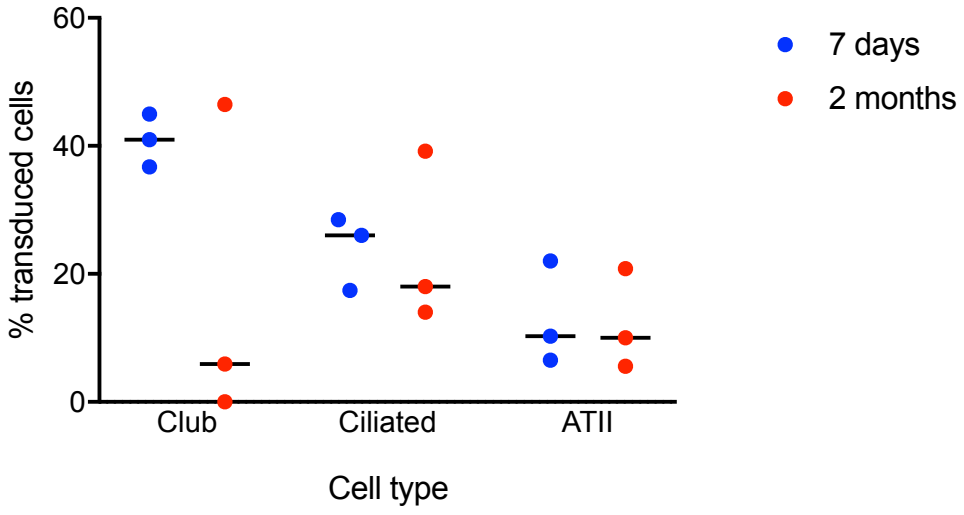

Figure 3.5. Proportion of EGFP-positive cells by cell type counted 7 days and 2 months after transduction of murine lung with rSIV.F/HN.

Female BALB/c mice (n = 3) were administered 3.02 x 10^8 TTU of rSIV.F/HN hCEF EGFP via intranasal instillation (Section 2.6.5.1). Seven days or 2 months after vector administration, the animals were culled and their lungs processed and sectioned (Section 2.6.9.1). Two sections per animal were immunostained for EGFP expression (green) and cell-specific markers (red) for club cells (uteroglobin), ciliated cells (β-tubulin), goblet cells (mucin 5AC), basal cells (cytokeratin 5), type I alveolar cells (ATI; podoplanin) and type II alveolar cells (ATII; surfactant protein C) (Section 2.6.9.2). Ten images were captured for each section and the total number of cells of a particular cell type and the number that were EGFP-positive counted (Section 2.6.9.3). (A) Representative images for each cell type are shown, with the scale bar (20 μm) and airway lumen (A) indicated. (B) Absolute numbers of cells counted across all sections from a single time-point. (C) The proportion of transduced cells for club, ciliated and ATII cells. Data are shown as individual values for each animal (each of which is an average of two sections) and median.

3.2.4 Expression of secretory reporter protein *Gaussia* luciferase (GLux) following intramuscular delivery of rAAV2/8 in mice

The use of rAAV2/8 to express mAb in the mouse circulation following IM delivery has been reported (Fang et al., 2005), indicating that this might be a useful strategy for systemic protein expression. An *in vivo* time-course experiment was undertaken to measure GLux activity after mice were administered 10^9, 10^{10} or 10^{11} GC of rAAV2/8 CASI soGLux (Table 2.2) via IM injection (Section 2.6.5.3). As shown in Figure 3.6 A, sustained GLux activity in the serum was observed for at least 12 months, with only a 3-fold decrease between 28 days and 12 months observed for the high dose (10^{11} GC/mouse) group. This is in contrast to the 9-fold decrease observed within that period following IN administration of rSIV.F/HN (Figure 3.4), and may reflect different turnover rates of lung and muscle cells (Rawlins and Hogan, 2008, Spalding et al., 2005). Glux expression following rAAV2/8 delivery appeared to be dose related, with significant differences observed between the treatment groups ($p<0.0001$). Significant GLux activity in the BALF (Figure 3.6 B) was also observed for the medium and high dose (10^{10} and 10^{11} GC/mouse, respectively) at 12 months post-delivery.

To compare the two delivery approaches (rAAV2/8 IM and rSIV.F/HN IN), expression in the high dose group from each experiment (10^8 TTU/mouse for rSIV.F/HN and 10^{11} GC/mouse for rAAV2/8) was considered. At 12 months post-delivery, rAAV2/8 IM administration resulted in >800-fold higher GLux activity in the serum than that achieved with rSIV.F/HN ($p<0.0001$; Figures 3.4 A and 3.6 A). In the BALF, however, rSIV.F/HN IN delivery achieved >900-fold higher levels of expression than rAAV2/8 ($p<0.0001$; Figures 3.4 B and 3.6 B). Based on these results with a secreted reporter protein, rAAV2/8 delivered to the muscle was

deemed to be the favoured vector for protein expression in serum, while rSIV.F/HN was superior for expression in the lung lumen.

It has been reported that IM injection of rAAV2/8 in mice and NHPs results in significant transduction and transgene expression in the liver (Greig et al., 2014). To determine whether protein production by the liver significantly contributed to the serum levels of GLux observed in the above study (Figure 3.6), an experiment was undertaken to quantify hepatic and muscle reporter gene activity following administration of the vector. Mice were administered 10^9, 10^{10} or 10^{11} GC of rAAV2/8 CASI EGFPLux (Table 2.2) IM (Section 2.6.5.3) and Lux expression quantified in the muscle and liver using *in vivo* BLI (Section 2.6.8). As shown in Figure 3.7, significant luciferase signal could only be detected in mice which received the highest dose (10^{11} GC) of the vector. In those animals, there was significant luciferase activity in the liver ($p<0.05$), although it was 460-fold lower than in the injected muscle. It was concluded that the relative contribution of the liver to protein expression following IM delivery of rAAV2/8 is negligible compared to that of the muscle, at least when GLux is expressed from the CASI promoter.

A

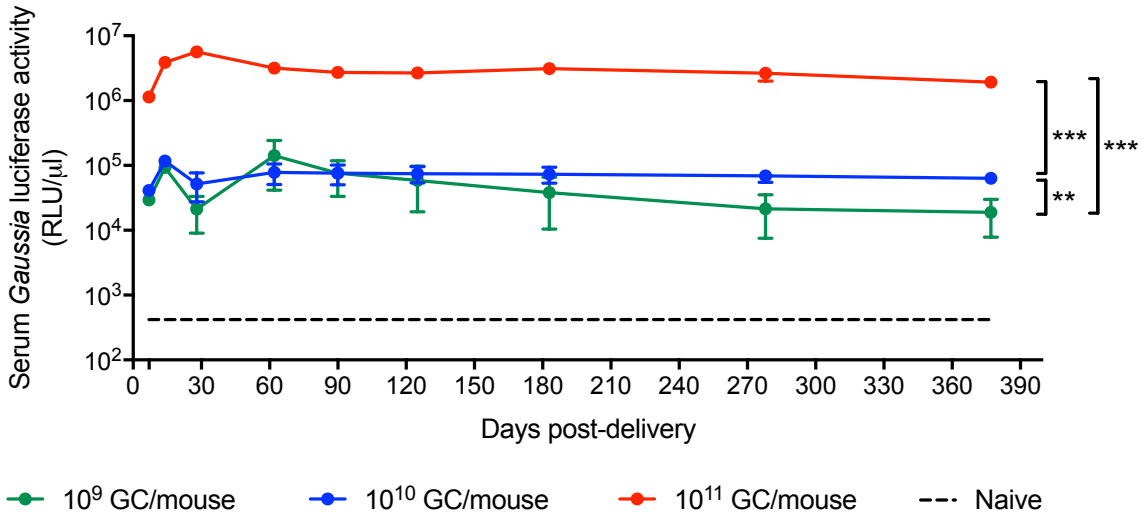
Serum Gaussia luciferase activity (RLU/μl)
10^7
10^6
10^5
10^4
10^3
10^2
0 30 60 90 120 150 180 210 240 270 300 330 360 390
Days post-delivery
***
***
**
10^9 GC/mouse
10^10 GC/mouse
10^11 GC/mouse
Naive

B

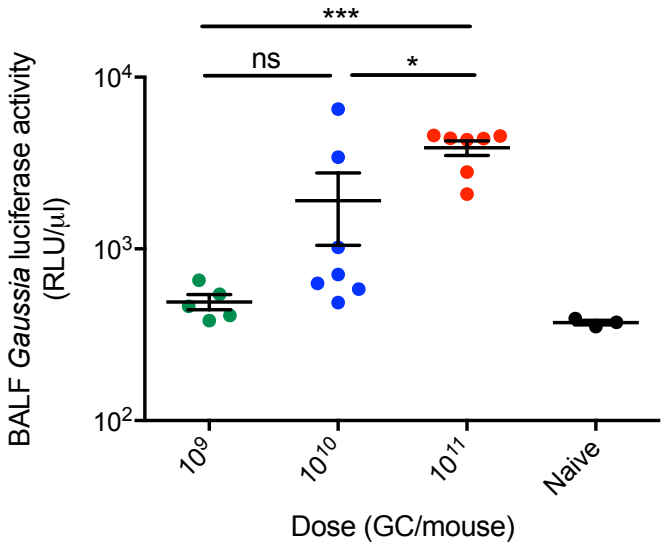
***
ns
*
BALF Gaussia luciferase activity (RLU/μl)
10^4
10^3
10^2
10^9
10^10
10^11
Naive
Dose (GC/mouse)

Figure 3.6. *Gaussia* luciferase activity in the serum and broncho-alveolar lavage fluid after intramuscular injection of rAAV2/8 CASI soGLux.

Female BALB/c mice (n = 12) were administered 10^9, 10^{10} or 10^{11} GC of rAAV2/8 CASI soGLux (Table 2.2) by intramuscular injection (Section 2.6.5.3). *Gaussia* luciferase activity in (A) the serum (Section 2.6.6.1, n = 7-19) and (B) broncho-alveolar lavage fluid (BALF) (Section 2.6.6.2, n = 3-7) collected at 12 months was measured using luminometry (Section 2.7.3). Data are shown as individual values and/or mean ± standard error of the mean. Statistical differences between groups were analysed by ANOVA on log-transformed data, with (A) Tukey's or (B) Dunn's post hoc test. A calculated p value of >0.05 was deemed non-significant as indicated with ns on figures. Calculated p values of <0.05, <0.01 or <0.001 were deemed a significant difference as indicated with one star (*), two stars (**) or three stars (***), respectively.

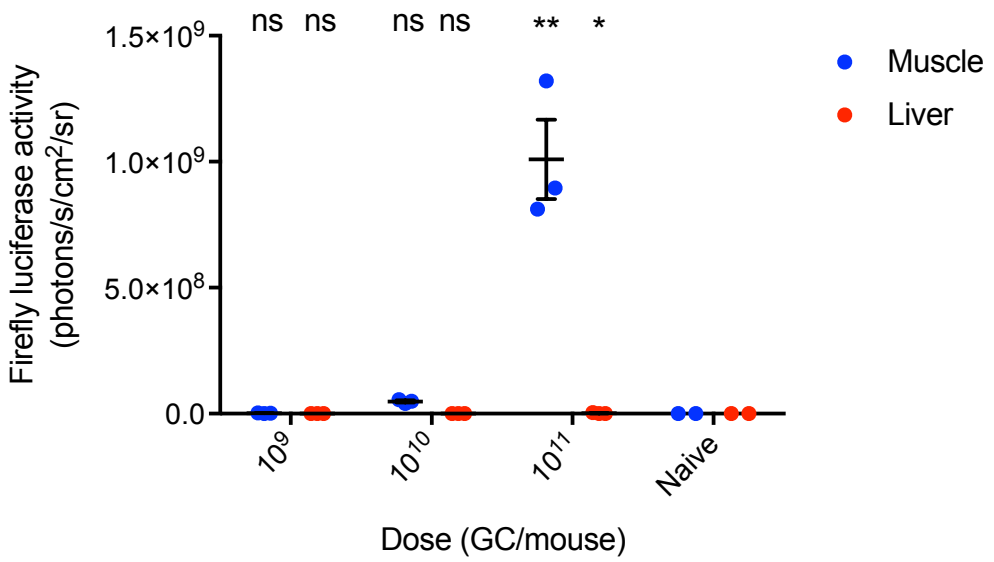

Figure 3.7. Luciferase activity in muscle and liver after intramuscular injection of rAAV2/8 CASI EGFPLux.

Female BALB/c mice (n = 3) were administered 10^9, 10^{10} or 10^{11} GC of rAAV2/8 CASI EGFPLux (Table 2.2) by intramuscular injection (Section 2.6.5.3). Twenty-eight days after administration, luciferase activity in the injected muscle and liver was measured using *in vivo* bioluminescence imaging (BLI) (Section 2.6.8, n = 3). Data are shown as individual values and mean ± standard error of the mean. Statistical differences between groups were analysed by Kruskal-Wallis test, with Dunn's post hoc test, compared with naïve values. A calculated p value of >0.05 was deemed non-significant as indicated with ns on figures. Calculated p values of <0.05 or <0.01 were deemed a significant difference as indicated with one star (*) or two stars (**), respectively.

3.2.5 Investigation into optimal method of administration of rAAV2/8 and rSIV.F/HN vectors

The IN delivery of rSIV.F/HN vector incorporating the hCEF promoter, and IM delivery of rAAV2/8 incorporating the CASI promoter were developed for delivery into the lung and muscle, respectively, based on experience and published results. However, it is possible that alternative administration routes for these vectors could result in higher secretory protein expression in the serum and/or lung lumen. For example, the rAAV2/8 vector was successful at producing therapeutic levels of factor IX when delivered intravenously (IV) in haemophilia B patients in a clinical trial (Nathwani et al., 2014). Therefore, a comparison of secretory protein levels following administration of the two vectors via different routes was performed. Mice were dosed with 10^{11} GC rAAV2/8 CASI soGLux (Table 2.2) via IM or IV injection (Sections 2.6.5.3 and 2.6.5.4), or with 10^{8} TTU of rSIV.F/HN hCEF soGLux (Table 2.2) via IN (Section 2.6.5.1), IM or IV delivery. Figure 3.8 A shows that highest GLux activity in the serum was achieved using rAAV2/8 CASI soGLux via the IM or IV route ($p<0.0001$). Lower but significant activity in the serum was also measured with IN delivery of rSIV.F/HN hCEF soGLux ($p<0.0001$), while no expression was observed when the vector was administered IM or IV ($p>0.05$). The highest level of GLux activity in BALF was achieved with IN administration of rSIV.F/HN hCEF soGLux ($p<0.0001$, Figure 3.8 B). Reporter activity in the BALF was also observed following rAAV2/8 CASI soGLux delivery via IM and IV injection ($p<0.0001$). Although IV injection of rAAV2/8 CASI soGLux achieved marginally higher activity in the serum compared with IM injection, this route of administration is more invasive and difficult to perform in mice, and the IM route is preferred for this vector. Detectable activity in the serum and BALF with rSIV.F/HN hCEF

soGLux was only observed when using the IN route. Therefore, this is the preferred delivery method of this vector for the purpose of expressing secretory protein.

3.2.6 Effect of serotype and promoter on secretory reporter protein *Gaussia* luciferase (GLux) expression following rAAV delivery to the lung

In Sections 3.2.2 and 3.2.5, rSIV.F/HN and rAAV2/8 were investigated for delivery of secretory reporter protein to the circulation and lung lumen. Administration of rAAV2/8 IM emerged as the most suitable method for delivery of protein to circulation, whilst rSIV.F/HN was preferred for expression of GLux in the lung lumen. Recombinant AAV2/8 was not tested for IN delivery in this thesis, as serotype 8 does not have a high tropism for the lung (Zincarelli et al., 2008). Serotype 9, on the other hand, has been demonstrated to efficiently transduce airway epithelia and direct sufficient expression of an anti-influenza mAb to protect mice and ferrets from infection with the virus (Limberis et al., 2013). An experiment was therefore undertaken to determine whether rAAV2/9 would be superior to rSIV.F/HN at directing secretory protein expression from the lung. Mice were administered 10^9, 10^{10} or 10^{11} GC of rAAV2/9 hCEFI soGLux (Table 2.2) via IN instillation (Section 2.6.5.1) and serum GLux activity measured for 4 months and in the BALF at the end of the experiment (Section 2.7.3).

A

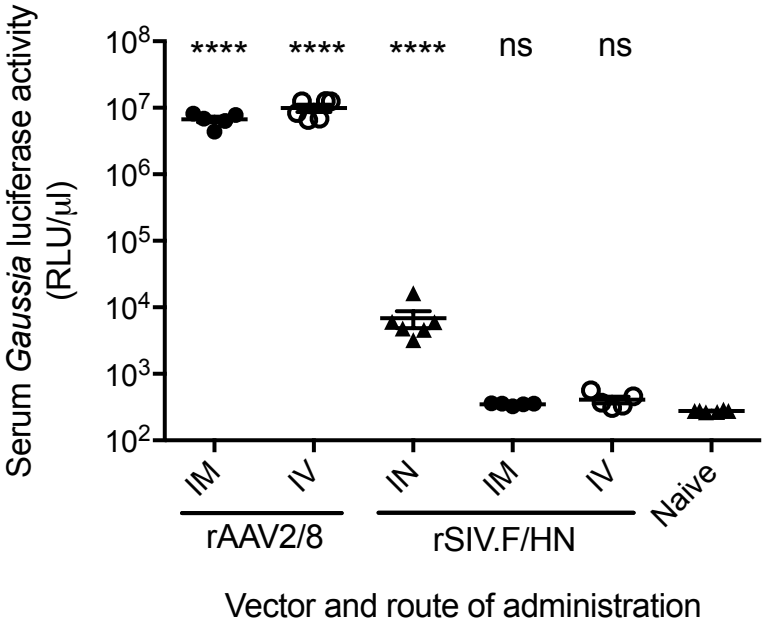
Serum Gaussia luciferase activity (RLU/μl)
10^8
10^7
10^6
10^5
10^4
10^3
10^2
**** **** **** ns ns
IM IV IN IM IV Naive
rAAV2/8
rSIV.F/HN
Vector and route of administration

B

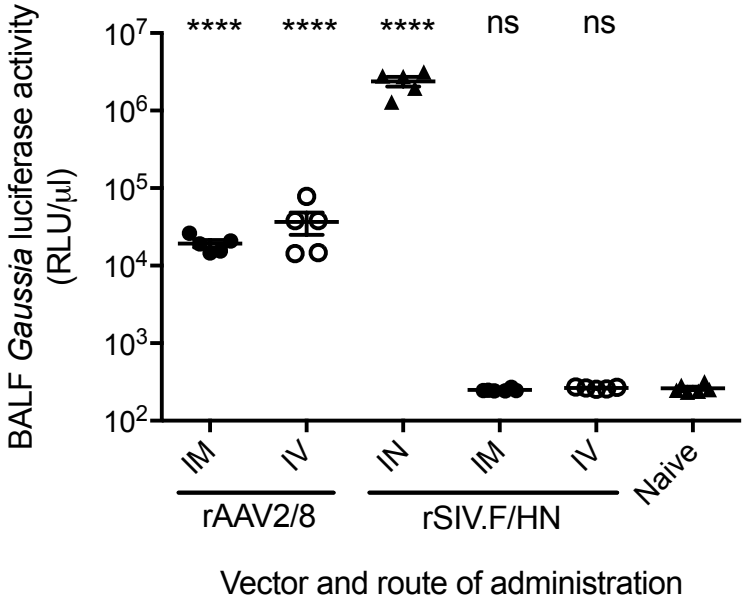
BALF Gaussia luciferase activity (RLU/μl)
10^7
10^6
10^5
10^4
10^3
10^2
**** **** **** ns ns
IM IV IN IM IV Naive
rAAV2/8
rSIV.F/HN
Vector and route of administration

Figure 3.8. *Gaussia* luciferase activity in the serum and broncho-alveolar lavage fluid after rSIV.F/HN hCEF soGLux and rAAV2/8 CASI soGLux administration via different routes.

Female BALB/c mice (n = 6) were administered 10^8 TTU of rSIV.F/HN hCEF soGLux (Table 2.2) via intranasal instillation (IN) (Section 2.6.5.1), intramuscular injection (IM) (Section 2.6.5.3) or intravenous injection (IV) (Section 2.6.5.4), or 10^{11} GC of rAAV2/8 CASI soGLux (Table 2.2) by IM or IV injection. Fifty-seven days after administration, *Gaussia* luciferase activity in (A) the serum (Section 2.6.6.1) and (B) broncho-alveolar lavage fluid (BALF) (Section 2.6.6.2) was measured using luminometry (Section 2.7.3, n = 5-6). Data are shown as individual values and mean ± standard error of the mean. Statistical differences between groups were analysed by ANOVA on log-transformed data with Dunnett's post hoc test, compared with naïve values. A calculated p value of >0.05 was deemed non-significant as indicated with ns on figures. A calculated p value of <0.0001 was deemed a significant difference as indicated with four stars (****).

As shown in Figure 3.9 A, dose-dependent expression of GLux in the circulation was observed, with sustained and significant secretion for at least 4 months following delivery of 10^{10} and 10^{11} GC of rAAV2/9 ($p<0.001$). Significant expression of the reporter was also detected in the BALF for all three doses (Figure 3.9 B). To compare the three delivery platforms (rAAV2/8 IM, rSIV.F/HN IN and rAAV2/9 IN), GLux levels achieved in the serum at 4 months post-delivery of each vector are shown in Figure 3.10 A. At this timepoint, rAAV2/8 delivered IM was superior for expression into circulation, yielding 25-fold higher levels than rAAV2/9 delivered IN ($p<0.001$), which in turn expressed 54-fold higher levels than rSIV.F/HN delivered IN ($p<0.001$). GLux levels in the BALF at the time of harvest were also compared for the three vectors (Figure 3.10 B). At 12 months post-delivery, rSIV.F/HN directed 25% higher levels of GLux expression in the lung lumen compared to rAAV2/9 at 4 months post-delivery, although this difference was not significant. Both vectors yielded over 700-fold higher GLux levels in the lung lumen than rAAV2/8 delivered IM (measured at 12 months post-delivery; $p<0.001$). Recombinant AAV2/8 delivered IM was therefore confirmed as the preferred platform for expression of protein into circulation, whilst rSIV.F/HN and rAAV2/9 delivered IN were approximately equivalent for secretion into lung lumen.

A

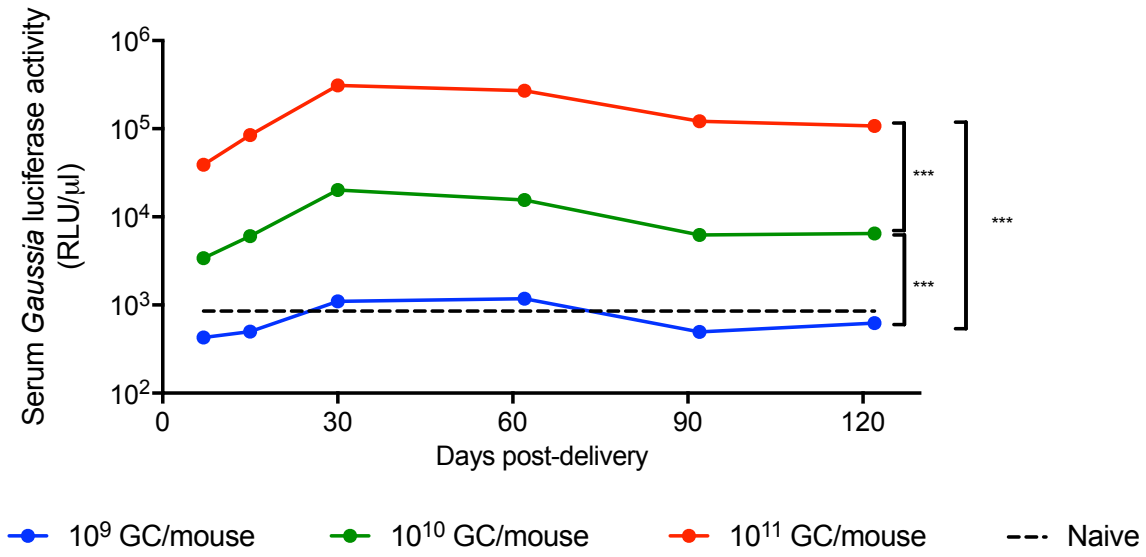
Serum Gaussia luciferase activity (RLU/μl)
10^6
10^5
10^4
10^3
10^2
0
30
60
90
120
Days post-delivery
***
***
***
10^9 GC/mouse
10^10 GC/mouse
10^11 GC/mouse
Naive

B

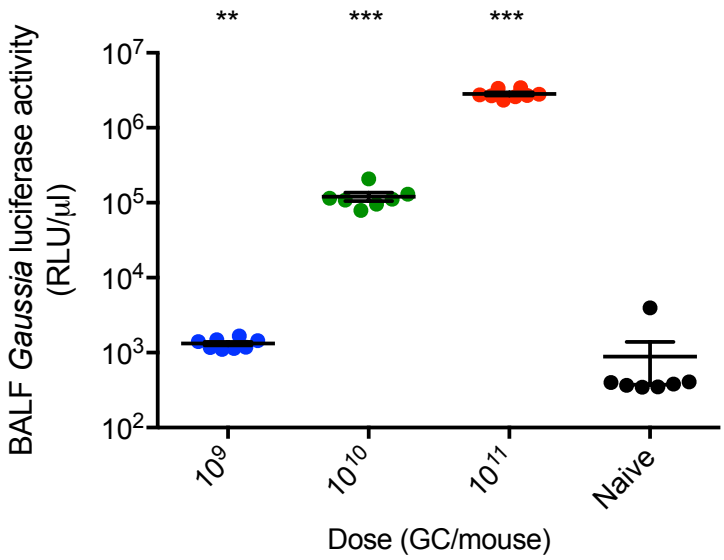
BALF Gaussia luciferase activity (RLU/μl)
10^7
10^6
10^5
10^4
10^3
10^2
**
***
***
10^9
10^10
10^11
Naive
Dose (GC/mouse)

Figure 3.9. Expression of *Gaussia* luciferase in the serum and broncho-alveolar lavage fluid after administration of rAAV2/9.

Female BALB/c mice (n = 8) were administered 10^9, 10^{10} or 10^{11} GC rAAV2/9 hCEFI soGLux (Table 2.2) via intranasal instillation (Section 2.6.5.1). Serum was sampled at the indicated time-points (Section 2.6.6.1) and broncho-alveolar lavage fluid (BALF) collected at 4 months after delivery (Section 2.6.6.2). *Gaussia* luciferase activity in the serum (A) and BALF (B) was measured using luminometry (Section 2.7.3). Data are shown as individual values and/or mean ± standard error of the mean. Statistical differences between groups were analysed by ANOVA on log-transformed data, with (A) Tukey's or (B) Dunn's post hoc test, compared with naïve values. Calculated p values of <0.01 or <0.001 were deemed a significant difference as indicated with two stars (**) or three stars (***), respectively.

A

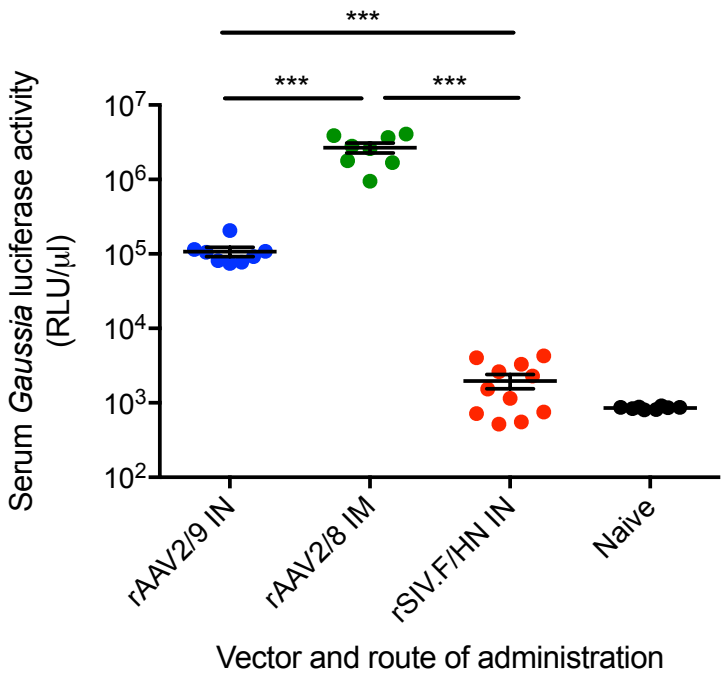
***
***
***
Serum Gaussia luciferase activity
(RLU/μl)
10^7
10^6
10^5
10^4
10^3
10^2
rAAV2/9 IN
rAAV2/8 IM
rSIV.F/HN IN
Naive
Vector and route of administration

B

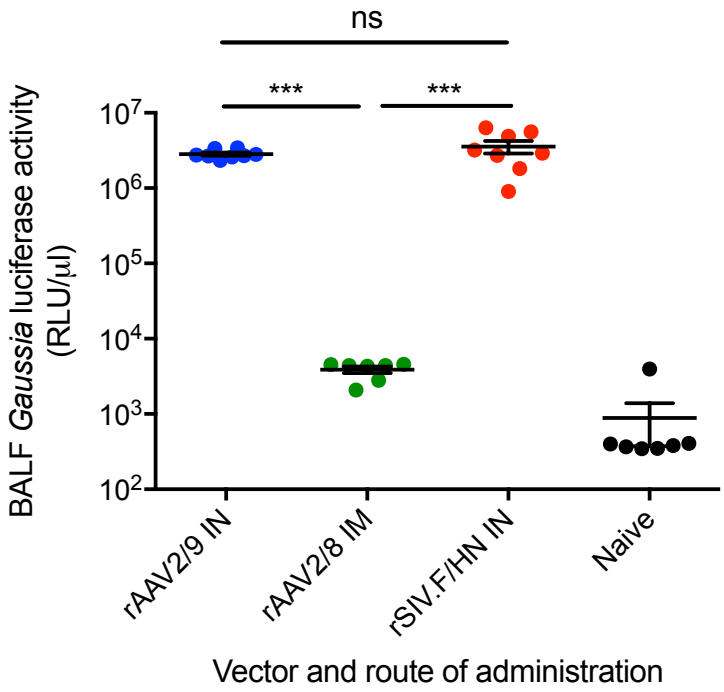
ns
***
***
BALF Gaussia luciferase activity
(RLU/μl)
10^7
10^6
10^5
10^4
10^3
10^2
rAAV2/9 IN
rAAV2/8 IM
rSIV.F/HN IN
Naive
Vector and route of administration

Figure 3.10. Comparison of *Gaussia* luciferase activity in the serum broncho-alveolar lavage fluid after administration of rAAV2/8, rAAV2/9 and rSIV.F/HN. Female BALB/c mice (n = 8-11) were administered 10^{11} GC of rAAV2/9 hCEFI soGLux via intranasal instillation (rAAV2/9 IN), 10^{11} GC of rAAV2/8 CASI soGLux by intramuscular injection (rAAV2/8 IM) (Section 2.6.5.3) or 10^{8} TTU of rSIV.F/HN hCEF soGLux via IN instillation (rSIV.F/HN IN) (Section 2.6.5.1). (A) *Gaussia* luciferase (GLux) activity in the serum (Section 2.6.6.1) at 28 days post-delivery was measured using luminometry (Section 2.7.3). (B) Broncho-alveolar lavage fluid (BALF) was collected (Section 2.6.6.2) 4 (rAAV2/9 IN) or 12 (rAAV2/8 IM and rSIV.F/HN) months after vector administration and GLux activity measured. Data are shown as individual values and mean ± standard error of the mean. Statistical differences between groups were analysed by ANOVA on log-transformed data, with Bonferroni's post hoc test. A calculated p value of >0.05 was deemed non-significant as indicated with ns on figures. A calculated p value of <0.001 was deemed a significant difference as indicated with three stars (***).

Recombinant AAV2/8 used in the above experiments utilised the CASI promoter, whilst rAAV2/9 and rSIV.F/HN vectors utilised the hCEF promoter. To determine whether expression levels from the lung could be improved by using the CASI promoter, rAAV2/9 CASI soGLux vector (Table 2.2) was manufactured (Section 2.5.3) and delivered into mice via the IN route. Levels of GLux in the serum and BALF were measured 28 days after administration and compared with serum and BALF collected at 28 days and 4 months, respectively, after administration of rAAV2/9 hCEFI soGLux. As shown in Figure 3.11, the hCEFI promoter is superior to CASI at directing expression of GLux from the lung into both serum (A) and BALF (B), yielding approximately 2-3-fold higher reporter activity in those two compartments for the top dose (10^{11} GC) of each vector ($p<0.0001$). The hCEFI promoter is therefore preferred to CASI for expression of secretory protein from the lung. Its activity in the muscle compared to CASI also ought to be investigated.

A

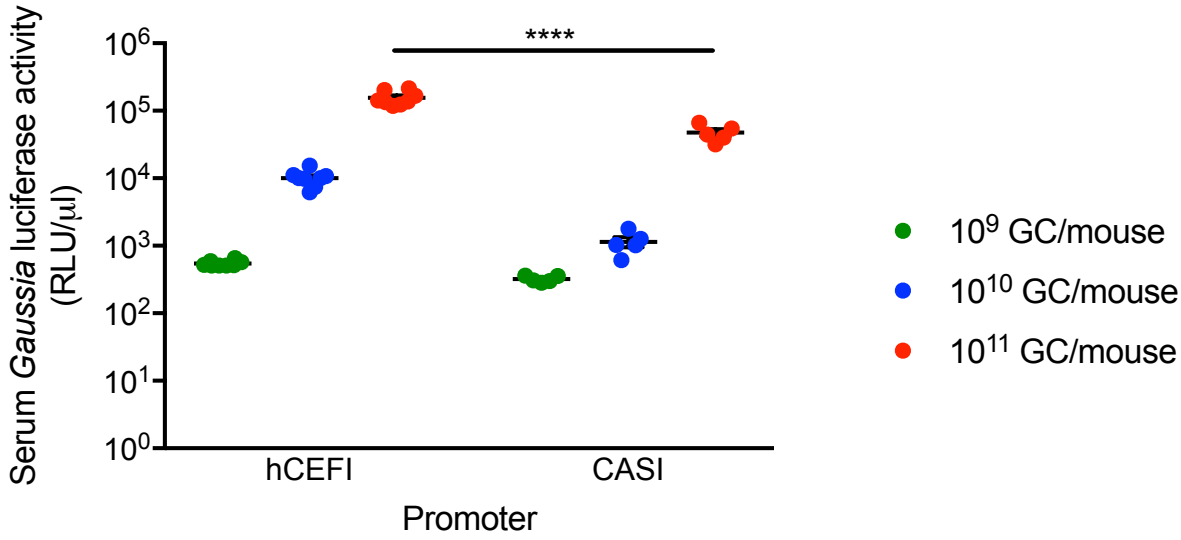
Serum Gaussia luciferase activity (RLU/µl)
10^6
10^5
10^4
10^3
10^2
10^1
10^0
****
hCEFI
CASI
Promoter
10^9 GC/mouse
10^10 GC/mouse
10^11 GC/mouse

B

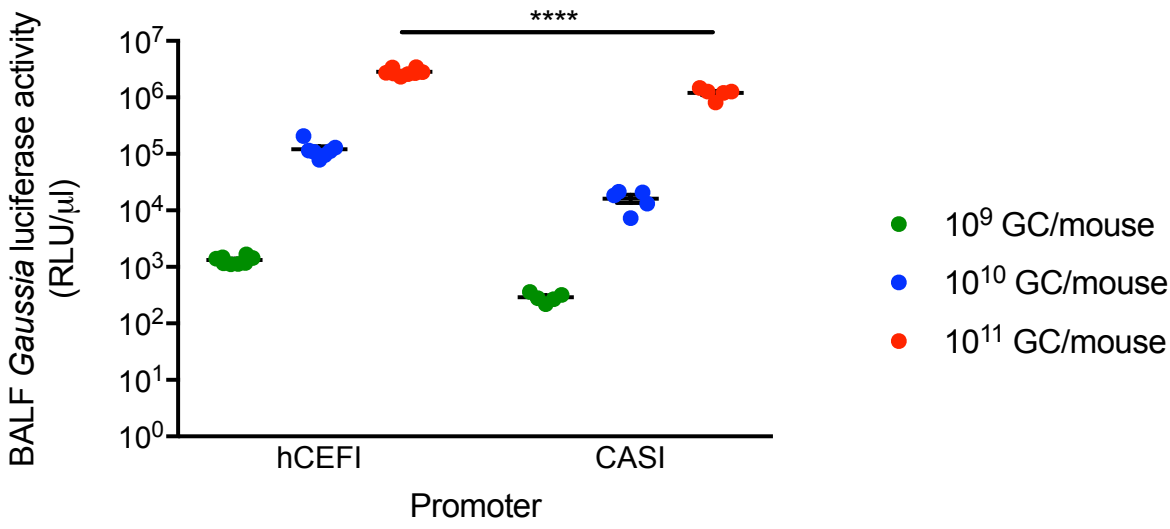
BALF Gaussia luciferase activity (RLU/µl)
10^7
10^6
10^5
10^4
10^3
10^2
10^1
10^0
****
hCEFI
CASI
Promoter
10^9 GC/mouse
10^10 GC/mouse
10^11 GC/mouse

Figure 3.11. Comparison of *Gaussia* luciferase activity in the serum and broncho-alveolar lavage fluid as directed by hCEFI and CASI promoters after administration of rAAV2/9 to the lung.

Female BALB/c mice (n = 5-8) were administered 10^9 (green), 10^{10} (blue) or 10^{11} (red) GC of rAAV2/9 hCEFI soGLux (hCEFI) or rAAV2/9 CASI soGLux (CASI) (Table 2.2) via intranasal instillation (Section 2.6.5.1). Levels of GLux activity in the serum (A) and broncho-alveolar lavage fluid (BALF; B) at 28 days post-delivery were measured using luminometry (Section 2.7.3). Data are shown as individual values and mean ± standard error of the mean. Statistical differences between the high dose groups (10^{11} GC) were analysed by Student's t-test on log-transformed data. A calculated p value of <0.0001 was deemed a significant difference as indicated with four stars (****).

3.3 Discussion

3.3.1 Non-viral gene transfer agents for delivery of secretory protein

The studies described in this chapter evaluated selected non-viral and viral gene delivery platforms as potential methods for establishing protein factories. Two non-viral formulations were investigated for delivery to the lung, selected on the basis of their efficient airway gene transfer in a large animal model (McLachlan et al., 2011) and, in the case of GL67A lipoplexes, safe use in clinical trials (Alton et al., 2015). Plasmid/GL67A complexes were initially selected since secretion of GLux into serum after nasal instillation of pDNA/GL67A polyplexes to mice has previously been demonstrated (Griesenbach et al., 2011). However, this formulation is associated with inflammation in the mouse lung (Eastman et al., 1997). Therefore, the preferred pDNA/GL67A aerosol formulation, which is safe in humans and capable of stabilising lung function of CF patients (Alton et al., 2015), was selected. However, no significant GLux expression was observed in the serum or lung lumen of mice following pG4.hCEFI.soGLux/GL67A aerosol delivery (Figure 3.2).

Non-viral formulations are continually being developed for delivery to the lung and other compartments, and optimisation of the plasmid sequence has the potential to increase the levels and persistence of transgene expression. It was previously shown that a minimal 93 bp region of the hC enhancer recapitulated the expression profile of the full-length sequence, and that a tandem dual minimal enhancer increased expression levels seven-fold relative to the single 93 bp sequence (Oliveira, 2015). Here, the effect of additional copies of the minimal 93 bp enhancer placed in tandem was investigated, but inclusion of three or four tandem minimal

enhancers did not result in an increase in gene expression following a pDNA/PEI aerosol (Figure 3.3), indicating that this type of modification was unlikely to lead to improved secretory protein expression in the mouse lung. The combination of novel, efficient, non-viral transfection agents with optimised plasmid sequences could be further explored for *in vivo* gene transfer for secretory protein production, but for the remainder of the studies described here, viral vectors were investigated.

3.3.2 Transduction profile of rSIV.F/HN in murine lung

The relatively poor efficiencies of non-viral vectors such as PEI and GL67A in the mouse lung mean that it has been difficult to identify the transfected cell types (Davies et al., 2007). However, high transduction rates achieved with viral vectors make it possible to identify transduced cells. Studies described in Section 3.2.3 investigated the transduction profile in the mouse lung at two time-points following administration of rSIV.F/HN. In agreement with the previously published report (Alton et al., 2017), the vector was found to transduce all of the investigated cell types (club, ciliated, goblet, type I and type II alveolar cells), with the exception of basal cells, suggesting inefficiency of transducing this cell type. A number of additional observations were also made. Firstly, there was an apparent difference in transduction rates of club cells at 7 days and 2 months after vector delivery (Figure 3.5). As club cells give rise to ciliated and goblet cells (Montoro et al., 2018, Rock et al., 2009), it is possible that differentiation of club cells is responsible for the reduction in the proportion of EGFP-positive club cells between the two analysis time-points.

Secondly, very few EGFP-positive ATI cells were identified in sections from any of the animals. Acquisition of ten images of the alveolar region at random did not capture any transduced ATI cells in the examined sections, and these cells could only be identified by direct localisation using the EGFP channel. This indicated a very low transduction rate which could not be quantified using the method employed in this study (Section 2.6.9.3). A more suitable method of quantifying the rates of transduction of these cells by rSIV.F/HN could be using a fully-automated fluorescence microscope, which would allow visualisation of the whole lung section and thus of all transduced ATI cells in a particular plane. The relative proportion of these cells which are transduced by the vector, albeit low, could then be quantified.

Thirdly, very low numbers of goblet cells, EGFP-positive or negative, could be identified at 2 months after administration of rSIV.F/HN, indicating that these cells are turned over within that period, either as a result of vector administration or ageing. Lastly, no transduced basal cells could be identified at either time-point. Although Alton et al. reported EGFP-positive basal cells, they noted their rarity (Alton et al., 2017); elsewhere, it was reported that basal cell transduction *in vivo* could only be achieved after pre-treatment of mouse airways with polidocanol, which removes the epithelium to expose basal cells (Leoni et al., 2015). Thus, the inability to identify transduced basal cells in the studies described in this chapter (Figure 3.5) is consistent with these findings. Interestingly, no basal cells could be identified 7 days after dosing of rSIV.F/HN. Although these cells are thought to be mainly confined to the trachea in mice (Rock et al., 2009), they have been detected in the murine bronchi (Alton et al., 2017, Hong et al., 2004), and abundant basal cells were detected at the 2-month time-point in this study (Figure 3.5). Wu et al. observed that porcine basal cells maintained in an air-liquid interface culture

system would be stimulated to differentiate into specialised cells upon infection with influenza virus (Wu et al., 2016). It is possible that administration of rSIV.F/HN stimulated basal cells in the mouse lung to differentiate such that few would be detectable at 7 days post-transduction and that by 2 months after administration their population would have expanded again.

Another potential explanation for the discrepancy between the presence of basal cells in sections from those two time-points could be a developmental one. It has been reported that the distribution of basal cells in respiratory epithelium of mice shifts with age such that basal cell numbers decline in the trachea of mice between 3 and 22 months of age (Wansleeben et al., 2014). In the study performed in this thesis, animals from the 7-day treatment group were between 6 and 8 weeks of age, while animals from the 2-month treatment cohort were 7 weeks older. The distribution of basal cells in their airways could therefore have shifted, resulting in these cells only being identifiable in the 2-month group. Whilst it was reported that transduced basal cells could be observed at 7 days after rSIV.F/HN delivery (Alton et al., 2017), the age of the animals at the time of procedure was also not stated. It is possible that the difference in age is responsible for the observed discrepancy in basal cell numbers in the lung at 7 weeks and 2 months. As naïve mice were only harvested at a single time-point, it was not possible to determine whether vector administration or age-related changes were responsible for the observed lack of basal cells at day 7, or the very low numbers of goblet cells at 2 months after delivery of rSIV.F/HN.

In this chapter, the six main cell types in the lung were investigated: club, goblet, ciliated and basal cells of the airway, and ATI and ATII cells of the parenchyma.

Other rarer cells types have been identified in the mouse and human lung, including tuft (also known as brush) cells and ionocytes, thought to function in osmotic homeostasis (Montoro et al., 2018, Plasschaert et al., 2018). Currently, it is unknown whether these rare cells are transduced by rSIV.F/HN and contribute to secretory protein expression following rSIV.F/HN administration.

3.3.3 Gene transfer platforms for delivery of secretory protein to circulation and lung lumen

Several gene transfer platforms were compared to evaluate expression of the secreted reporter GLux into the circulation and lung lumen. The rAAV serotypes 8 and 9 were selected for study based on their reported efficiency of gene transfer in the murine muscle and lung, respectively, and ability to direct therapeutically relevant levels of mAb expression in mice (Sections 1.1.5.4 and 3.1). In this study, rAAV2/8 administered via IM injection led to the highest GLux levels in the circulation, with robust and sustained secretion observed for at least 12 months (Figure 3.6 A). Furthermore, rAAV2/8 delivered IM was reported to direct expression of a mAb in mice for 64 weeks (Balazs et al., 2013). For secretion of protein to the lung lumen, rSIV.F/HN and rAAV2/9 vectors delivered IN were equivalent (Figure 3.10 B). Duration of expression from rAAV2/9 was only confirmed at 4 months, whilst rSIV.F/HN was shown to direct GLux expression in BALF for at least 12 months (Figure 3.4), and was thus selected for further study. It was decided to investigate both platforms (rAAV2/8 delivered IM and rSIV.F/HN delivered IN) for expression of mAbs in two model applications in the following chapters.

In future studies, novel rAAV serotypes, developed through approaches like rational design and directed evolution for more targeted tropism, superior transduction efficiency and/or reduced seropositivity in the human population, could be investigated for secretory protein expression. A number of such AAV serotypes were developed for muscle gene therapy, and were reported to exhibit up to 84-fold higher transduction efficiency in the human muscle *ex vivo* and reduced humoral seroreactivity, compared to serotype 8 (Paulk et al., 2018a). Use of such serotypes for expression of mAbs from skeletal muscle could allow achievement of therapeutically relevant expression levels with lower vector doses, potentially translating into reduced cost of treatment per patient.

Chapter 4: Development of palivizumab factories for prophylaxis of RSV infection

4.1 Introduction

Respiratory syncytial virus (RSV) is a prevalent respiratory pathogen causing hospitalisations in young children and the elderly. As described in Section 1.2.3.2, prophylaxis with the mAb palivizumab is practised in the absence of a licensed vaccine. This chapter describes studies using RSV infection to evaluate the potential of selected gene transfer agents to deliver therapeutic mAbs *in vivo*. Because RSV infections begin in the respiratory tract, which is also the main site of viral replication, the presence of neutralising mAbs might be advantageous in the fluid lining the lung, as well as in the circulation. Indeed, it has been reported that levels of anti-RSV IgG in the nasal mucosa are more strongly inversely correlated with the severity of infection in infants than serum IgG levels (Vissers et al., 2016). For this reason, both vectors delivering mAb genes to the lung for local production and those mediating systemic delivery could be useful for protection against RSV infection.

Based on the results of studies in Chapter 3 using the secretory reporter GLux, two viral vectors were selected for gene transfer of palivizumab: rSIV.F/HN and rAAV2/8, delivered to the lung and muscle, respectively. Palivizumab expression levels achieved by these vectors *in vivo* must reach a certain target level to be protective against RSV infection, and this can be evaluated in an animal model. Several models of RSV infection are available, including murine, bovine and NHP models (reviewed in Taylor, 2017). Inbred mouse strains are permissive for RSV

replication to varying degrees (Prince et al., 1979). BALB/c mice are semi-permissive to infection and exhibit clinical signs such as weight loss and increased respiratory rate when challenged with a sufficiently high (10^6 to 2 x 10^7 ffu) dose of RSV (van Schaik et al., 1998). Functional readouts of viral replication and disease severity can include measurement of weight loss, enumeration of inflammatory cells and mediators in the BALF, and quantification of viral titres using plaque assay or polymerase chain reaction (PCR) (Openshaw, 2013). Due to the ease of use, the BALB/c strain was selected to model protection against RSV infection.

The aims of the experiments presented in this chapter included: (i) to generate palivizumab-expressing rSIV.F/HN and rAAV2/8 vectors, (ii) to measure palivizumab levels in the serum and BALF following vector delivery to mice and (iii) to determine whether the levels of palivizumab produced *in vivo* are protective against RSV infection in an animal model.

4.2 Results

4.2.1 Production and validation of rSIV.F/HN and rAAV2/8 vectors expressing palivizumab

Due to the packaging constraints of rAAV, the single-open reading frame (ORF) strategy (Fang et al., 2005) (Figure 4.1), in which the light and heavy chain sequences are fused with a cleavage site combining the 2A self-processing peptide derived from the foot-and-mouth disease virus, and furin target sequence, was used to design mAb cDNAs in this thesis. Palivizumab cDNA was constructed from

the original heavy and light chain sequences (Johnson et al., 1997) (Appendix) using MacVector software, codon-optimised for *Homo sapiens*, depleted of CpG dinucleotides and synthesised by GeneArt (Thermo Fisher Scientific). The transgene was sub-cloned as described in Section 2.3.5 to generate the rSIV genome plasmid pSIV.hCEF.palivizumab and the rAAV genome plasmid pAAV2.CASI.palivizumab (Table 2.1; Figure 4.2). When used to transfect HEK293T cells (Section 2.4.2), both genome plasmids directed abundant expression of IgG (Section 2.7.4), as shown in Figure 4.3. Production of rAAV2/8 and rSIV.F/HN viral vectors was therefore performed using the respective genome plasmids. The rAAV2/8 CASI palivizumab (Table 2.2) was produced in adherent HEK293T cells cultured in HYPERFlasks and purified from cell lysates using a two-step process (Section 2.5.4), resulting in a highly concentrated preparation. Purity was confirmed using SDS-PAGE (Section 2.7.6.2). The rSIV.F/HN hCEF palivizumab (Table 2.2) was produced by Steve Hyde in suspension HEK293T cells cultured in serum-free media in a WAVE bioreactor and purified from the supernatants with a two-step process (Section 2.5.2). Titres of both vectors were determined using TaqMan real-time PCR assay (Sections 2.5.3 and 2.5.5) with the assistance of Ian Pringle and Eoin Mac Ráemoinn and expressed as genome copies (GC) or TaqMan transducing units (TTU) per unit volume for rAAV and rLV, respectively.

Vectors rAAV2/8 CASI palivizumab and rSIV.F/HN hCEF palivizumab (Table 2.2) were used to transduce HEK293T cells and palivizumab levels assessed in the supernatants using human IgG ELISA (Section 2.7.4). As shown in Figure 4.4, both vectors directed expression of the mAb in cell culture, supporting progression to animal studies.

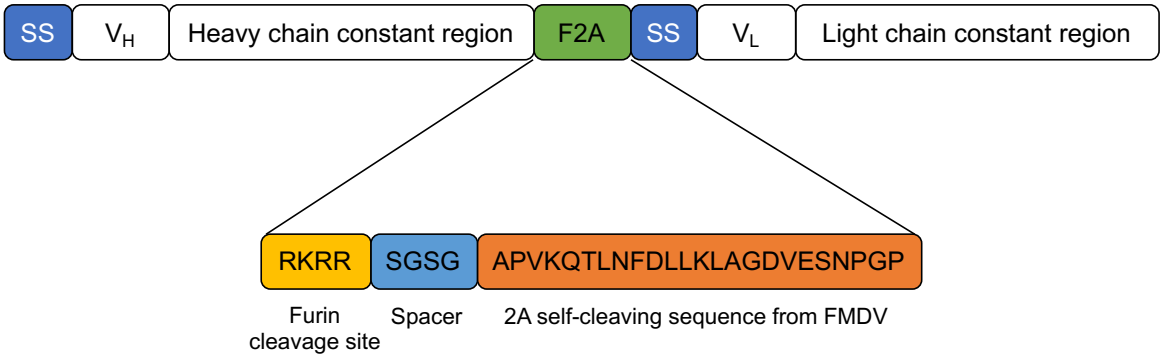

Figure 4.1. Single-ORF antibody expression system.

Both the heavy and light chain sequences of the antibody, consisting of a variable (V_H or V_L) and constant region, are preceded by a signal sequence (SS, dark blue) from the human growth hormone (hGH), which facilitates secretion. The two chains are fused by a cleavage site (F2A, green), which combines the furin target sequence (yellow) with the 2A self-processing peptide derived from the foot-and-mouth disease virus (FMDV, orange), connected by a four-amino acid spacer (light blue).

A

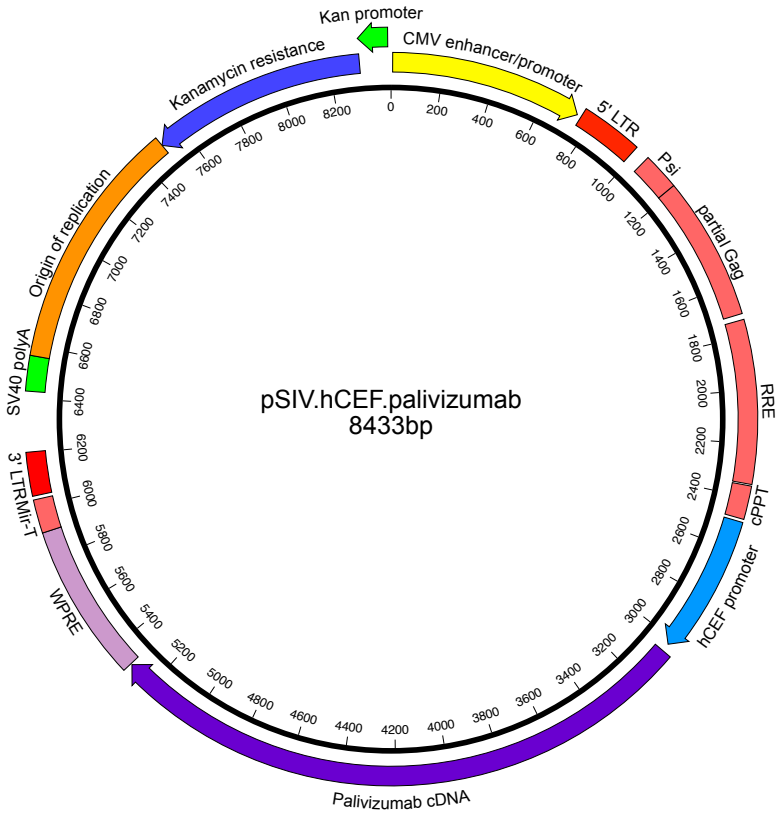
Kan promoter
CMV enhancer/promoter
5' LTR
Psi
partial Gag
RRE
cPPT
hCEF promoter
Palivizumab cDNA
WPRE
Mir-T
3' LTR
SV40 polyA
Origin of replication
Kanamycin resistance
pSIV.hCEF.palivizumab
8433bp

B

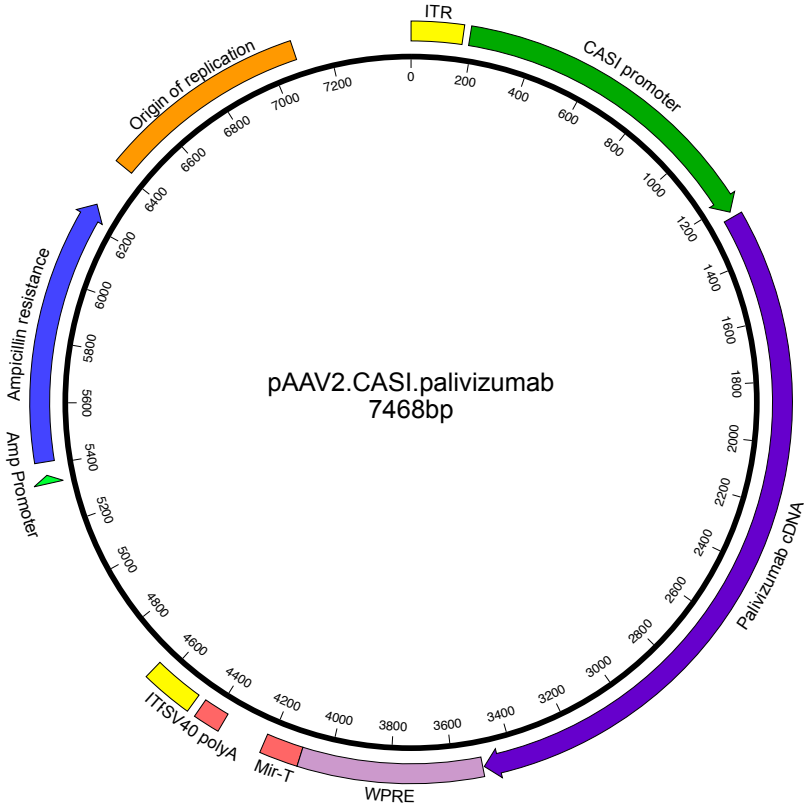
ITR
CASI promoter
Palivizumab cDNA
WPRE
Mir-T
ITR
SV40 polyA
Amp Promoter
Ampicillin resistance
Origin of replication
pAAV2.CASI.palivizumab
7468bp

Figure 4.2. Recombinant lentiviral and rAAV vector genomes encoding palivizumab.

(A) Palivizumab was expressed from the CASI promoter (compound promoter comprising CMV enhancer, chicken β-actin promoter and ubiquitin enhancer) in the rAAV genome plasmid, and (B) from the hCEF promoter (CpG-free version of the human cytomegalovirus (CMV) enhancer with the CpG-free version of the elongation factor 1 alpha (EF1α) promoter) in the rSIV genome plasmid (Table 2.1). WPRE, woodchuck hepatitis virus regulatory element; Mir-T, micro RNA 142-p target sequence; SV40 polyA, simian virus 40 polyadenylation signal; CMV, cytomegalovirus; ITR, inverted terminal repeat; LTR, long terminal repeat; RRE, Rev response element; cPPT, central polypurine tract.

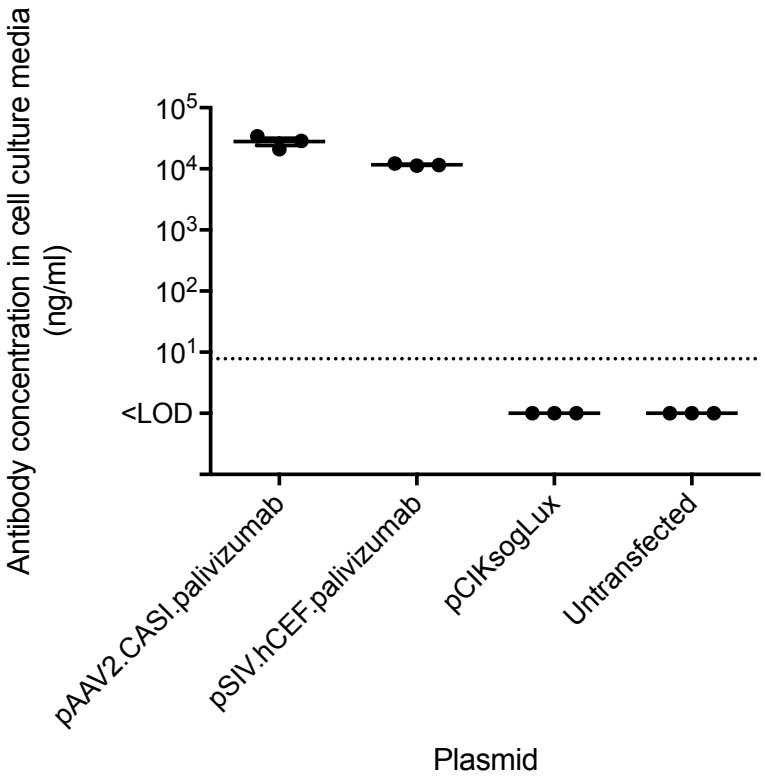

Figure 4.3. Palivizumab expression following transfection of rSIV and rAAV vector genomes in cell culture.

Adherent HEK293T cells (n = 3 wells per group) were transfected (Section 2.4.2) with vector genome plasmids pAAV2.CASI.palivizumab and pSIV.hCEF.palivizumab, along with control plasmid pCIKsoGLux (Table 2.1). Ninety-six hours after transfection, antibody levels in the supernatant was measured using human IgG ELISA (Section 2.7.4). Data are shown as individual values and mean ± standard error of the mean. Dotted line denotes lower limit of detection (7.8 ng/ml).

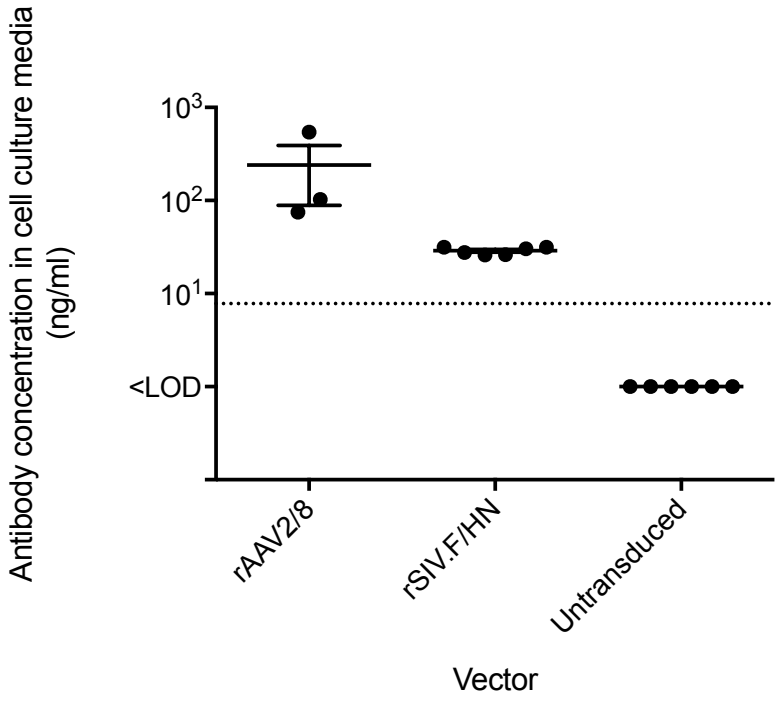

Figure 4.4. Palivizumab expression following transduction of rAAV2/8 and rSIV.F/HN in cell culture.

For rAAV2/8, 5 x 10^5 adherent HEK293T cells were transduced with 10^{10} GC of rAAV2/8 CASI palivizumab (Table 2.2). Six days post-transduction, antibody levels in the supernatant were measured using human IgG ELISA (Section 2.7.4; n = 3). For rSIV.F/HN, 5 x 10^5 HEK293T cells grown in suspension were infected with 10^6 TTUs of rSIV.F/HN hCEF palivizumab (Table 2.2) in the presence of 8 μM polybrene (Sigma-Aldrich). Seven days post-transduction, antibody levels in the supernatant were measured using human IgG ELISA (Section 2.7.4; n = 6). Data are shown as individual values and mean ± standard error of the mean. Dotted line denotes lower limit of detection (7.8 ng/ml).

4.2.2 *In vivo* palivizumab production using rSIV.F/HN and rAAV2/8

The aims of the study described in this section were to measure the level and duration of palivizumab expression from rSIV.F/HN and rAAV2/8 *in vivo* as has been previously observed for the secretory protein GLux with both vectors (Sections 3.2.2 and 3.2.3). Mice were administered three different doses of each vector: 10^9, 10^{10} or 10^{11} GC of rAAV2/8 CASI palivizumab via IM injection (Section 2.6.5.3), or 10^6, 10^7 or 10^8 TTU rSIV.F/HN hCEF palivizumab via IN instillation (Section 2.6.5.1). Blood samples were collected at intervals up to 6 months post-delivery (Section 2.6.6.1). The BALF was also collected (Section 2.6.6.2) from a proportion of mice from each group at 1 month, and from the remainder at the end of the experiment, 6 months after dosing. Palivizumab levels in the serum and BALF samples were determined using human IgG ELISA (Section 2.7.4).

As shown in Figure 4.5 A, IM administration of 10^{10} or 10^{11} GC of rAAV2/8 resulted in robust and sustained expression of palivizumab into circulation, with average serum concentrations of 15.0 and 89.3 µg/ml ($p<0.05$ and $p<0.001$, respectively, compared with naïve mice) at 6 months (Figure 4.5 B). Delivery of the lowest dose (10^9 GC) of the vector initially resulted in marginally detectable expression, which declined to undetectable levels from day 28 onwards. Only marginal levels of palivizumab expression could be detected in the serum of mice administered doses ranging between 10^6 and 10^8 TTU of rSIV.F/HN by IN instillation (Figure 4.5 B). Serum palivizumab levels of 25-30 µg/ml have been reported to reduce RSV titres in the lungs of cotton rats by >99% (Johnson et al., 1997). Comparison of this figure with the levels observed in this study, which reached 89.3 µg/ml in mice

administered 10^{11} GC of rAAV2/8 (Figure 4.5), warranted progression to RSV infection studies in mice (Section 4.2.4).

In the BALF, palivizumab levels were measured at 1 and 6 months post-delivery (Figure 4.5 C & D). For rSIV.F/HN, significant BALF expression was observed at 1 month for the highest dose group (10^8 TTU, $p<0.05$), with average levels of 22 ng/ml. Although not significant, expression was also detected at 6 months, with average levels in the BALF of 15 and 17 ng/ml for mice administered 10^7 and 10^8 TTU of the vector, respectively. In mice administered 10^{10} and 10^{11} GC of rAAV2/8, antibody levels in the BALF reached 18 and 230 ng/ml at 1 month ($p<0.05$ and $p<0.001$, respectively, compared with naïve mice). These levels were sustained for the duration of the experiment, averaging 55 and 324 ng/ml in the BALF of those groups at 6 months ($p<0.05$ and $p<0.001$, respectively, compared with naïve values). Comparison of urea concentration in BALF and serum samples can be used to calculate the dilution factor of BALF relative to epithelial lining fluid (ELF) in the lung (Paul-Smith et al., 2018). Measurement of urea concentration in serum and BALF samples collected using the same methods as in this study (Sections 2.6.6.1 and 2.6.6.2) indicated that the BALF is on average diluted by a factor of 28 relative to the ELF (Tan, 2017). Using this approximate conversion, the ELF levels of the mAb at 6 months post-delivery can be estimated as 9 and 0.5 µg/ml for mice administered the highest dose of rAAV2/8 and rSIV.F/HN, respectively.

A

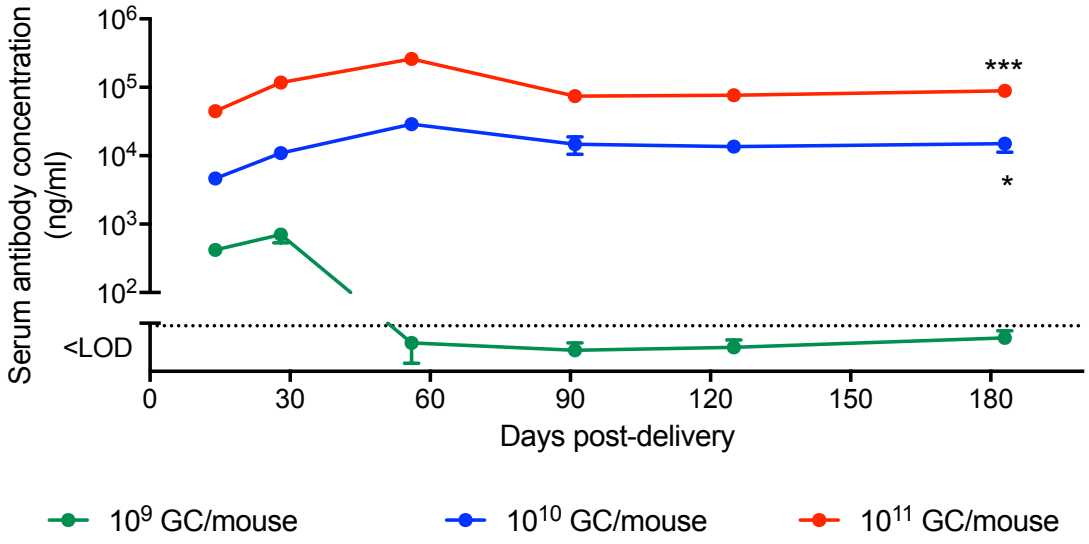
Serum antibody concentration (ng/ml)
10^6
10^5
10^4
10^3
10^2
<LOD
***
*
0
30
60
90
120
150
180
Days post-delivery
10^9 GC/mouse
10^{10} GC/mouse
10^{11} GC/mouse

B

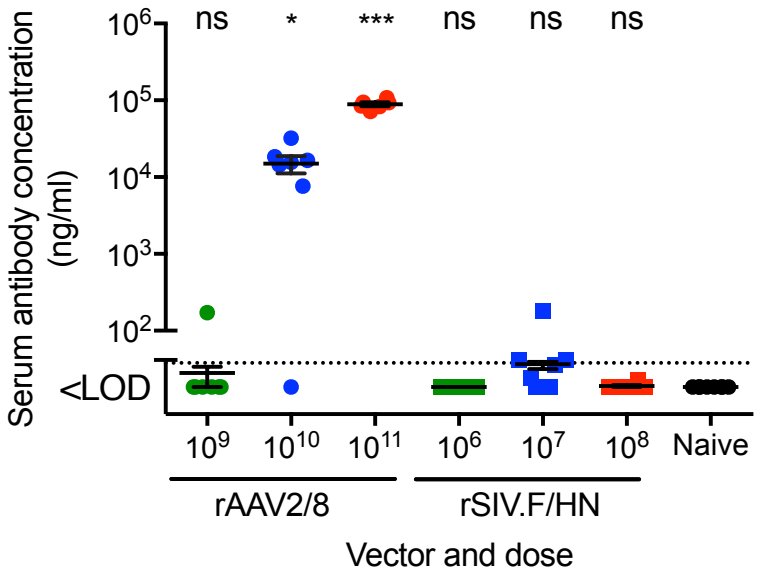
Serum antibody concentration (ng/ml)
10^6
10^5
10^4
10^3
10^2
<LOD
ns
*
***
ns
ns
ns
10^9
10^{10}
10^{11}
10^6
10^7
10^8
Naive
rAAV2/8
rSIV.F/HN
Vector and dose

C

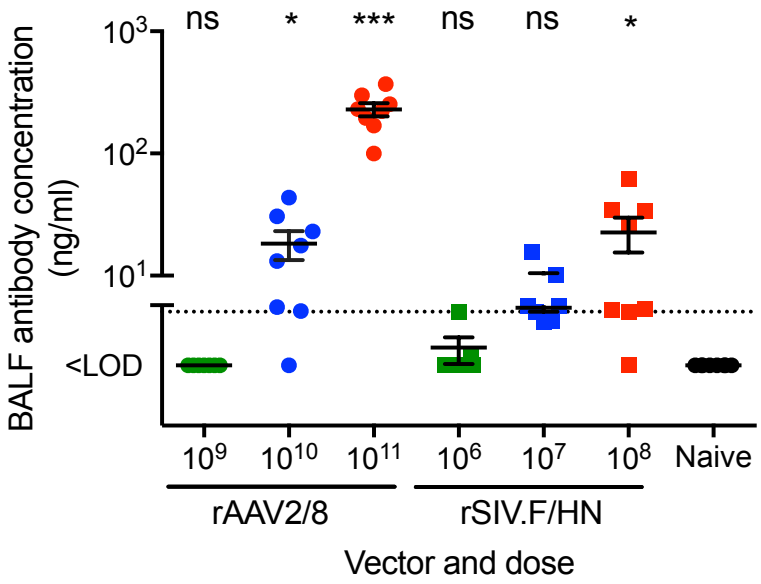
ns
*
***
ns
ns
*
10^3
10^2
10^1
<LOD
BALF antibody concentration (ng/ml)
10^9
10^{10}
10^{11}
10^6
10^7
10^8
Naive
rAAV2/8
rSIV.F/HN
Vector and dose

D

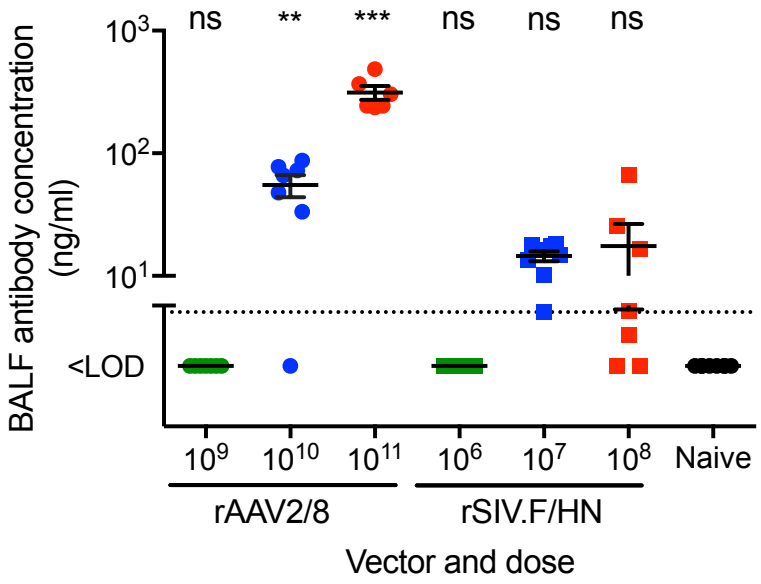
ns
**
***
ns
ns
ns
10^3
10^2
10^1
<LOD
BALF antibody concentration (ng/ml)
10^9
10^{10}
10^{11}
10^6
10^7
10^8
Naive
rAAV2/8
rSIV.F/HN
Vector and dose

Figure 4.5. Palivizumab expression following administration of rAAV2/8 and rSIV.F/HN to mice.

Female BALB/c mice (n = 16) were administered 10^9 (green circles), 10^{10} (blue circles) or 10^{11} (red circles) GC of rAAV2/8 CASI palivizumab via intramuscular injection (Section 2.6.5.3), or 10^6 (green squares), 10^7 (blue squares) or 10^8 (red squares) TTU of rSIV.F/HN hCEF palivizumab via intranasal instillation (Section 2.6.5.1). Serum was obtained by collecting blood (Section 2.6.6.1) at the indicated time-points (A). Eight mice from each group were culled at 1 month post-delivery to obtain broncho-alveolar lavage fluid (BALF), whilst the remaining animals were culled at 6 months for BALF collection (Section 2.6.6.2). Antibody titre in the serum and BALF samples was measured using human IgG ELISA (Section 2.7.4). (A) Palivizumab concentration in the serum throughout the duration of the experiment is shown for rAAV2/8 only, as serum antibody levels for mice treated with rSIV.F/HN were not significantly different from naive at most time-points (not shown). (B) The individual values for serum concentration at 6 months post-delivery. (C) Palivizumab concentration in the BALF at 1 and (D) 6 months post-delivery. Data are shown as individual values and/or mean ± standard error of the mean. Significant differences between the values were determined using Kruskal-Wallis test with Dunn's post hoc multiple comparison test compared with naïve mice. A calculated p value of >0.05 was deemed non-significant as indicated with ns on figures. Calculated p values of <0.05, <0.01 or <0.001 were deemed a significant difference as indicated with one (*), two (**) or three stars (***), respectively. Dotted line denotes lower limit of detection: 78 ng/ml for serum (A and B) and 7.8 ng/ml for BALF (C and D).

4.2.3 Neutralising activity of *in vivo* produced palivizumab

Before proceeding to studies with animal models of RSV infection, it was necessary to demonstrate that the *in vivo* produced palivizumab is functionally active and possesses neutralising capacity against RSV. A serum and BALF sample containing the highest concentration of mAb from day 28 after administration of rAAV2/8 or rSIV.F/HN expressing palivizumab (see Figure 4.5 for details of the experiment), were selected for evaluation. Neutralising activity against RSV was measured using the plaque reduction assay (Section 2.4.4) for a series of dilutions of each sample and presented as the absolute number of viral immunoplaques per well, or expressed as percent neutralisation relative to the negative control (serum and BALF obtained from a naïve BALB/c mouse). A commercial formulation of palivizumab in the form of Synagis 100 mg/ml solution for injection (MedImmune) was included in the experiment as a positive control (Figure 4.6 E and F).

As shown in Figure 4.6 A and B, serum obtained from a mouse administered 10^{11} GC of rAAV2/8 via IM injection exhibits near-complete neutralisation of RSV at 1:50 dilution, indicating that the antibody present in the sample is biologically active. Partial neutralisation is also achieved with serum from the animal in the medium dose group (10^{10} GC of rAAV2/8). Serum samples obtained from mice administered rSIV.F/HN and 10^{9} GC of rAAV2/8 did not exhibit neutralising activity, likely due to the concentration of palivizumab being too low, as previously measured using ELISA (Section 4.2.2). The neutralising activity of BALF was more difficult to ascertain, as a clear trend for decreasing neutralisation as the dilution factor increased was not apparent for any of the samples (Figure 4.6 D), likely due

to palivizumab levels being too low in those samples, which were further diluted for the assay.

Comparison of the number of RSV immunoplaques observed for the serum sample from the highest dose (10^{11} GC) rAAV2/8 group with that obtained for Synagis 100 mg/ml solution (MedImmune) indicates that the serum from this animal had a neutralising activity equivalent to approximately 390 µg/ml of palivizumab. The observed biological activity of the *in vivo* produced antibody supported progression to studies with a mouse model of RSV infection.

4.2.4 Protection from RSV in a mouse model of infection

The BALB/c mouse strain was selected for evaluation of the protective capacity of the rAAV and rSIV gene delivery platforms, with weight loss as the primary readout. Mice were administered 10^{10} or 10^{11} GC of rAAV2/8 CASI palivizumab via IM injection (Section 2.6.5.3), or 1.7 x 10^6 or 1.7 x 10^7 TTU rSIV.F/HN hCEF palivizumab via IN instillation (Section 2.6.5.1). Animal weight was recorded for up to 5 days (Figure 4.7 A) to ensure no interference with the readout following subsequent infection with RSV. Twenty-eight days after vector delivery, a dose of 7.5 x 10^5 ffu of RSV (gift of Cecilia Johansson), or PBS for an untreated control group, was administered via IN instillation. The weight of individual animals was recorded and expressed as percentage of measurement performed on the day of challenge with the infectious agent (Figure 4.7 B); statistical analysis is summarised in Figure 4.7 C. The study was performed with the assistance of Cecilia Johansson and Freja Kirsebom.

A

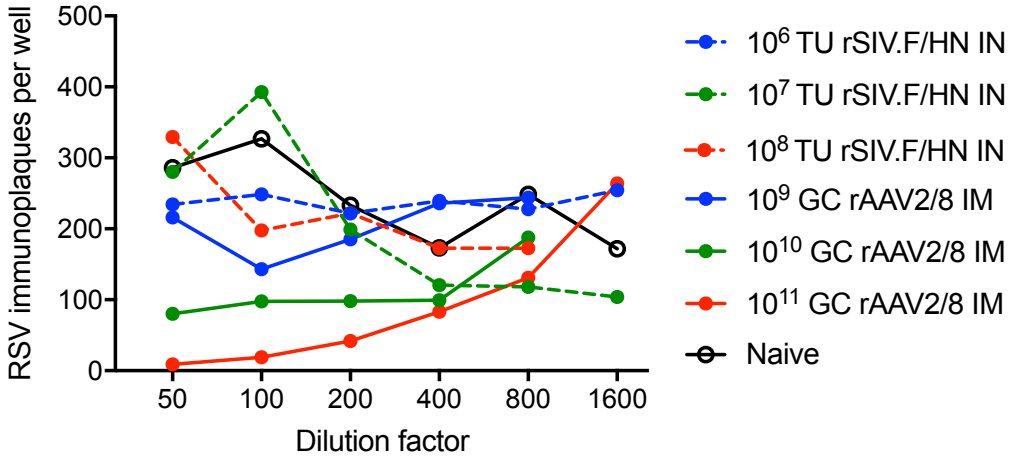
RSV immunoplaques per well
500
400
300
200
100
0
50
100
200
400
800
1600
Dilution factor
10^6 TU rSIV.F/HN IN
10^7 TU rSIV.F/HN IN
10^8 TU rSIV.F/HN IN
10^9 GC rAAV2/8 IM
10^10 GC rAAV2/8 IM
10^11 GC rAAV2/8 IM
Naive

B

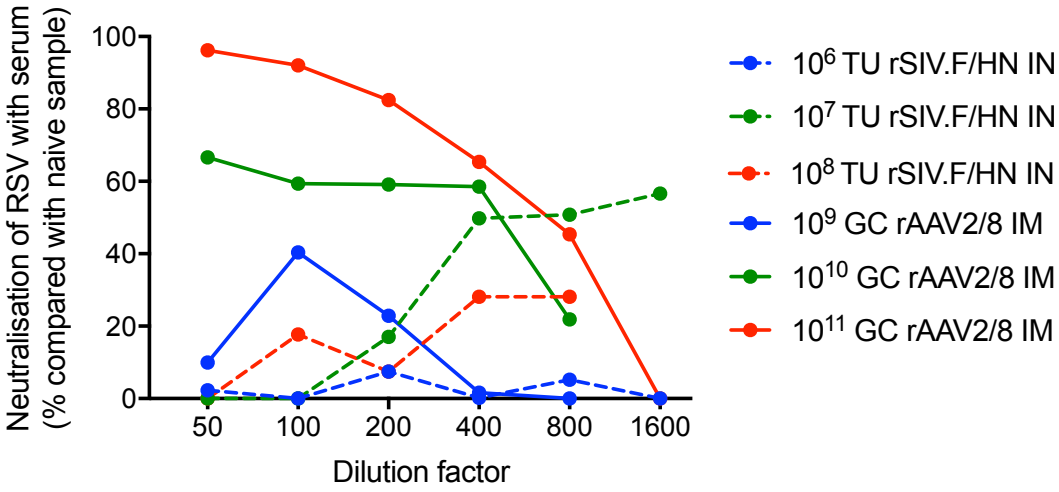
Neutralisation of RSV with serum
(% compared with naive sample)
100
80
60
40
20
0
50
100
200
400
800
1600
Dilution factor
10^6 TU rSIV.F/HN IN
10^7 TU rSIV.F/HN IN
10^8 TU rSIV.F/HN IN
10^9 GC rAAV2/8 IM
10^10 GC rAAV2/8 IM
10^11 GC rAAV2/8 IM

C

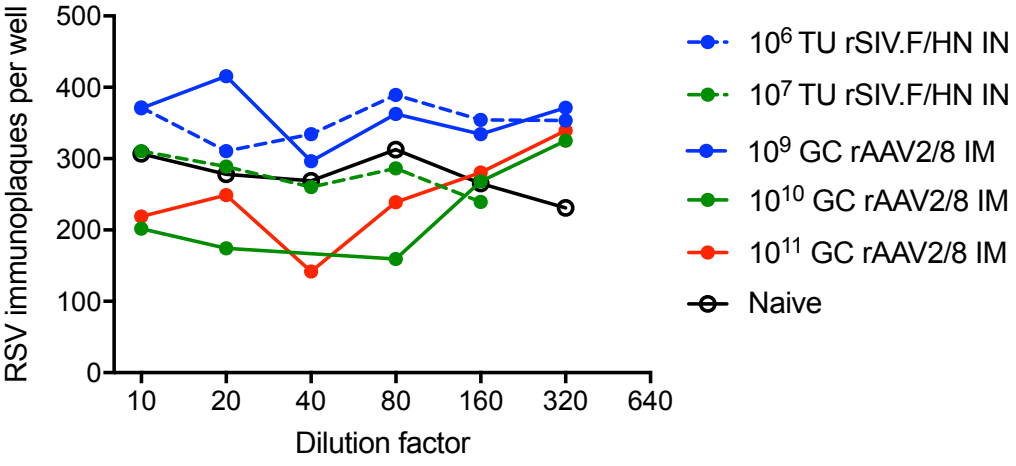
RSV immunoplaques per well
500
400
300
200
100
0
10
20
40
80
160
320
640
Dilution factor
10^6 TU rSIV.F/HN IN
10^7 TU rSIV.F/HN IN
10^9 GC rAAV2/8 IM
10^10 GC rAAV2/8 IM
10^11 GC rAAV2/8 IM
Naive

D

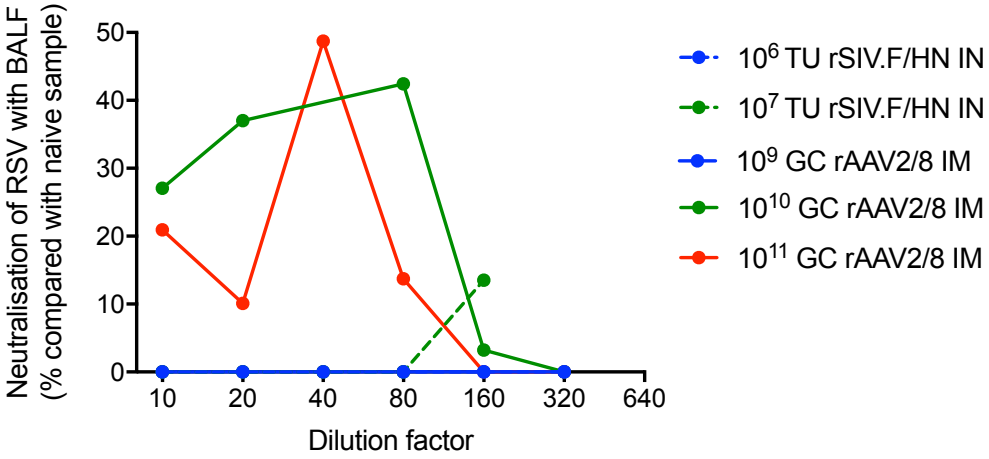
Neutralisation of RSV with BALF
(% compared with naive sample)
50
40
30
20
10
0
10
20
40
80
160
320
640
Dilution factor
10^6 TU rSIV.F/HN IN
10^7 TU rSIV.F/HN IN
10^9 GC rAAV2/8 IM
10^10 GC rAAV2/8 IM
10^11 GC rAAV2/8 IM

E

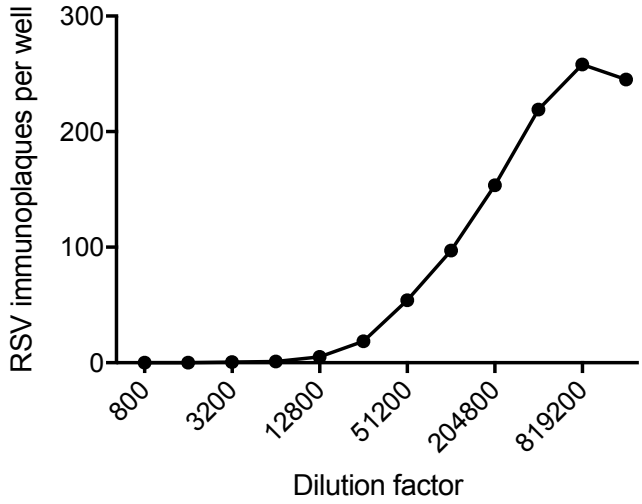
RSV immunoplaques per well
300
200
100
0
800
3200
12800
51200
204800
819200
Dilution factor

F

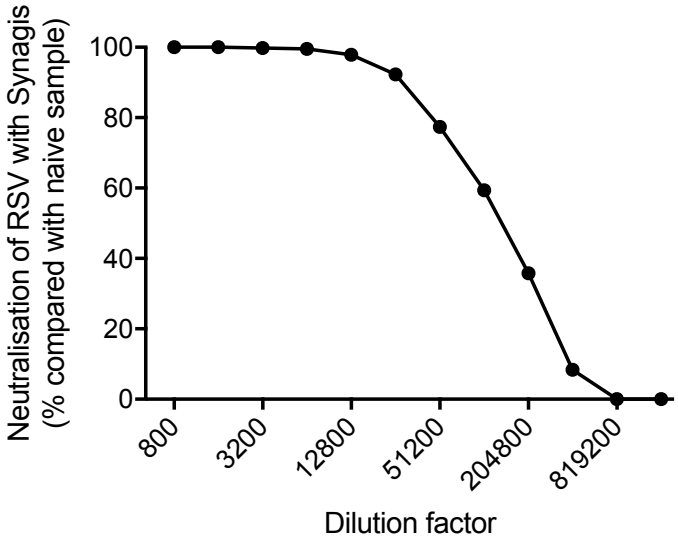
Neutralisation of RSV with Synagis
(% compared with naive sample)
100
80
60
40
20
0
800
3200
12800
51200
204800
819200
Dilution factor

Figure 4.6. Neutralising activity of *in vivo* produced palivizumab.

As described in Figure 4.5, female BALB/c mice were administered 10^9 (green solid line) 10^{10} (blue solid line) or 10^{11} (red solid line) GC of rAAV2/8 CASI palivizumab via intramuscular injection (Section 2.6.5.3), or 10^6 (green dashed line), 10^7 (blue dashed line) or 10^8 (red dashed line) TTU of rSIV.F/HN hCEF palivizumab via intranasal instillation (Section 2.6.5.1). Serum and BALF were obtained (Sections 2.6.6.1 and 2.6.6.2) 28 days later. From each group, the sample with the highest level of palivizumab, as measured using human IgG ELISA (Section 2.7.4), was selected for evaluation of neutralising activity against RSV using plaque reduction assay (Section 2.4.4), the results of which are shown here. The absolute number of plaques per well and the calculated neutralising activity expressed as percentage (compared with naïve sample) are shown for serum (A and B) and BALF (C and D). A sample of BALF from the group dosed with 10^8 TTU of rSIV.F/HN was not available. A commercial preparation of palivizumab (Synagis, 100 mg/ml; MedImmune) was used as a positive control (E and F). Each data point represents the mean of duplicate readings.

A

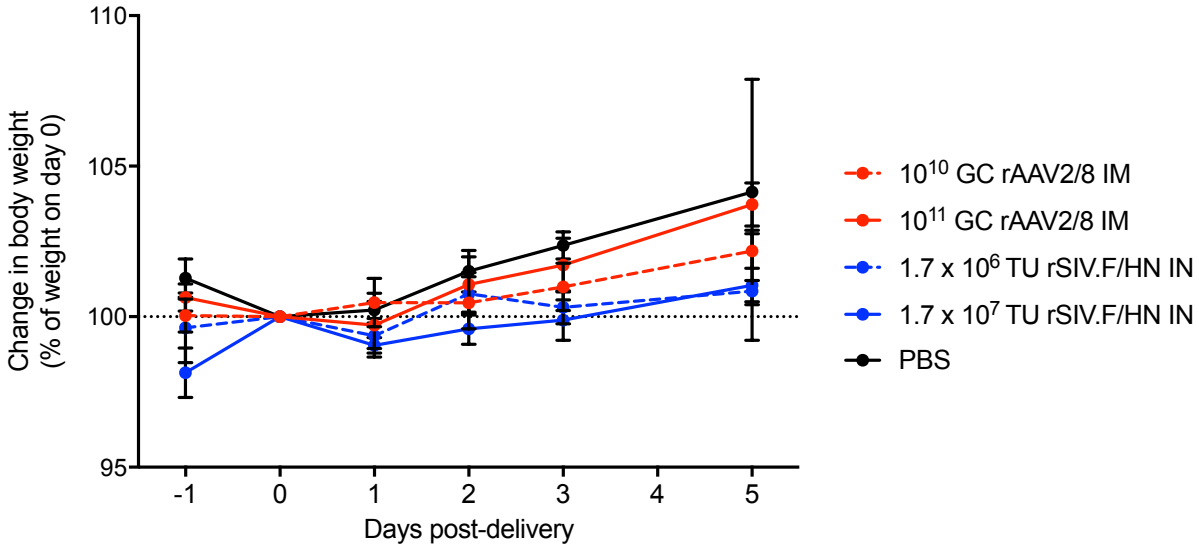
110
105
100
95
Change in body weight
(% of weight on day 0)
-1
0
1
2
3
4
5
Days post-delivery
10^10 GC rAAV2/8 IM
10^11 GC rAAV2/8 IM
1.7 x 10^6 TU rSIV.F/HN IN
1.7 x 10^7 TU rSIV.F/HN IN
PBS

B

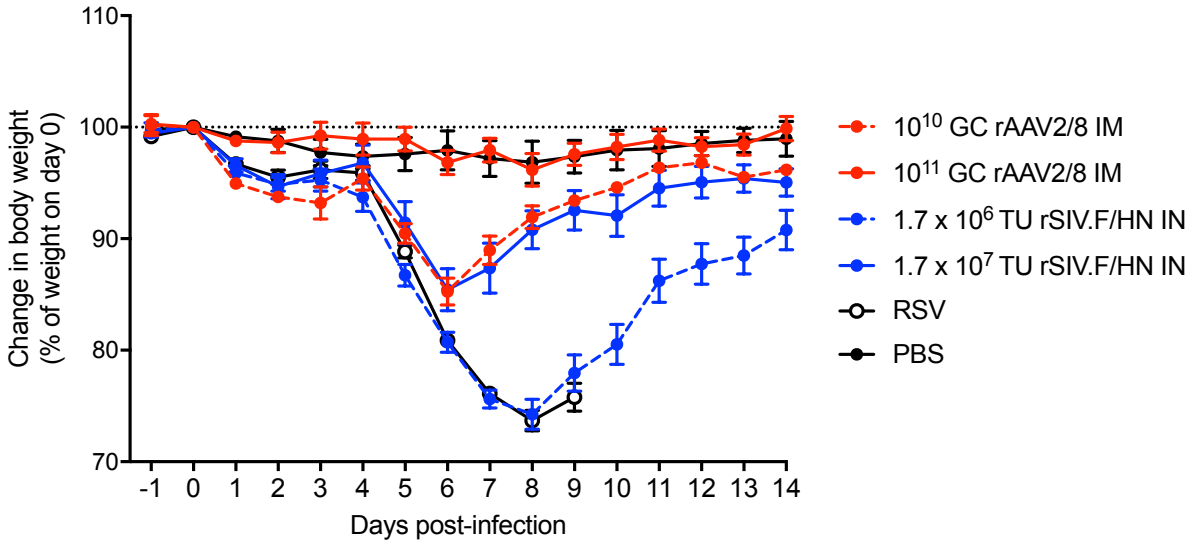
110
100
90
80
70
Change in body weight
(% of weight on day 0)
-1 0 1 2 3 4 5 6 7 8 9 10 11 12 13 14
Days post-infection
10^10 GC rAAV2/8 IM
10^11 GC rAAV2/8 IM
1.7 x 10^6 TU rSIV.F/HN IN
1.7 x 10^7 TU rSIV.F/HN IN
RSV
PBS

C

Comparison	Significance
RSV vs 10^{10} GC rAAV2/8 CASI palivizumab	*
RSV vs 10^{11} GC rAAV2/8 CASI palivizumab	****
RSV vs 1.7 x 10^6 TTU rSIV.F/HN hCEF palivizumab	ns
RSV vs 1.7 x 10^7 TTU rSIV.F/HN hCEF palivizumab	*
RSV vs PBS	****

Figure 4.7. Protection from RSV infection following rAAV2/8- and rSIV.F/HN-mediated palivizumab gene transfer.

Female BALB/c mice (n = 5) were administered 10^{10} or 10^{11} GC of rAAV2/8 CASI palivizumab via intramuscular injection (Section 2.6.5.3) and 1.7 x 10^6 or 1.7 x 10^7 TTU of rSIV.F/HN hCEF palivizumab via intranasal (IN) instillation (Section 2.6.5.1). Twenty-eight days later, the mice received 7.5 x 10^5 pfu of RSV or PBS via IN instillation. Mouse weight following (A) vector delivery and (B) RSV infection was recorded for 5 and 14 days, respectively. Mice with weight falling below 75% of the initial measurement were culled in agreement with the Home Office project licence. Data are shown as mean ± standard error of the mean. (C) Significant differences between treatment groups were determined using two-way ANOVA with Dunnett's post hoc test on data up to day 8 after RSV infection. A calculated p value of >0.05 was deemed non-significant as indicated with ns in the table. Calculated p values of <0.05 or <0.0001 were deemed a significant difference as indicated with one (*) or four stars (****), respectively.

All mice in the untreated group and two animals from the 1.7 x 10^6 TTU of rSIV.F/HN group had to be culled due to reaching the 25% weight loss limit; all other mice treated with palivizumab-expressing vectors survived the RSV challenge. Mice which had received 1.7 x 10^7 TTU of rSIV.F/HN and 10^{10} GC of rAAV2/8 were partially protected from RSV-induced weight loss ($p<0.05$), whilst administration of 10^{11} GC of rAAV2/8 resulted in complete prevention of weight loss ($p<0.0001$). At the end of the experiment (14 days after RSV infection), serum and BALF was collected from the surviving animals and mAb levels measured using human IgG ELISA (Section 2.7.4). Palivizumab could be detected in the serum of mice administered 10^{10} and 10^{11} GC of rAAV2/8, and there was a significant difference between the two doses ($p<0.0001$; Figure 4.8 A). These animals, along with those dosed with 1.7 x 10^7 TTU of rSIV.F/HN, also had detectable palivizumab levels in the BALF. The high (10^{11} GC) rAAV2/8 dose group had significantly higher expression levels than either of the other two groups. No significant difference between the high (1.7 x 10^7 TTU) dose group of rSIV.F/HN and low dose (10^{10} GC) of rAAV2/8 was observed (Figure 4.8 B), which is consistent with these groups experiencing similar levels of weight loss following RSV infection (Figure 4.7 B). A potential caveat of measuring palivizumab levels in the serum and BALF after an RSV infection is that some of the antibody might have been bound by the virus and would not be detectable. Nonetheless, levels of palivizumab reported here (Figure 4.8) were in broad agreement with the observed level of protection from virus-induced weight loss (Figure 4.7).

A

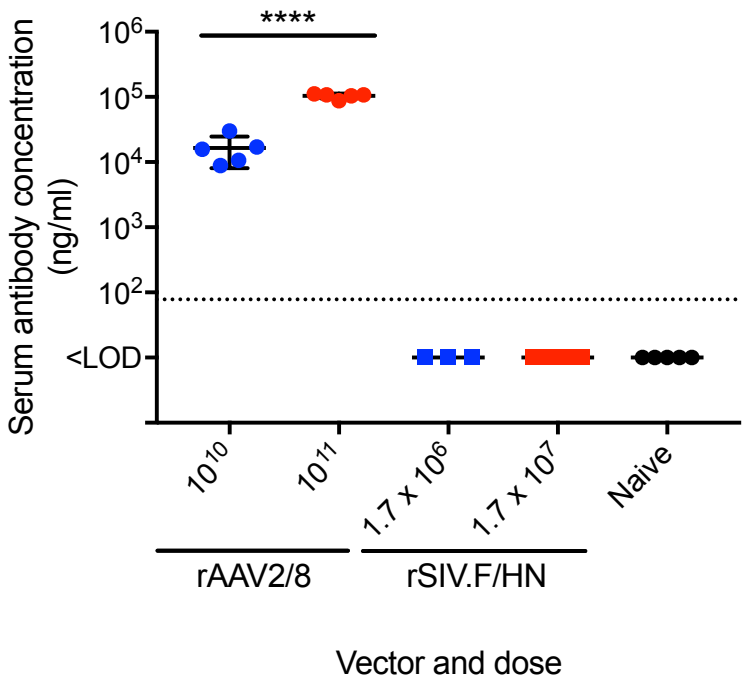
****
Serum antibody concentration (ng/ml)
10^6
10^5
10^4
10^3
10^2
≤LOD
10^10
10^11
1.7 x 10^6
1.7 x 10^7
Naive
rAAV2/8
rSIV.F/HN
Vector and dose

B

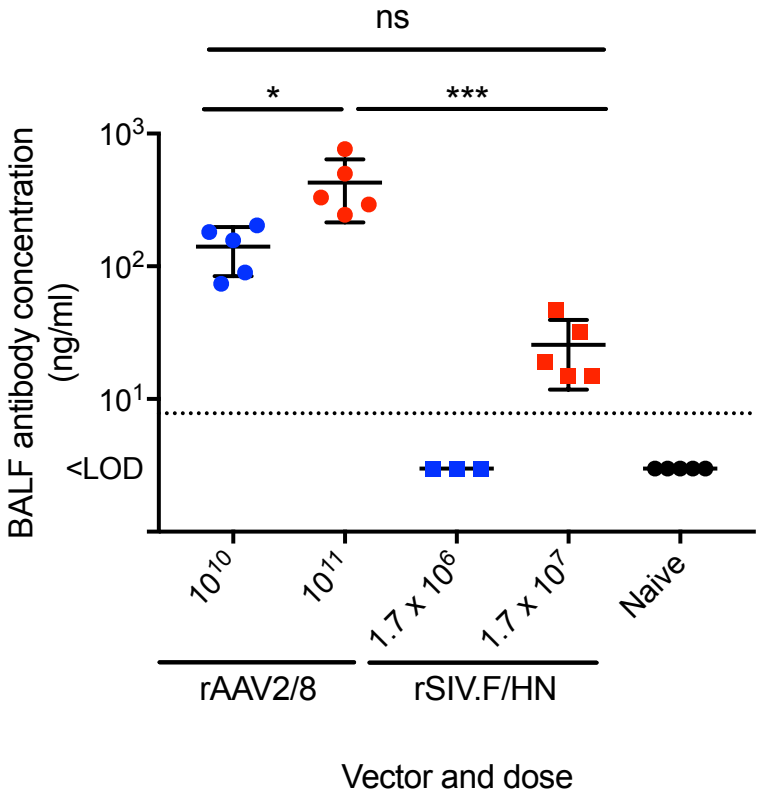
ns
*
***
BALF antibody concentration (ng/ml)
10^3
10^2
10^1
≤LOD
10^10
10^11
1.7 x 10^6
1.7 x 10^7
Naive
rAAV2/8
rSIV.F/HN
Vector and dose

Figure 4.8. Palivizumab expression in the serum and BALF following RSV infection in mice administered rAAV2/8 and rSIV.F/HN.

As described in Figure 4.7, female BALB/c mice (n = 5) were administered 10^{10} or 10^{11} GC of rAAV2/8 CASI palivizumab via intramuscular injection (Section 2.6.5.3) and 1.7 x 10^6 or 1.7 x 10^7 TTU of rSIV.F/HN hCEF palivizumab via intranasal (IN) instillation (Section 2.6.5.1). Twenty-eight days later, the mice received 7.5 x 10^5 pfu of RSV or PBS via IN instillation. Fourteen days after the infection, the animals were culled and their serum (Section 2.6.6.1) and broncho-alveolar lavage fluid (BALF) (Section 2.6.6.2) collected. Palivizumab levels in the (A) serum and (B) BALF were measured using human anti-IgG ELISA (Section 2.7.4). Data are shown as individual values and mean ± standard error of the mean. Significant differences between treatment groups were determined using (A) Student's t-test or (B) ANOVA with Tukey's post hoc test. A calculated p value of >0.05 was deemed non-significant as indicated with ns on figures. Calculated p values of <0.05, <0.001 or <0.0001 were deemed a significant difference as indicated with one (*), three (***) or four stars (****), respectively.

Recruitment of immune cells is a hallmark of inflammation, therefore total and differential cell quantification (Section 2.6.7) was carried out on the collected BAL samples to evaluate the numbers and types of cells recruited into the lung following RSV infection. Figure 4.9 A shows the relative proportions of macrophages, lymphocytes and neutrophils present in the BAL. The total number of lymphocytes in the different groups is shown in Figure 4.9 B. Mice which had received either 10^{10} or 10^{11} GC of rAAV2/8 IM did not show significant lymphocyte infiltration in the lung compared with naïve animals (PBS) ($p>0.05$). Mice administered 1.7×10^6 or 1.7×10^7 TTU of rSIV.F/HN IN experienced significantly greater lymphocyte infiltration than the uninfected group ($p>0.001$ and $p>0.01$, respectively), reflecting inflammation in the lung in response to RSV infection.

To confirm the results obtained in this experiment (Figure 4.7), to delineate the non-specific effects of the vectors upon response to infection, and to evaluate the protective potential of higher doses of rSIV.F/HN, an additional RSV challenge study was undertaken. Mice were administered 10^{10} or 10^{11} GC of rAAV2/8 CASI palivizumab via IM injection (Section 2.6.5.3), as previously, or 10^8 or 1.95×10^8 TTU (the maximal feasible dose) of rSIV.F/HN hCEF palivizumab via IN instillation (Section 2.6.5.1). Two groups of mice received matched high doses of control vectors expressing an irrelevant GLux transgene: 10^{11} GC of rAAV2/8 CASI GLux via IM injection and 1.95×10^8 TTU rSIV.F/HN hCEF GLux via IN instillation. The dose of RSV was reduced slightly from 7.5×10^5 to 7×10^5 ffu to minimise the risk of animals reaching the weight loss limit (75% of weight on day 0). Twenty-eight days after vector delivery, the mice were administered the RSV via IN instillation (Section 2.6.5.1). The weight of individual animals was recorded and expressed as percentage of the weight measured immediately prior to challenge with RSV

(Figure 4.10). The study was performed with the assistance of Cecilia Johansson and Freja Kirsebom.

Results in Figure 4.10 showed that, in agreement with previous observations (Figure 4.7), mice that received 10^{11} GC of rAAV2/8 CASI palivizumab were completely protected from RSV-induced weight loss ($p<0.0001$). Complete protection was also observed in groups which received 10^8 or 1.95×10^8 TTU rSIV.F/HN hCEF palivizumab ($p<0.001$; Figure 4.10). In contrast to previous results, which indicated that partial protection is conferred by administration of the lower (10^{10} GC) dose of rAAV2/8 CASI palivizumab (Figure 4.7), this treatment group was not protected from weight loss on this occasion ($p>0.05$; Figure 4.10), and one animal had to be culled on day 9 post-infection due to reaching the weight loss limit. Although administration of either rAAV2/8 or rSIV.F/HN expressing GLux did not appear to have a significant effect on weight loss ($p>0.05$), all but one animal in the rAAV2/8 control group needed to be culled by day 8, indicating a possible (albeit unconfirmed) negative effect of this vector on response to RSV infection. Although not statistically significant, there appeared to be a partially protective effect in the group administered rSIV.F/HN hCEF GLux.

A

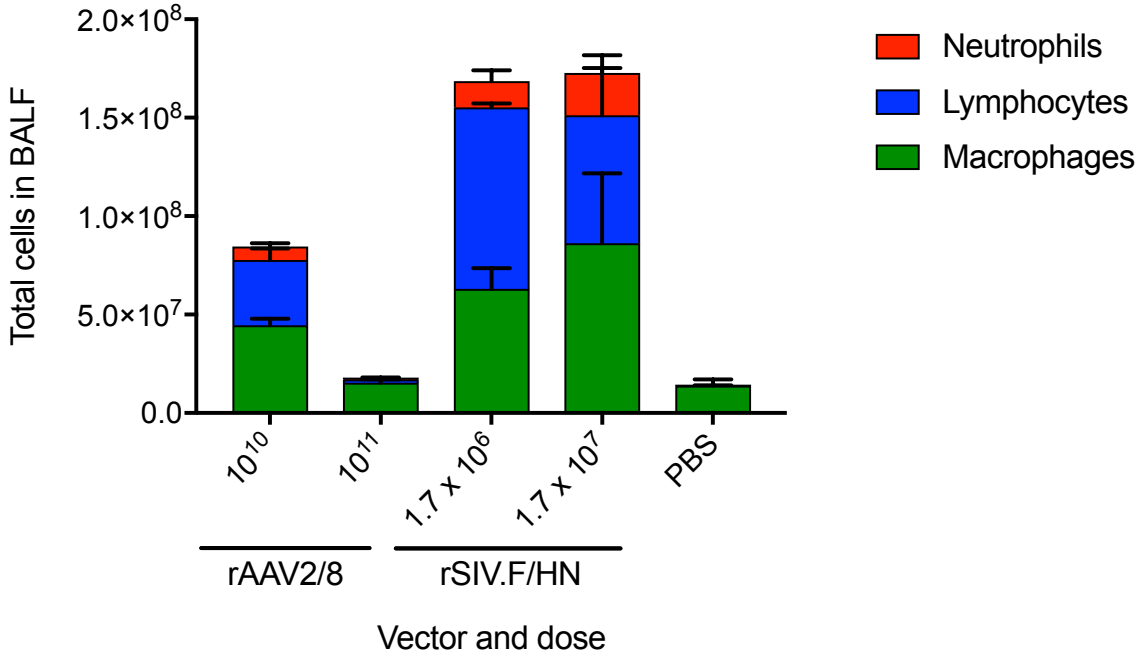
Total cells in BALF
2.0×10^8
1.5×10^8
1.0×10^8
5.0×10^7
0.0
Neutrophils
Lymphocytes
Macrophages
10^10
10^11
1.7 x 10^6
1.7 x 10^7
PBS
rAAV2/8
rSIV.F/HN
Vector and dose

B

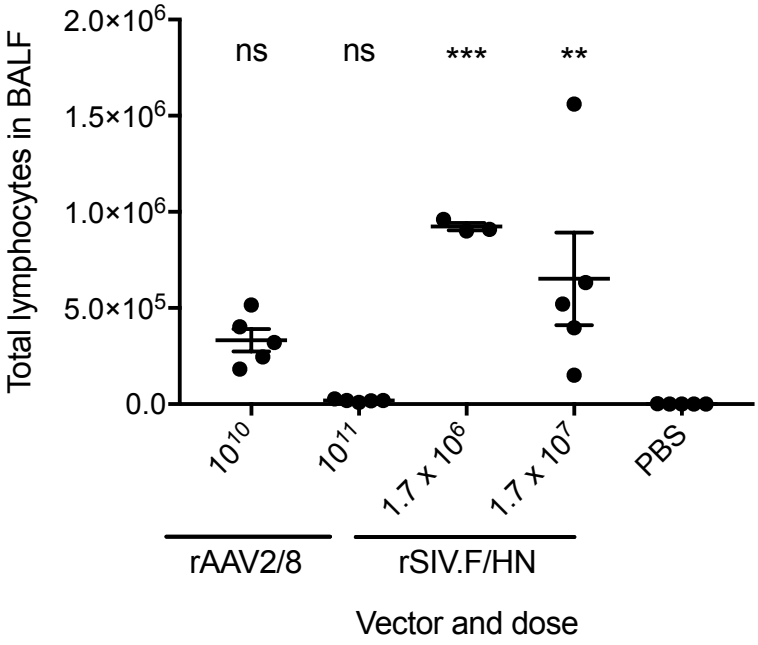
Total lymphocytes in BALF
2.0×10^6
1.5×10^6
1.0×10^6
5.0×10^5
0.0
ns
ns
***
**
10^10
10^11
1.7 x 10^6
1.7 x 10^7
PBS
rAAV2/8
rSIV.F/HN
Vector and dose

Figure 4.9. Pulmonary leukocyte infiltration following infection with RSV in mice treated with rAAV2/8 and rSIV.F/HN.

As described in Figure 4.7, female BALB/c mice (n = 5) were administered 10^{10} or 10^{11} GC of rAAV2/8 CASI palivizumab via intramuscular injection (Section 2.6.5.3) and 1.7 x 10^6 or 1.7 x 10^7 TTU of rSIV.F/HN hCEF palivizumab via intranasal (IN) instillation (Section 2.6.5.1). Twenty-eight days later, the mice received 7.5 x 10^5 ffu of RSV or PBS via IN instillation. Fourteen days after the infection, the animals were culled and total and differential leukocyte quantification (Section 2.6.7) of the broncho-alveolar lavage (BAL) samples (Section 2.6.6.2) undertaken. (A) The total numbers of different types of leukocytes in the BAL: macrophages (green), lymphocytes (blue) and neutrophils (red); the height of the combined bar indicates the total number of leukocytes. (B) The total number of lymphocytes in BAL. Data are shown as individual values and mean ± standard error of the mean. Significant differences between treatment groups were determined using ANOVA with Dunnett's post hoc test, compared with naïve values. A calculated p value of >0.05 was deemed non-significant as indicated with ns on figures. Calculated p values of <0.01 or <0.001 were deemed a significant difference as indicated with two (**) or three (***), respectively.

A

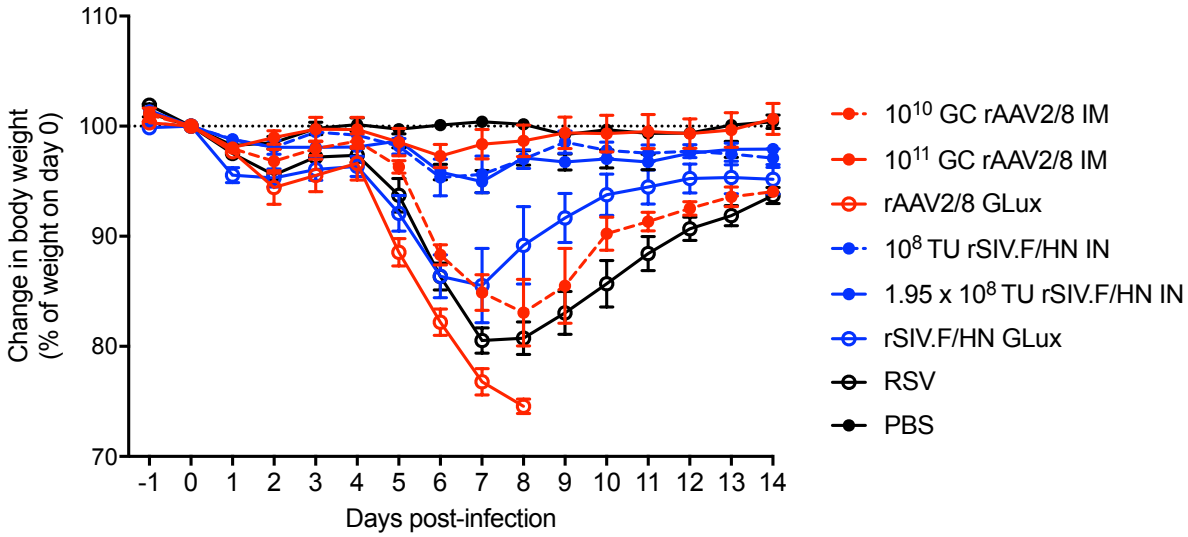

B

Comparison	**Significance**
RSV vs 10^{10} GC rAAV2/8 CASI palivizumab	ns
RSV vs 10^{11} GC rAAV2/8 CASI palivizumab	****
RSV vs 10^{8} TTU rSIV.F/HN hCEF palivizumab	***
RSV vs 1.95 x 10^{8} TTU rSIV.F/HN hCEF palivizumab	***
RSV vs 10^{11} GC rAAV2/8 CASI GLux	ns
RSV vs 1.95 x 10^{8} TTU rSIV.F/HN hCEF GLux	ns
RSV vs PBS	****

Figure 4.10. Effect of rAAV2/8 and rSIV.F/HN on weight loss in mice upon infection with RSV.

Female BALB/c mice (n = 5) were administered 10^{10} or 10^{11} GC of rAAV2/8 CASI palivizumab or 10^{11} GC of rAAV2/8 CASI GLux via intramuscular injection (Section 2.6.5.3), or 10^{8} or 1.95 x 10^{8} TTU rSIV.F/HN hCEF palivizumab or 1.95 x 10^{8} TTU rSIV.F/HN hCEF GLux via intranasal (IN) instillation (Section 2.6.5.1). Twenty-eight days later, the mice received 7 x 10^{5} ffu of RSV or PBS via IN instillation (Section 2.6.5.1) and their weight was recorded daily for 14 days (A). Mice whose weight dropped below 75% of the initial measurement were culled in agreement with the Home Office project licence. Data are shown as mean ± standard error of the mean. (B) Significant differences between treatment groups were determined using two-way ANOVA with Dunnett's post hoc test on data up to day 7 after RSV infection. A calculated p value of >0.05 was deemed non-significant as indicated with ns in the table. Calculated p values of <0.001 or <0.0001 were deemed a significant difference as indicated with three (***) or four stars (****), respectively.

4.3 Discussion

The studies described in this chapter aimed to demonstrate the feasibility of using passive antibody gene transfer for prophylaxis of RSV infection.

4.3.1 Transport of antibody and GLux across lung epithelium

Results obtained in Chapter 3 with the secretory reporter protein GLux (Figures 3.4 and 3.6), showed that IN delivery of rSIV.F/HN yielded nearly three orders of magnitude greater GLux in the BALF compared with IM delivery of rAAV2/8. However, for palivizumab, rAAV2/8 administered IM resulted in approximately 10- and 20-fold higher expression in the BALF than rSIV.F/HN at 1 and 6 months post-administration, respectively (Figure 4.5 C and D). Thus, GLux reporter activity did not predict the result with the mAb. A possible explanation could be that GLux and mAb secretion occurs via different transport pathways across the lung epithelia. It has been reported that the uptake of GLux into cultured mammalian cells is likely to be mediated by non-specific pinocytosis (El-Amouri et al., 2013). The transport of IgG into the lung lumen, on the other hand, occurs via a well-characterised receptor-specific transcytosis pathway involving the neonatal Fc receptor (FcRn) (reviewed in Kuo et al., 2010). Thus, IgG is first taken up into polarised epithelial cells via non-specific endocytosis, then bound by FcRn in the acidic environment of the endosome and subsequently released at the apical or basolateral surface (Kuo et al., 2010). Transcytosis of IgG is important for a number of immunologic functions, including passive transfer of antibody from mother to offspring via the placenta and breast milk, and bidirectional transport of IgG across the mucosa to

sample antigens (Stapleton et al., 2015). Whilst murine FcRn appears more efficient at trafficking in the apical to basolateral direction (McCarthy et al., 2000), conflicting reports exist about the predominant direction of IgG transport by human FcRn (Claypool et al., 2004, Praetor et al., 1999). Nonetheless, the results obtained in this chapter suggest that transport from the basolateral to apical surface of the airway epithelium is more efficient for IgG than GLux.

4.3.2 *In vivo* production of therapeutically relevant levels of palivizumab

Intramuscular delivery of rAAV2/8 resulted in sustained expression of palivizumab into circulation, with the highest dose achieving an average serum concentration of 89 µg/ml at 6 months (Figure 4.5). The likelihood of these levels to be protective against RSV infection can be inferred by comparison with literature reporting serum levels conferring protection in animal models of infection and trough serum levels in patients receiving Synagis. In the cotton rat model of RSV infection, a >99% reduction in lung RSV titres was observed with serum levels of 25-30 µg/ml (Johnson et al., 1997), which has been used as a target serum concentration in clinical trials (Subramanian et al., 1998). In patients receiving Synagis, serum levels reach 131.2 µg/ml at 24 hours post-injection (Malley et al., 1998) and thereafter decline to 37 and 72 µg/ml prior to the second and fifth injection, respectively (Null et al., 1998). Comparison of serum palivizumab levels achieved in mice in the present study (up to 89 µg/ml; Figure 4.5) with the predicted protective level of 25-30 µg/ml in rodents and 70-130 µg/ml in patients warranted proceeding to RSV infection studies.

The estimated palivizumab ELF levels were 9 and 0.5 μg/ml for mice administered the highest dose of rAAV2/8 and rSIV.F/HN, respectively. The relevant palivizumab concentration in the lung lining fluid has not been measured in animal models or patients. However, the ELF antibody levels obtained in this study can be compared with the half maximal effective concentration (EC_{50}) of palivizumab to determine whether they may have an effect on RSV infection. The EC_{50} has been measured *in vitro* using plaque-reduction (also performed in this study; Section 2.4.4), microneutralisation and fusion inhibition assays and reported as 2, 0.10 and 0.17 μg/ml, respectively (Johnson et al., 1997). The estimated ELF levels observed in this study (up to 9 μg/ml) compared favourably with these figures, indicating possible protective effect.

Before proceeding to RSV challenge studies, the biological activity of the *in vivo* produced antibody was assessed using plaque reduction assay (Section 2.4.4). Whilst serum from a mouse administered rAAV2/8 blocked RSV infection *in vitro* (Figure 4.6), the neutralising activity of the BALF samples could not be confirmed, likely due to the mAb levels being too low. Additionally, only one serum and BALF sample per treatment group were tested. Nevertheless, the biological activity of the palivizumab produced *in vivo* was confirmed and comparison of the most concentrated serum sample with the neutralising activity of Synagis solution indicated even greater potency (equivalent to 390 μg/ml) than expected from the IgG levels measured with ELISA (138 μg/ml; Figure 4.5).

4.3.3 Demonstration of protection from RSV infection

Several animal models of RSV infection are available, including the cotton rat *Sigmodon hispidus* which is often regarded as the gold standard model for this and other respiratory viral infections (Boukhvalova and Blanco, 2013, Boukhvalova et al., 2009). In this study, the BALB/c mouse model was selected due to the ease of use and relatively low cost. Whilst not a natural host for the virus, the mouse is a reliable and widely used model in RSV research (Openshaw, 2013). It recapitulates a number of clinical signs of disease and has been used to demonstrate the ability of mAbs, including palivizumab, to protect against RSV infection (Johnson et al., 1997, Taylor et al., 1984). The scoring of disease severity by measuring weight loss upon RSV infection is considered a convenient, reproducible and objective measure (Openshaw, 2013) and was therefore selected as the primary readout in the RSV challenge experiments.

In agreement with the predicted efficacy of administration of the highest dose (10^{11} GC) of rAAV2/8 via IM injection, based on the observed levels of palivizumab in the serum and BALF (Figure 4.6), this treatment group was completely protected from RSV-induced weight loss (Figures 4.7 and 4.10). Administration of the lower dose of this vector (10^{10} GC) yielded inconsistent results, with partial protection observed in the first study (Figure 4.7), but not in the second study (Figure 4.10). Possible reasons for this discrepancy might include experimental variation in administration of vector or infection with RSV. Administration of 1.7×10^7 TTU of rSIV.F/HN via IN insufflation was partially protective (Figure 4.7), whilst higher doses of 10^8 and 1.95×10^8 TTU resulted in complete protection from RSV-induced weight loss (Figure 4.10). Additionally, rAAV2/8 was shown to prevent lymphocyte

infiltration in the lungs of mice (Figure 4.9), indicating that the vector prevented inflammation upon infection with the virus. Whilst mice administered 1.7 x 10^6 or 1.7 x 10^7 TTU of rSIV.F/HN showed increased numbers of lymphocytes in their BAL relative to uninfected mice (Figure 4.9), it was not possible to determine whether these levels were lower than in untreated mice, as these were all culled due to significant weight loss prior to completion of the experiment. Nonetheless, the results obtained in Section 4.2.4 indicate that both vectors are effective at preventing RSV infection in mice. The duration of expression conferred by these vectors, especially rAAV2/8 at 6 months (Figure 4.5), suggests that the protection could be long-lasting and therefore relevant as prophylaxis to cover the entire RSV season, which lasts for 31 weeks (Rose et al., 2018).

Although administration of 10^8 TTU of rSIV.F/HN resulted in expression of lower levels of palivizumab in the BALF at 1 month compared with 10^{11} GC of rAAV2/8 (Figure 4.5 C), the two groups showed equivalent protection from RSV-induced weight loss (Figures 4.7 and 4.10). It is possible that production of the mAb in the lung is advantageous, resulting in more potent protection than predicted by the observed IgG levels. When mAb levels were measured in the BALF of mice at the end of the experiment, however, there was no significant difference in palivizumab levels between these two groups (Figure 4.8), indicating possible inter-experimental variation.

Interestingly, administration of rSIV.F/HN hCEF GLux appeared to have a partially protective effect, whilst mice dosed with rAAV2/8 CASI GLux experienced exacerbated weight loss. Neither of these results was, however, statistically significant (Figure 4.10). It is possible that administration of the lentiviral vector to

the lungs of mice primed the animals through an unknown mechanism for improved clearance of RSV following infection. Viral load in the lungs of mice administered palivizumab-expressing and control vectors ought to be measured following infection to determine whether this is the case, and to demonstrate that delivery of rSIV.F/HN hCEF palivizumab and rAAV2/8 CASI palivizumab reduces RSV-induced weight loss by blocking infection with and replication of the virus.

4.3.4 Alternative gene transfer options for RSV prophylaxis

The results described in this chapter could be extended to new anti-RSV mAbs currently in development. The mAb MEDI8897 is a modified anti-F protein mAb which has been shown to be nine-fold more potent than palivizumab in reducing RSV replication in cotton rats, and has a half-life three-fold greater than palivizumab in NHPs (Zhu et al., 2017). This mAb is currently being evaluated in clinical trials, with an aim for a single IM dose to provide protection for an entire season (Griffin et al., 2017). Another mAb in development for RSV prophylaxis is REGN2222, which has also been reported to exceed the potency and stability of palivizumab and is being tested in clinical trials (Sivapalasingam et al., 2015). Structurally different is ALX-0171, a trimeric camel-derived “Nanobody” designed for inhalation. The neutralising activity of this compound against RSV is superior to palivizumab i*n vitro*, and it is currently being evaluated in clinical trials (Detalle et al., 2016). However, it has been reported that the antiviral activity of Nanobodies following inhalation lasts for only for 48 hours in mice (Schepens et al., 2011). The increased persistence of protein expression achieved with rSIV.F/HN and rAAV2/8 could offer improved duration of prophylaxis with ALX-0171.

An alternative strategy to utilising mAb gene transfer for RSV prophylaxis in infants is the administration of vector to pregnant or breastfeeding mothers. Indeed, maternal immunisation is already being investigated as a vaccination strategy for RSV (Section 1.2.3), with Novavax's F-protein/alum vaccine currently undergoing a phase III clinical trial. Maternal immunisation has the added advantage of protecting both mother and infant and could overcome the challenge of eliciting effective immune responses to a vaccine in neonates (Kaaijk et al., 2013). For maternal gene transfer, IM administration of rAAV2/8 would be preferred, as it yields the highest levels of palivizumab in the serum (Section 4.2.2). This strategy is expected to maximise transfer of the mAb across the placenta and into milk (Fouda et al., 2011), providing protection against RSV infection in first months of life.

Chapter 5: Development of anti-TNFα factories for treatment of rheumatoid arthritis

5.1 Introduction

Rheumatoid arthritis is a debilitating autoimmune disease affecting about 1% of the general population (Gabriel, 2001). Due to the high cost of treatment with biologic TNFα antagonists (discussed in Section 1.1.1), development of an alternative delivery method using gene transfer is highly desirable. Based on the results presented in Chapter 3, IM delivery of rAAV2/8 was identified as an effective method of delivering secretory protein to the circulation and therefore this approach was investigated for expression of two anti-TNFα biologics: infliximab and etanercept (described in Section 1.3.3).

As TNFα is a key player in the inflammatory response, biologics targeting this cytokine are immunosuppressive and associated with an increased risk of infections and cancer (Furst et al., 2013); cessation of therapy might be necessary if patients develop such diseases. In the context of *in vivo* anti-TNFα production following gene transfer, it would be helpful if expression of the biologic could be regulated. One of the additional aims of this chapter was therefore to investigate the possibility of controlling anti-TNFα expression following gene delivery to the muscle using rAAV. Potential methods for controlling protein expression are summarised in Table 5.1 and can be broadly divided into pharmacological, and those utilising inflammation-inducible regulatory elements. In the context of rheumatoid arthritis, a number of regulatory elements from inflammation-related genes have been investigated, including those encoding matrix metalloproteases

(Vermeij et al., 2014), NF-κB (Aalbers et al., 2015, Bevaart et al., 2015), complement protein C3 (Miagkov et al., 2002), and the cell adhesion molecule E-selectin (Garaulet et al., 2013). With the exception of the C3 promoter, each of these elements have been used in the context of intra-articular gene delivery, and it is unclear whether they would be subject to sufficient inflammation-dependent activation when delivered to the muscle in an individual experiencing RA.

An alternative method of controlling protein expression is pharmacological. Following delivery of a vector encoding a regulatable cassette to a patient with RA, expression of the biologic could be induced to respond to disease flares and subsequently discontinued by administration or withdrawal of a small molecule drug. The doxycycline-inducible Tet-ON system (Table 5.1) has been used to control transgene expression following rAAV delivery to rodents and NHPs, although it was found to be refractory to repeated stimulation and failed to respond on the third cycle (Perez et al., 2004). This is thought to be due to the cellular and humoral immune responses to the bacterial TetR protein, which abrogate expression from transduced tissue in NHPs (Favre et al., 2002, Le Guiner et al., 2014).

The dimeriser system, developed by ARIAD therapeutics (Johnston et al., 2003) comprises two components: one encoding two transcription factors which dimerise upon administration of rapamycin, and another with the gene of interest under the control of a promoter responsive to the dimerised transcription factor complex. This system has been successfully used to control expression of erythropoietin in NHPs following rAAV delivery to the muscle for up to 26 cycles (Rivera et al., 2005). It was also effective at inducing expression of a mAb in mice, although the system

was ‘leaky’ in the absence of inducer drug and required the use of dual rAAV due to the packaging constraints of the vector (Fang et al., 2007).

A conceptually different approach is small molecule-assisted shutoff (SMASh) (Chung et al., 2015). The SMASh tag (Figure 5.1 A and B) contains non-structural protein 3 (NS3) which is a serine protease from hepatitis C virus (HCV). A protein of interest is tagged at its C-terminus with the NS3 protease, with the NS3 protease cleavage target sequence positioned between the desired protein and the NS3 protease. Fused to the C-terminus of the NS3 protease is a degron – a peptide domain whose presence confers a greatly increased rate of protein degradation (Ravid and Hochstrasser, 2008). In the presence of an NS3 protease inhibitor, the NS3 protease is unable to cleave the NS3 protease cleavage target sequence, which leads to degron-mediated degradation of the entire fusion protein. In the absence of an NS3 protease inhibitor, the NS3 protease cleaves its target sequence, generating the desired protein and an NS3 protease-degron fusion which is targeted for protein degradation. Thus, in the absence of an NS3 protease inhibitor the desired protein is produced, while in the presence of an NS3 protease inhibitor, little or no desired protein-NS3 protease-degron fusion is accumulated (Figure 5.1 C). *In vitro*, SMASh facilitated 98.1% suppression of protein expression with a concentration of the NS3 inhibitor asunaprevir that is non-toxic *in vivo*, and offered tuneable repression with over 50-fold dynamic range (Chung et al., 2015). Importantly, the entire SMASh sequence can be encoded within a 0.9-kb DNA fragment, allowing construction of a 2.4 kb etanercept-SMASh cDNA which is small enough to be packaged, complete with a CASI enhancer/promoter, within a single rAAV vector, removing the need for a dual vector system. The studies described in

this chapter investigated the use of SMASh to control anti-TNFα expression following gene transfer.

The aims of the work presented in this chapter included: (i) to generate infliximab and etanercept-expressing rAAV2/8 vectors, (ii) to measure expression levels achieved in the serum following delivery of those vectors to mice, and (iii) to develop a regulatable expression system for anti-TNFα based on SMASh.

5.2 Results

5.2.1 *In vivo* infliximab production using rAAV2/8

The single-ORF strategy (Figure 4.1) utilised for palivizumab was also used to design the cDNA for expression of infliximab. The original heavy and light chain variable protein sequences (Appendix) were sourced from patent number US5698195A (Le, 1991) and a cDNA construct, codon optimised for *Homo sapiens* and depleted of CpG dinucleotides, was designed using MacVector software and synthesised by GeneArt (Thermo Fisher Scientific). The transgene was sub-cloned into the rAAV2 genome plasmid to generate pAAV2.CASI.infliximab (Table 2.1; Figure 5.2 A) as described in Section 2.3.5. This plasmid was found to direct robust IgG expression in HEK293T cells following transfection (Section 2.4.2) (Figure 5.2 B) and used to produce an rAAV2/8 vector (Section 2.5.4). Transduction of rAAV2/8 CASI infliximab (Table 2.2) in HEK293T cells also resulted in secretion of IgG into the cell culture media supernatants (Figure 5.3).

Table 5.1. Methods for controlling protein expression following gene transfer.

Method	Mechanism	Advantages	Disadvantages	References
Inflammation-responsive regulatory elements	Regulatory elements from genes encoding proteins involved in inflammation are used to control anti-TNFα expression	Self-regulating; no foreign, potentially immunogenic components	Only tested for intra-articular gene delivery; transgene expression unlikely to be induced in the context of IM delivery	Aalbers et al., 2015, Bevaart et al., 2015, Garaulet et al., 2013, Miagkov et al., 2002, Varley et al., 1997, Vermeij et al., 2014
Tet-ON	Tetracycline-dependent transactivator (TA) protein enables expression of transgene under control of Tet-response element (TRE)	Extensively used and researched	Would require a dual rAAV system; refractory to repeated stimulation; the TA protein is immunogenic, which limits duration of expression	Favre et al., 2002, Le Guiner et al., 2014, Perez et al., 2004
Dimeriser	The DNA-binding and activation domain fusion proteins of human origin dimerise in the presence of inducer molecule and activate expression	Shown to be effective in the context of rAAV	Rapamycin is immunosuppressive (although rapalogues can be used); would require a dual rAAV system; leaky	Fang et al., 2007, Johnston et al., 2003, Nguyen et al., 2007, Rivera et al., 2005
SMASh	A degron-containing tag is fused to the protein of interest; self-cleavage of the tag is regulated with a protease inhibitor	Can be accommodated into a single rAAV vector; clinically tested protease inhibitors available	Not tested *in vivo* yet	Chung et al., 2015

A

DEMEEC^SQHLPGAGSSGDIMDYKDDDDKGSSGTGSGSGTSAPITAYAQQTR

GLLGCIITSLTGRDKNQVEGEVQIVSTATQTFLATCINGVCWAVYHGAGTRTIAS

PKGPVIQMYTNVDQDLVGWPAPQGSRSLTPCTCGSSDLYLVTRHADVIPVRRR

GDSRGSLLSPRPISYLKGSSGGPLLCPAGHAVGLFRAAVCTRGVAKAVDFIPVE

NLETTMRSPVFTDNSSPPAVTLTHPITKIDTKYIMTCMSADLEVVTSTWVLVGGV

LAALAAYCLSTGCVVIVGRIVLSGKPAIIPDREVLY

B

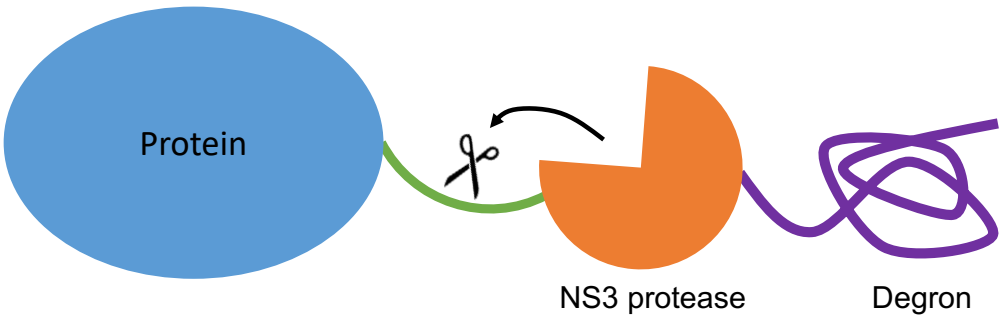

C

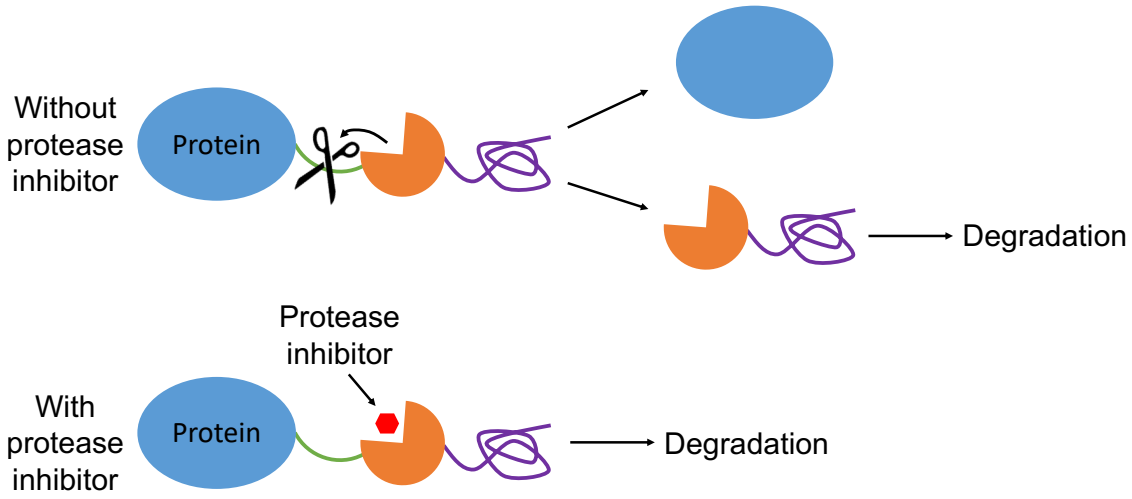

Figure 5.1. Schematic showing key features of the small molecule-assisted shutoff (SMASh) system.

(A) The sequence of non-structural protein 3 (NS3) protease from hepatitis C virus (HCV) is shown in orange. In the SMASh tag, it is joined to its cleavage target sequence (green, with the cleavage site indicated) by a linker (black) containing the Flag tag sequence (red). The NS3 protease sequence is followed by a truncated NS3 helicase domain (grey) and the non-structural protein 4A (NS4A) cofactor (purple). The truncated helicase domain and the NS4A sequence are thought to act as a degron. (B) The protein of interest (blue) is fused to the SMASh tag, comprising the cleavage sequence (green), the NS3 protease (orange) and the degron (purple). (C) In the absence of NS3 protease inhibitor, the protease cleaves its target sequence, thereby separating the native protein from the SMASh tag, which is degraded. When NS3 protease inhibitor is present, it prevents the protease from cleaving the tag and the degron directs degradation of the entire fusion protein, thereby abrogating expression of the protein of interest.

A

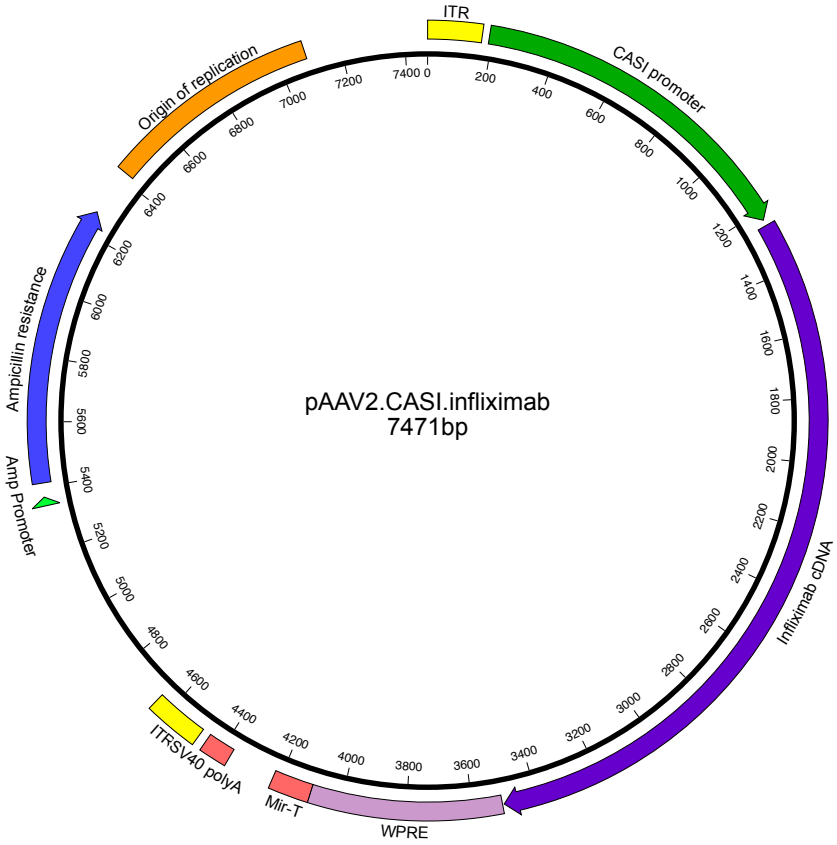
ITR
CASI promoter
Origin of replication
Ampicillin resistance
Amp Promoter
Infliximab cDNA
ITRSV40 polyA
Mir-T
WPRE
pAAV2.CASI.infliximab
7471bp

B

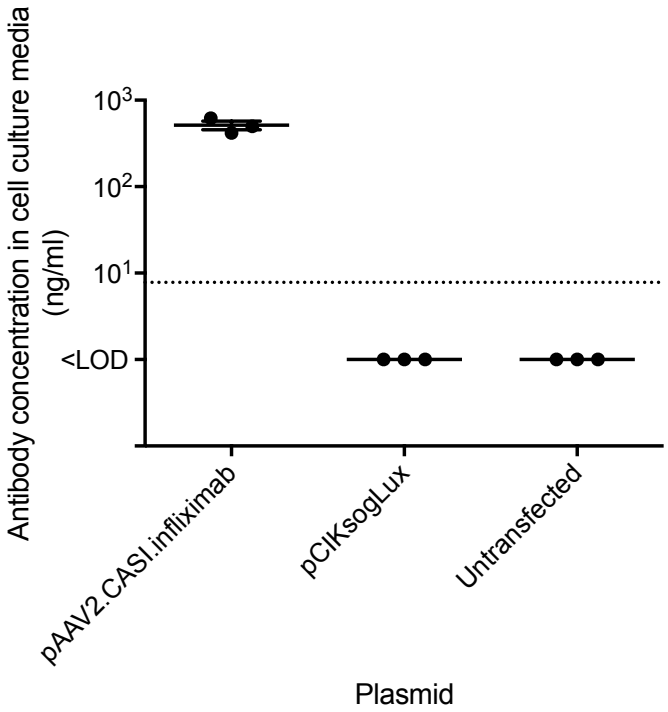
Antibody concentration in cell culture media (ng/ml)
10^3
10^2
10^1
<LOD
pAAV2.CASI.infliximab
pCIKsogLux
Untransfected
Plasmid

Figure 5.2. Infliximab expression following transfection of an rAAV vector genome plasmid in cell culture.

(A) pAAV2.CASI.infliximab vector genome (Table 2.1). WPRE, woodchuck hepatitis virus regulatory element; Mir-T, micro RNA 142-p target sequence; SV40 polyA, simian virus 40 polyadenylation signal; CMV, cytomegalovirus; ITR, inverted terminal repeat; CASI, compound promoter comprising CMV enhancer, chicken β-actin promoter and ubiquitin enhancer. (B) Adherent HEK293T cells (seeded at 5 x 10^5 cells/well in 12-well plates, n = 3 wells) were transfected with pAAV2.CASI.infliximab or pCIKsoGLux (a control plasmid, encoding *Gaussia* luciferase) (Table 2.1; Section 2.4.2). Ninety-six hours after transfection, antibody concentration in the supernatant was measured using human IgG ELISA (Section 2.7.4). Data are shown as individual values and mean ± standard error of the mean. Dotted line denotes lower limit of detection (LOD) (7.8 ng/ml).

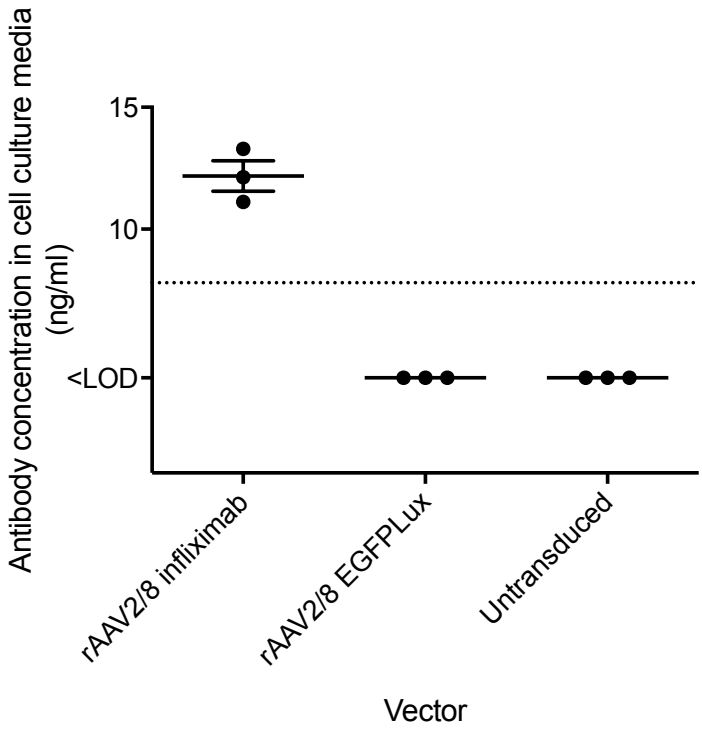

Figure 5.3. Infliximab expression following transduction of rAAV2/8 in cell culture.

Adherent HEK293T cells (seeded at 5 x 10^5 cells/well in 6-well plates, n = 3 wells) were transduced with 10^{10} GC of rAAV2/8 CASI palivizumab or rAAV2/8 CASI EGFPLux (Table 2.2) per well. Six days post-transduction, antibody levels in the supernatant were measured using Human IgG ELISA (Section 2.7.4). Data are shown as individual values and mean ± standard error of the mean. Dotted line denotes lower limit of detection (LOD) (7.8 ng/ml).

Following confirmation that the vector expressed infliximab in mammalian cell culture, an *in vivo* experiment was undertaken to determine the level and duration of infliximab expression that can be achieved using rAAV2/8. Mice were administered 10^9, 10^{10} or 10^{11} GC of rAAV2/8 CASI infliximab via IM injection (Section 2.6.5.3). Blood samples were collected at intervals up to 6 months post-delivery (Section 2.6.6.1) and infliximab levels in the isolated serum measured using human IgG ELISA (Section 2.7.4). As shown in Figure 5.4 A, administration of the two highest doses of the vector (10^{10} or 10^{11} GC, respectively) resulted in robust, persistent expression of infliximab in the serum for at least 6 months. At the latest time-point (Figure 5.4 B), the average infliximab serum levels in the 10^{10} and 10^{11} GC treatment groups were 9.81 and 88.9 µg/ml, respectively ($p<0.01$ and $p<0.001$ compared with naïve mice). Delivery of the lowest dose (10^9 GC) of the vector resulted in initially detectable, but not significant, expression that declined to undetectable levels in most animals by 6 months (Figure 5.4 B).

As infliximab does not cross-react with murine TNFα, a mouse model expressing human TNFα, such as the Tg197 transgenic strain (Keffer et al., 1991) (further discussed in Section 5.3.2) would be required to investigate the effectiveness of rAAV-mediated infliximab gene transfer in ameliorating arthritis. However, due to difficulties in obtaining and maintaining this model, assessing the functional effects of rAAV-mediated infliximab expression had to be de-prioritised. Instead, etanercept, which does cross-react with mouse TNFα and is also widely used in the treatment of RA (Haraoui and Bykerk, 2007), was selected as an alternative anti-TNFα biologic for further study in the remainder of this chapter.

A

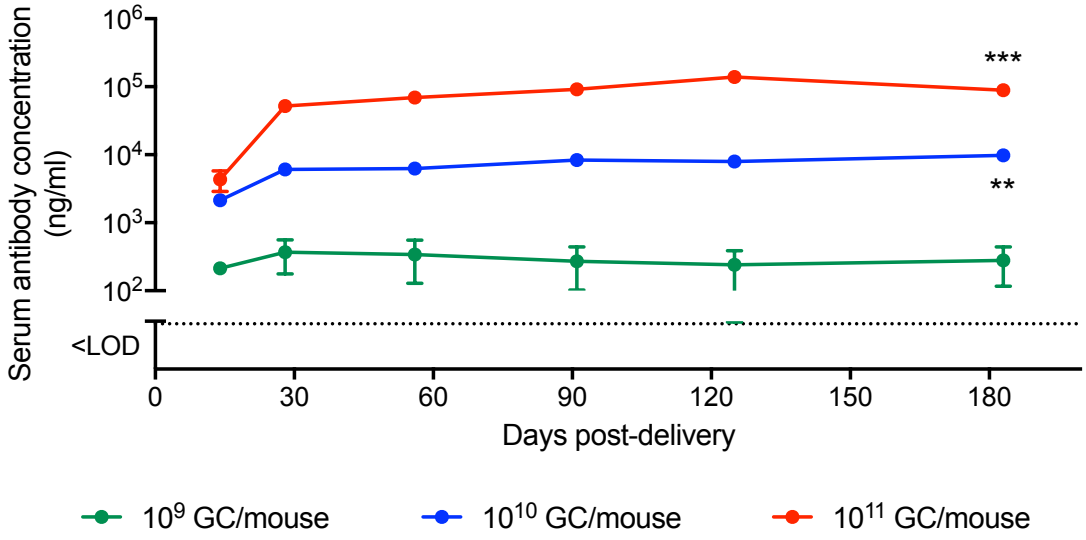
Serum antibody concentration (ng/ml)
10^6
10^5
10^4
10^3
10^2
<LOD
***
**
0
30
60
90
120
150
180
Days post-delivery
10^9 GC/mouse
10^{10} GC/mouse
10^{11} GC/mouse

B

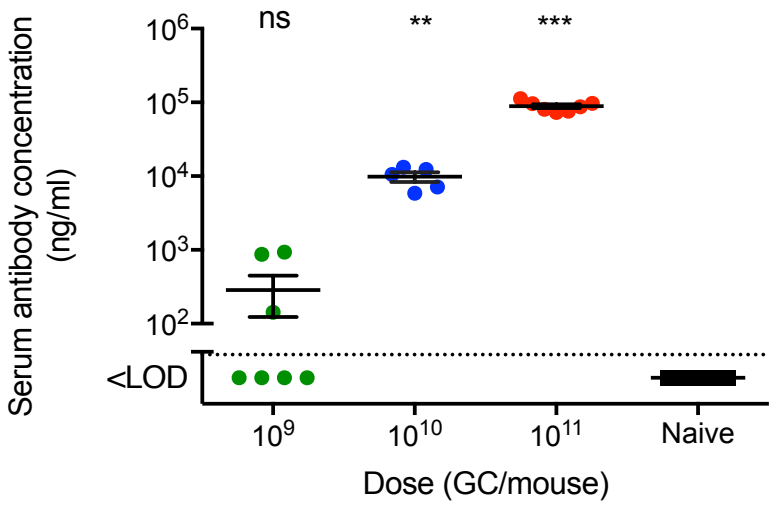
Serum antibody concentration (ng/ml)
10^6
10^5
10^4
10^3
10^2
<LOD
ns
**
***
10^9
10^{10}
10^{11}
Naive
Dose (GC/mouse)

Figure 5.4. Infliximab expression following administration of rAAV2/8 to mice.

Female BALB/c mice (n = 8) were administered 10^9, 10^{10} or 10^{11} GC of rAAV2/8 CASI infliximab via intramuscular injection (Section 2.6.5.3). Serum was obtained by collecting blood from the tail vein (Section 2.6.6.1) at the indicated time-points (A). Antibody concentration in the serum was measured using human IgG ELISA (Section 2.7.4). (A) Infliximab concentration in the serum throughout the duration of the experiment. (B) Individual values for serum antibody concentration at 6 months post-delivery. Data are shown as individual values and/or mean ± standard error of the mean. Significant differences between the values were determined using Kruskal-Wallis test with Dunn's post hoc test compared with naïve mice. A calculated p value of >0.05 was deemed non-significant as indicated with ns. Calculated p values of <0.01 or <0.001 were deemed a significant difference as indicated with two (**) or three stars (***), respectively. Dotted line denotes lower limit of detection (LOD) (78 ng/ml).

5.2.2 *In vivo* etanercept production using rAAV2/8 vectors

The protein sequence of etanercept (Appendix) was sourced from patent number US7276477B2 (Osslund, 2003). The TNFR2, from which etanercept is derived (Section 1.3.3), has a native signal sequence for secretion and it was speculated that this might offer an improvement over the hGH signal sequence included in palivizumab and infliximab cDNAs (Figure 4.1). Two cDNA constructs were therefore designed for etanercept: one including the hGH signal sequence, and the other containing the native TNFR2 signal sequence (Figure 5.5 A). The constructs were codon optimised for *Homo sapiens*, depleted of CpG dinucleotides, synthesised by GeneArt (Thermo Fisher Scientific) and sub-cloned into rAAV2 genome plasmid (Section 2.3.6) to create pAAV2.CASI.hGH-etanercept and pAAV2.CASI.TNFR2-etanercept genomes (Table 2.1). Upon transfection in HEK293T cells (Section 2.4.1), both genomes were found to direct detectable and similar levels of expression of etanercept in the cell culture media supernatant (Figure 5.5 B), and were used to produce rAAV2/8 CASI hGH-etanercept and rAAV2/8 CASI TNFR2-etanercept (Table 2.2; Section 2.5.4). Both vectors were found capable of transducing HEK293T cells and directing secretion of etanercept into the cell culture media supernatant (Figure 5.6).

To determine whether expression of etanercept can be achieved *in vivo* following rAAV2/8 delivery, mice received 10^{10} or 10^{11} GC of each vector via IM injection (Section 2.6.5.3). Blood was sampled at intervals (Section 2.6.6.1) and etanercept levels in the serum were measured using human IgG ELISA (Section 2.7.4). As shown in Figure 5.7 A, the higher dose (10^{11} GC) of each vector directed detectable expression of etanercept in the serum for at least 56 days. At this time-point, the

average concentration reached 5.02 and 5.73 μg/ml for rAAV2/8 CASI hGH-etanercept and rAAV2/8 CASI TNFR2-etanercept, respectively (Figure 5.7 B). Administration of the lower dose (10^{10} GC) of either vector did not result in detectable etanercept expression in the serum. There was no difference in expression levels between the two vectors at any time-point ($p<0.05$), and the hGH signal sequence-containing construct was selected for subsequent studies, as this signal sequence has already been demonstrated to facilitate persistent mAb expression from mouse muscle for at least 6 months (Figure 5.4).

For rAAV2/8-mediated *in vivo* etanercept gene transfer to be more applicable for clinical use in RA patients, a method of controlling expression of the protein after administration is highly desirable. The next section describes the investigation into using SMASh for this purpose.

A

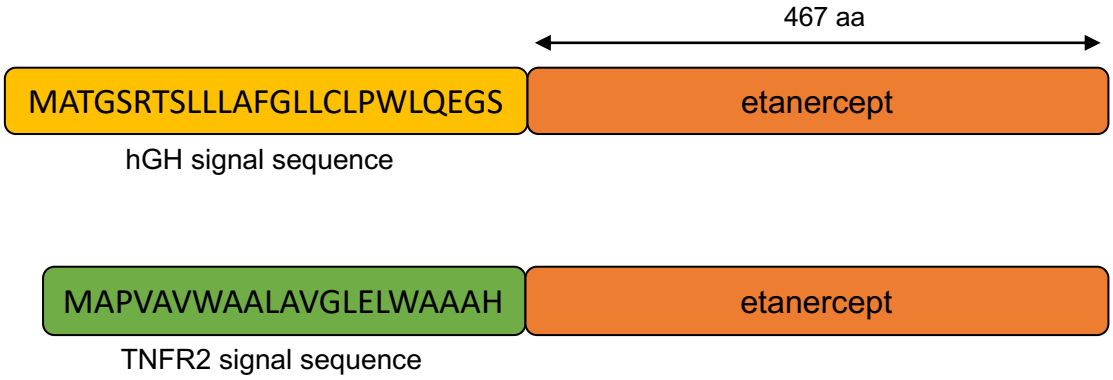
467 aa
MATGSRTSLLLAFGLLCLPWLQEGS
etanercept
hGH signal sequence
MAPVAVWAALAVGLELWAAAH
etanercept
TNFR2 signal sequence

B

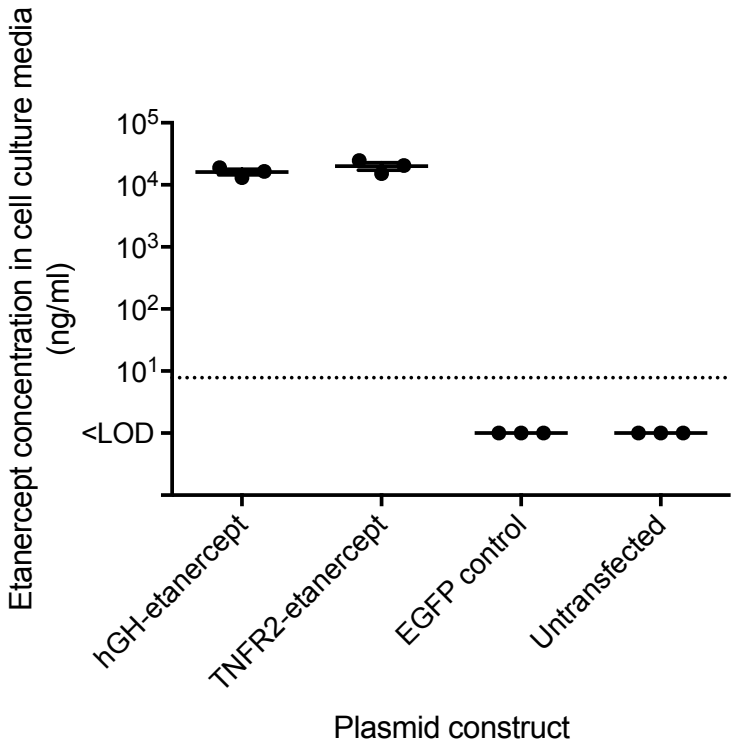
Etanercept concentration in cell culture media (ng/ml)
10^5
10^4
10^3
10^2
10^1
<LOD
hGH-etanercept
TNFR2-etanercept
EGFP control
Untransfected
Plasmid construct

Figure 5.5. Confirmation of etanercept expression following transfection of rAAV vector genomes in cell culture.

(A) Signal sequences from the human growth hormone (hGH) and tumour necrosis factor alpha receptor 2 (TNFR2) were fused to etanercept, which is 467 amino acids (aa) long, at the N-terminus. (B) Adherent HEK293T cells (n = 3 wells) were transfected with pAAV2.CASI.hGH-etanercept (hGH-etanercept), pAAV2.CASI.TNFR2-etanercept (TNFR2-etanercept) or pEGFP-N1 (EGFP control) (Table 2.1; Section 2.4.2). Ninety-six hours after transfection, antibody concentration in the supernatant was measured using human IgG ELISA (Section 2.7.4). Data are shown as individual values and mean ± standard error of the mean. Dotted line denotes lower limit of detection (LOD) (7.8 ng/ml).

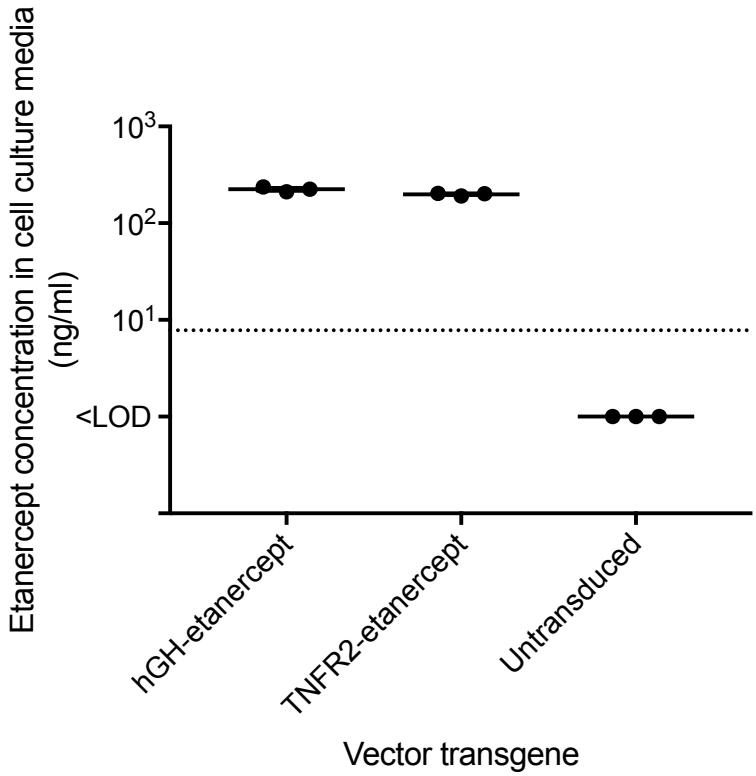

Figure 5.6. Etanercept expression following transduction of rAAV2/8 in cell culture.

Adherent HEK293T cells (seeded in 6-well plates at 10^6 cells per well, n = 3 wells) were transduced with 10^{10} GC of rAAV2/8 CASI hGH-etanercept or rAAV2/8 CASI TNFR2-etanercept (Table 2.2). Six days post-transduction, antibody levels in the supernatant were measured using human IgG ELISA (Section 2.7.4). Data are shown as individual values and mean ± standard error of the mean. Dotted line denotes lower limit of detection (LOD) (7.8 ng/ml).

A

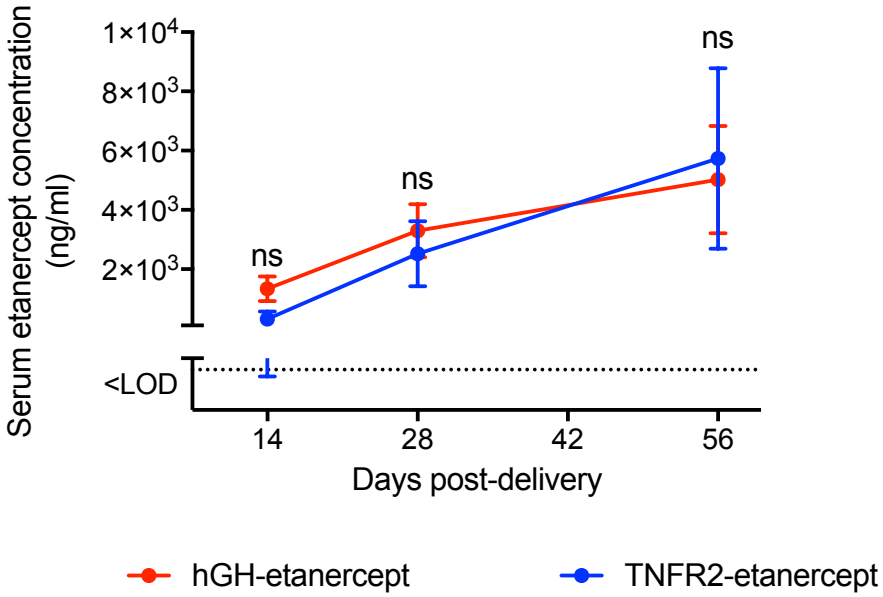
Serum etanercept concentration (ng/ml)
1×10^4
8×10^3
6×10^3
4×10^3
2×10^3
<LOD
ns
ns
ns
14
28
42
56
Days post-delivery
hGH-etanercept
TNFR2-etanercept

B

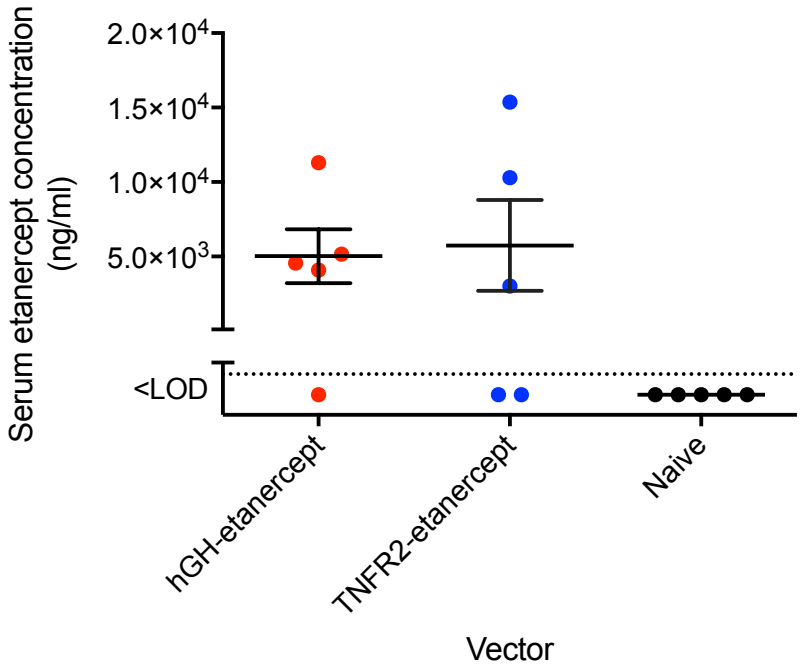
Serum etanercept concentration (ng/ml)
2.0×10^4
1.5×10^4
1.0×10^4
5.0×10^3
<LOD
hGH-etanercept
TNFR2-etanercept
Naive
Vector

Figure 5.7. Etanercept expression following administration of rAAV2/8 to mice.

Female BALB/c mice (n = 5) were administered 10^{10} or 10^{11} GC of rAAV2/8 CASI hGH-etanercept or rAAV2/8 CASI TNFR2-etanercept via intramuscular injection (Section 2.6.5.3). Serum was obtained by collecting blood from the tail vein (Section 2.6.6.1) at the indicated time-points. (A) Etanercept concentration in the serum was measured using human IgG ELISA (Section 2.7.4). Results are only displayed for animals dosed with 10^{11} GC of rAAV, as there was no detectable expression in the serum of animals from the lower dose (10^{10} GC) treatment groups. (B) Individual values for serum antibody concentration at 56 days post-delivery. Data are shown as individual values and/or mean ± standard error of the mean. Significant differences between the values were determined using Kruskal-Wallis test. A calculated p value of >0.05 was deemed non-significant as indicated with ns. Dotted line denotes lower limit of detection (LOD) (78 ng/ml).

5.2.3 Regulation of anti-TNFα expression using SMASh

A study was undertaken to demonstrate the ability of SMASh (Figure 5.1) to control protein expression *in vitro* and thus replicate the findings of the study first describing the tag (Chung et al., 2015). HEK293T cells were transfected (Section 2.4.2) with pG6.hCEFI.Lux-SMASh, which encodes firefly luciferase fused to SMASh at the C-terminus, pG6.hCEFI.Lux (encoding luciferase without SMASh; both gifts of Ian Pringle), or a control plasmid pEGFP-N1 (Table 2.1) in the presence or absence of 1 μM of the NS3 protease inhibitor asunaprevir (ASV). Addition of ASV to cell culture media at the time of transfection resulted in a 24-fold reduction in luciferase protein expression from pG6.hCEFI.Lux-SMASh ($p<0.001$, Figure 5.9 A). The addition of ASV had no effect on luciferase expression from the pG6.hCEFI.Lux control plasmid which did not contain SMASh.

To demonstrate that suppression of protein expression using SMASh is reversible, Madin-Darby Canine Kidney (MDCK) cells, which are strongly adherent and do not easily detach upon washing and replacement of media, were transfected (Section 2.4.2) with pG6.hCEFI.Lux-SMASh, pG6.hCEFI.Lux or the control plasmid pEGFP-N1 (Table 2.1) in the presence or absence of 1 μM ASV. After 24 hours, the cells were washed and the media replaced with one either containing or not containing 1 μM ASV. A further 48 hours later, luciferase activity in the lysates was measured. The schematic timeline of the experiment is shown in Figure 5.8 B. Figure 5.9 C shows that the 32-fold reduction in luciferase expression from pG6.hCEFI.Lux-SMASh after a 24-hour incubation with ASV ($p<0.001$) is reversible, with luciferase activity returning to levels that are not significantly

different from those recorded in the unsuppressed samples within 48 hours of removal of the drug.

Having demonstrated reversible control of luciferase expression, an experiment was undertaken to determine whether SMASh is effective in suppressing expression of secretory proteins *in vitro*, in preparation for the possible use of SMASh *in vivo*. Plasmids pG6.hCEFI.soGLux-SMASh and pG6.hCEFI.etanercept-SMASh (Table 2.1), encoding the secretory reporter protein GLux and etanercept, respectively, fused to SMASh tag, were generated as described in Section 2.3.7. HEK293T cells were transfected (Section 2.4.2) with pG6.hCEFI.soGLux-SMASh, pG6.hCEFI.soGLux, pG6.hCEFI.etanercept-SMASh, pG6.hCEFI.etanercept or the control plasmid pEGFP-N1 (Table 2.1) in the presence or absence of asunaprevir. After 24 hours, GLux activity or etanercept concentration in the supernatants were measured, as appropriate (Sections 2.7.3 and 2.7.4). As shown in Figure 5.10 A, SMASh was only partially successful in suppressing expression of GLux, with a 1.5-fold reduction in activity in the cell culture media supernatant in the presence of asunaprevir ($p<0.001$). Expression from pG6.hCEFI.soGLux-SMASh in the absence of the inhibitor was over 800-fold lower than from pG6.hCEFI.soGLux, indicating that the presence of the tag impairs the expression or activity of GLux. In the case of etanercept, the protein was undetectable in the supernatant of cells transfected with pG6.hCEFI.etanercept-SMASh, with or without inclusion of asunaprevir, even though abundant expression from pG6.hCEFI.etanercept was observed (Figure 5.10 B).

A

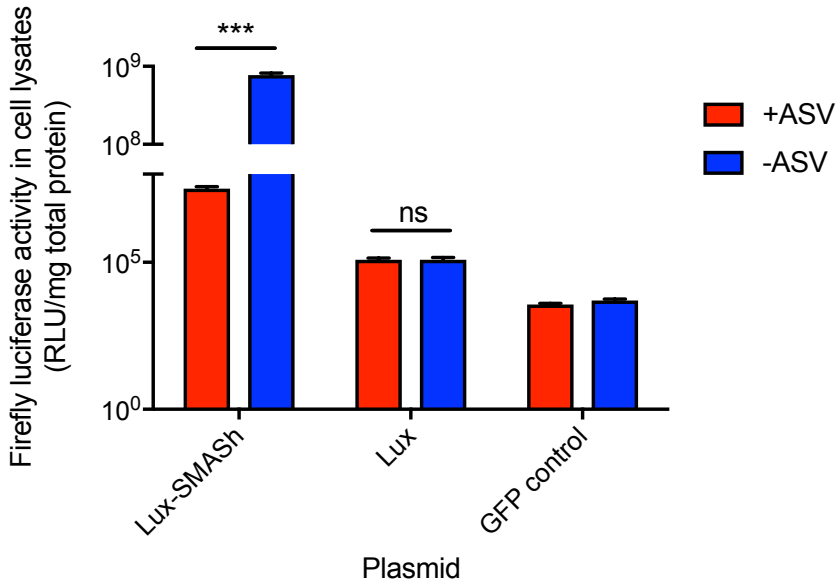
***
ns
10^9
10^8
10^5
10^0
Firefly luciferase activity in cell lysates
(RLU/mg total protein)
+ASV
-ASV
Lux-SMASh
Lux
GFP control
Plasmid

B

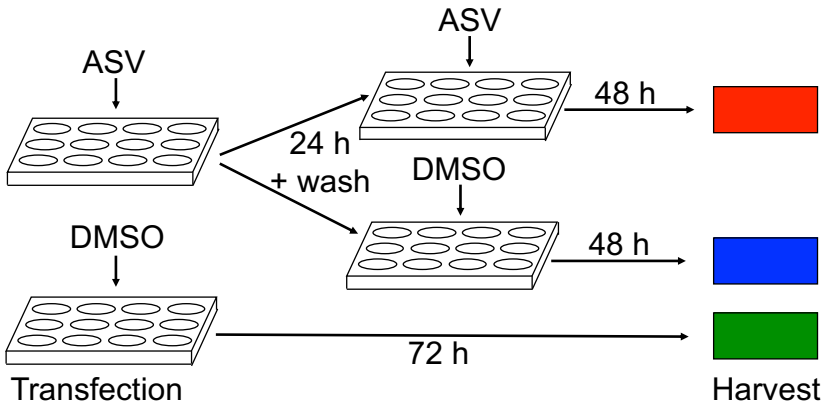
ASV
ASV
48 h
24 h
+ wash
DMSO
DMSO
48 h
72 h
Transfection
Harvest

C

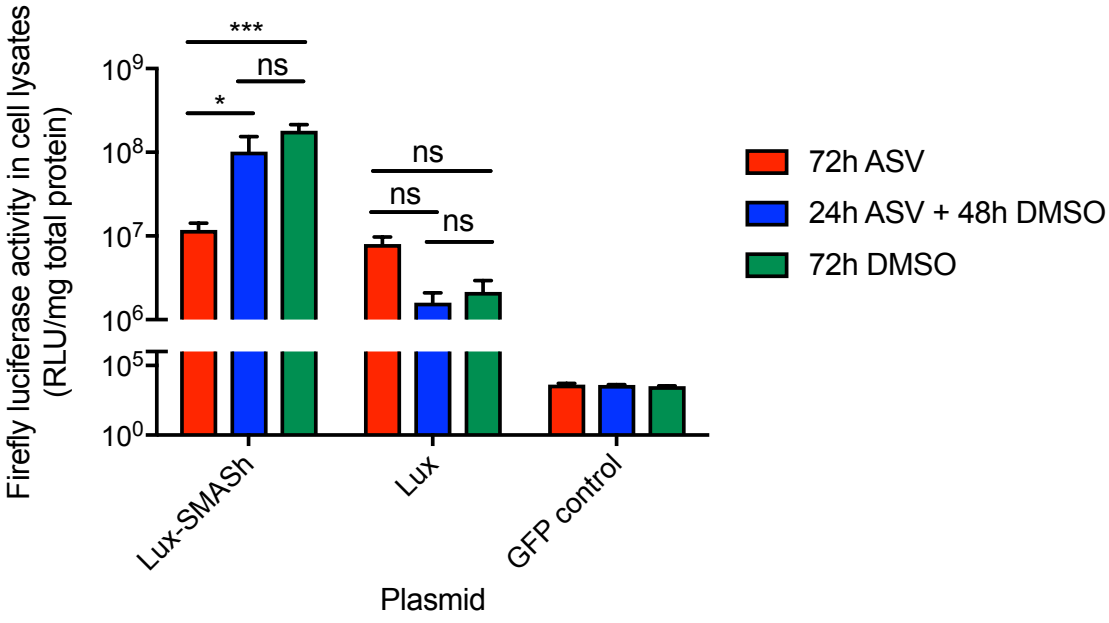
***
ns
*
ns
ns
ns
10^9
10^8
10^7
10^6
10^5
10^0
Firefly luciferase activity in cell lysates
(RLU/mg total protein)
72h ASV
24h ASV + 48h DMSO
72h DMSO
Lux-SMASh
Lux
GFP control
Plasmid

Figure 5.8. Reversible suppression of luciferase expression using SMASh.

(A) Adherent HEK293T cells (seeded at 5 x 10^5 cells/well in 12-well plates, n = 6 wells) were transfected with pG6.hCEFI.Lux-SMASh (Lux-SMASh), pG4.hCEFI.Lux (Lux) or pEGFP-N1 (GFP control) (Table 2.1; Section 2.4.2) in the presence or absence of 1 μM asunaprevir (ASV). After 24 hours, luciferase activity in the lysates was measured using luminometry (Section 2.7.2). (B) Schematic of experimental design. MDCK cells (seeded at 2 x 10^4 cells/well in 12-well plates, n = 6 wells per group) were transfected with pG6.hCEFI.Lux-SMASh (Lux-SMASh), pG6.hCEFI.Lux (Lux) or pEGFP-N1 (GFP control) (Section 2.4.2) in the presence or absence of 1 μM ASV or equivalent amount of the diluent dimethyl sulfoxide (DMSO, Sigma-Aldrich). After 24 hours, the cells were washed and fresh media added containing either 1 μM ASV or DMSO. The cells were incubated for a further 48 hours, after which the cell lysates were collected (Section 2.4.3) and firefly luciferase activity in the lysates measured using luminometry (Section 2.7.2). (C) Firefly luciferase activity in the cell lysates. Data are shown as mean ± standard error of the mean. Significant differences between the values were determined using ANOVA with Bonferroni's post hoc test. A calculated p value of >0.05 was deemed non-significant as indicated with ns. Calculated p values of <0.05 or <0.001 were deemed a significant difference as indicated with one (*) or three stars (***), respectively.

A

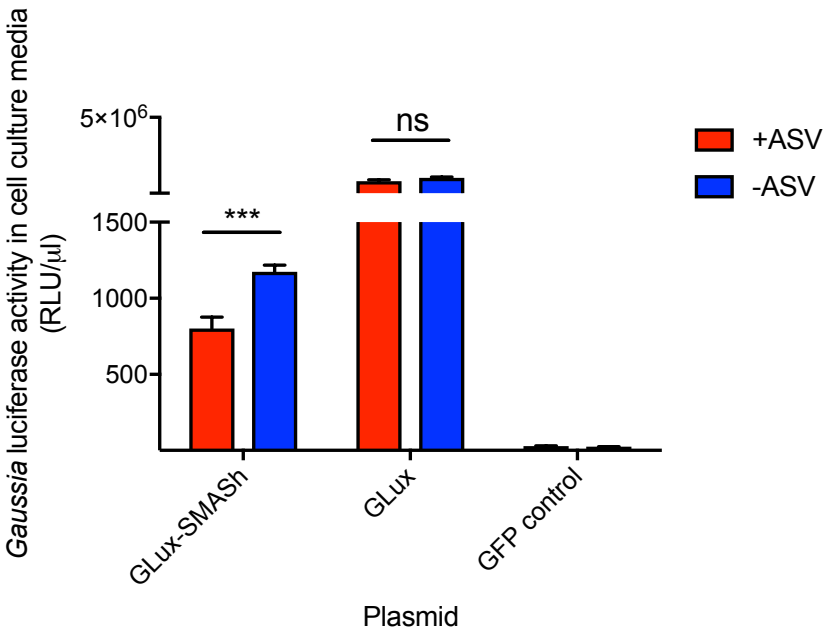
Gaussia luciferase activity in cell culture media (RLU/µl)
5×10^6
1500
1000
500
***
ns
+ASV
-ASV
GLux-SMASh
GLux
GFP control
Plasmid

B

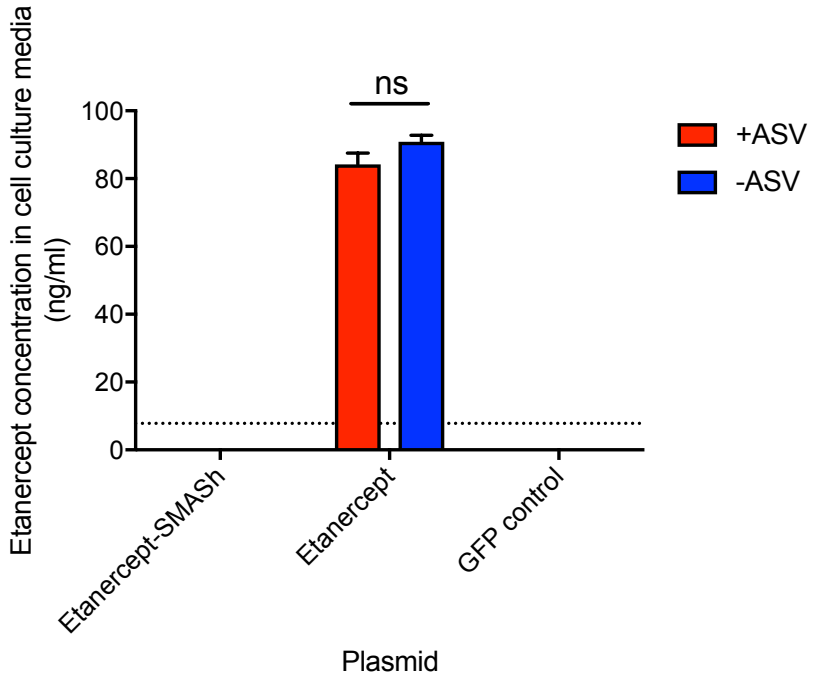
Etanercept concentration in cell culture media (ng/ml)
100
80
60
40
20
0
ns
+ASV
-ASV
Etanercept-SMASh
Etanercept
GFP control
Plasmid

Figure 5.9. Control of *Gaussia* luciferase and etanercept expression using SMASh.

Adherent HEK293T cells (seeded at 5 x 10^5 cells/well in 12-well plates, n = 6 wells) were transfected (Section 2.4.2) with pG6.hCEFI.soGLux-SMASh (GLux-SMASh), pG6.hCEFI.soGLux (GLux), pG6.hCEFI.etanercept-SMASh (etanercept-SMASh), pG6.hCEFI.etanercept (etanercept) or pEGFP-N1 (GFP control) (Table 2.1) in the presence or absence of 1 μM asunaprevir (ASV). After 24 hours, the supernatants were collected and (A) GLux and (B) etanercept levels measured, using GLux assay (Section 2.7.3) and human IgG ELISA (Section 2.7.4), respectively. Data are shown as mean ± standard error of the mean. Significant differences between the values were determined using ANOVA with Bonferroni's post hoc test (A) or Student's t-test (B). A calculated p value of >0.05 was deemed non-significant as indicated with ns. A calculated p value of <0.001 was deemed a significant difference as indicated with three stars (***). Dotted line denotes lower limit of detection for human IgG ELISA (7.8 ng/ml).

The lack of etanercept expression from pG6.hCEFI.etanercept-SMASh was unexpected. DNA sequencing revealed that no mutations were present in the etanercept-SMASh cDNA or anywhere else in the plasmid (data not shown). Quantification of mRNA expression using TaqMan reverse-transcriptase PCR assay (Section 2.7.5) demonstrated that the amount of mRNA transcribed from pG6.hCEFI.etanercept-SMASh was not significantly different from that transcribed from pG6.hCEFI.etanercept (Figure 5.10). This indicated that there was no specific feature of the plasmid preventing mRNA transcription and instead suggested there may be an issue at the level of translation or thereafter.

Further investigation into the biochemistry of NS3 protease suggested a possible mechanism for the lack of expression of etanercept, which is outlined in Figure 5.11. The NS3 protease, which is normally localised to the cytoplasm (Wolk et al., 2000), contains a cluster of three cysteine residues coordinating a zinc ion (Love et al., 1996), which is required for correct folding of the protein (Stempniak et al., 1997). It was hypothesised that the cysteine residues could become oxidised as the etanercept-SMASh fusion protein is being translated in the ER, preventing the binding of zinc to the cysteine cluster and thus blocking cleavage of the NS3 target sequence even in the absence of ASV. Consequently, the entire SMASh tag would, in all circumstances, remain fused to the protein of interest and the degron would direct degradation of the whole fusion protein, such that no etanercept could be expressed in the absence or presence of NS3 protease inhibitor.

To test this hypothesis, the SMASh tag was modified to remove the degron sequence (Figure 5.12 A), which should prevent protein degradation and indicate whether cleavage at the NS3 protease target site takes place when fused to

etanercept. The NS3 protease is preceded by a Flag tag, enabling detection of either the fusion protein or the cleaved NS3 protease by immunoblotting (Figure 5.12 B). A plasmid encoding etanercept fused to the modified, degron-less SMASh tag was constructed as described in Section 2.3.7, generating pG6.hCEFI.etanercept-NS3 (Table 2.1). HEK293T cells were transfected (Section 2.4.2) with the plasmid in the presence or absence of 1 μM ASV, and the lysates and supernatants subjected to SDS-PAGE and immunoblotting for Flag (Section 2.7.6).

The results of immunoblotting are shown in Figure 5.13. The lysates from cells transfected with pG6.hCEFI.etanercept-NS3 which have not been subjected to deglycosylation exhibit a single band, corresponding in size to dimeric etanercept fused to NS3 protease (~200 kDa). This band is visible irrespective of incubation of the cells with asunaprevir (ASV + and ASV -). Denaturation and deglycosylation of protein samples (D +) resulted in a single band corresponding to monomeric etanercept fused to NS3 protease (~100 kDa). A 23-kDa band, which would represent the cleaved portion of the fusion protein, was not observed regardless of whether ASV was present. It was therefore concluded that cleavage of NS3 target sequence does not take place when the protease is fused to etanercept. No protein bands were detected in the supernatants of transfected cells, suggesting that the fusion protein was not secreted but remained inside the cell. The SMASh system was therefore deemed an inadequate method with which to control expression of etanercept *in vivo* following gene transfer. An alternative solution is discussed in the next section.

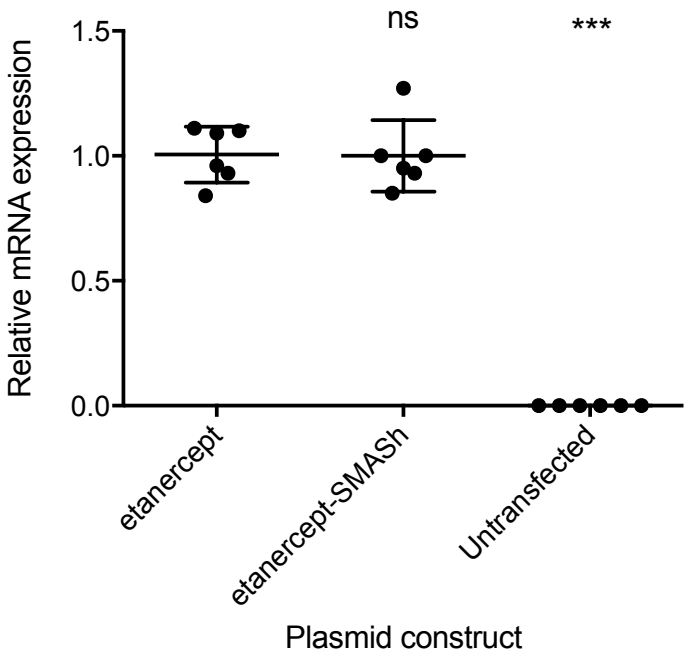

Figure 5.10. Quantification of mRNA expression from etanercept-SMASh plasmid construct.

Adherent HEK293T cells (seeded at 5 x 10^5 cells/well in 12-well plates, n = 6 wells) were transfected with pG6.hCEFI.etanercept (etanercept) or pG6.hCEFI.etanercept-SMASh (etanercept-SMASh) (Table 2.1; Section 2.4.2). After 24 hours, total RNA was extracted from the cell lysates and etanercept and glyceraldehyde 3-phosphate dehydrogenase (GAPDH) transcripts were quantified using TaqMan reverse transcriptase-PCR assay. The relative abundance of etanercept-encoding transcripts was normalised to GAPDH expression and expressed as a proportion of expression from pG6.hCEFI.etanercept (Section 2.7.5). Data are shown as individual values and mean ± standard error of the mean. Significant differences between the values were determined using ANOVA with Dunnett's post hoc test compared with pG6.hCEFI.etanercept. A calculated p value of >0.05 was deemed non-significant as indicated with ns. A calculated p value of <0.001 was deemed a significant difference as indicated with three stars (***).

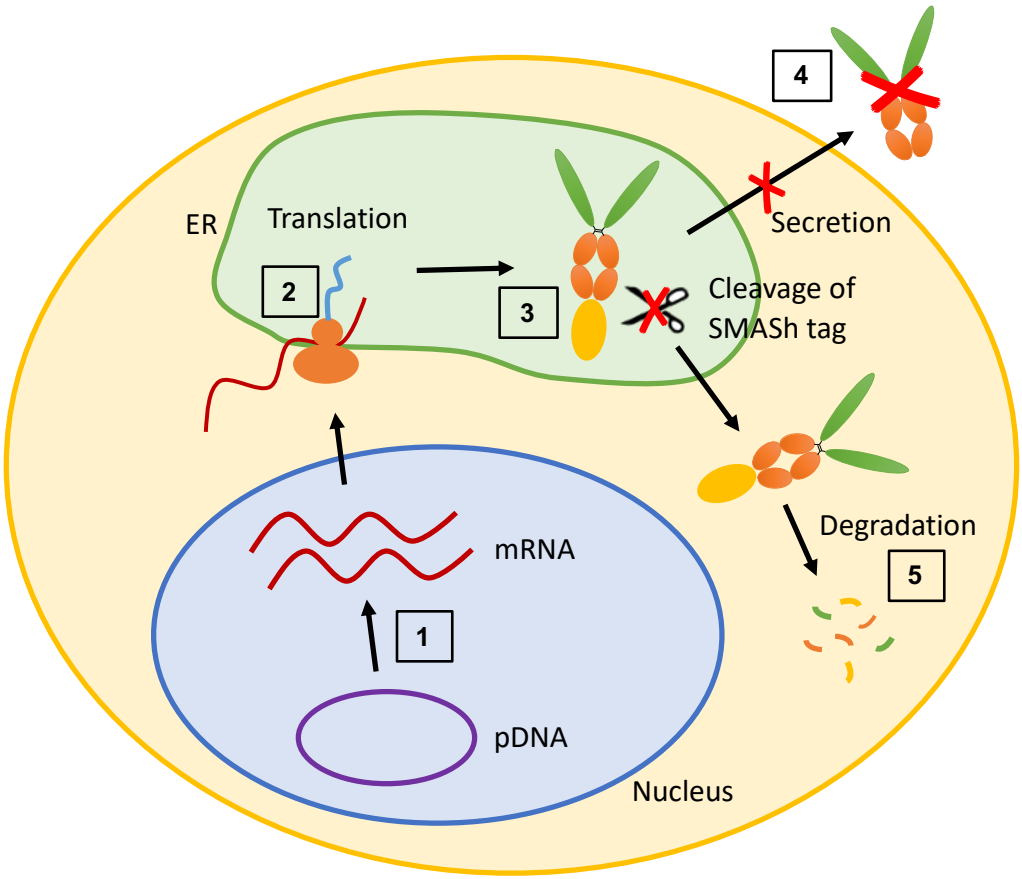

Figure 5.11. Schematic of consequence of fusing SMASh tag with a secreted protein.

Following delivery to the cell, plasmid encoding the etanercept-SMASh fusion construct is transcribed (1) and the mRNA translated. The secretory signal sequence leads to docking of the ribosome-mRNA-nascent chain complex onto the endoplasmic reticulum (ER), where the signal peptide is removed by a signal peptidase and protein synthesis continues (2). In the absence of an inhibitor of NS3 protease, SMASh tag should remove itself (3) and etanercept should be secreted from the cell (4). However, a cysteine cluster in the NS3 protease is presumed to be oxidised in the ER, preventing correct folding and activity of the protein. The tag therefore remains fused to etanercept and the degron directs degradation of the entire fusion protein (5), such that no etanercept can be detected.

A

DEMEEC^SQHLPGAGSSGDIMDYKDDDDKGSSGTGSGSGTSAPITAYAQQTR

GLLGCIITSLTGRDKNQVEGEVQIVSTATQTFLATCINGVCWAVYHGAGTRTIAS

PKGPVIQMYTNVDQDLVGWPAPQGSRSLTPCTCGSSDLYLVTRHADVIPVRRR

GDSRGSLLSPRPISYLKGSSGGPLLCPAGHAVGLFRAAVCTRGVAKAVDFIPVE

NLETTMRSPVFTD

B

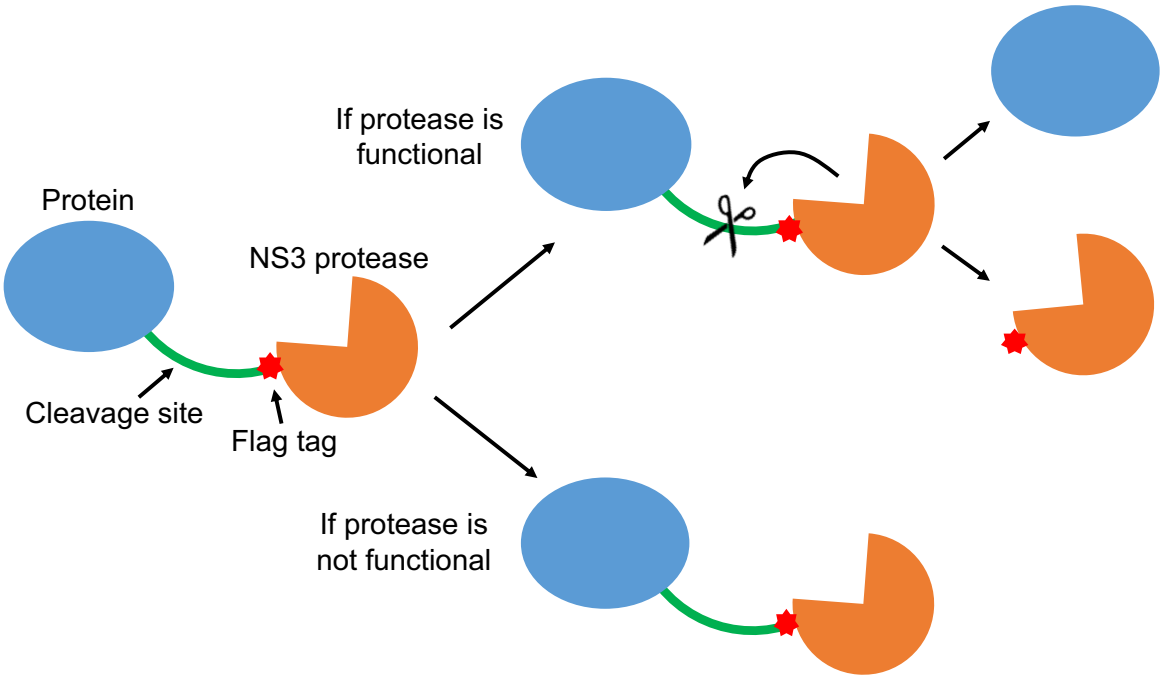

Figure 5.12. Cleavage by NS3 protease in the absence of degron sequence. (A) The putative degron was removed from the SMASh tag by deletion of the truncated NS3 helicase domain and the NS4A cofactor (Figure 5.7 A), leaving behind the cleavage signal sequence (green), the linker (black) with a Flag tag (red) and NS3 protease (orange). (B) In the absence of NS3 protease inhibitor, the protease should cleave its substrate, releasing the protein of interest. If the protease is not functional, it will remain fused to the protein of interest, and the entire fusion protein can be detected.

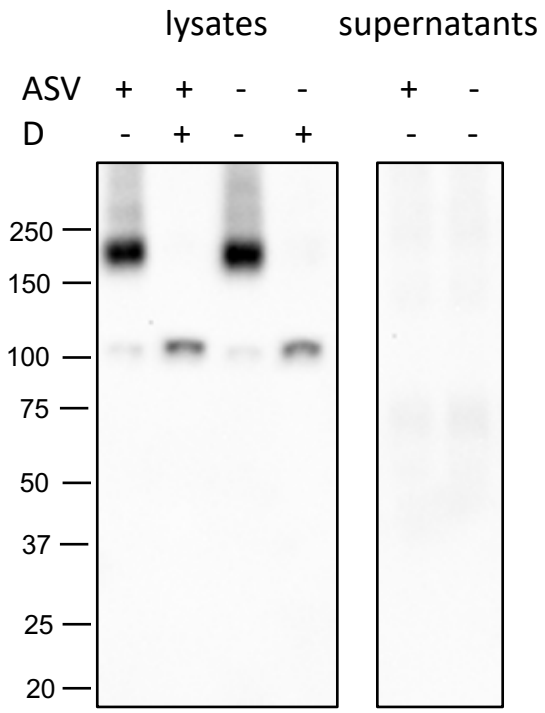

Figure 5.13. Cleavage activity of NS3 protease fused to etanercept.

Adherent HEK293T cells (seeded at 10^6 cells/well in 6-well plates) were transfected (Section 2.4.2) with pG6.hCEFI.etanercept-NS3 (Table 2.1) in the presence or absence of 1 μM asunaprevir (ASV). After 24 hours, cell culture media supernatants were collected and total protein was extracted from cell lysates and optionally deglycosylated in denaturing conditions using Protein Deglycosylation Mix II (NEB) according to the manufacturer's protocol (D + or -). The protein samples were then subjected to SDS-PAGE, transferred onto a nitrocellulose membrane and immunoblotted for Flag tag (Section 2.7.6). Molecular weight markers, along with their weight in kDa, are indicated.

5.3 Discussion

5.3.1 Serum anti-TNFα levels following rAAV2/8 administration

The studies presented in this chapter demonstrate sustained and robust expression of anti-TNFα following rAAV2/8 administration to the muscle. Serum levels of infliximab at 6 months post-delivery reached an average of 89 μg/ml in the highest dose group (Figure 5.4). To estimate whether these levels are likely to be therapeutically relevant, they were compared with literature reports of trough serum levels in RA patients that correlate with remission of the disease. Following injection of infliximab, trough serum levels of 1.15 or 2.03 μg/ml were found to be associated with moderate and good clinical response, respectively (Mori, 2007). Elsewhere, it was concluded that a trough level of approximately 1 μg/ml is required to observe a response (St Clair et al., 2002). The levels of infliximab observed in Figure 5.4 exceeded those quoted in the above studies, warranting progression to investigations in an animal model. Due to the lack of cross-reactivity between infliximab and mouse TNFα, the transgenic Tg197 mouse model expressing human TNFα would have to be used for this purpose, but difficulties in sourcing and maintaining this strain supported the decision to switch to a biologic which cross-reacts with mouse TNFα. Etanercept was therefore selected for further studies in this chapter such that a simpler mouse model could be used in which RA is induced, such as the collagen-induced arthritis (CIA) model (further discussed in Section 5.3.2). Etanercept has a further advantage of being encoded by a smaller cDNA (1.5 kb), enabling accommodation of the SMASh tag into a single vector and removing the need for a dual vector system. The levels of etanercept achieved in the serum following rAAV2/8 administration reached

approximately 5 µg/ml at 56 days post-delivery. This is markedly lower than the levels observed for infliximab at this time-point (69.2 µg/ml for a matched vector dose) and likely reflects the difference in the half-lives of the two proteins: 7-12 days for infliximab (Klotz et al., 2007) and 68 hours for etanercept (Korth-Bradley et al., 2000). Nonetheless, serum etanercept levels observed in this study compare favourably with the 1-1.56 µg/ml trough levels in patients that are associated with remission (Chen et al., 2015, Sanmarti et al., 2015), suggesting they could have a therapeutic effect.

5.3.2 Future studies in animal models of RA

To demonstrate the therapeutic potential of rAAV2/8-mediated anti-TNFα gene transfer, the ability of the vector to ameliorate disease symptoms in an animal model could be tested. A number of transgenic and induced murine models have been developed to aid research into treatment for RA (reviewed in Bevaart et al., 2010). Transgenic lines develop RA spontaneously, an example of which is the Tg197 line, which carries five copies of the human TNFα gene, with the 3' untranslated region (UTR) replaced by that of the beta-globin gene leading to high levels of expression of both soluble and membrane-bound human TNFα (Keffer et al., 1991). Since this model expresses the human form of the cytokine, it would be suitable for testing anti-TNFα biologics which do not cross-react with the mouse protein, such as infliximab and golimumab (Shealy et al., 2010). To test the effectiveness of rAAV-mediated etanercept gene transfer *in vivo*, an induced model of RA could be used, such as the commonly used CIA. In this model, arthritis is triggered by immunising the animals with type II collagen with complete Freund's

adjuvant (Kannan et al., 2005). Pathological features are similar to those observed in human RA (McNamee et al., 2015), as are the immunological mechanisms, including the involvement of T-cells and cytokine-mediated signalling. The CIA mouse model has been used to demonstrate that anti-TNFα is effective in both prophylaxis and treatment of arthritic symptoms (Williams et al., 1992), setting precedent for development of anti-TNFα biologics for treatment of RA. This model would therefore be suitable to test whether administration of rAAV2/8 CASI etanercept has the capability to reduce RA symptoms *in vivo*, and this is currently being explored as an extension to the studies described in this chapter.

5.3.3 Regulation of anti-TNFα production following gene transfer

In this chapter, SMASh was investigated as a method of controlling etanercept expression. Its main advantage is that it can be accommodated into a single rAAV vector, removing the need for a dual vector system which would reduce transgene expression levels compared to a single rAAV vector (Colella et al., 2014, Trapani et al., 2014). Despite successful suppression of firefly luciferase expression (Figure 5.8), SMASh was not effective at controlling expression of secretory proteins GLux and etanercept (Figure 5.10), presumably due to the lack of NS3 protease activity when fused to a secretory protein. A potential solution to this issue could be inclusion of a transmembrane (TM) region between etanercept and the SMASh tag, as suggested in Figure 5.14 A. This would allow the SMASh portion of the fusion protein to remain outside the ER and thus the NS3 protease to retain its function. If a suitable linker containing a protease cleavage site was included, etanercept could be cleaved from the TM region by an endogenous protease

present in the Golgi apparatus or at the cell membrane, and ultimately secreted (Figure 5.14 B). An example of a protease which could be utilised is TACE, also called ADAM metallopeptidase domain 17 (ADAM17). It is a membrane-tethered protein located in the trans-Golgi network and at the cell membrane which naturally cleaves transmembrane molecules such as TNFα, TNFR1, TNFR2 and other proteins to release their soluble portions (Figure 1.11). It is expressed in a wide variety of tissues, including skeletal muscle (Black et al., 1997), rendering it potentially useful for gene delivery to this site.

A hurdle to implementation of this proposal is the limited packaging capacity of rAAV. In TNFR2, the region spanning the TACE cleavage site and the transmembrane helix is at least 83 amino acids long, meaning an additional region of ~250 bp would have to be accommodated in the vector. In the case of etanercept, this would increase the genome size to 5.04 kb, which exceeds the 4.1-4.9 kb range reported to be optimal for packaging efficiency (Dong et al., 1996). For this and other, larger transgenes such as single-ORF mAbs, the possibility of substituting the 1.04 kb CASI enhancer/promoter for a smaller transcriptional element would need to be explored in order to accommodate the SMASh system into a single vector. A possible alternative could be the widely used 0.51 kb CMV enhancer/promoter, which directs robust, long-term expression from the murine muscle following rAAV2/8-mediated gene transfer, albeit at levels lower than CASI (Balazs et al., 2011). The 0.70 kb hCEFI enhancer/promoter, developed for persistent expression in the murine lung (Hyde et al., 2008), was used in vectors delivered IN in Chapters 3 and 4. Its activity in the mouse muscle has not been evaluated and could be investigated in the future in the context of rAAV2/8-mediated gene transfer. Alternatively, a synthetic design approach could be

employed (Schlabach et al., 2010) to develop compact transcriptional elements capable of driving high-level, persistent transgene expression from the muscle that would allow accommodation of large cDNA constructs into a single rAAV vector. Regrettably, such vector engineering and optimisation was outside of the time available for this thesis and this approach was not explored. Further solutions which could be explored to regulate expression of biologics following gene transfer are discussed in Section 6.2.

A

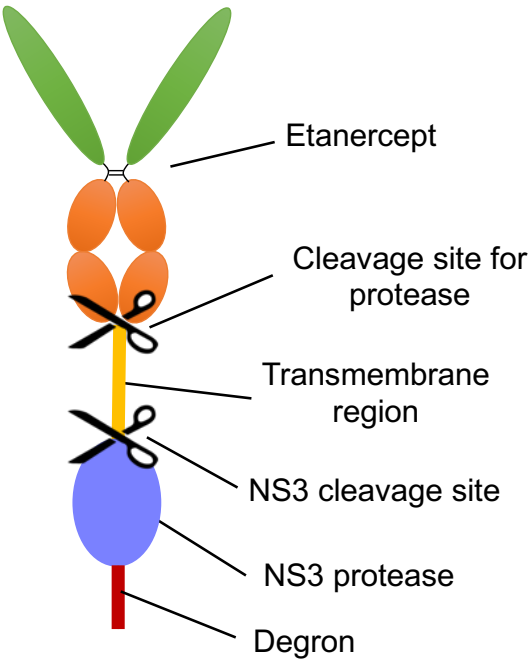
Etanercept
Cleavage site for protease
Transmembrane region
NS3 cleavage site
NS3 protease
Degron

B

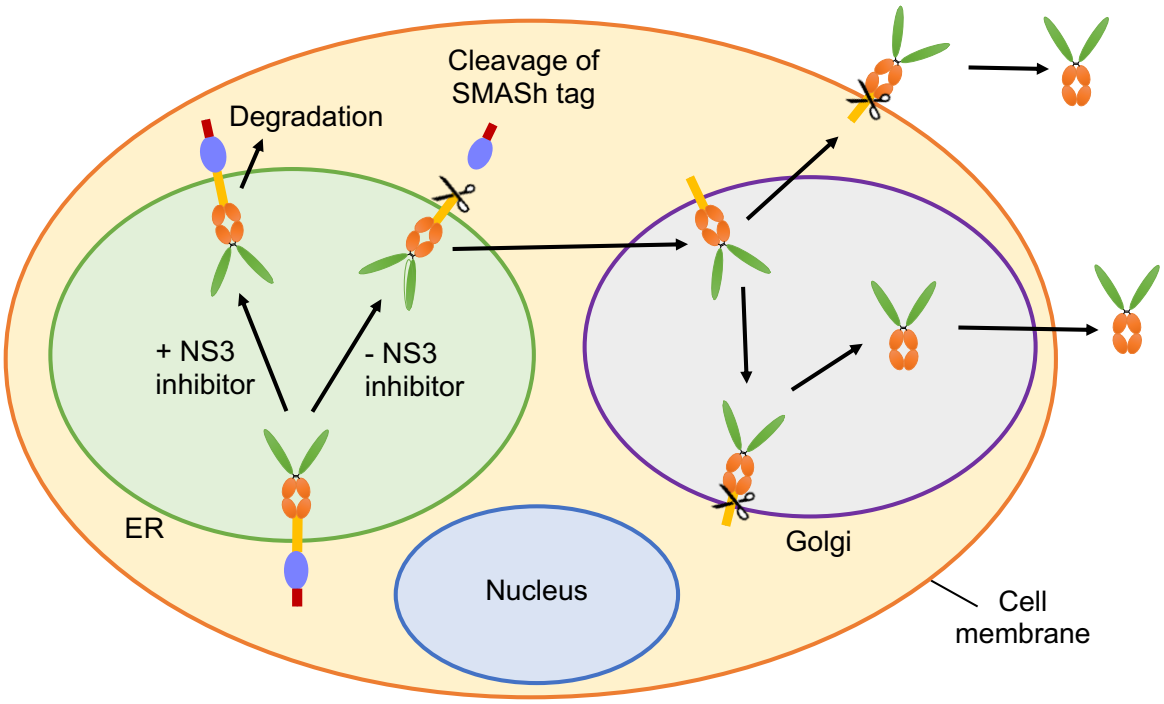
Cleavage of SMASh tag
Degradation
+ NS3 inhibitor
- NS3 inhibitor
ER
Golgi
Nucleus
Cell membrane

Figure 5.14. Proposed solution for retaining function of NS3 protease when fused to a secretory protein.

(A) Schematic structure of the proposed fusion protein, with an intervening transmembrane region between etanercept and SMASh tag. The transmembrane region includes a cleavage site for a membrane protease present either in the Golgi network, or at the cell membrane. (B) When the fusion protein is synthesised, the transmembrane region ensures the SMASh tag remains outside the ER, thus retaining functional activity of NS3 protease. In the presence of NS3 protease inhibitor, cleavage of SMASh tag does not occur, and the entire fusion protein is degraded. In the absence of NS3 protease inhibitor, NS3 protease cleaves its target sequence in the transmembrane region, releasing etanercept from the tag, which is subsequently degraded. The transmembrane etanercept is transported from the ER to Golgi apparatus, where it may be processed by a resident protease to release soluble etanercept into the lumen, from where it is secreted. The transmembrane region may also be cleaved by a protease at the cell surface, thereby releasing etanercept into the extracellular space.

Chapter 6: Discussion

6.1. *In vivo* antibody expression following gene transfer

Parenteral administration of mAbs is used in the treatment of many diseases, particularly cancer and autoimmune diseases, with the potential to increase patients' quality or even duration of life. However, due to the costs related to the complexity of manufacture and purification, their use may be restricted if it is not deemed cost-effective. For example, the anti-RSV mAb palivizumab, which costs up to £6,000 per patient for a five-dose regimen (Marshall et al., 2008), is recommended for use only in preterm neonates or infants with congenital heart and lung disease (Section 1.2.3.2), despite the associated disease symptoms and complications representing a considerable burden in the wider paediatric population (Section 1.2.1). Another example is the anti-cancer drug trastuzumab, which, despite being effective at treating metastatic breast cancer (Marty et al., 2005, Vogel et al., 2002), has not been deemed cost-effective (Norum et al., 2005) compared with the commonly used $50,000 per life-year threshold (Neumann et al., 2014). Utilising gene therapy vectors to deliver therapeutic antibody genes directly to individuals could offer an alternative solution if the cost of treatment per patient can be reduced, with the added benefit of easing patient burden, as a single dose of the gene transfer agent could offer long-lasting effects.

Direct expression of mAbs *in vivo* has been shown to be effective in animal models for a number of applications, including HIV (Balazs et al., 2011), influenza (Balazs et al., 2013) and Ebola infections (Robert et al., 2017), amongst others. As expression levels *in vivo* appear to be antibody-specific (Balazs et al., 2011), the

use of different mAbs in the reported studies makes it difficult to draw definitive conclusions about the relative efficiency of the various gene delivery platforms used for mAb gene transfer (reviewed in Hollevoet and Declerck, 2017). The aim of this thesis was to perform direct comparison of available gene transfer agents for delivery of secretory protein to the circulation and lung lumen, and to evaluate their efficacy using two model diseases: rheumatoid arthritis (RA) and RSV infection.

In Chapter 3, a number of non-viral and viral gene transfer vectors were investigated for delivery of secretory reporter protein to the circulation and lung lumen. Non-viral gene transfer formulations have several advantages compared with viral vectors, such as lower manufacturing costs and the lack of pre-existing immunity (discussed in Section 1.1.4). A previous study evaluated three non-viral gene transfer agents in sheep lung, employed as a large animal model of human aerosol delivery: 25-kDa branched PEI, the cationic liposome GL67A (both described in Section 1.1.4) and compacted DNA nanoparticles formulated with polyethylene glycol-substituted lysine 30-mer (McLachlan et al., 2011). The aerosol delivery efficiencies for PEI and GL67A were equivalent and superior to the nanoparticle formulation in sheep (McLachlan et al., 2011); studies described in Section 3.3.1 therefore focused on these two gene transfer agents. It was hypothesised that the cationic lipid GL67A, which has been evaluated in the clinic for treatment of CF (Alton et al., 2015), may be successful at delivering secretory protein to the lung lumen and circulation. However, as shown in Figure 3.2, no significant expression of GLux reporter protein was observed in the lung lumen or circulation following delivery of a GL67A aerosol to the murine lung. New non-viral formulations with improved efficiencies are continually being developed, such as

novel nanoparticles comprising a nucleus-targeting core and a negatively charged capsid-like shell, which can reportedly achieve >95% transfection efficiency *in vitro* (Li et al., 2017a). It is rare that such high efficiencies *in vitro* translate into animal models, but many lessons are being learned which may ultimately contribute to improved transduction *in vivo* (van Haasteren et al., 2018). Optimisation of the constituent plasmid sequence within non-viral formulations is an additional strategy for increasing the levels and persistence of transgene expression. For example, inclusion of scaffold/matrix attachment regions (S/MARs) – sequences which mediate attachment of DNA to the nuclear matrix and facilitate replication of the exogenous plasmid – was shown to facilitate expression of a reporter protein for up to 1 year following delivery of pDNA to the retina of mice (Koirala et al., 2014). The combination of emerging, highly efficient non-viral formulations with plasmid sequences optimised for *in vivo* use could be explored for the purpose of secretory protein production.

Studies in Chapter 3 also investigated the use of the viral gene transfer agents rAAV and rSIV.F/HN. As outlined in Section 1.1.5.4, recombinant AAV has emerged as a versatile vector for delivery of mAbs to the circulation, including for prophylaxis against infectious agents such as influenza (Balazs et al., 2013), HIV (Balazs et al., 2011) and Ebola (Robert et al., 2017), and was therefore selected for study. The rAAV serotypes 8 and 9 were investigated in this thesis (Sections 3.2.4 and 3.2.6), since they have already been demonstrated to direct robust expression of mAbs from the murine muscle (Fang et al., 2005) and lung (Limberis et al., 2013), respectively. Excitingly, new capsids are continually being developed through combinatorial and rational approaches that have desirable features such as reduced sensitivity to pre-existing immunity (further discussed in Section 6.2),

altered tropism and improved efficiency of tissue-specific transduction and transgene expression; these could be explored in the future for mAb gene transfer (also discussed in Section 3.3.3). The lentiviral vector rSIV.F/HN, which is currently under investigation for treatment of CF lung disease (Alton et al., 2017), was studied for lung gene transfer because of its ability to direct sustained expression of secretory protein from the mouse lung (Paul-Smith et al., 2018). Delivery of rAAV2/8 to the muscle was found to direct the highest levels of secretory reporter GLux expression in the circulation, with robust expression maintained for at least 12 months (Figure 3.6). The lentiviral vector rSIV.F/HN was preferred for delivery of protein to the lung lumen, resulting in sustained expression of GLux in this compartment for at least 12 months (Figure 3.4).

The studies presented in Chapter 4 investigated transfer of palivizumab cDNA for prophylaxis of RSV infection, used here as an application requiring delivery of mAb to the lung and serum (Section 4.1). As described in Section 1.2.3, in the absence of a licensed RSV vaccine, there is an urgent, unmet need for cost-effective prophylaxis against this respiratory pathogen. Based on the sustained expression of the GLux secretory reporter protein in the lung lining and circulation of mice (Figures 3.4 and 3.6), rAAV2/8 and rSIV.F/HN were investigated for delivery of the anti-RSV mAb palivizumab to the muscle and lung, respectively. Recombinant AAV2/8 directed robust and sustained antibody expression in the serum, whilst both vectors resulted in delivery of the mAb to the lung lumen (Figure 4.5). The rSIV.F/HN was found to direct approximately 10-20-fold lower levels of expression in the lung lining fluid compared with rAAV2/8 (Fig 4.5). This is at odds with results obtained for GLux (Figures 3.4 and 3.6) and likely reflective of the differing modes of transport of the two proteins across the lung epithelium, namely: non-specific

pinocytosis for GLux (El-Amouri et al., 2013) and FcRn receptor-mediated transcytosis for IgG (Roopenian and Akilesh, 2007) (Section 4.3.1). Importantly, this suggests that GLux is not a useful indicator with which to predict levels of mAb expression.

Despite the lower than expected palivizumab levels achieved with rSIV.F/HN in the mouse lung (Fig 4.5), successful protection from RSV infection-induced weight loss in mice was conferred by both rSIV.F/HN and rAAV2/8 (Figures 4.7 and 4.10), indicating that both delivery platforms could be useful for this indication. In the present study, the RSV challenge was carried out 28 days following vector delivery, demonstrating protection for at least as long as is provided by a single dose of palivizumab, which is administered monthly (Section 1.2.3.2). Ideally, a single dose of a gene transfer vector would result in expression for the duration of the RSV season, which lasts for 31 weeks (Rose et al., 2018), or even extend into subsequent seasons, as children tend to be repeatedly infected (Glezen et al., 1986) due to the lack of an effective acquired immune response (Chang and Braciale, 2002). Expression conferred by IM delivery of rAAV2/8 IM is long-lasting, with reports of sustained mAb production in the serum of mice for at least 64 weeks (Balazs et al., 2013), and robust expression of palivizumab demonstrated here for at least 6 months (Figure 4.5). If similar longevity could be recapitulated in patients, protection conferred by this vector might be expected to last for at least 6 months to >1 year. With rSIV.F/HN, significant palivizumab expression in the serum or BALF could not be detected at 6 months post-delivery (Figure 4.5). The duration of protection conferred by the vector therefore ought to be investigated in an experiment where RSV challenge takes place 6 months after palivizumab gene transfer in mice. If such sustained protection is not achieved with a single dose,

subsequent doses of rSIV.F/HN could be used to boost palivizumab levels, as successful readministration of the vector has been previously demonstrated in mice without loss of activity (Alton et al., 2017). The possibility of achieving long-term palivizumab expression through multiple administrations of rSIV.F/HN could therefore be explored.

In Chapter 5, the use of rAAV2/8 to transfer anti-TNFα biologic genes for treatment of rheumatoid arthritis (RA) was investigated. This application was selected as a model disease for delivery of mAbs to the circulation because of the high cost of biologic treatment and prevalence of this condition in the general population (Sections 1.1.7 and 1.3). Delivery of rAAV2/8 to the muscle of BALB/c mice was found to direct robust expression of two anti-TNFα agents: infliximab and etanercept (Figures 5.4 and 5.7). Due to the immunosuppressive nature of anti-TNFα, small molecule-assisted shutoff (SMASh) was investigated as a method of suppressing protein production. The system was however ineffective at controlling expression of etanercept, as a component of the system – NS3 protease from HCV – lost activity upon fusion to the biologic (Section 5.2.4). Alternative methods of controlling expression *in vivo* following gene delivery need to be investigated, which are further discussed in the section below.

6.2. Control of transgene expression following gene delivery

In theory, constitutive expression of mAbs against exogenous targets such as infectious agents should not be harmful to patients, but a risk exists that this could lead to the development of paraproteinaemia. Also called monoclonal

gammopathy, this condition is characterised by the presence of excessive monoclonal immunoglobulin in the blood and in severe cases may lead to complications such as neuropathy (Rison and Beydoun, 2016). Although commonly presenting in lymphoproliferative disorders such as multiple myeloma (Percy and D'Sa, 2009), the majority of cases of paraproteinaemia are monoclonal gammopathy of undetermined significance (MGUS) (Kyle et al., 2003), which affects as many as 6% of the elderly (60-80 years old) population (Crawford et al., 1987). These patients exhibit IgG serum levels of <30 mg/ml and do not usually require active treatment, unless they progress to multiple myeloma, for which there is a risk of 1% per year (Kyle et al., 2006). The levels of IgG expression achieved in mice using rAAV2/8 (~90 μg/ml serum for palivizumab and infliximab at 6 months; Figures 4.5 and 5.4) are more than 300-fold lower than the 30 mg/ml cut-off for asymptomatic myeloma (Cook and Macdonald, 2007), and thus unlikely to be pathogenic in humans, especially if the delivered dose is carefully assessed.

In addition to minimising the risk of paraproteinaemia, the ability to control mAb production following gene transfer might also reduce the chance of the patient developing anti-drug immune responses and thus prolong or potentiate the therapeutic effect of mAb gene transfer. Generation of anti-drug antibodies (ADA) is associated with higher clearance, and thus lower serum levels, of palivizumab in infants receiving RSV prophylaxis (Robbie et al., 2012). If mAb expression from a single dose of vector lasted for more than a year, one might envisage upregulating/switching on palivizumab expression during the RSV season and downregulating/switching off expression outside of that period, which might help minimise the risk of developing ADA.

The ability to control the expression of a biologic following gene transfer will be particularly helpful for indications such as RA, where the immunosuppressive nature of the medication may necessitate cessation of therapy (Ding et al., 2010); discussed in Section 5.2). Ideally, a regulatable expression system could also allow physicians to fine-tune expression of the mAb to match the severity of the disease. For example, RA patients experience periods of worsening disease activity called “flares”, which are associated with particularly intense pain (Hewlett et al., 2012) and are often unexplained and debilitating (Bykerk et al., 2014). Severe flares may necessitate changes in treatment plan, such as an increase in the dose of a biologic drug (Bykerk et al., 2016). The ability to regulate the expression of anti-TNFα following gene transfer could therefore be useful for managing RA disease flares and would also allow tapering of dose if symptoms are in remission.

Experiments in Section 5.2.3 were designed to explore the possibility of using SMASh for controlling expression of a protein following gene transfer. This system emerged as a promising candidate due to its effective suppression of protein production and the ability to be accommodated within a single rAAV vector (Table 5.1). The SMASh system was, however, unsuccessful at controlling etanercept expression *in vitro* (Figure 5.10), as the NS3 protease component of the tag appeared to lose its function upon fusion to etanercept (Figure 5.14).

An alternative system which could be explored the ecdysone receptor-based inducible gene regulation system called RheoSwitch (Karzenowski et al., 2006), shown to be inducible upon administration of a small, pharmacologically inert ligand activator veledimex and exhibiting undetectable basal activity (Palli et al., 2003). RheoSwitch is currently being investigated for intratumoural administration

of adenoviral vectors for treatment of glioblastoma (Barrett et al., 2018), with preliminary results from a phase I trial indicating a good safety profile in humans (Lebel et al., 2016). The system has also been shown to work in the context of rAAV-mediated delivery of a reporter gene 1.5 kb in size (Karzenowski et al., 2006), meaning that it could be used in combination with etanercept without the need for a dual rAAV vector system. Although RheoSwitch successfully achieved a single cycle of induction in mice and NHPs (Barrett et al., 2018), the ability of the system to be repeatedly stimulated over a long period has not been tested and this is currently being investigated as an extension to the studies presented in this thesis.

6.3. Immunity against rAAV and rSIV.F/HN

A key challenge to the effective translation of viral vector-mediated gene therapy is likely to be pre-existing immunity to the vector. This is especially important for rAAV as pre-existing immunity against naturally occurring AAV is common; neutralising antibodies against AAV are present in a significant proportion of the population, with highest seropositivity rates for AAV1 and 2 (67% and 72%, respectively), followed by AAV9 (47%), AAV6 (46%), AAV5 (40%) and AAV8 (38%) (Boutin et al., 2010). Ultimately, such pre-existing immunity could prevent a substantial proportion of patients from benefiting from rAAV gene transfer. Potential solutions have been proposed, including the addition of empty vector particles, or “capsid decoys”, to final vector formulation for delivery, a strategy shown to facilitate rAAV-mediated transduction in mice and NHPs in the presence of neutralising anti-AAV antibodies (Mingozzi et al., 2013a).

Alternatively, administration of two doses of B-cell depleting mAb rituximab to patients resulted in a decrease in neutralising antibody titres against AAV5, although the treatment was ineffective in a third of the studied subjects (Mingozzi et al., 2013b). Combination of rituximab and the immunosuppressant cyclosporine A in NHPs eliminated neutralising antibodies against transgene protein expressed from rAAV2/8, and allowed readministration of an alternative serotype expressing the same protein (factor IX) (Mingozzi et al., 2012). This indicates that transient immunosuppression might be used to not only eliminate pre-existing immunity to the wild-type virus, but also acquired immunity to the transgene protein, potentially prolonging duration of transgene expression. An alternative method of depleting neutralising antibodies against AAV which does not increase the risk of infections (Pohl et al., 1991) is plasmapheresis (Monteilhet et al., 2011). It is, however, an invasive procedure which involves the replacement of plasma with a 20% solution of albumin in saline and can cause serious adverse effects such as haemolysis, drop in arterial blood pressure and arrhythmias in 2% of recipients (Szczeklik et al., 2013, Wozniak et al., 2015).

A third approach involves the use of serotypes to which pre-existing immunity is low, such as serotypes which naturally seldom occur in the human population. This includes the NHP-derived AAVrh10 (Thwaite et al., 2014) and AAVrh74 (Duncan et al., 2015), currently under investigation in clinical trials (Naso et al., 2017), and a number of porcine serotypes (Bello et al., 2014). Strategies such as directed evolution (Maheshri et al., 2006) and targeted mutagenesis (Lochrie et al., 2006) have also been used to alter vector tropism and aid evasion of neutralising antibodies (reviewed in Bartel et al., 2011). For example, novel serotypes generated through capsid shuffling and recombination exhibited reduced

seroreactivity against human sera compared to AAV1, 6 and 8 (Paulk et al., 2018a). Altogether, a number of strategies have the potential to address the problem of pre-existing neutralising antibodies to AAV in candidate patients for gene transfer. The route of administration may also have an impact on the effect of pre-existing immunity; it has been suggested that intramuscular delivery might minimise the exposure of the vector to neutralising antibodies in the serum, compared with intravenous injection (Calcedo and Wilson, 2013). This is consistent with observations made in NHPs, where the same levels of naturally-occurring neutralising antibodies that blocked hepatic transduction upon IV administration did not block efficient expression following IM delivery in another study (Greig et al., 2016, Li et al., 2011). These results indicate that pre-existing immunity might be less of a problem in the context of IM delivery compared to the IV route.

Although pre-existing immunity in the population is regarded as less of an obstacle in the context of lentiviral gene transfer (Annoni et al., 2013), innate immune responses stimulated by the vector might limit the duration of expression. A type I interferon response was observed in mice following IV administration of rLV pseudotyped with VSV-G and GP64 glycoproteins, which limited the efficiency of transduction and duration of expression in the liver (Brown et al., 2007). In contrast, administration of F/HN-pseudotyped rLV to the mouse lung has been shown here (Figure 3.4) and by others (Griesenbach et al., 2012, Mitomo et al., 2010, Paul-Smith et al., 2018) to direct transgene expression sustained for 12-22 months. Although mild acute toxicity was observed in animals which received rSIV.F/HN IN (Alton et al., 2017), cytokine responses were not assessed, and the effect of innate immune responses on the efficiency or stability of rSIV.F/HN-mediated gene transfer in the lung ought to be investigated. Acquired immune responses to the

envelope protein could also potentially interfere with the ability of the vector to transduce human lungs. The rSIV.F/HN is pseudotyped with surface glycoproteins from Sendai virus, which is a murine pathogen that does not naturally infect humans (Section 1.1.6.2). The F and HN proteins, however, have a high sequence homology with human parainfluenza virus (hPIV) (Gorman et al., 1990), for which up to 80% of children are seropositive by 4 years of age (Parrott et al., 1962). Thus, pre-existing immunity to hPIV could ultimately limit rSIV.F/HN transduction efficiency in humans. Administration of human sera containing anti-hPIV antibodies to mice via IP injection or IN instillation, however, did not appear to block or diminish transduction with the vector 24 hours later (Alton et al., 2017). The mechanism for this is unclear and may be related to the ability of lentiviral vectors to be successfully re-administered without loss of efficacy (Alton et al., 2017, Sinn et al., 2008). Nonetheless, the effect of pre-existing immunity on rSIV.F/HN-mediated gene transfer in patients should be examined.

6.4. Delivery of antibody genes for other diseases

The two disease applications investigated in this thesis represented exemplars for lung and systemic delivery which could be applicable to the use of other mAbs. Observations from delivery of palivizumab cDNA as prophylaxis for RSV infection could be applied to other respiratory infectious agents. Successful protection against influenza challenge has been demonstrated in animal models via rAAV2/8 gene delivery to the muscle (Balazs et al., 2013) and rAAV2/9 lung (Limberis et al., 2013). Gene transfer to the lung with rSIV.F/HN may also be suitable for delivering mAbs to the lung lumen to treat non-infectious diseases such as asthma. Examples

include mepolizumab (Nucala; GlaxoSmithKline, Brentford, UK) (Fala, 2016) and reslizumab (Cinqair; Teva, Petah Tikva, Israel) (Hom and Pisano, 2017), which target interleukin-5 (IL-5), and omalizumab (Xolair; Genentech, San Francisco, CA, USA) which targets immunoglobulin E (IgE) (Thomson and Chaudhuri, 2012). These are currently administered systemically (Matucci et al., 2018), but expressing them directly in the patient's lungs might be beneficial. Interleukin-5 found in the BALF of asthma patients is associated with higher recruitment of eosinophils (Ohnishi et al., 1993, Robinson et al., 1993), which play a central role in pulmonary inflammation in asthma (Durham and Kay, 1985). Blocking the cytokine directly in the lung through a sustained local expression of mepolizumab or reslizumab could therefore be a useful strategy for treating this disease. Localised production of the mAb with limited secretion into circulation, as observed with rSIV.F/HN gene delivery (Figure 3.4), might be advantageous to limit systemic effects of anti-IL-5 mAbs, including side effects such as infection with herpes zoster virus, cases of which have been observed in patients receiving mepolizumab (Fala, 2016). It might however be possible that both systemic and local action of the mAb is required for effective treatment. Aerosolisation of the anti-IgE mAb omalizumab to lungs of asthma patients was ineffective at relieving symptoms (Fahy et al., 1999), suggesting that the presence of the mAb in lung alone is insufficient. However, administration of an anti-interleukin-13 Fab fragment via inhaled aerosol was shown to reduce allergic airway responses in an NHP model of asthma (Lightwood et al., 2018). It remains to be seen whether the anti-IL-5 mAbs mepolizumab and reslizumab are required predominantly in the lung or whether systemic expression is also necessary.

Another lung disease for which local mAb gene delivery could be useful is chronic obstructive pulmonary disease (COPD), which is one of the top five leading causes of death worldwide (Mathers and Loncar, 2006) and new treatments for which are urgently needed. Clinical trials investigating the use of biologic antagonists of TNFα (Aaron et al., 2013, Rennard et al., 2007), interleukin-8 (IL-8) (Mahler et al., 2004) and IL-1 receptor (Calverley et al., 2017) in COPD patients have not shown clinical benefit, and some observed an increased risk of cancer (Rennard et al., 2013). Approximately 40% of COPD patients have an eosinophilic phenotype (Singh et al., 2014), providing precedent for treatment of this subset with IL-5 antagonists, which has preliminarily proved effective (Pavord et al., 2017). Delivery of mepolizumab or other immunosuppressant mAb cDNA for local production in the lung by rSIV.F/HN could offer an effective treatment whilst also minimising risks associated with systemic administration. A potential barrier to inhaled gene therapy for this disease could be the mucus hypersecretion and airway obstruction observed in COPD lungs, although the success of the inhaled non-viral formulation GL67A/pGM169 for treatment of CF (Alton et al., 2015) suggests that gene delivery to a lung partially obstructed with mucus is possible. First-in-human clinical trials with rSIV.F/HN in CF patients should be performed in the next few years (Alton et al., 2017) and the results will indicate whether this might be a feasible strategy for COPD gene therapy.

Local delivery of mAbs through gene transfer could also be a useful approach in the treatment of lung cancer, which is the leading cause of cancer-related deaths (Siegel et al., 2018). Examples of mAbs which could be delivered in this way include bevacizumab (Avastin), an anti-vascular endothelial growth factor (VEGF) mAb approved for treatment of non-small cell lung cancer (Sandler et al., 2006).

Cetuximab has also been investigated for treatment of lung cancer, although its effect is modest (Pirker et al., 2009) and it has not been approved for this indication. For metastatic disease, systemic administration of the mAb might be preferred.

Studies in Chapter 5 described delivery of TNFα antagonists infliximab and etanercept for treatment of RA, with robust and sustained expression achieved from rAAV2/8 (Figures 5.4 and 5.7). These drugs are used to treat a number of other autoimmune diseases the pathoaetiology of which involves TNFα: Crohn's disease, ulcerative colitis, psoriasis and ankylosing spondylitis (Section 1.3.3). Delivery of cDNA encoding those biologics through rAAV2/8 injection could therefore offer alternative means of treatment for those disorders. Due to the immunosuppressive nature of treatment with anti-TNFα biologics, development of regulatable expression system (discussed in Section 6.2) will be important for the success of such applications.

6.5. Implications and future directions

Intramuscular delivery of rAAV2/8 has previously emerged as an effective vehicle for mAb gene transfer (Section 1.1.5.4), including for respiratory applications such as influenza infection (Balazs et al., 2013). For such indications, delivery of mAb to the lung could directly target the site of infection or disease whilst limiting systemic side-effects (discussed in Section 6.4). Here, it was shown that rSIV.F/HN delivered IN was equally effective at protecting mice from RSV-induced weight loss as rAAV2/8 delivered IM (Section 4.2.4), indicating that this delivery platform could be used if systemic expression of the mAb is undesirable. For mAbs which are

associated with serious side effects, such as TNFα antagonists, the ability to regulate expression following gene transfer will be crucial. Although SMASh (Chung et al., 2015) was identified as a promising candidate system (Section 5.1), it failed to control expression of secretory proteins (Section 5.2.4). Alternative means of controlling expression therefore need to be developed to ensure acceptable safety of stable gene transfer of such mAbs in patients.

For mAb gene transfer using rAAV2/8 or rSIV.F/HN to be feasible in the clinic, the cost of the vector must offer substantial savings relative to parenteral administration. The costs of gene therapy based on viral vectors have thus far been prohibitive; the most notable case is perhaps Glybera's (alipogene tiparvovec) $1-million price tag (Morrison, 2015), which, combined with limited demand, ultimately led to its withdrawal from the market (Senior, 2017). However, continued improvements are being made to large-scale viral vector production (reviewed in Clément and Grieger, 2016, van der Loo and Wright, 2016), which, combined with a high demand for the product, as is the case for many mAbs, should progressively reduce the costs of therapy such that in the future, antibody gene transfer might become a cost-effective alternative to parenteral administration.

References

AALBERS, C. J., BEVAART, L., LOILER, S., DE CORTIE, K., WRIGHT, J. F., MINGOZZI, F., TAK, P. P. & VERVOORDELDONK, M. J. 2015. Preclinical Potency and Biodistribution Studies of an AAV 5 Vector Expressing Human Interferon-beta (ART-I02) for Local Treatment of Patients with Rheumatoid Arthritis. *PLoS One,* 10**,** e0130612.

AARON, S. D., VANDEMHEEN, K. L., MALTAIS, F., FIELD, S. K., SIN, D. D., BOURBEAU, J., MARCINIUK, D. D., FITZGERALD, J. M., NAIR, P. & MALLICK, R. 2013. TNFalpha antagonists for acute exacerbations of COPD: a randomised double-blind controlled trial. *Thorax,* 68**,** 142-8.

AFIONE, S. A., CONRAD, C. K., KEARNS, W. G., CHUNDURU, S., ADAMS, R., REYNOLDS, T. C., GUGGINO, W. B., CUTTING, G. R., CARTER, B. J. & FLOTTE, T. R. 1996. In vivo model of adeno-associated virus vector persistence and rescue. *J Virol,* 70**,** 3235-41.

AFONSO, C. L., AMARASINGHE, G. K., BÁNYAI, K., BÀO, Y., BASLER, C. F., BAVARI, S., BEJERMAN, N., BLASDELL, K. R., BRIAND, F.-X., BRIESE, T., BUKREYEV, A., CALISHER, C. H., CHANDRAN, K., CHÉNG, J., CLAWSON, A. N., COLLINS, P. L., DIETZGEN, R. G., DOLNIK, O., DOMIER, L. L., DÜRRWALD, R., DYE, J. M., EASTON, A. J., EBIHARA, H., FARKAS, S. L., FREITAS-ASTÚA, J., FORMENTY, P., FOUCHIER, R. A. M., FÙ, Y., GHEDIN, E., GOODIN, M. M., HEWSON, R., HORIE, M., HYNDMAN, T. H., JIĀNG, D., KITAJIMA, E. W., KOBINGER, G. P., KONDO, H., KURATH, G., LAMB, R. A., LENARDON, S., LEROY, E. M., LI, C.-X., LIN, X.-D., LIÚ, L., LONGDON, B., MARTON, S., MAISNER, A., MÜHLBERGER, E., NETESOV, S. V., NOWOTNY, N., PATTERSON, J. L., PAYNE, S. L., PAWESKA, J. T., RANDALL, R. E., RIMA, B. K., ROTA, P., RUBBENSTROTH, D., SCHWEMMLE, M., SHI, M., SMITHER, S. J., STENGLEIN, M. D., STONE, D. M., TAKADA, A., TERREGINO, C., TESH, R. B., TIAN, J.-H., TOMONAGA, K., TORDO, N., TOWNER, J. S., VASILAKIS, N., VERBEEK, M., VOLCHKOV, V. E., WAHL-JENSEN, V., WALSH, J. A., WALKER, P. J., WANG, D., WANG, L.-F., WETZEL, T., WHITFIELD, A. E., XIÈ, J., YUEN, K.-Y., ZHANG, Y.-Z. & KUHN, J. H. 2016. Taxonomy of the order Mononegavirales: update 2016. *Archives of Virology,* 161**,** 2351-2360.

AIHARA, H. & MIYAZAKI, J.-I. 1998. Gene transfer into muscle by electroporation in vivo. *Nature Biotechnology,* 16**,** 867.

ALLOCCA, M., DORIA, M., PETRILLO, M., COLELLA, P., GARCIA-HOYOS, M., GIBBS, D., KIM, S. R., MAGUIRE, A., REX, T. S., DI VICINO, U., CUTILLO, L., SPARROW, J. R., WILLIAMS, D. S., BENNETT, J. & AURICCHIO, A. 2008. Serotype-dependent packaging of large genes in adeno-associated viral vectors results in effective gene delivery in mice. *J Clin Invest,* 118**,** 1955-64.

ALTON, E., ARMSTRONG, D. K., ASHBY, D., BAYFIELD, K. J., BILTON, D., BLOOMFIELD, E. V., BOYD, A. C., BRAND, J., BUCHAN, R., CALCEDO, R., CARVELLI, P., CHAN, M., CHENG, S. H., COLLIE, D. D. S., CUNNINGHAM, S., DAVIDSON, H. E., DAVIES, G., DAVIES, J. C., DAVIES, L. A., DEWAR, M. H., DOHERTY, A., DONOVAN, J., DWYER, N. S., ELGMATI, H. I., FEATHERSTONE, R. F., GAVINO, J., GEA-SORLI, S., GEDDES, D. M., GIBSON, J. S. R., GILL, D. R., GREENING, A. P., GRIESENBACH, U., HANSELL, D. M., HARMAN, K., HIGGINS, T. E., HODGES, S. L., HYDE, S. C., HYNDMAN, L., INNES, J. A., JACOB, J., JONES, N., KEOGH, B. F., LIMBERIS, M. P., LLOYD-EVANS, P., MACLEAN, A. W., MANVELL, M. C., MCCORMICK, D., MCGOVERN, M., MCLACHLAN, G., MENG, C., MONTERO, M. A., MILLIGAN, H., MOYCE, L. J., MURRAY, G. D., NICHOLSON, A. G., OSADOLOR, T., PARRA-LEITON, J., PORTEOUS, D. J., PRINGLE, I. A., PUNCH, E. K., PYTEL, K. M., QUITTNER, A. L., RIVELLINI, G., SAUNDERS, C. J., SCHEULE, R. K., SHEARD, S., SIMMONDS, N. J., SMITH, K., SMITH, S. N., SOUSSI, N.,

SOUSSI, S., SPEARING, E. J., STEVENSON, B. J., SUMNER-JONES, S. G., TURKKILA, M., URETA, R. P., WALLER, M. D., WASOWICZ, M. Y., WILSON, J. M., WOLSTENHOLME-HOGG, P. & CONSORTIUM, U. K. C. F. G. T. 2015. Repeated nebulisation of non-viral CFTR gene therapy in patients with cystic fibrosis: a randomised, double-blind, placebo-controlled, phase 2b trial. *Lancet Respir Med,* 3**,** 684-691.

ALTON, E. W., BEEKMAN, J. M., BOYD, A. C., BRAND, J., CARLON, M. S., CONNOLLY, M. M., CHAN, M., CONLON, S., DAVIDSON, H. E., DAVIES, J. C., DAVIES, L. A., DEKKERS, J. F., DOHERTY, A., GEA-SORLI, S., GILL, D. R., GRIESENBACH, U., HASEGAWA, M., HIGGINS, T. E., HIRONAKA, T., HYNDMAN, L., MCLACHLAN, G., INOUE, M., HYDE, S. C., INNES, J. A., MAHER, T. M., MORAN, C., MENG, C., PAUL-SMITH, M. C., PRINGLE, I. A., PYTEL, K. M., RODRIGUEZ-MARTINEZ, A., SCHMIDT, A. C., STEVENSON, B. J., SUMNER-JONES, S. G., TOSHNER, R., TSUGUMINE, S., WASOWICZ, M. W. & ZHU, J. 2017. Preparation for a first-in-man lentivirus trial in patients with cystic fibrosis. *Thorax,* 72**,** 137-147.

ALTON, E. W., STERN, M., FARLEY, R., JAFFE, A., CHADWICK, S. L., PHILLIPS, J., DAVIES, J., SMITH, S. N., BROWNING, J., DAVIES, M. G., HODSON, M. E., DURHAM, S. R., LI, D., JEFFERY, P. K., SCALLAN, M., BALFOUR, R., EASTMAN, S. J., CHENG, S. H., SMITH, A. E., MEEKER, D. & GEDDES, D. M. 1999. Cationic lipid-mediated CFTR gene transfer to the lungs and nose of patients with cystic fibrosis: a double-blind placebo-controlled trial. *Lancet,* 353**,** 947-54.

AMERICAN ACADEMY OF PEDIATRICS COMMITTEE ON INFECTIOUS, D. & AMERICAN ACADEMY OF PEDIATRICS BRONCHIOLITIS GUIDELINES, C. 2014. Updated guidance for palivizumab prophylaxis among infants and young children at increased risk of hospitalization for respiratory syncytial virus infection. *Pediatrics,* 134**,** 415-20.

ANDREWS, C. D., LUO, Y., SUN, M., YU, J., GOFF, A. J., GLASS, P. J., PADTE, N. N., HUANG, Y. & HO, D. D. 2017. In Vivo Production of Monoclonal Antibodies by Gene Transfer via Electroporation Protects against Lethal Influenza and Ebola Infections. *Mol Ther Methods Clin Dev,* 7**,** 74-82.

ANNONI, A., CANTORE, A., DELLA VALLE, P., GOUDY, K., AKBARPOUR, M., RUSSO, F., BARTOLACCINI, S., D'ANGELO, A., RONCAROLO, M. G. & NALDINI, L. 2013. Liver gene therapy by lentiviral vectors reverses anti-factor IX pre-existing immunity in haemophilic mice. *EMBO Molecular Medicine,* 5**,** 1684-1697.

ARRUDA, V. R., SCHUETTRUMPF, J., HERZOG, R. W., NICHOLS, T. C., ROBINSON, N., LOTFI, Y., MINGOZZI, F., XIAO, W., COUTO, L. B. & HIGH, K. A. 2004. Safety and efficacy of factor IX gene transfer to skeletal muscle in murine and canine hemophilia B models by adeno-associated viral vector serotype 1. *Blood,* 103**,** 85-92.

ATCHISON, R. W., CASTO, B. C. & HAMMON, W. M. 1965. Adenovirus-Associated Defective Virus Particles. *Science,* 149**,** 754-6.

AUGUST, A., GLENN, G. M., KPAMEGAN, E., HICKMAN, S. P., JANI, D., LU, H., THOMAS, D. N., WEN, J., PIEDRA, P. A. & FRIES, L. F. 2017. A Phase 2 randomized, observer-blind, placebo-controlled, dose-ranging trial of aluminum-adjuvanted respiratory syncytial virus F particle vaccine formulations in healthy women of childbearing age. *Vaccine,* 35**,** 3749-3759.

AURICCHIO, A., O'CONNOR, E., WEINER, D., GAO, G.-P., HILDINGER, M., WANG, L., CALCEDO, R. & WILSON, J. M. 2002. Noninvasive gene transfer to the lung for systemic delivery of therapeutic proteins. *The Journal of Clinical Investigation,* 110**,** 499-504.

AVINA-ZUBIETA, J. A., CHOI, H. K., SADATSAFAVI, M., ETMINAN, M., ESDAILE, J. M. & LACAILLE, D. 2008. Risk of cardiovascular mortality in patients with rheumatoid arthritis: a meta-analysis of observational studies. *Arthritis Rheum,* 59**,** 1690-7.

BACH, P. B., GIRALT, S. A. & SALTZ, L. B. 2017. Fda approval of tisagenlecleucel: Promise and complexities of a $475 000 cancer drug. *JAMA,* 318**,** 1861-1862.

BALAZS, A. B., BLOOM, J. D., HONG, C. M., RAO, D. S. & BALTIMORE, D. 2013. Broad protection against influenza infection by vectored immunoprophylaxis in mice. *Nat Biotechnol,* 31**,** 647-52.

BALAZS, A. B., CHEN, J., HONG, C. M., RAO, D. S., YANG, L. & BALTIMORE, D. 2011. Antibody-based protection against HIV infection by vectored immunoprophylaxis. *Nature,* 481**,** 81-4.

BALAZS, A. B., OUYANG, Y., HONG, C. M., CHEN, J., NGUYEN, S. M., RAO, D. S., AN, D. S. & BALTIMORE, D. 2014. Vectored immunoprophylaxis protects humanized mice from mucosal HIV transmission. *Nat Med,* 20**,** 296-300.

BARRETT, J. A., CAI, H., MIAO, J., KHARE, P. D., GONZALEZ, P., DALSING-HERNANDEZ, J., SHARMA, G., CHAN, T., COOPER, L. J. N. & LEBEL, F. 2018. Regulated intratumoral expression of IL-12 using a RheoSwitch Therapeutic System((R)) (RTS((R))) gene switch as gene therapy for the treatment of glioma. *Cancer Gene Ther*.

BARTEL, M. A., SCHAFFER, D. V. & BÜNING, H. 2011. Enhancing the Clinical Potential of AAV Vectors by Capsid Engineering to Evade Pre-Existing Immunity. *Frontiers in Microbiology,* 2**,** 204.

BARTLETT, J. S., WILCHER, R. & SAMULSKI, R. J. 2000. Infectious entry pathway of adeno-associated virus and adeno-associated virus vectors. *J Virol,* 74**,** 2777-85.

BARTON, L. L., GRANT, K. L. & LEMEN, R. J. 2001. Respiratory syncytial virus immune globulin: Decisions and costs. *Pediatric Pulmonology,* 32**,** 20-28.

BEELER, J. A. & COELINGH, K. V. 1989. Neutralization Epitopes of the F-Glycoprotein of Respiratory Syncytial Virus - Effect of Mutation Upon Fusion Function. *Journal of Virology,* 63**,** 2941-2950.

BEHERA, A. K., MATSUSE, H., KUMAR, M., KONG, X., LOCKEY, R. F. & MOHAPATRA, S. S. 2001. Blocking intercellular adhesion molecule-1 on human epithelial cells decreases respiratory syncytial virus infection. *Biochem Biophys Res Commun,* 280**,** 188-95.

BELLO, A., CHAND, A., AVILES, J., SOULE, G., AURICCHIO, A. & KOBINGER, G. P. 2014. Novel Adeno-associated Viruses Derived From Pig Tissues Transduce Most Major Organs in Mice. *Scientific Reports,* 4**,** 6644.

BENNETT, R. M., GABOR, G. T. & MERRITT, M. M. 1985. DNA binding to human leukocytes. Evidence for a receptor-mediated association, internalization, and degradation of DNA. *Journal of Clinical Investigation,* 76**,** 2182-2190.

BERNS, K. I., BYRNE, B. J., FLOTTE, T. R., GAO, G., HAUSWIRTH, W. W., HERZOG, R. W., MUZYCZKA, N., VANDENDRIESSCHE, T., XIAO, X., ZOLOTUKHIN, S. & SRIVASTAVA, A. 2015. Adeno-Associated Virus Type 2 and Hepatocellular Carcinoma? *Hum Gene Ther,* 26**,** 779-81.

BERNS, K. I. & ROSE, J. A. 1970. Evidence for a single-stranded adenovirus-associated virus genome: isolation and separation of complementary single strands. *J Virol,* 5**,** 693-9.

BEVAART, L., AALBERS, C. J., VIERBOOM, M. P., BROEKSTRA, N., KONDOVA, I., BREEDVELD, E., HAUCK, B., WRIGHT, J. F., TAK, P. P. & VERVOORDELDONK, M. J. 2015. Safety, Biodistribution, and Efficacy of an AAV-5 Vector Encoding Human Interferon-Beta (ART-I02) Delivered via Intra-Articular Injection in Rhesus Monkeys with Collagen-Induced Arthritis. *Hum Gene Ther Clin Dev,* 26**,** 103-12.

BEVAART, L., VERVOORDELDONK, M. J. & TAK, P. P. 2010. Evaluation of therapeutic targets in animal models of arthritis: how does it relate to rheumatoid arthritis? *Arthritis Rheum,* 62**,** 2192-205.

BLACK, R. A., RAUCH, C. T., KOZLOSKY, C. J., PESCHON, J. J., SLACK, J. L., WOLFSON, M. F., CASTNER, B. J., STOCKING, K. L., REDDY, P., SRINIVASAN, S., NELSON, N., BOIANI, N., SCHOOLEY, K. A., GERHART, M., DAVIS, R., FITZNER, J. N., JOHNSON, R. S., PAXTON, R. J., MARCH, C. J. & CERRETTI, D. P. 1997. A metalloproteinase disintegrin that releases tumour-necrosis factor-alpha from cells. *Nature,* 385**,** 729-33.

BMA. Available: www.medicinescomplete.com [Accessed 13th Feb 2018].
BONAFEDE, M., JOSEPH, G. J., SHAH, N., PRINCIC, N. & HARRISON, D. J. 2014. Cost of tumor necrosis factor blockers per patient with rheumatoid arthritis in a multistate Medicaid population. *Clinicoecon Outcomes Res,* 6**,** 381-8.
BONAFEDE, M. M., GANDRA, S. R., WATSON, C., PRINCIC, N. & FOX, K. M. 2012. Cost per treated patient for etanercept, adalimumab, and infliximab across adult indications: a claims analysis. *Adv Ther,* 29**,** 234-48.
BORROK, M. J., DIGIANDOMENICO, A., BEYAZ, N., MARCHETTI, G. M., BARNES, A. S., LEKSTROM, K. J., PHIPPS, S. S., MCCARTHY, M. P., WU, H., DALL'ACQUA, W. F., TSUI, P. & GUPTA, R. 2018. Enhancing IgG distribution to lung mucosal tissue improves protective effect of anti–Pseudomonas aeruginosa antibodies. *JCI Insight,* 3.
BOSHART, M., WEBER, F., JAHN, G., DORSCH-H⇒LER, K., FLECKENSTEIN, B. & SCHAFFNER, W. 1985. A very strong enhancer is located upstream of an immediate early gene of human cytomegalovirus. *Cell,* 41**,** 521-530.
BOUKHVALOVA, M. S. & BLANCO, J. C. 2013. The cotton rat Sigmodon hispidus model of respiratory syncytial virus infection. *Curr Top Microbiol Immunol,* 372**,** 347-58.
BOUKHVALOVA, M. S., PRINCE, G. A. & BLANCO, J. C. 2009. The cotton rat model of respiratory viral infections. *Biologicals,* 37**,** 152-9.
BOURGEOIS, C., BOUR, J. B., LIDHOLT, K., GAUTHRAY, C. & POTHIER, P. 1998. Heparin-like structures on respiratory syncytial virus are involved in its infectivity in vitro. *J Virol,* 72**,** 7221-7.
BOUSSIF, O., LEZOUALC'H, F., ZANTA, M. A., MERGNY, M. D., SCHERMAN, D., DEMENEIX, B. & BEHR, J. P. 1995. A versatile vector for gene and oligonucleotide transfer into cells in culture and in vivo: polyethylenimine. *Proc Natl Acad Sci U S A,* 92**,** 7297-301.
BOUTIN, S., MONTEILHET, V., VERON, P., LEBORGNE, C., BENVENISTE, O., MONTUS, M. F. & MASURIER, C. 2010. Prevalence of Serum IgG and Neutralizing Factors Against Adeno-Associated Virus (AAV) Types 1, 2, 5, 6, 8, and 9 in the Healthy Population: Implications for Gene Therapy Using AAV Vectors. *Human Gene Therapy,* 21**,** 704-712.
BRADY, J. M., BALTIMORE, D. & BALAZS, A. B. 2017. Antibody gene transfer with adeno-associated viral vectors as a method for HIV prevention. *Immunol Rev,* 275**,** 324-333.
BRENNAN, F. M., CHANTRY, D., JACKSON, A., MAINI, R. & FELDMANN, M. 1989. Inhibitory effect of TNF alpha antibodies on synovial cell interleukin-1 production in rheumatoid arthritis. *Lancet,* 2**,** 244-7.
BROWN, B. D., SITIA, G., ANNONI, A., HAUBEN, E., SERGI, L. S., ZINGALE, A., RONCAROLO, M. G., GUIDOTTI, L. G. & NALDINI, L. 2007. In vivo administration of lentiviral vectors triggers a type I interferon response that restricts hepatocyte gene transfer and promotes vector clearance. *Blood,* 109**,** 2797-2805.
BUDKER, V., ZHANG, G., DANKO, I., WILLIAMS, P. & WOLFF, J. 1998. The efficient expression of intravascularly delivered DNA in rat muscle. *Gene Ther,* 5**,** 272-6.
BURNS, J. C., FRIEDMANN, T., DRIEVER, W., BURRASCANO, M. & YEE, J. K. 1993. Vesicular stomatitis virus G glycoprotein pseudotyped retroviral vectors: concentration to very high titer and efficient gene transfer into mammalian and nonmammalian cells. *Proc Natl Acad Sci U S A,* 90**,** 8033-7.
BURRAGE, P. S., MIX, K. S. & BRINCKERHOFF, C. E. 2006. Matrix metalloproteinases: role in arthritis. *Front Biosci,* 11**,** 529-43.
BYINGTON, C. L., WILKES, J., KORGENSKI, K. & SHENG, X. 2015. Respiratory syncytial virus-associated mortality in hospitalized infants and young children. *Pediatrics,* 135**,** e24-31.
BYKERK, V. P., BINGHAM, C. O., CHOY, E. H., LIN, D., ALTEN, R., CHRISTENSEN, R., FURST, D. E., HEWLETT, S., LEONG, A., MARCH, L., WOODWORTH, T., BOIRE, G., HARAOUI, B., HITCHON, C., JAMAL, S., KEYSTONE, E. C., POPE, J., TIN, D., THORNE, J. C. & BARTLETT, S. J. 2016. Identifying flares in rheumatoid arthritis:

reliability and construct validation of the OMERACT RA Flare Core Domain Set. *RMD Open,* 2.
BYKERK, V. P., LIE, E., BARTLETT, S. J., ALTEN, R., BOONEN, A., CHRISTENSEN, R., FURST, D. E., HEWLETT, S., LEONG, A. L., LYDDIATT, A., MARCH, L., MAY, J. E., MONTIE, P., ORBAI, A.-M., POHL, C., SCHOLTE VOSHAAR, M., WOODWORTH, T., BINGHAM , C. O. & CHOY, E. H. 2014. Establishing a Core Domain Set to Measure Rheumatoid Arthritis Flares: Report of the OMERACT 11 RA Flare Workshop. *The Journal of Rheumatology*.
CALCEDO, R. & WILSON, J. M. 2013. Humoral Immune Response to AAV. *Frontiers in Immunology,* 4**,** 341.
CALVERLEY, P. M. A., SETHI, S., DAWSON, M., WARD, C. K., FINCH, D. K., PENNEY, M., NEWBOLD, P. & VAN DER MERWE, R. 2017. A randomised, placebo-controlled trial of anti-interleukin-1 receptor 1 monoclonal antibody MEDI8968 in chronic obstructive pulmonary disease. *Respir Res,* 18**,** 153.
CARBONELL-ESTRANY, X., SIMOES, E. A. F., DAGAN, R., HALL, C. B., HARRIS, B., HULTQUIST, M., CONNOR, E. M., LOSONSKY, G. A. & GRP, M. S. 2010. Motavizumab for Prophylaxis of Respiratory Syncytial Virus in High-Risk Children: A Noninferiority Trial. *Pediatrics,* 125**,** E35-E51.
CARTER, B. J., FIFE, K. H., DE LA MAZA, L. M. & BERNS, K. I. 1976. Genome localization of adeno-associated virus RNA. *J Virol,* 19**,** 1044-53.
CHAN, S. Y., SPECK, R. F., MA, M. C. & GOLDSMITH, M. A. 2000. Distinct mechanisms of entry by envelope glycoproteins of Marburg and Ebola (Zaire) viruses. *J Virol,* 74**,** 4933-7.
CHANG, J. & BRACIALE, T. J. 2002. Respiratory syncytial virus infection suppresses lung CD8+ T-cell effector activity and peripheral CD8+ T-cell memory in the respiratory tract. *Nature Medicine,* 8**,** 54.
CHANG, K., YANG, S. M., KIM, S. H., HAN, K. H., PARK, S. J. & SHIN, J. I. 2014. Smoking and rheumatoid arthritis. *Int J Mol Sci,* 15**,** 22279-95.
CHAO, H., LIU, Y., RABINOWITZ, J., LI, C., SAMULSKI, R. J. & WALSH, C. E. 2000. Several Log Increase in Therapeutic Transgene Delivery by Distinct Adeno-Associated Viral Serotype Vectors. *Molecular Therapy,* 2**,** 619-623.
CHEN, D.-Y., CHEN, Y.-M., TSAI, W.-C., TSENG, J.-C., CHEN, Y.-H., HSIEH, C.-W., HUNG, W.-T. & LAN, J.-L. 2015. Significant associations of antidrug antibody levels with serum drug trough levels and therapeutic response of adalimumab and etanercept treatment in rheumatoid arthritis. *Annals of the Rheumatic Diseases,* 74**,** e16-e16.
CHEN, X., KUBE, D. M., COOPER, M. J. & DAVIS, P. B. 2008a. Cell Surface Nucleolin Serves as Receptor for DNA Nanoparticles Composed of Pegylated Polylysine and DNA. *Molecular Therapy,* 16**,** 333-342.
CHEN, Z.-Y., HE, C.-Y., EHRHARDT, A. & KAY, M. A. 2003. Minicircle DNA vectors devoid of bacterial DNA result in persistent and high-level transgene expression in vivo. *Molecular Therapy,* 8**,** 495-500.
CHEN, Z.-Y., RIU, E., HE, C.-Y., XU, H. & KAY, M. A. 2008b. Silencing of Episomal Transgene Expression in Liver by Plasmid Bacterial Backbone DNA Is Independent of CpG Methylation. *Molecular Therapy,* 16**,** 548-556.
CHEUNG, A. K., HOGGAN, M. D., HAUSWIRTH, W. W. & BERNS, K. I. 1980. Integration of the adeno-associated virus genome into cellular DNA in latently infected human Detroit 6 cells. *J Virol,* 33**,** 739-48.
CHINGCUANCO, F., SEGAL, J. B., KIM, S. C. & ALEXANDER, G. C. 2016. Bioequivalence of Biosimilar Tumor Necrosis Factor-alpha Inhibitors Compared With Their Reference Biologics: A Systematic Review. *Ann Intern Med,* 165**,** 565-574.
CHOLLET, P., FAVROT, M. C., HURBIN, A. & COLL, J. L. 2002. Side-effects of a systemic injection of linear polyethylenimine-DNA complexes. *J Gene Med,* 4**,** 84-91.
CHUNG, H. K., JACOBS, C. L., HUO, Y., YANG, J., KRUMM, S. A., PLEMPER, R. K., TSIEN, R. Y. & LIN, M. Z. 2015. Tunable and reversible drug control of protein production via a self-excising degron. *Nat Chem Biol,* 11**,** 713-20.

CLAYPOOL, S. M., DICKINSON, B. L., WAGNER, J. S., JOHANSEN, F. E., VENU, N., BORAWSKI, J. A., LENCER, W. I. & BLUMBERG, R. S. 2004. Bidirectional transepithelial IgG transport by a strongly polarized basolateral membrane Fcgamma-receptor. *Mol Biol Cell,* 15**,** 1746-59.

CLÉMENT, N. & GRIEGER, J. C. 2016. Manufacturing of recombinant adeno-associated viral vectors for clinical trials. *Molecular Therapy - Methods & Clinical Development,* 3.

COLELLA, P., TRAPANI, I., CESI, G., SOMMELLA, A., MANFREDI, A., PUPPO, A., IODICE, C., ROSSI, S., SIMONELLI, F., GIUNTI, M., BACCI, M. L. & AURICCHIO, A. 2014. Efficient gene delivery to the cone-enriched pig retina by dual AAV vectors. *Gene Therapy,* 21**,** 450.

COLLINS, P. L., DICKENS, L. E., BUCKLER-WHITE, A., OLMSTED, R. A., SPRIGGS, M. K., CAMARGO, E. & COELINGH, K. V. 1986. Nucleotide sequences for the gene junctions of human respiratory syncytial virus reveal distinctive features of intergenic structure and gene order. *Proceedings of the National Academy of Sciences of the United States of America,* 83**,** 4594-4598.

COLLINS, P. L. & MOTTET, G. 1991. Post-translational processing and oligomerization of the fusion glycoprotein of human respiratory syncytial virus. *J Gen Virol,* 72 (Pt 12)**,** 3095-101.

COLOSIA, A. D., YANG, J., HILLSON, E., MAUSKOPF, J., COPLEY-MERRIMAN, C., SHINDE, V. & STODDARD, J. 2017. The epidemiology of medically attended respiratory syncytial virus in older adults in the United States: A systematic review. *PLoS One,* 12**,** e0182321.

CONNOR, E., TOP, F., KRAMER, A., SCHNEIDER, M., LOVE, J., CARLIN, D., SIBER, G., LESZCZYNSKI, J., MCIVER, J., HEMMING, V., HENSON, S., SPRUILL, S., COLVEN, C., WITTES, J., VIDYASAGAR, D., PARK, L., MODLIN, J. F., RHODES, T., PRAMANIK, A. K., JUE, S., SMITH, M., RABALAIS, G. P., FRANCO, S., WILKERSON, S., BIBB, K., PICHOFF, B. E., REMICH, S., RETTKE, M., WEISMAN, L. E., MCDONALD, M. C., JOHNSON, K. E., ADAMS, K., CHARTRAND, S. A., WILSON, M. C., REDDING, G. J., MAYOCK, D., HANNA, H. J. S., STEVENSON, D. K., ARIAGNO, R. L., ADAMS, M. M., MODLER, S., SUBRAMANIAN, S., SMITH, Y. A., HOY, D. A., KUNOS, I., ANGELUS, P., YOGEV, R., DAVIS, M., MILLARD, D. D., STEICHEN, J. J., GRATTON, T., BERNBAUM, J., BANKS, B., ZIRIN, S., FRICKO, J., CORCORAN, L., BARRETT, C. T., PUSSER, N. L., STIEHM, R., COOPER, E. R., FUJII, A., GIVNER, L. B., OSHEA, T. M., NORMAN, B., JENNINGS, T. L., KIMURA, R. E., VASAN, U., HENNESSY, A., KOVACS, A., DELEMOS, R., KHOURY, M., NACHMAN, S. A., STOBIE, P. E., COGGINS, J., PEREA, K. M., ARONOFF, S. C., LYNCH, S., POLAK, M., BAER, L. S., HALL, C. B., LONG, C., INWOOD, R., ANTONIO, E., RAI, B. C., GOYAL, M., SOLECKI, L. E., LEPOW, M. L., HORGAN, M., SWANSON, H., MAYNARD, R. C., BRASEL, D., WERNER, K., OELBERG, D. G., SANCHEZ, P. J., BROYLES, S., ZERAY, F., BAREFIELD, E. S., COLLINS, M. V., DESAI, S. A., WISWELL, T. E., et al. 1997. Reduction of respiratory syncytial virus hospitalization among premature infants and infants with bronchopulmonary dysplasia using respiratory syncytial virus immune globulin prophylaxis. *Pediatrics,* 99**,** 93-99.

COOK, L. & MACDONALD, D. H. C. 2007. Management of paraproteinaemia. *Postgraduate Medical Journal,* 83**,** 217-223.

CORNILLIE, F., SHEALY, D., D'HAENS, G., GEBOES, K., VAN ASSCHE, G., CEUPPENS, J., WAGNER, C., SCHAIBLE, T., PLEVY, S. E., TARGAN, S. R. & RUTGEERTS, P. 2001. Infliximab induces potent anti-inflammatory and local immunomodulatory activity but no systemic immune suppression in patients with Crohn's disease. *Alimentary Pharmacology & Therapeutics,* 15**,** 463-473.

CRAIGO, J. K. & MONTELARO, R. C. 2011. Equine Infectious Anemia Virus Infection and Immunity: Lessons for Aids Vaccine Development. *Future Virol,* 6**,** 139-142.

CRAWFORD, J., EYE, M. K. & COHEN, H. J. 1987. Evaluation of monoclonal gammopathies in the "well" elderly. *The American Journal of Medicine,* 82**,** 39-45.

CURTIS, J. R., PATKAR, N., XIE, A., MARTIN, C., ALLISON, J. J., SAAG, M., SHATIN, D. & SAAG, K. G. 2007. Risk of serious bacterial infections among rheumatoid arthritis patients exposed to tumor necrosis factor alpha antagonists. *Arthritis Rheum,* 56**,** 1125-33.

DALKARA, D., BYRNE, L. C., KLIMCZAK, R. R., VISEL, M., YIN, L., MERIGAN, W. H., FLANNERY, J. G. & SCHAFFER, D. V. 2013. In vivo-directed evolution of a new adeno-associated virus for therapeutic outer retinal gene delivery from the vitreous. *Sci Transl Med,* 5**,** 189ra76.

DARQUET, A. M., CAMERON, B., WILS, P., SCHERMAN, D. & CROUZET, J. 1997. A new DNA vehicle for nonviral gene delivery: supercoiled minicircle. *Gene Therapy,* 4**,** 1341.

DAVIES, L. A., HYDE, S. C., NUNEZ-ALONSO, G., BAZZANI, R. P., HARDING-SMITH, R., PRINGLE, I. A., LAWTON, A. E., ABDULLAH, S., ROBERTS, T. C., MCCORMICK, D., SUMNER-JONES, S. G. & GILL, D. R. 2012. The use of CpG-free plasmids to mediate persistent gene expression following repeated aerosol delivery of pDNA/PEI complexes. *Biomaterials,* 33**,** 5618-27.

DAVIES, L. A., MCLACHLAN, G., SUMNER-JONES, S. G., FERGUSON, D., BAKER, A., TENNANT, P., GORDON, C., VRETTOU, C., BAKER, E., ZHU, J., ALTON, E. W., COLLIE, D. D., PORTEOUS, D. J., HYDE, S. C. & GILL, D. R. 2008. Enhanced lung gene expression after aerosol delivery of concentrated pDNA/PEI complexes. *Mol Ther,* 16**,** 1283-90.

DAVIES, L. A., NUNEZ-ALONSO, G. A., HEBEL, H. L., SCHEULE, R. K., CHENG, S. H., HYDE, S. C. & GILL, D. R. 2010. A novel mixing device for the reproducible generation of nonviral gene therapy formulations. *BioTechniques,* 49**,** 666-668.

DAVIES, L. A., SEGUELA, C., VARATHALINGAM, A., CHENG, S. H., HYDE, S. C. & GILL, D. R. 2007. Identification of transfected cell types following non-viral gene transfer to the murine lung. *The Journal of Gene Medicine,* 9**,** 184-196.

DAYA, S. & BERNS, K. I. 2008. Gene therapy using adeno-associated virus vectors. *Clin Microbiol Rev,* 21**,** 583-93.

DAYA, S., CORTEZ, N. & BERNS, K. I. 2009. Adeno-associated virus site-specific integration is mediated by proteins of the nonhomologous end-joining pathway. *J Virol,* 83**,** 11655-64.

DE SILVA, S. R., MCCLEMENTS, M. E., HANKINS, M. W. & MACLAREN, R. E. 2015. Adeno-Associated Viral Gene Therapy for Retinal Disorders. *In:* BO, X. & VERHAAGEN, J. (eds.) *Gene Delivery and Therapy for Neurological Disorders.* New York, NY: Springer New York.

DEAN, D. A., MACHADO-ARANDA, D., BLAIR-PARKS, K., YELDANDI, A. V. & YOUNG, J. L. 2003. Electroporation as a method for high-level nonviral gene transfer to the lung. *Gene Therapy,* 10**,** 1608.

DEKELVER, R. C., CHOI, V. M., MOEHLE, E. A., PASCHON, D. E., HOCKEMEYER, D., MEIJSING, S. H., SANCAK, Y., CUI, X., STEINE, E. J., MILLER, J. C., TAM, P., BARTSEVICH, V. V., MENG, X., RUPNIEWSKI, I., GOPALAN, S. M., SUN, H. C., PITZ, K. J., ROCK, J. M., ZHANG, L., DAVIS, G. D., REBAR, E. J., CHEESEMAN, I. M., YAMAMOTO, K. R., SABATINI, D. M., JAENISCH, R., GREGORY, P. D. & URNOV, F. D. 2010. Functional genomics, proteomics, and regulatory DNA analysis in isogenic settings using zinc finger nuclease-driven transgenesis into a safe harbor locus in the human genome. *Genome Res,* 20**,** 1133-42.

DELGADO, M. F., COVIELLO, S., MONSALVO, A. C., MELENDI, G. A., HERNANDEZ, J. Z., BATALLE, J. P., DIAZ, L., TRENTO, A., CHANG, H. Y., MITZNER, W., RAVETCH, J., MELERO, J. A., IRUSTA, P. M. & POLACK, F. P. 2009. Lack of antibody affinity maturation due to poor Toll-like receptor stimulation leads to enhanced respiratory syncytial virus disease. *Nat Med,* 15**,** 34-41.

DESHANE, J., SIEGAL, G. P., ALVAREZ, R. D., WANG, M. H., FENG, M., CABRERA, G., LIU, T., KAY, M. & CURIEL, D. T. 1995. Targeted tumor killing via an intracellular antibody against erbB-2. *J Clin Invest,* 96**,** 2980-9.

DESOUBEAUX, G., REICHERT, J. M., SLEEMAN, M., RECKAMP, K. L., RYFFEL, B., ADAMCZEWSKI, J. P., SWEENEY, T. D., VANBEVER, R., DIOT, P., OWEN, C. A., PAGE, C., LERONDEL, S., LE PAPE, A. & HEUZE-VOURC'H, N. 2016. Therapeutic monoclonal antibodies for respiratory diseases: Current challenges and perspectives, March 31 – April 1, 2016, Tours, France. *mAbs,* 8**,** 999-1009.

DETALLE, L., STOHR, T., PALOMO, C., PIEDRA, P. A., GILBERT, B. E., MAS, V., MILLAR, A., POWER, U. F., STORTELERS, C., ALLOSERY, K., MELERO, J. A. & DEPLA, E. 2016. Generation and Characterization of ALX-0171, a Potent Novel Therapeutic Nanobody for the Treatment of Respiratory Syncytial Virus Infection. *Antimicrob Agents Chemother,* 60**,** 6-13.

DEYLE, D. R. & RUSSELL, D. W. 2009. Adeno-associated virus vector integration. *Current opinion in molecular therapeutics,* 11**,** 442-447.

DING, T., ON BEHALF OF THE STANDARDS, A., GUIDELINES WORKING GROUP OF, B. S. R. C. A. C., BHPR, LEDINGHAM, J., ON BEHALF OF THE STANDARDS, A., GUIDELINES WORKING GROUP OF, B. S. R. C. A. C., BHPR, LUQMANI, R., ON BEHALF OF THE STANDARDS, A., GUIDELINES WORKING GROUP OF, B. S. R. C. A. C., BHPR, WESTLAKE, S., ON BEHALF OF THE STANDARDS, A., GUIDELINES WORKING GROUP OF, B. S. R. C. A. C., BHPR, HYRICH, K., ON BEHALF OF THE STANDARDS, A., GUIDELINES WORKING GROUP OF, B. S. R. C. A. C., BHPR, LUNT, M., ON BEHALF OF THE STANDARDS, A., GUIDELINES WORKING GROUP OF, B. S. R. C. A. C., BHPR, KIELY, P., ON BEHALF OF THE STANDARDS, A., GUIDELINES WORKING GROUP OF, B. S. R. C. A. C., BHPR, BUKHARI, M., ON BEHALF OF THE STANDARDS, A., GUIDELINES WORKING GROUP OF, B. S. R. C. A. C., BHPR, ABERNETHY, R., ON BEHALF OF THE STANDARDS, A., GUIDELINES WORKING GROUP OF, B. S. R. C. A. C., BHPR, BOSWORTH, A., ON BEHALF OF THE STANDARDS, A., GUIDELINES WORKING GROUP OF, B. S. R. C. A. C., BHPR, OSTOR, A., ON BEHALF OF THE STANDARDS, A., GUIDELINES WORKING GROUP OF, B. S. R. C. A. C., BHPR, GADSBY, K., ON BEHALF OF THE STANDARDS, A., GUIDELINES WORKING GROUP OF, B. S. R. C. A. C., BHPR, MCKENNA, F., ON BEHALF OF THE STANDARDS, A., GUIDELINES WORKING GROUP OF, B. S. R. C. A. C., BHPR, FINNEY, D., ON BEHALF OF THE STANDARDS, A., GUIDELINES WORKING GROUP OF, B. S. R. C. A. C., BHPR, DIXEY, J., ON BEHALF OF THE STANDARDS, A., GUIDELINES WORKING GROUP OF, B. S. R. C. A. C., BHPR, DEIGHTON, C., ON BEHALF OF THE STANDARDS, A., GUIDELINES WORKING GROUP OF, B. S. R. C. A. C. & BHPR 2010. BSR and BHPR rheumatoid arthritis guidelines on safety of anti-TNF therapies. *Rheumatology,* 49**,** 2217-2219.

DOMACHOWSKE, J. B., KHAN, A. A., ESSER, M. T., JENSEN, K., TAKAS, T., VILLAFANA, T., DUBOVSKY, F. & GRIFFIN, M. P. 2018. Safety, Tolerability and Pharmacokinetics of MEDI8897, an Extended Half-life Single-dose Respiratory Syncytial Virus Prefusion F-targeting Monoclonal Antibody Administered as a Single Dose to Healthy Preterm Infants. *Pediatr Infect Dis J,* 37**,** 886-892.

DONG, J. Y., FAN, P. D. & FRIZZELL, R. A. 1996. Quantitative analysis of the packaging capacity of recombinant adeno-associated virus. *Hum Gene Ther,* 7**,** 2101-12.

DUAN, D., LI, Q., KAO, A. W., YUE, Y., PESSIN, J. E. & ENGELHARDT, J. F. 1999. Dynamin is required for recombinant adeno-associated virus type 2 infection. *J Virol,* 73**,** 10371-6.

DUAN, D., SHARMA, P., YANG, J., YUE, Y., DUDUS, L., ZHANG, Y., FISHER, K. J. & ENGELHARDT, J. F. 1998. Circular intermediates of recombinant adeno-associated virus have defined structural characteristics responsible for long-term episomal persistence in muscle tissue. *J Virol,* 72**,** 8568-77.

DULL, T., ZUFFEREY, R., KELLY, M., MANDEL, R. J., NGUYEN, M., TRONO, D. & NALDINI, L. 1998. A third-generation lentivirus vector with a conditional packaging system. *J Virol,* 72**,** 8463-71.

DUNCAN, F., NAUGHTON, B., ZARASPE, K., MURREY, D., S MEADOWS, A., CLARK, R., E NEWSOME, D., WHITE, P., FU, H. & M MCCARTY, D. 2015. *Broad functional correction of molecular impairments by systemic delivery of scAAVrh74-hSGSH gene delivery in MPS IIIA mice*.

DURHAM, S. R. & KAY, A. B. 1985. Eosinophils, bronchial hyperreactivity and late-phase asthmatic reactions. *Clin Allergy,* 15**,** 411-8.

EARLEY, L. F., POWERS, J. M., ADACHI, K., BAUMGART, J. T., MEYER, N. L., XIE, Q., CHAPMAN, M. S. & NAKAI, H. 2017. Adeno-associated Virus (AAV) Assembly-Activating Protein Is Not an Essential Requirement for Capsid Assembly of AAV Serotypes 4, 5, and 11. *Journal of Virology,* 91**,** e01980-16.

EASTMAN, S. J., LUKASON, M. J., TOUSIGNANT, J. D., MURRAY, H., LANE, M. D., ST GEORGE, J. A., AKITA, G. Y., CHERRY, M., CHENG, S. H. & SCHEULE, R. K. 1997. A concentrated and stable aerosol formulation of cationic lipid:DNA complexes giving high-level gene expression in mouse lung. *Hum Gene Ther,* 8**,** 765-73.

ECKER, D. M., JONES, S. D. & LEVINE, H. L. 2015. The therapeutic monoclonal antibody market. *MAbs,* 7**,** 9-14.

EILAND, L. S. 2009. Respiratory syncytial virus: diagnosis, treatment and prevention. *J Pediatr Pharmacol Ther,* 14**,** 75-85.

EL-AMOURI, S. S., CAO, P., MIAO, C. & PAN, D. 2013. Secreted Luciferase for In Vivo Evaluation of Systemic Protein Delivery in Mice. *Molecular biotechnology,* 53**,** 63-73.

ELLIOTT, M. J., MAINI, R. N., FELDMANN, M., LONG-FOX, A., CHARLES, P., KATSIKIS, P., BRENNAN, F. M., WALKER, J., BIJL, H., GHRAYEB, J. & ET AL. 1993. Treatment of rheumatoid arthritis with chimeric monoclonal antibodies to tumor necrosis factor alpha. *Arthritis Rheum,* 36**,** 1681-90.

ERHORN, S. 2016. Etanercept Biosimilar (Benepali®). *In:* REGIONAL DRUG & THERAPEUTICS CENTRE, N. (ed.).

FAHY, J. V., COCKCROFT, D. W., BOULET, L. P., WONG, H. H., DESCHESNES, F., DAVIS, E. E., RUPPEL, J., SU, J. Q. & ADELMAN, D. C. 1999. Effect of aerosolized anti-IgE (E25) on airway responses to inhaled allergen in asthmatic subjects. *Am J Respir Crit Care Med,* 160**,** 1023-7.

FALA, L. 2016. Nucala (Mepolizumab): First IL-5 Antagonist Monoclonal Antibody FDA Approved for Maintenance Treatment of Patients with Severe Asthma. *Am Health Drug Benefits,* 9**,** 106-10.

FANG, J., QIAN, J. J., YI, S., HARDING, T. C., TU, G. H., VANROEY, M. & JOOSS, K. 2005. Stable antibody expression at therapeutic levels using the 2A peptide. *Nat Biotechnol,* 23**,** 584-90.

FANG, J., YI, S., SIMMONS, A., TU, G. H., NGUYEN, M., HARDING, T. C., VANROEY, M. & JOOSS, K. 2007. An antibody delivery system for regulated expression of therapeutic levels of monoclonal antibodies in vivo. *Mol Ther,* 15**,** 1153-9.

FARBER, H. J., BUCKWOLD, F. J., LACHMAN, B., SIMPSON, J. S., BUCK, E., ARUN, M., VALADEZ, A. M., RUIZ, T., ALONZO, J., HENRY, A., COS-OKPALLA, N., NGUYEN, K., BRENDEL, W., SMALL, J. & GLOMB, W. B. 2016. Observed Effectiveness of Palivizumab for 29-36-Week Gestation Infants. *Pediatrics,* 138.

FARFAN-PORTET, M.-I., GERKENS, S., LEPAGE-NEFKENS, I., VINCK, I. & HULSTAERT, F. 2014. Are biosimilars the next tool to guarantee cost-containment for pharmaceutical expenditures? *The European Journal of Health Economics,* 15**,** 223-228.

FASANMADE, A. A., ADEDOKUN, O. J., FORD, J., HERNANDEZ, D., JOHANNS, J., HU, C., DAVIS, H. M. & ZHOU, H. 2009. Population pharmacokinetic analysis of infliximab in patients with ulcerative colitis. *European Journal of Clinical Pharmacology,* 65**,** 1211-1228.

FASBENDER, A., MARSHALL, J., MONINGER, T. O., GRUNST, T., CHENG, S. & WELSH, M. J. 1997. Effect of co-lipids in enhancing cationic lipid-mediated gene transfer in vitro and in vivo. *Gene Therapy,* 4**,** 716.

FAUROUX, B., SIMÕES, E. A. F., CHECCHIA, P. A., PAES, B., FIGUERAS-ALOY, J., MANZONI, P., BONT, L. & CARBONELL-ESTRANY, X. 2017. The Burden and Long-term Respiratory Morbidity Associated with Respiratory Syncytial Virus Infection in Early Childhood. *Infectious Diseases and Therapy,* 6**,** 173-197.

FAUSTMAN, D. L. & DAVIS, M. 2013. TNF receptor 2 and disease: autoimmunity and regenerative medicine. *Frontiers in Immunology,* 4.

FAVRE, D., BLOUIN, V., PROVOST, N., SPISEK, R., PORROT, F., BOHL, D., MARME, F., CHEREL, Y., SALVETTI, A., HURTREL, B., HEARD, J. M., RIVIERE, Y. & MOULLIER, P. 2002. Lack of an immune response against the tetracycline-dependent transactivator correlates with long-term doxycycline-regulated transgene expression in nonhuman primates after intramuscular injection of recombinant adeno-associated virus. *J Virol,* 76**,** 11605-11.

FELTES, T. F., CABALKA, A. K., MEISSNER, C., PIAZZA, F. M., CARLIN, D. A., TOP, F. H., CONNOR, E. M., SONDHEIMER, H. M. & GRP, C. S. S. 2003. Palivizumab prophylaxis reduces hospitalization due to respiratory syncytial virus in young children with hemodynamically significant congenital heart disease. *Journal of Pediatrics,* 143**,** 532-540.

FELTES, T. F., SONDHEIMER, H. M., TULLOH, R. M. R., HARRIS, B. S., JENSEN, K. M., LOSONSKY, G. A., GRIFFIN, M. P. & GRP, M. C. S. 2011. A Randomized Controlled Trial of Motavizumab Versus Palivizumab for the Prophylaxis of Serious Respiratory Syncytial Virus Disease in Children With Hemodynamically Significant Congenital Heart Disease. *Pediatric Research,* 70**,** 186-191.

FERRARI, F. K., SAMULSKI, T., SHENK, T. & SAMULSKI, R. J. 1996. Second-strand synthesis is a rate-limiting step for efficient transduction by recombinant adeno-associated virus vectors. *Journal of Virology,* 70**,** 3227-3234.

FERRARI, S., PETTENAZZO, A., GARBATI, N., ZACCHELLO, F., BEHR, J. P. & SCARPA, M. 1999. Polyethylenimine shows properties of interest for cystic fibrosis gene therapy. *Biochim Biophys Acta,* 1447**,** 219-25.

FIGURSKA, M. & STANKIEWICZ, A. 2011. Effectiveness of ranibizumab intravitreal injections for exudative age-related macular degeneration treatment: 12-month outcomes. *Medical Science Monitor : International Medical Journal of Experimental and Clinical Research,* 17**,** CR485-CR490.

FLOTTE, T., CARTER, B., CONRAD, C., GUGGINO, W., REYNOLDS, T., ROSENSTEIN, B., TAYLOR, G., WALDEN, S. & WETZEL, R. 1996. A phase I study of an adeno-associated virus-CFTR gene vector in adult CF patients with mild lung disease. *Hum Gene Ther,* 7**,** 1145-59.

FOUDA, G. G., YATES, N. L., POLLARA, J., SHEN, X., OVERMAN, G. R., MAHLOKOZERA, T., WILKS, A. B., KANG, H. H., SALAZAR-GONZALEZ, J. F., SALAZAR, M. G., KALILANI, L., MESHNICK, S. R., HAHN, B. H., SHAW, G. M., LOVINGOOD, R. V., DENNY, T. N., HAYNES, B., LETVIN, N. L., FERRARI, G., MONTEFIORI, D. C., TOMARAS, G. D., PERMAR, S. R. & THE CENTER FOR, H. I. V. A. V. I. 2011. HIV-Specific Functional Antibody Responses in Breast Milk Mirror Those in Plasma and Are Primarily Mediated by IgG Antibodies. *Journal of Virology,* 85**,** 9555-9567.

FUKASAWA, M., MIURA, T., HASEGAWA, A., MORIKAWA, S., TSUJIMOTO, H., MIKI, K., KITAMURA, T. & HAYAMI, M. 1988. Sequence of simian immunodeficiency virus from African green monkey, a new member of the HIV/SIV group. *Nature,* 333**,** 457.

FURST, D. E., KEYSTONE, E. C., SO, A. K., BRAUN, J., BREEDVELD, F. C., BURMESTER, G. R., DE BENEDETTI, F., DORNER, T., EMERY, P., FLEISCHMANN, R., GIBOFSKY, A., KALDEN, J. R., KAVANAUGH, A., KIRKHAM, B., MEASE, P., RUBBERT-ROTH, A., SIEPER, J., SINGER, N. G., SMOLEN, J. S., VAN RIEL, P. L. C. M., WEISMAN, M. H. & WINTHROP, K. L. 2013. Updated consensus statement on biological agents for the treatment of rheumatic diseases, 2012. *Annals of the Rheumatic Diseases,* 72**,** 2-34.

GABRIEL, S. E. 2001. The epidemiology of rheumatoid arthritis. *Rheum Dis Clin North Am,* 27**,** 269-81.
GABRIEL, S. E., CROWSON, C. S. & O'FALLON, M. 1999. The epidemiology of rheumatoid arthritis in Rochester, Minnesota, 1955–1985. *Arthritis & Rheumatism,* 42**,** 415-420.
GARAULET, G., ALFRANCA, A., TORRENTE, M., ESCOLANO, A., LOPEZ-FONTAL, R., HORTELANO, S., REDONDO, J. M. & RODRIGUEZ, A. 2013. IL10 released by a new inflammation-regulated lentiviral system efficiently attenuates zymosan-induced arthritis. *Mol Ther,* 21**,** 119-30.
GARDNER, M. R., KATTENHORN, L. M., KONDUR, H. R., VON SCHAEWEN, M., DORFMAN, T., CHIANG, J. J., HAWORTH, K. G., DECKER, J. M., ALPERT, M. D., BAILEY, C. C., NEALE, E. S., JR., FELLINGER, C. H., JOSHI, V. R., FUCHS, S. P., MARTINEZ-NAVIO, J. M., QUINLAN, B. D., YAO, A. Y., MOUQUET, H., GORMAN, J., ZHANG, B., POIGNARD, P., NUSSENZWEIG, M. C., BURTON, D. R., KWONG, P. D., PIATAK, M., JR., LIFSON, J. D., GAO, G., DESROSIERS, R. C., EVANS, D. T., HAHN, B. H., PLOSS, A., CANNON, P. M., SEAMAN, M. S. & FARZAN, M. 2015. AAV-expressed eCD4-Ig provides durable protection from multiple SHIV challenges. *Nature,* 519**,** 87-91.
GAUDET, D., MÉTHOT, J., DÉRY, S., BRISSON, D., ESSIEMBRE, C., TREMBLAY, G., TREMBLAY, K., DE WAL, J., TWISK, J., VAN DEN BULK, N., SIER-FERREIRA, V. & VAN DEVENTER, S. 2013. Efficacy and long term safety of alipogene tiparvovec (AAV1-LPL(S447X)) gene therapy for lipoprotein lipase deficiency: an open label trial. *Gene therapy,* 20**,** 361-369.
GENESTIER, L., PAILLOT, R., FOURNEL, S., FERRARO, C., MIOSSEC, P. & REVILLARD, J. P. 1998. Immunosuppressive properties of methotrexate: apoptosis and clonal deletion of activated peripheral T cells. *J Clin Invest,* 102**,** 322-8.
GILCHRIST, S., TOROK, T. J., GARY, H. E., ALEXANDER, J. P. & ANDERSON, L. J. 1994. National Surveillance for Respiratory Syncytial Virus, United-States, 1985-1990. *Journal of Infectious Diseases,* 170**,** 986-990.
GILL, D. R., BAZZANI, R. P., CONNOLLY, M. M., SCHLEEF, M., HYDE, S. C. & PRINGLE, I. A. 2016. 743. Minicircles Are Similar to Plasmids in Providing High Level, Long-Term Expression in the Lung. *Molecular Therapy,* 24**,** S293.
GLEZEN, W. P., TABER, L. H., FRANK, A. L. & KASEL, J. A. 1986. Risk of primary infection and reinfection with respiratory syncytial virus. *Am J Dis Child,* 140**,** 543-6.
GORMAN, W. L., GILL, D. S., SCROGGS, R. A. & PORTNER, A. 1990. The hemagglutinin-neuraminidase glycoproteins of human parainfluenza virus type 1 and Sendai virus have high structure-function similarity with limited antigenic cross-reactivity. *Virology,* 175**,** 211-221.
GRAHAM, F. L., SMILEY, J., RUSSELL, W. C. & NAIRN, R. 1977. Characteristics of a human cell line transformed by DNA from human adenovirus type 5. *J Gen Virol,* 36**,** 59-74.
GRAMPP, G. & RAMANAN, S. 2015. The Diversity of Biosimilar Design and Development: Implications for Policies and Stakeholders. *Biodrugs,* 29**,** 365-372.
GREIG, J. A., CALCEDO, R., GRANT, R. L., PENG, H., MEDINA-JASZEK, C. A., AHONKHAI, O., QIN, Q., ROY, S., TRETIAKOVA, A. P. & WILSON, J. M. 2016. Intramuscular administration of AAV overcomes pre-existing neutralizing antibodies in rhesus macaques. *Vaccine,* 34**,** 6323-6329.
GREIG, J. A., PENG, H., OHLSTEIN, J., MEDINA-JASZEK, C. A., AHONKHAI, O., MENTZINGER, A., GRANT, R. L., ROY, S., CHEN, S.-J., BELL, P., TRETIAKOVA, A. P. & WILSON, J. M. 2014. Intramuscular Injection of AAV8 in Mice and Macaques Is Associated with Substantial Hepatic Targeting and Transgene Expression. *PLoS ONE,* 9**,** e112268.
GRIESENBACH, U., INOUE, M., MENG, C., FARLEY, R., CHAN, M., NEWMAN, N. K., BRUM, A., YOU, J., KERTON, A., SHOEMARK, A., BOYD, A. C., DAVIES, J. C., HIGGINS, T. E., GILL, D. R., HYDE, S. C., INNES, J. A., PORTEOUS, D. J.,

HASEGAWA, M. & ALTON, E. W. 2012. Assessment of F/HN-pseudotyped lentivirus as a clinically relevant vector for lung gene therapy. *Am J Respir Crit Care Med,* 186**,** 846-56.

GRIESENBACH, U., VICENTE, C. C., ROBERTS, M. J., MENG, C., SOUSSI, S., XENARIOU, S., TENNANT, P., BAKER, A., BAKER, E., GORDON, C., VRETTOU, C., MCCORMICK, D., COLES, R., GREEN, A. M., LAWTON, A. E., SUMNER-JONES, S. G., CHENG, S. H., SCHEULE, R. K., HYDE, S. C., GILL, D. R., COLLIE, D. D., MCLACHLAN, G. & ALTON, E. W. 2011. Secreted Gaussia luciferase as a sensitive reporter gene for in vivo and ex vivo studies of airway gene transfer. *Biomaterials,* 32**,** 2614-24.

GRIFFIN, M. P., KHAN, A. A., ESSER, M. T., JENSEN, K., TAKAS, T., KANKAM, M. K., VILLAFANA, T. & DUBOVSKY, F. 2017. Safety, Tolerability, and Pharmacokinetics of MEDI8897, the Respiratory Syncytial Virus Prefusion F-Targeting Monoclonal Antibody with an Extended Half-Life, in Healthy Adults. *Antimicrobial Agents and Chemotherapy,* 61.

HACEIN-BEY-ABINA, S., VON KALLE, C., SCHMIDT, M., MCCORMACK, M. P., WULFFRAAT, N., LEBOULCH, P., LIM, A., OSBORNE, C. S., PAWLIUK, R., MORILLON, E., SORENSEN, R., FORSTER, A., FRASER, P., COHEN, J. I., DE SAINT BASILE, G., ALEXANDER, I., WINTERGERST, U., FREBOURG, T., AURIAS, A., STOPPA-LYONNET, D., ROMANA, S., RADFORD-WEISS, I., GROSS, F., VALENSI, F., DELABESSE, E., MACINTYRE, E., SIGAUX, F., SOULIER, J., LEIVA, L. E., WISSLER, M., PRINZ, C., RABBITTS, T. H., LE DEIST, F., FISCHER, A. & CAVAZZANA-CALVO, M. 2003. LMO2-associated clonal T cell proliferation in two patients after gene therapy for SCID-X1. *Science,* 302**,** 415-9.

HALBERT, C. L., STANDAERT, T. A., WILSON, C. B. & MILLER, A. D. 1998. Successful readministration of adeno-associated virus vectors to the mouse lung requires transient immunosuppression during the initial exposure. *J Virol,* 72**,** 9795-805.

HALL, C. B. & DOUGLAS, R. G., JR. 1981. Modes of transmission of respiratory syncytial virus. *J Pediatr,* 99**,** 100-3.

HALL, C. B., DOUGLAS, R. G., SCHNABEL, K. C. & GEIMAN, J. M. 1981. Infectivity of Respiratory Syncytial Virus by Various Routes of Inoculation. *Infection and Immunity,* 33**,** 779-783.

HARAOUI, B. & BYKERK, V. 2007. Etanercept in the treatment of rheumatoid arthritis. *Therapeutics and Clinical Risk Management,* 3**,** 99-105.

HAWKES, N. 2015. Biosimilar versions of anti-TNF drugs could save NHS money, drug company claims. *Bmj-British Medical Journal,* 351.

HAWORTH, C., BRENNAN, F. M., CHANTRY, D., TURNER, M., MAINI, R. N. & FELDMANN, M. 1991. Expression of granulocyte-macrophage colony-stimulating factor in rheumatoid arthritis: regulation by tumor necrosis factor-alpha. *Eur J Immunol,* 21**,** 2575-9.

HEFENEIDER, S. H., BENNETT, R. M., PHAM, T. Q., CORNELL, K., MCCOY, S. L. & HEINRICH, M. C. 1990. Identification of a Cell-Surface DNA Receptor and Its Association with Systemic Lupus Erythematosus. *Journal of Investigative Dermatology,* 94**,** s79-s84.

HEIKKINEN, T., VALKONEN, H., WARIS, M. & RUUSKANEN, O. 2015. Transmission of Respiratory Syncytial Virus Infection Within Families. *Open Forum Infectious Diseases,* 2.

HENDERSON, F. W., COLLIER, A. M., CLYDE, W. A., JR. & DENNY, F. W. 1979. Respiratory-syncytial-virus infections, reinfections and immunity. A prospective, longitudinal study in young children. *N Engl J Med,* 300**,** 530-4.

HERMAN, S. A. & COFFIN, J. M. 1987. Efficient packaging of readthrough RNA in ALV: implications for oncogene transduction. *Science,* 236**,** 845-8.

HEWLETT, S., SANDERSON, T., MAY, J., ALTEN, R., BINGHAM, C. O., 3RD, CROSS, M., MARCH, L., POHL, C., WOODWORTH, T. & BARTLETT, S. J. 2012. 'I'm hurting, I want to kill myself': rheumatoid arthritis flare is more than a high joint count--an

international patient perspective on flare where medical help is sought. *Rheumatology (Oxford),* 51**,** 69-76.
HINDERER, C., KATZ, N., BUZA, E. L., DYER, C., GOODE, T., BELL, P., RICHMAN, L. & WILSON, J. M. 2018. Severe toxicity in nonhuman primates and piglets following high-dose intravenous administration of an AAV vector expressing human SMN. *Hum Gene Ther*.
HOLLEVOET, K., DE SMIDT, E., GEUKENS, N. & DECLERCK, P. 2018. Prolonged in vivo expression and anti-tumor response of DNA-based anti-HER2 antibodies. *Oncotarget,* 9**,** 13623-13636.
HOLLEVOET, K. & DECLERCK, P. J. 2017. State of play and clinical prospects of antibody gene transfer. *J Transl Med,* 15**,** 131.
HOM, S. & PISANO, M. 2017. Reslizumab (Cinqair): An Interleukin-5 Antagonist for Severe Asthma of the Eosinophilic Phenotype. *Pharmacy and Therapeutics,* 42**,** 564-568.
HONG, K. U., REYNOLDS, S. D., WATKINS, S., FUCHS, E. & STRIPP, B. R. 2004. Basal Cells Are a Multipotent Progenitor Capable of Renewing the Bronchial Epithelium. *The American Journal of Pathology,* 164**,** 577-588.
HONGRONG CAI, H. 2017. *Therapeutic Monoclonal Antibodies Approved by FDA in 2016*.
HOWE, S. J., MANSOUR, M. R., SCHWARZWAELDER, K., BARTHOLOMAE, C., HUBANK, M., KEMPSKI, H., BRUGMAN, M. H., PIKE-OVERZET, K., CHATTERS, S. J., DE RIDDER, D., GILMOUR, K. C., ADAMS, S., THORNHILL, S. I., PARSLEY, K. L., STAAL, F. J., GALE, R. E., LINCH, D. C., BAYFORD, J., BROWN, L., QUAYE, M., KINNON, C., ANCLIFF, P., WEBB, D. K., SCHMIDT, M., VON KALLE, C., GASPAR, H. B. & THRASHER, A. J. 2008. Insertional mutagenesis combined with acquired somatic mutations causes leukemogenesis following gene therapy of SCID-X1 patients. *J Clin Invest,* 118**,** 3143-50.
HUANG, K., INCOGNITO, L., CHENG, X., ULBRANDT, N. D. & WU, H. 2010. Respiratory Syncytial Virus-Neutralizing Monoclonal Antibodies Motavizumab and Palivizumab Inhibit Fusion. *Journal of Virology,* 84**,** 8132-8140.
HUANG, M., CHEN, Z., HU, S., JIA, F., LI, Z., HOYT, G., ROBBINS, R. C., KAY, M. A. & WU, J. C. 2009. Novel Minicircle Vector for Gene Therapy in Murine Myocardial Infarction. *Circulation,* 120**,** S230-S237.
HUANG, Y. T., ROMITO, R. R., DE, B. P. & BANERJEE, A. K. 1993. Characterization of the in vitro system for the synthesis of mRNA from human respiratory syncytial virus. *Virology,* 193**,** 862-7.
HUANG, Y. T. & WERTZ, G. W. 1982. The genome of respiratory syncytial virus is a negative-stranded RNA that codes for at least seven mRNA species. *Journal of Virology,* 43**,** 150-157.
HUENNEKENS, F. M. 1994. The methotrexate story: a paradigm for development of cancer chemotherapeutic agents. *Adv Enzyme Regul,* 34**,** 397-419.
HYDE, S. C., PRINGLE, I. A., ABDULLAH, S., LAWTON, A. E., DAVIES, L. A., VARATHALINGAM, A., NUNEZ-ALONSO, G., GREEN, A. M., BAZZANI, R. P., SUMNER-JONES, S. G., CHAN, M., LI, H., YEW, N. S., CHENG, S. H., BOYD, A. C., DAVIES, J. C., GRIESENBACH, U., PORTEOUS, D. J., SHEPPARD, D. N., MUNKONGE, F. M., ALTON, E. W. & GILL, D. R. 2008. CpG-free plasmids confer reduced inflammation and sustained pulmonary gene expression. *Nat Biotechnol,* 26**,** 549-51.
INNALA, L., BERGLIN, E., MOLLER, B., LJUNG, L., SMEDBY, T., SODERGREN, A., MAGNUSSON, S., RANTAPAA-DAHLQVIST, S. & WALLBERG-JONSSON, S. 2014. Age at onset determines severity and choice of treatment in early rheumatoid arthritis: a prospective study. *Arthritis Res Ther,* 16**,** R94.
ISAACSON, J. 2016. Analysis of Orphan Drug Market. *In:* CAPITAL, L. (ed.).
JAKOVLJEVIC, M., GUTZWILLER, F., SCHWENKGLENKS, M., MILOVANOVIC, O., RANCIC, N., VARJACIC, M., STOJADINOVIC, D., DAGOVIC, A. & MATTER-

WALSTRA, K. 2014. Costs differences among monoclonal antibodies-based first-line oncology cancer protocols for breast cancer, colorectal carcinoma and non-Hodgkin's lymphoma. *J BUON,* 19**,** 1111-20.
JEPSEN, M. T., TREBBIEN, R., EMBORG, H. D., KRAUSE, T. G., SCHØNNING, K., VOLDSTEDLUND, M., NIELSEN, J. & FISCHER, T. K. 2018. Incidence and seasonality of respiratory syncytial virus hospitalisations in young children in Denmark, 2010 to 2015. *Eurosurveillance,* 23**,** 17-00163.
JERE, D., JIANG, H. L., AROTE, R., KIM, Y. K., CHOI, Y. J., CHO, M. H., AKAIKE, T. & CHO, C. S. 2009. Degradable polyethylenimines as DNA and small interfering RNA carriers. *Expert Opin Drug Deliv,* 6**,** 827-34.
JOHNSON, F. B., OZER, H. L. & HOGGAN, M. D. 1971. Structural proteins of adenovirus-associated virus type 3. *J Virol,* 8**,** 860-63.
JOHNSON, L. G., OLSEN, J. C., NALDINI, L. & BOUCHER, R. C. 2000. Pseudotyped human lentiviral vector-mediated gene transfer to airway epithelia in vivo. *Gene Therapy,* 7**,** 568.
JOHNSON, P. R. & COLLINS, P. L. 1988. The fusion glycoproteins of human respiratory syncytial virus of subgroups A and B: sequence conservation provides a structural basis for antigenic relatedness. *J Gen Virol,* 69 (Pt 10)**,** 2623-8.
JOHNSON, S., OLIVER, C., PRINCE, G. A., HEMMING, V. G., PFARR, D. S., WANG, S. C., DORMITZER, M., O'GRADY, J., KOENIG, S., TAMURA, J. K., WOODS, R., BANSAL, G., COUCHENOUR, D., TSAO, E., HALL, W. C. & YOUNG, J. F. 1997. Development of a humanized monoclonal antibody (MEDI-493) with potent in vitro and in vivo activity against respiratory syncytial virus. *J Infect Dis,* 176**,** 1215-24.
JOHNSON, S. M., MCNALLY, B. A., IOANNIDIS, I., FLANO, E., TENG, M. N., OOMENS, A. G., WALSH, E. E. & PEEPLES, M. E. 2015. Respiratory Syncytial Virus Uses CX3CR1 as a Receptor on Primary Human Airway Epithelial Cultures. *Plos Pathogens,* 11.
JOHNSTON, J., TAZELAAR, J., RIVERA, V. M., CLACKSON, T., GAO, G. P. & WILSON, J. M. 2003. Regulated expression of erythropoietin from an AAV vector safely improves the anemia of beta-thalassemia in a mouse model. *Mol Ther,* 7**,** 493-7.
JUN-ICHI, M., SATOSHI, T., KIMI, A., FUMI, T., AKIRA, T., KIYOSHI, T. & KEN-ICHI, Y. 1989. Expression vector system based on the chicken β-actin promoter directs efficient production of interleukin-5. *Gene,* 79**,** 269-277.
KAAIJK, P., LUYTJES, W. & ROTS, N. Y. 2013. Vaccination against RSV: Is maternal vaccination a good alternative to other approaches? *Human Vaccines & Immunotherapeutics,* 9**,** 1263-1267.
KANNAN, K., ORTMANN, R. A. & KIMPEL, D. 2005. Animal models of rheumatoid arthritis and their relevance to human disease. *Pathophysiology,* 12**,** 167-81.
KAPIKIAN, A. Z., MITCHELL, R. H., CHANOCK, R. M., SHVEDOFF, R. A. & STEWART, C. E. 1969. An epidemiologic study of altered clinical reactivity to respiratory syncytial (RS) virus infection in children previously vaccinated with an inactivated RS virus vaccine. *Am J Epidemiol,* 89**,** 405-21.
KARRON, R. A., BUONAGURIO, D. A., GEORGIU, A. F., WHITEHEAD, S. S., ADAMUS, J. E., CLEMENTS-MANN, M. L., HARRIS, D. O., RANDOLPH, V. B., UDEM, S. A., MURPHY, B. R. & SIDHU, M. S. 1997. Respiratory syncytial virus (RSV) SH and G proteins are not essential for viral replication in vitro: clinical evaluation and molecular characterization of a cold-passaged, attenuated RSV subgroup B mutant. *Proc Natl Acad Sci U S A,* 94**,** 13961-6.
KARZENOWSKI, D., CHEN, Z., POTTER, D. & PADIDAM, M. 2006. 501. RheoSwitch® Therapeutic System-Inducible Recombinant AAV Vectors for Tightly Regulated Transgene Expression. *Molecular Therapy,* 13**,** S194.
KEFFER, J., PROBERT, L., CAZLARIS, H., GEORGOPOULOS, S., KASLARIS, E., KIOUSSIS, D. & KOLLIAS, G. 1991. Transgenic mice expressing human tumour necrosis factor: a predictive genetic model of arthritis. *EMBO J,* 10**,** 4025-31.

KEIZER, R. J., HUITEMA, A. D., SCHELLENS, J. H. & BEIJNEN, J. H. 2010. Clinical pharmacokinetics of therapeutic monoclonal antibodies. *Clin Pharmacokinet,* 49**,** 493-507.
KEYSTONE, E. C., SCHIFF, M. H., KREMER, J. M., KAFKA, S., LOVY, M., DEVRIES, T. & BURGE, D. J. 2004. Once-weekly administration of 50 mg etanercept in patients with active rheumatoid arthritis - Results of a multicenter, randomized, double-blind, placebo-controlled trial. *Arthritis and Rheumatism,* 50**,** 353-363.
KIM, H. W., CANCHOLA, J. G., BRANDT, C. D., PYLES, G., CHANOCK, R. M., JENSEN, K. & PARROTT, R. H. 1969. Respiratory syncytial virus disease in infants despite prior administration of antigenic inactivated vaccine. *Am J Epidemiol,* 89**,** 422-34.
KLOTZ, U., TEML, A. & SCHWAB, M. 2007. Clinical Pharmacokinetics and Use of Infliximab. *Clinical Pharmacokinetics,* 46**,** 645-660.
KNIGHT, D. M., TRINH, H., LE, J. M., SIEGEL, S., SHEALY, D., MCDONOUGH, M., SCALLON, B., MOORE, M. A., VILCEK, J., DADDONA, P. & GHRAYEB, J. 1993. Construction and Initial Characterization of a Mouse-Human Chimeric Anti-Tnf Antibody. *Molecular Immunology,* 30**,** 1443-1453.
KOBAYASHI, M., IIDA, A., UEDA, Y. & HASEGAWA, M. 2003. Pseudotyped lentivirus vectors derived from simian immunodeficiency virus SIVagm with envelope glycoproteins from paramyxovirus. *J Virol,* 77**,** 2607-14.
KOBINGER, G. P., WEINER, D. J., YU, Q. C. & WILSON, J. M. 2001. Filovirus-pseudotyped lentiviral vector can efficiently and stably transduce airway epithelia in vivo. *Nat Biotechnol,* 19**,** 225-30.
KOCZOT, F. J., CARTER, B. J., GARON, C. F. & ROSE, J. A. 1973. Self-complementarity of terminal sequences within plus or minus strands of adenovirus-associated virus DNA. *Proc Natl Acad Sci U S A,* 70**,** 215-9.
KOIRALA, A., CONLEY, S. M. & NAASH, M. I. Episomal Maintenance of S/MAR-Containing Non-Viral Vectors for RPE-Based Diseases. 2014 New York, NY. Springer New York, 703-709.
KORTH-BRADLEY, J. M., RUBIN, A. S., HANNA, R. K., SIMCOE, D. K. & LEBSACK, M. E. 2000. The Pharmacokinetics of Etanercept in Healthy Volunteers. *Annals of Pharmacotherapy,* 34**,** 161-164.
KOTIN, R. M., MENNINGER, J. C., WARD, D. C. & BERNS, K. I. 1991. Mapping and direct visualization of a region-specific viral DNA integration site on chromosome 19q13-qter. *Genomics,* 10**,** 831-4.
KOTTERMAN, M. A. & SCHAFFER, D. V. 2014. Engineering adeno-associated viruses for clinical gene therapy. *Nature reviews. Genetics,* 15**,** 445-451.
KUMAR, M., BRADOW, B. P. & ZIMMERBERG, J. 2003. Large-scale production of pseudotyped lentiviral vectors using baculovirus GP64. *Hum Gene Ther,* 14**,** 67-77.
KUO, T. T., BAKER, K., YOSHIDA, M., QIAO, S. W., AVESON, V. G., LENCER, W. I. & BLUMBERG, R. S. 2010. Neonatal Fc receptor: from immunity to therapeutics. *J Clin Immunol,* 30**,** 777-89.
KYLE, R. A., GERTZ, M. A., WITZIG, T. E., LUST, J. A., LACY, M. Q., DISPENZIERI, A., FONSECA, R., RAJKUMAR, S. V., OFFORD, J. R., LARSON, D. R., PLEVAK, M. E., THERNEAU, T. M. & GREIPP, P. R. 2003. Review of 1027 Patients With Newly Diagnosed Multiple Myeloma. *Mayo Clinic Proceedings,* 78**,** 21-33.
KYLE, R. A., THERNEAU, T. M., RAJKUMAR, S. V., LARSON, D. R., PLEVAK, M. F., OFFORD, J. R., DISPENZIERI, A., KATZMANN, J. A. & MELTON, L. J. 2006. Prevalence of Monoclonal Gammopathy of Undetermined Significance. *New England Journal of Medicine,* 354**,** 1362-1369.
LATROCHE, C., GITIAUX, C., CHRÉTIEN, F., DESGUERRE, I., MOUNIER, R. & CHAZAUD, B. 2015. Skeletal Muscle Microvasculature: A Highly Dynamic Lifeline. *Physiology,* 30**,** 417-427.
LE GUINER, C., STIEGER, K., TOROMANOFF, A., GUILBAUD, M., MENDES-MADEIRA, A., DEVAUX, M., GUIGAND, L., CHEREL, Y., MOULLIER, P., ROLLING, F. & ADJALI, O. 2014. Transgene regulation using the tetracycline-inducible TetR-KRAB system

after AAV-mediated gene transfer in rodents and nonhuman primates. *PLoS One,* 9**,** e102538.
LE, J. V., J.; DADDONA, P.; GHRAYEB, J.; KNIGHT, D.; SIEGEL, S. 1991. *Methods of treating rheumatoid arthritis using chimeric anti-TNF antibodies*.
LEADER, S. & KOHLHASE, K. 2003. Recent trends in severe respiratory syncytial virus (RSV) among US infants, 1997 to 2000. *J Pediatr,* 143**,** S127-32.
LEBEL, F. M., BARRETT, J. A., CHIOCCA, E. A., YU, J., LUKAS, R. V., NAGPAL, S., KUMTHEKAR, P., KRISHNAN, S. & COOPER, L. J. 2016. Effect of controlled intratumoral viral delivery of Ad-RTS-hIL-12 + oral veledimex in subjects with recurrent or progressive glioma. *Journal of Clinical Oncology,* 34**,** 2052-2052.
LEONI, G., WASOWICZ, M. Y., CHAN, M., MENG, C., FARLEY, R., BRODY, S. L., INOUE, M., HASEGAWA, M., ALTON, E. W. & GRIESENBACH, U. 2015. Ex Vivo and In Vivo Lentivirus-Mediated Transduction of Airway Epithelial Progenitor Cells. *Curr Gene Ther,* 15**,** 581-90.
LEWIS, A. D., CHEN, R., MONTEFIORI, D. C., JOHNSON, P. R. & CLARK, K. R. 2002. Generation of neutralizing activity against human immunodeficiency virus type 1 in serum by antibody gene transfer. *J Virol,* 76**,** 8769-75.
LEWIS, P., HENSEL, M. & EMERMAN, M. 1992. Human immunodeficiency virus infection of cells arrested in the cell cycle. *EMBO J,* 11**,** 3053-8.
LI, C., NARKBUNNAM, N., SAMULSKI, R. J., ASOKAN, A., HU, G., JACOBSON, L. J., MANCO-JOHNSON, M. J. & MONAHAN, P. E. 2011. Neutralizing antibodies against adeno-associated virus examined prospectively in pediatric patients with hemophilia. *Gene Therapy,* 19**,** 288.
LI, J., OLVERA, A. I., AKBARI, O. S., MORADIAN, A., SWEREDOSKI, M. J., HESS, S. & HAY, B. A. 2015. Vectored antibody gene delivery mediates long-term contraception. *Curr Biol,* 25**,** R820-2.
LI, L., LI, X., WU, Y., SONG, L., YANG, X., HE, T., WANG, N., YANG, S., ZENG, Y., WU, Q., QIAN, Z., WEI, Y. & GONG, C. 2017a. Multifunctional Nucleus-targeting Nanoparticles with Ultra-high Gene Transfection Efficiency for In Vivo Gene Therapy. *Theranostics,* 7**,** 1633-1649.
LI, M., WU, Y., QIU, Y., YAO, Z., LIU, S., LIU, Y., SHI, J. & ZHENG, D. 2012. 2A peptide-based, lentivirus-mediated anti-death receptor 5 chimeric antibody expression prevents tumor growth in nude mice. *Mol Ther,* 20**,** 46-53.
LI, P., ZHENG, Y. & CHEN, X. 2017b. Drugs for Autoimmune Inflammatory Diseases: From Small Molecule Compounds to Anti-TNF Biologics. *Frontiers in Pharmacology,* 8.
LIGHTWOOD, D., TSERVISTAS, M., ZEHENTLEITNER, M., SARKAR, K., TURNER, A., BRACHER, M., SMITH, B., LAMOUR, S., BOURNE, T., SHAW, S., GOZZARD, N. & PALFRAMAN, R. T. 2018. Efficacy of an Inhaled Interleukin-13 Antibody Fragment in a Model of Chronic Asthma. *American Journal of Respiratory and Critical Care Medicine,* 198, 610-619.
LIMBERIS, M. P., ADAM, V. S., WONG, G., GREN, J., KOBASA, D., ROSS, T. M., KOBINGER, G. P., TRETIAKOVA, A. & WILSON, J. M. 2013. Intranasal Antibody Gene Transfer in Mice and Ferrets Elicits Broad Protection Against Pandemic Influenza. *Science Translational Medicine,* 5**,** 187ra72-187ra72.
LIMBERIS, M. P., TRETIAKOVA, A., NAMBIAR, K., WONG, G., RACINE, T., CROSARIOL, M., XIANGGUO, Q., KOBINGER, G. & WILSON, J. M. 2016. Adeno-Associated Virus Serotype 9-Expressed ZMapp in Mice Confers Protection Against Systemic and Airway-Acquired Ebola Virus Infection. *The Journal of Infectious Diseases,* 214**,** 1975-1979.
LIU, F., SONG, Y. & LIU, D. 1999. Hydrodynamics-based transfection in animals by systemic administration of plasmid DNA. *Gene Ther,* 6**,** 1258-66.
LOCHRIE, M. A., TATSUNO, G. P., CHRISTIE, B., MCDONNELL, J. W., ZHOU, S., SUROSKY, R., PIERCE, G. F. & COLOSI, P. 2006. Mutations on the external surfaces

of adeno-associated virus type 2 capsids that affect transduction and neutralization. *J Virol,* 80**,** 821-34.
LOPEZ-OLIVO, M. A., SIDDHANAMATHA, H. R., SHEA, B., TUGWELL, P., WELLS, G. A. & SUAREZ-ALMAZOR, M. E. 2014. Methotrexate for treating rheumatoid arthritis. *Cochrane Database Syst Rev***,** CD000957.
LOUBOUTIN, J. P., WANG, L. & WILSON, J. M. 2005. Gene transfer into skeletal muscle using novel AAV serotypes. *J Gene Med,* 7**,** 442-51.
LOVE, R. A., PARGE, H. E., WICKERSHAM, J. A., HOSTOMSKY, Z., HABUKA, N., MOOMAW, E. W., ADACHI, T. & HOSTOMSKA, Z. 1996. The crystal structure of hepatitis C virus NS3 proteinase reveals a trypsin-like fold and a structural zinc binding site. *Cell,* 87**,** 331-42.
MAHESHRI, N., KOERBER, J. T., KASPAR, B. K. & SCHAFFER, D. V. 2006. Directed evolution of adeno-associated virus yields enhanced gene delivery vectors. *Nature Biotechnology,* 24**,** 198.
MAHLER, D. A., HUANG, S., TABRIZI, M. & BELL, G. M. 2004. Efficacy and safety of a monoclonal antibody recognizing interleukin-8 in COPD: a pilot study. *Chest,* 126**,** 926-34.
MAINI, R., ST CLAIR, E. W., BREEDVELD, F., FURST, D., KALDEN, J., WEISMAN, M., SMOLEN, J., EMERY, P., HARRIMAN, G., FELDMANN, M. & LIPSKY, P. 1999. Infliximab (chimeric anti-tumour necrosis factor alpha monoclonal antibody) versus placebo in rheumatoid arthritis patients receiving concomitant methotrexate: a randomised phase III trial. ATTRACT Study Group. *Lancet,* 354**,** 1932-9.
MAINI, R. N., BREEDVELD, F. C., KALDEN, J. R., SMOLEN, J. S., DAVIS, D., MACFARLANE, J. D., ANTONI, C., LEEB, B., ELLIOTT, M. J., WOODY, J. N., SCHAIBLE, T. F. & FELDMANN, M. 1998. Therapeutic efficacy of multiple intravenous infusions of anti-tumor necrosis factor alpha monoclonal antibody combined with low-dose weekly methotrexate in rheumatoid arthritis. *Arthritis Rheum,* 41**,** 1552-63.
MALHOTRA, R., WARD, M., BRIGHT, H., PRIEST, R., FOSTER, M. R., HURLE, M., BLAIR, E. & BIRD, M. 2003. Isolation and characterisation of potential respiratory syncytial virus receptor(s) on epithelial cells. *Microbes Infect,* 5**,** 123-33.
MALLEY, R., DEVINCENZO, J., RAMILO, O., DENNEHY, P. H., MEISSNER, H. C., GRUBER, W. C., SANCHEZ, P. J., JAFRI, H., BALSLEY, J., CARLIN, D., BUCKINGHAM, S., VERNACCHIO, L. & AMBROSINO, D. M. 1998. Reduction of respiratory syncytial virus (RSV) in tracheal aspirates in intubated infants by use of humanized monoclonal antibody to RSV F protein. *J Infect Dis,* 178**,** 1555-61.
MARSHALL, L., KELSALL, W. & GOODING, N. 2008. A cost-effective approach to administering palivizumab in a centralised nurse-led community clinic. *Archives of Disease in Childhood,* 93**,** 638-638.
MARTY, M., COGNETTI, F., MARANINCHI, D., SNYDER, R., MAURIAC, L., TUBIANA-HULIN, M., CHAN, S., GRIMES, D., ANTÓN, A., LLUCH, A., KENNEDY, J., O'BYRNE, K., CONTE, P., GREEN, M., WARD, C., MAYNE, K. & EXTRA, J.-M. 2005. Randomized Phase II Trial of the Efficacy and Safety of Trastuzumab Combined With Docetaxel in Patients With Human Epidermal Growth Factor Receptor 2–Positive Metastatic Breast Cancer Administered As First-Line Treatment: The M77001 Study Group. *Journal of Clinical Oncology,* 23**,** 4265-4274.
MATHERS, C. D. & LONCAR, D. 2006. Projections of global mortality and burden of disease from 2002 to 2030. *PLoS Med,* 3**,** e442.
MATROSOVICH, M., MATROSOVICH, T., CARR, J., ROBERTS, N. A. & KLENK, H.-D. 2003. Overexpression of the α-2,6-Sialyltransferase in MDCK Cells Increases Influenza Virus Sensitivity to Neuraminidase Inhibitors. *Journal of Virology,* 77**,** 8418-8425.
MATUCCI, A., VULTAGGIO, A. & DANESI, R. 2018. The use of intravenous versus subcutaneous monoclonal antibodies in the treatment of severe asthma: a review. *Respiratory Research,* 19**,** 154.

MCCARTHY, K. M., YOONG, Y. & SIMISTER, N. E. 2000. Bidirectional transcytosis of IgG by the rat neonatal Fc receptor expressed in a rat kidney cell line: a system to study protein transport across epithelia. *J Cell Sci,* 113 (Pt 7)**,** 1277-85.

MCINNES, I. B., LEUNG, B. P. & LIEW, F. Y. 2000. Cell-cell interactions in synovitis - Interactions between T lymphocytes and synovial cells. *Arthritis Research,* 2**,** 374-378.

MCLACHLAN, G., DAVIDSON, H., HOLDER, E., DAVIES, L. A., PRINGLE, I. A., SUMNER-JONES, S. G., BAKER, A., TENNANT, P., GORDON, C., VRETTOU, C., BLUNDELL, R., HYNDMAN, L., STEVENSON, B., WILSON, A., DOHERTY, A., SHAW, D. J., COLES, R. L., PAINTER, H., CHENG, S. H., SCHEULE, R. K., DAVIES, J. C., INNES, J. A., HYDE, S. C., GRIESENBACH, U., ALTON, E. W. F. W., BOYD, A. C., PORTEOUS, D. J., GILL, D. R. & COLLIE, D. D. S. 2011. Pre-clinical evaluation of three non-viral gene transfer agents for cystic fibrosis after aerosol delivery to the ovine lung. *Gene Therapy,* 18**,** 996.

MCLELLAN, J. S., CHEN, M., JOYCE, M. G., SASTRY, M., STEWART-JONES, G. B. E., YANG, Y., ZHANG, B., CHEN, L., SRIVATSAN, S., ZHENG, A., ZHOU, T., GRAEPEL, K. W., KUMAR, A., MOIN, S., BOYINGTON, J. C., CHUANG, G.-Y., SOTO, C., BAXA, U., BAKKER, A. Q., SPITS, H., BEAUMONT, T., ZHENG, Z., XIA, N., KO, S.-Y., TODD, J.-P., RAO, S., GRAHAM, B. S. & KWONG, P. D. 2013a. Structure-Based Design of a Fusion Glycoprotein Vaccine for Respiratory Syncytial Virus. *Science (New York, N.Y.),* 342**,** 592-598.

MCLELLAN, J. S., CHEN, M., LEUNG, S., GRAEPEL, K. W., DU, X., YANG, Y., ZHOU, T., BAXA, U., YASUDA, E., BEAUMONT, T., KUMAR, A., MODJARRAD, K., ZHENG, Z., ZHAO, M., XIA, N., KWONG, P. D. & GRAHAM, B. S. 2013b. Structure of RSV Fusion Glycoprotein Trimer Bound to a Prefusion-Specific Neutralizing Antibody. *Science (New York, N.Y.),* 340**,** 1113-1117.

MCNAMEE, K., WILLIAMS, R. & SEED, M. 2015. Animal models of rheumatoid arthritis: How informative are they? *Eur J Pharmacol,* 759**,** 278-86.

MEJIAS, A. & RAMILO, O. 2015. New options in the treatment of respiratory syncytial virus disease. *J Infect,* 71 Suppl 1**,** S80-7.

MELIANI, A., BOISGERAULT, F., RONZITTI, G., COLLAUD, F., LEBORGNE, C., KISHIMOTO, T. K. & MINGOZZI, F. 2016. Antigen-Specific Modulation of Capsid Immunogenicity with Tolerogenic Nanoparticles Results in Successful AAV Vector Readministration. *Molecular Therapy,* 24**,** S34-S34.

MELLSTEDT, H. 2013. Clinical considerations for biosimilar antibodies. *European Journal of Cancer Supplements,* 11**,** 1-11.

MENDELL, J. R., AL-ZAIDY, S., SHELL, R., ARNOLD, W. D., RODINO-KLAPAC, L. R., PRIOR, T. W., LOWES, L., ALFANO, L., BERRY, K., CHURCH, K., KISSEL, J. T., NAGENDRAN, S., L'ITALIEN, J., SPROULE, D. M., WELLS, C., CARDENAS, J. A., HEITZER, M. D., KASPAR, A., CORCORAN, S., BRAUN, L., LIKHITE, S., MIRANDA, C., MEYER, K., FOUST, K. D., BURGHES, A. H. M. & KASPAR, B. K. 2017. Single-Dose Gene-Replacement Therapy for Spinal Muscular Atrophy. *N Engl J Med,* 377**,** 1713-1722.

MIAGKOV, A. V., VARLEY, A. W., MUNFORD, R. S. & MAKAROV, S. S. 2002. Endogenous regulation of a therapeutic transgene restores homeostasis in arthritic joints. *J Clin Invest,* 109**,** 1223-9.

MINGOZZI, F., ANGUELA, X. M., PAVANI, G., CHEN, Y., DAVIDSON, R. J., HUI, D. J., YAZICIOGLU, M., ELKOUBY, L., HINDERER, C. J., FAELLA, A., HOWARD, C., TAI, A., PODSAKOFF, G. M., ZHOU, S., BASNER-TSCHAKARJAN, E., WRIGHT, J. F. & HIGH, K. A. 2013a. Overcoming Preexisting Humoral Immunity to AAV Using Capsid Decoys. *Science translational medicine,* 5**,** 194ra92-194ra92.

MINGOZZI, F., CHEN, Y., EDMONSON, S. C., ZHOU, S., THURLINGS, R. M., TAK, P. P., HIGH, K. A. & VERVOORDELDONK, M. J. 2013b. Prevalence and pharmacological modulation of humoral immunity to AAV vectors in gene transfer to synovial tissue. *Gene Therapy,* 20**,** 417-424.

MINGOZZI, F., CHEN, Y., MURPHY, S. L., EDMONSON, S. C., TAI, A., PRICE, S. D., METZGER, M. E., ZHOU, S., WRIGHT, J. F., DONAHUE, R. E., DUNBAR, C. E. & HIGH, K. A. 2012. Pharmacological Modulation of Humoral Immunity in a Nonhuman Primate Model of AAV Gene Transfer for Hemophilia B. *Molecular Therapy,* 20**,** 1410-1416.

MITOMO, K., GRIESENBACH, U., INOUE, M., SOMERTON, L., MENG, C., AKIBA, E., TABATA, T., UEDA, Y., FRANKEL, G. M., FARLEY, R., SINGH, C., CHAN, M., MUNKONGE, F., BRUM, A., XENARIOU, S., ESCUDERO-GARCIA, S., HASEGAWA, M. & ALTON, E. W. 2010. Toward gene therapy for cystic fibrosis using a lentivirus pseudotyped with Sendai virus envelopes. *Mol Ther,* 18**,** 1173-82.

MOCHIZUKI, H., SCHWARTZ, J. P., TANAKA, K., BRADY, R. O. & REISER, J. 1998. High-titer human immunodeficiency virus type 1-based vector systems for gene delivery into nondividing cells. *J Virol,* 72**,** 8873-83.

MOGHADDAM, A., OLSZEWSKA, W., WANG, B., TREGONING, J. S., HELSON, R., SATTENTAU, Q. J. & OPENSHAW, P. J. M. 2006. A potential molecular mechanism for hypersensitivity caused by formalin-inactivated vaccines. *Nature Medicine,* 12**,** 905.

MOHLER, K. M., TORRANCE, D. S., SMITH, C. A., GOODWIN, R. G., STREMLER, K. E., FUNG, V. P., MADANI, H. & WIDMER, M. B. 1993. Soluble Tumor-Necrosis-Factor (Tnf) Receptors Are Effective Therapeutic Agents in Lethal Endotoxemia and Function Simultaneously as Both Tnf Carriers and Tnf Antagonists. *Journal of Immunology,* 151**,** 1548-1561.

MONACO, C., NANCHAHAL, J., TAYLOR, P. & FELDMANN, M. 2015. Anti-TNF therapy: past, present and future. *International Immunology,* 27**,** 55-62.

MONTEILHET, V., SAHEB, S., BOUTIN, S., LEBORGNE, C., VERON, P., MONTUS, M.-F., MOULLIER, P., BENVENISTE, O. & MASURIER, C. 2011. A 10 Patient Case Report on the Impact of Plasmapheresis Upon Neutralizing Factors Against Adeno-associated Virus (AAV) Types 1, 2, 6, and 8. *Molecular Therapy,* 19**,** 2084-2091.

MONTINI, E., CESANA, D., SCHMIDT, M., SANVITO, F., PONZONI, M., BARTHOLOMAE, C., SERGI SERGI, L., BENEDICENTI, F., AMBROSI, A., DI SERIO, C., DOGLIONI, C., VON KALLE, C. & NALDINI, L. 2006. Hematopoietic stem cell gene transfer in a tumor-prone mouse model uncovers low genotoxicity of lentiviral vector integration. *Nat Biotechnol,* 24**,** 687-96.

MONTORO, D. T., HABER, A. L., BITON, M., VINARSKY, V., LIN, B., BIRKET, S. E., YUAN, F., CHEN, S., LEUNG, H. M., VILLORIA, J., ROGEL, N., BURGIN, G., TSANKOV, A. M., WAGHRAY, A., SLYPER, M., WALDMAN, J., NGUYEN, L., DIONNE, D., ROZENBLATT-ROSEN, O., TATA, P. R., MOU, H., SHIVARAJU, M., BIHLER, H., MENSE, M., TEARNEY, G. J., ROWE, S. M., ENGELHARDT, J. F., REGEV, A. & RAJAGOPAL, J. 2018. A revised airway epithelial hierarchy includes CFTR-expressing ionocytes. *Nature*.

MOORE, A. E., SABACHEWSKY, L. & TOOLAN, H. W. 1955. Culture Characteristics of Four Permanent Lines of Human Cancer Cells. *Cancer Research,* 15**,** 598-602.

MOOTS, R. J., XAVIER, R. M., MOK, C. C., RAHMAN, M. U., TSAI, W. C., AL-MAINI, M. H., PAVELKA, K., MAHGOUB, E., KOTAK, S., KORTH-BRADLEY, J., PEDERSEN, R., MELE, L., SHEN, Q. & VLAHOS, B. 2017. The impact of anti-drug antibodies on drug concentrations and clinical outcomes in rheumatoid arthritis patients treated with adalimumab, etanercept, or infliximab: Results from a multinational, real-world clinical practice, non-interventional study. *Plos One,* 12.

MORI, S. 2007. A relationship between pharmacokinetics (PK) and the efficacy of infliximab for patients with rheumatoid arthritis: characterization of infliximab-resistant cases and PK-based modified therapy. *Mod Rheumatol,* 17**,** 83-91.

MORRISON, C. 2015. $1-million price tag set for Glybera gene therapy. *Nature Biotechnology,* 33**,** 217.

NAIR, H., NOKES, D. J., GESSNER, B. D., DHERANI, M., MADHI, S. A., SINGLETON, R. J., O'BRIEN, K. L., ROCA, A., WRIGHT, P. F., BRUCE, N., CHANDRAN, A., THEODORATOU, E., SUTANTO, A., SEDYANINGSIH, E. R., NGAMA, M.,

MUNYWOKI, P. K., KARTASASMITA, C., SIMOES, E. A., RUDAN, I., WEBER, M. W. & CAMPBELL, H. 2010. Global burden of acute lower respiratory infections due to respiratory syncytial virus in young children: a systematic review and meta-analysis. *Lancet,* 375**,** 1545-55.

NAIR, K., GHUSHCHYAN, V. & NAIM, A. 2013. Effectiveness and Costs of TNF-Alpha Blocker Use for Patients with Rheumatoid Arthritis. *Am Health Drug Benefits,* 6**,** 126-36.

NALDINI, L., BLOMER, U., GALLAY, P., ORY, D., MULLIGAN, R., GAGE, F. H., VERMA, I. M. & TRONO, D. 1996. In vivo gene delivery and stable transduction of nondividing cells by a lentiviral vector. *Science,* 272**,** 263-7.

NASO, M. F., TOMKOWICZ, B., PERRY, W. L. & STROHL, W. R. 2017. Adeno-Associated Virus (AAV) as a Vector for Gene Therapy. *Biodrugs,* 31**,** 317-334.

NATHWANI, A. C., REISS, U. M., TUDDENHAM, E. G. D., ROSALES, C., CHOWDARY, P., MCINTOSH, J., DELLA PERUTA, M., LHERITEAU, E., PATEL, N., RAJ, D., RIDDELL, A., PIE, J., RANGARAJAN, S., BEVAN, D., RECHT, M., SHEN, Y.-M., HALKA, K. G., BASNER-TSCHAKARJAN, E., MINGOZZI, F., HIGH, K. A., ALLAY, J., KAY, M. A., NG, C. Y. C., ZHOU, J., CANCIO, M., MORTON, C. L., GRAY, J. T., SRIVASTAVA, D., NIENHUIS, A. W. & DAVIDOFF, A. M. 2014. Long-Term Safety and Efficacy of Factor IX Gene Therapy in Hemophilia B. *New England Journal of Medicine,* 371**,** 1994-2004.

NAULT, J. C., DATTA, S., IMBEAUD, S., FRANCONI, A., MALLET, M., COUCHY, G., LETOUZE, E., PILATI, C., VERRET, B., BLANC, J. F., BALABAUD, C., CALDERARO, J., LAURENT, A., LETEXIER, M., BIOULAC-SAGE, P., CALVO, F. & ZUCMAN-ROSSI, J. 2015. Recurrent AAV2-related insertional mutagenesis in human hepatocellular carcinomas. *Nat Genet,* 47**,** 1187-93.

NAVAS, L., WANG, E., DE CARVALHO, V. & ROBINSON, J. 1992. Improved outcome of respiratory syncytial virus infection in a high-risk hospitalized population of Canadian children. Pediatric Investigators Collaborative Network on Infections in Canada. *J Pediatr,* 121**,** 348-54.

NEUMANN, E., SCHAEFER-RIDDER, M., WANG, Y. & HOFSCHNEIDER, P. H. 1982. Gene transfer into mouse lyoma cells by electroporation in high electric fields. *EMBO J,* 1**,** 841-5.

NEUMANN, P. J., COHEN, J. T. & WEINSTEIN, M. C. 2014. Updating Cost-Effectiveness — The Curious Resilience of the $50,000-per-QALY Threshold. *New England Journal of Medicine,* 371**,** 796-797.

NEUZIL, K. M. 2016. Progress toward a Respiratory Syncytial Virus Vaccine. *Clin Vaccine Immunol,* 23**,** 186-8.

NEWS. 2018. FDA approves hereditary blindness gene therapy. *Nature Biotechnology,* 36**,** 6.

NGUYEN, M., HUAN-TU, G., GONZALEZ-EDICK, M., RIVERA, V. M., CLACKSON, T., JOOSS, K. U. & HARDING, T. C. 2007. Rapamycin-regulated control of antiangiogenic tumor therapy following rAAV-mediated gene transfer. *Mol Ther,* 15**,** 912-20.

NOEL, D., PELEGRIN, M., MARIN, M., BIARD-PIECHACZYK, M., OURLIN, J. C., MANI, J. C. & PIECHACZYK, M. 1997. In vitro and in vivo secretion of cloned antibodies by genetically modified myogenic cells. *Hum Gene Ther,* 8**,** 1219-29.

NORUM, J., RISBERG, T. & OLSEN, J. A. 2005. A monoclonal antibody against HER-2 (trastuzumab) for metastatic breast cancer: a model-based cost-effectiveness analysis. *Annals of Oncology,* 16**,** 909-914.

NRAS 2010. The economic burden of rheumatoid arthritis. National Rheumatoid Arthritis Society.

NULL, D., BIMLE, C., WEISMAN, L., JOHNSON, K., STEICHEN, J., SINGH, S., WANG, E., ASZTALOS, E., LOEFFLER, A. M., AZIMI, P. H., LIEBERMAN, J. M., O'DONNELL, N. E., COOKE, R. J., MCCORMICK, K., KOO, W., HAMMAMI, M., MILNER, A. D., GAON, P., NACHMAN, S., TARPEY, K. P., SANCHEZ, P. J., BROYLES, R. S., BRATCHER, D., BALL, M. V., DUDA, F. J., DECUIR, P. M., POLLARA, B., NELSON,

L. S., BALBUS, M., SCHULTZ, M. J., CHIPPS, B. E., GIVNER, L. B., O'SHEA, M., EVERARD, M., PFEFFER, K., PAGE, A. J., DENNEHY, P. H., MODLIN, J., RHODES, T., DEVINCENZO, N., NICKERSON, B., ARRIETA, A., BOUCHER, F. D., KEENEY, R. E., YOUNG, T. E., STEVENS, J. C., ARIAGNO, R., ADAMS, M., POLAK, M. J., LYNCH, S. K., GERDES, J. S., KUBA, M., AOUTHMANY, M., LAMAR, K., CHANG, G. Y. W., SHELTON, M. M., HADEED, S. K. W., VASAN, U., HENNESSY, A., YOGEV, R., WELLIVER, R. C., TRISTRAM, D., ALBIN, C., JEFFERSON, T. T., PURDY, G. D., BUCKNER, C. M., SCHLESSEL, J., SIA, C., TAN, B., SANKARAN, K., MORLEY, C. J., WHITE, D. K., MEISSNER, H. C., FRANTZ, I., DESAI, S. A., STANLEY, C. W., INWOOD, R., SOLECKI, L. E., WALD, E., SMAIL, K., FOX, R. E., TACIAK, V., PARK, C. L., VIDYASAGAR, D., REDDING, G., MAYOCK, D. E., REUMAN, P. D., BIFANO, E. M., ESTRADA, B., MANCAO, M. Y., HOOK, B., MCDAVID, G., ROWEN, J. L., PATEL, J. A., ROBINSON, J., LEE, B., RODRIGUEZ, W., ARROBIO, J., HOCKER, J. R., MCCONNELL, C., et al. 1998. Palivizumab, a humanized respiratory syncytial virus monoclonal antibody, reduces hospitalization from respiratory syncytial virus infection in high-risk infants. *Pediatrics,* 102**,** 531-537.

NYE, S., WHITLEY, R. J. & KONG, M. 2016. Viral Infection in the Development and Progression of Pediatric Acute Respiratory Distress Syndrome. *Frontiers in Pediatrics,* 4**,** 128.

O'BRIEN, K. L., CHANDRAN, A., WEATHERHOLTZ, R., JAFRI, H. S., GRIFFIN, M. P., BELLAMY, T., MILLAR, E. V., JENSEN, K. M., HARRIS, B. S., REID, R., MOULTON, L. H., LOSONSKY, G. A., KARRON, R. A., SANTOSHAM, M. & RSV, R. S. V. 2015. Efficacy of motavizumab for the prevention of respiratory syncytial virus disease in healthy Native American infants: a phase 3 randomised double-blind placebo-controlled trial. *Lancet Infectious Diseases,* 15**,** 1398-1408.

OHMIT, S. E., MOLER, F. W., MONTO, A. S. & KHAN, A. S. 1996. Ribavirin utilization and clinical effectiveness in children hospitalized with respiratory syncytial virus infection. *J Clin Epidemiol,* 49**,** 963-7.

OHNISHI, T., SUR, S., COLLINS, D. S., FISH, J. E., GLEICH, G. J. & PETERS, S. P. 1993. Eosinophil survival activity identified as interleukin-5 is associated with eosinophil recruitment and degranulation and lung injury twenty-four hours after segmental antigen lung challenge. *J Allergy Clin Immunol,* 92**,** 607-15.

OKADA, Y., WU, D., TRYNKA, G., RAJ, T., TERAO, C., IKARI, K., KOCHI, Y., OHMURA, K., SUZUKI, A., YOSHIDA, S., GRAHAM, R. R., MANOHARAN, A., ORTMANN, W., BHANGALE, T., DENNY, J. C., CARROLL, R. J., EYLER, A. E., GREENBERG, J. D., KREMER, J. M., PAPPAS, D. A., JIANG, L., YIN, J., YE, L., SU, D. F., YANG, J., XIE, G., KEYSTONE, E., WESTRA, H. J., ESKO, T., METSPALU, A., ZHOU, X., GUPTA, N., MIREL, D., STAHL, E. A., DIOGO, D., CUI, J., LIAO, K., GUO, M. H., MYOUZEN, K., KAWAGUCHI, T., COENEN, M. J., VAN RIEL, P. L., VAN DE LAAR, M. A., GUCHELAAR, H. J., HUIZINGA, T. W., DIEUDE, P., MARIETTE, X., BRIDGES, S. L., JR., ZHERNAKOVA, A., TOES, R. E., TAK, P. P., MICELI-RICHARD, C., BANG, S. Y., LEE, H. S., MARTIN, J., GONZALEZ-GAY, M. A., RODRIGUEZ-RODRIGUEZ, L., RANTAPAA-DAHLQVIST, S., ARLESTIG, L., CHOI, H. K., KAMATANI, Y., GALAN, P., LATHROP, M., CONSORTIUM, R., CONSORTIUM, G., EYRE, S., BOWES, J., BARTON, A., DE VRIES, N., MORELAND, L. W., CRISWELL, L. A., KARLSON, E. W., TANIGUCHI, A., YAMADA, R., KUBO, M., LIU, J. S., BAE, S. C., WORTHINGTON, J., PADYUKOV, L., KLARESKOG, L., GREGERSEN, P. K., RAYCHAUDHURI, S., STRANGER, B. E., DE JAGER, P. L., FRANKE, L., VISSCHER, P. M., BROWN, M. A., YAMANAKA, H., MIMORI, T., TAKAHASHI, A., XU, H., BEHRENS, T. W., SIMINOVITCH, K. A., MOMOHARA, S., MATSUDA, F., YAMAMOTO, K. & PLENGE, R. M. 2014. Genetics of rheumatoid arthritis contributes to biology and drug discovery. *Nature,* 506**,** 376-81.

OLIVEIRA, C. 2015. *An Investigation into Persistent Transgene Expression from Plasmid Vectors in the Lung.* DPhil Thesis, University of Oxford.

OPENSHAW, P. J. 2013. The Mouse Model of Respiratory Syncytial Virus Disease. *Challenges and Opportunities for Respiratory Syncytial Virus Vaccines,* 372**,** 359-369.
OSSLUND, T. C., C.; CRAMPTON, S.; BASS, R. 2003. *Crystals of etanercept and methods of making thereof*.
PALLI, S. R., KAPITSKAYA, M. Z., KUMAR, M. B. & CRESS, D. E. 2003. Improved ecdysone receptor-based inducible gene regulation system. *Eur J Biochem,* 270**,** 1308-15.
PARK, T., GRIGGS, S. K. & SUH, D. C. 2015. Cost Effectiveness of Monoclonal Antibody Therapy for Rare Diseases: A Systematic Review. *BioDrugs,* 29**,** 259-74.
PARROTT, R. H., VARGOSKO, A. J., KIM, H. W., BELL, J. A. & CHANOCK, R. M. 1962. III. Myxoviruses: Parainfluenza. *American Journal of Public Health and the Nations Health,* 52**,** 907-917.
PATEL, M., GIDDINGS, A. M., SECHELSKI, J. & OLSEN, J. C. 2013. High efficiency gene transfer to airways of mice using influenza hemagglutinin pseudotyped lentiviral vectors. *J Gene Med,* 15**,** 51-62.
PAUL-SMITH, M. C., PYTEL, K. M., GELINAS, J.-F., MCINTOSH, J., PRINGLE, I., DAVIES, L., CHAN, M., MENG, C., BELL, R., CAMMACK, L., MORAN, C., CAMERON, L., INOUE, M., TSUGUMINE, S., HIRONAKA, T., GILL, D. R., HYDE, S. C., NATHWANI, A., ALTON, E. W. F. W. & GRIESENBACH, U. 2018. The murine lung as a factory to produce secreted intrapulmonary and circulatory proteins. *Gene Therapy*.
PAULK, N. K., PEKRUN, K., CHARVILLE, G. W., MAGUIRE-NGUYEN, K., WOSCZYNA, M. N., XU, J., ZHANG, Y., LISOWSKI, L., YOO, B., VILCHES-MOURE, J. G., LEE, G. K., SHRAGER, J. B., RANDO, T. A. & KAY, M. A. 2018a. Bioengineered Viral Platform for Intramuscular Passive Vaccine Delivery to Human Skeletal Muscle. *Molecular Therapy. Methods & Clinical Development,* 10**,** 144-155.
PAULK, N. K., PEKRUN, K., ZHU, E., NYGAARD, S., LI, B., XU, J., CHU, K., LEBORGNE, C., DANE, A. P., HAFT, A., ZHANG, Y., ZHANG, F., MORTON, C., VALENTINE, M. B., DAVIDOFF, A. M., NATHWANI, A. C., MINGOZZI, F., GROMPE, M., ALEXANDER, I. E., LISOWSKI, L. & KAY, M. A. 2018b. Bioengineered AAV Capsids with Combined High Human Liver Transduction In Vivo and Unique Humoral Seroreactivity. *Molecular Therapy,* 26**,** 289-303.
PAVELKA, M. & ROTH, J. 2010. Myofibrils and Sarcomere. *In:* PAVELKA, M. & ROTH, J. (eds.) *Functional Ultrastructure: Atlas of Tissue Biology and Pathology.* Vienna: Springer Vienna.
PAVILACK, M., CLIFFORD, R. A., GONZALES, T., KONG, A. M., WADE, S. & MCLAURIN, K. K. 2017. Trends in Utilization of Outpatient Respiratory Syncytial Virus Prophylaxis with Palivizumab among Medicaid- and Commercially Insured Infants. *Infect Dis Ther*.
PAVORD, I. D., CHANEZ, P., CRINER, G. J., KERSTJENS, H. A. M., KORN, S., LUGOGO, N., MARTINOT, J. B., SAGARA, H., ALBERS, F. C., BRADFORD, E. S., HARRIS, S. S., MAYER, B., RUBIN, D. B., YANCEY, S. W. & SCIURBA, F. C. 2017. Mepolizumab for Eosinophilic Chronic Obstructive Pulmonary Disease. *N Engl J Med,* 377**,** 1613-1629.
PENAUD-BUDLOO, M., LE GUINER, C., NOWROUZI, A., TOROMANOFF, A., CHEREL, Y., CHENUAUD, P., SCHMIDT, M., VON KALLE, C., ROLLING, F., MOULLIER, P. & SNYDER, R. O. 2008. Adeno-associated virus vector genomes persist as episomal chromatin in primate muscle. *J Virol,* 82**,** 7875-85.
PERCY, L. A. & D'SA, S. 2009. Multiple myeloma and paraproteinaemia. *Medicine,* 37**,** 212-216.
PEREZ, N., BIGEY, P., SCHERMAN, D., DANOS, O., PIECHACZYK, M. & PELEGRIN, M. 2004. Regulatable systemic production of monoclonal antibodies by in vivo muscle electroporation. *Genet Vaccines Ther,* 2**,** 2.
PIGUET, P. F., GRAU, G. E., VESIN, C., LOETSCHER, H., GENTZ, R. & LESSLAUER, W. 1992. Evolution of collagen arthritis in mice is arrested by treatment with anti-

tumour necrosis factor (TNF) antibody or a recombinant soluble TNF receptor. *Immunology,* 77**,** 510-4.

PIRKER, R., PEREIRA, J. R., SZCZESNA, A., VON PAWEL, J., KRZAKOWSKI, M., RAMLAU, R., VYNNYCHENKO, I., PARK, K., YU, C. T., GANUL, V., ROH, J. K., BAJETTA, E., O'BYRNE, K., DE MARINIS, F., EBERHARDT, W., GODDEMEIER, T., EMIG, M., GATZEMEIER, U. & TEAM, F. S. 2009. Cetuximab plus chemotherapy in patients with advanced non-small-cell lung cancer (FLEX): an open-label randomised phase III trial. *Lancet,* 373**,** 1525-31.

PLASSCHAERT, L. W., ŽILIONIS, R., CHOO-WING, R., SAVOVA, V., KNEHR, J., ROMA, G., KLEIN, A. M. & JAFFE, A. B. 2018. A single-cell atlas of the airway epithelium reveals the CFTR-rich pulmonary ionocyte. *Nature*.

POHL, M. A., LAN, S., BERL, T. & LUPUS NEPHRITIS COLLABORATIVE STUDY, G. 1991. PLasmapheresis does not increase the risk for infection in immunosuppressed patients with severe lupus nephritis. *Annals of Internal Medicine,* 114**,** 924-929.

PRAETOR, A., ELLINGER, I. & HUNZIKER, W. 1999. Intracellular traffic of the MHC class I-like IgG Fc receptor, FcRn, expressed in epithelial MDCK cells. *J Cell Sci,* 112 (Pt 14)**,** 2291-9.

PRINCE, G. A., HORSWOOD, R. L., BERNDT, J., SUFFIN, S. C. & CHANOCK, R. M. 1979. Respiratory syncytial virus infection in inbred mice. *Infect Immun,* 26**,** 764-6.

PRINGLE, I. A., MCLACHLAN, G., COLLIE, D. D. S., SUMNER-JONES, S. G., LAWTON, A. E., TENNANT, P., BAKER, A., GORDON, C., BLUNDELL, R., VARATHALINGAM, A., DAVIES, L. A., SCHMID, R. A., CHENG, S. H., PORTEOUS, D. J., GILL, D. R. & HYDE, S. C. 2007. Electroporation enhances reporter gene expression following delivery of naked plasmid DNA to the lung. *The Journal of Gene Medicine,* 9**,** 369-380.

PRITCHARD, C. H., GREENWALD, M. W., KREMER, J. M., GAYLIS, N. B., RIGBY, W., ZLOTNICK, S., CHUNG, C., JABER, B. & REISS, W. 2014. Safety of infusing rituximab at a more rapid rate in patients with rheumatoid arthritis: results from the RATE-RA study. *BMC Musculoskeletal Disorders,* 15**,** 177-177.

PUTRIK, P., RAMIRO, S., KVIEN, T. K., SOKKA, T., PAVLOVA, M., UHLIG, T. & BOONEN, A. 2014. Inequities in access to biologic and synthetic DMARDs across 46 European countries. *Annals of the Rheumatic Diseases,* 73**,** 198-206.

RAVID, T. & HOCHSTRASSER, M. 2008. Diversity of degradation signals in the ubiquitin–proteasome system. *Nature Reviews Molecular Cell Biology,* 9**,** 679.

RAWLINS, E. L. & HOGAN, B. L. M. 2008. Ciliated epithelial cell lifespan in the mouse trachea and lung. *American Journal of Physiology. Lung Cellular and Molecular Physiology,* 295**,** L231-L234.

RENNARD, S. I., FLAVIN, S. K., AGARWAL, P. K., LO, K. H. & BARNATHAN, E. S. 2013. Long-term safety study of infliximab in moderate-to-severe chronic obstructive pulmonary disease. *Respir Med,* 107**,** 424-32.

RENNARD, S. I., FOGARTY, C., KELSEN, S., LONG, W., RAMSDELL, J., ALLISON, J., MAHLER, D., SAADEH, C., SILER, T., SNELL, P., KORENBLAT, P., SMITH, W., KAYE, M., MANDEL, M., ANDREWS, C., PRABHU, R., DONOHUE, J. F., WATT, R., LO, K. H., SCHLENKER-HERCEG, R., BARNATHAN, E. S., MURRAY, J. & INVESTIGATORS, C. 2007. The safety and efficacy of infliximab in moderate to severe chronic obstructive pulmonary disease. *Am J Respir Crit Care Med,* 175**,** 926-34.

RISON, R. A. & BEYDOUN, S. R. 2016. Paraproteinemic neuropathy: a practical review. *BMC Neurology,* 16**,** 13.

RIVERA, V. M., GAO, G. P., GRANT, R. L., SCHNELL, M. A., ZOLTICK, P. W., ROZAMUS, L. W., CLACKSON, T. & WILSON, J. M. 2005. Long-term pharmacologically regulated expression of erythropoietin in primates following AAV-mediated gene transfer. *Blood,* 105**,** 1424-30.

ROBBIE, G. J., ZHAO, L., MONDICK, J., LOSONSKY, G. & ROSKOS, L. K. 2012. Population pharmacokinetics of palivizumab, a humanized anti-respiratory syncytial virus monoclonal antibody, in adults and children. *Antimicrob Agents Chemother,* 56**,** 4927-36.

ROBERT, M. A., NASSOURY, N., CHAHAL, P. S., VENNE, M. H., RACINE, T., QIU, X., KOBINGER, G., KAMEN, A., GILBERT, R. & GAILLET, B. 2017. Gene Transfer of ZMapp Antibodies Mediated By Recombinant Adeno-Associated Virus Protects Against Ebola Infections. *Hum Gene Ther*.

ROBINSON, D., HAMID, Q., BENTLEY, A., YING, S., KAY, A. B. & DURHAM, S. R. 1993. Activation of CD4+ T cells, increased TH2-type cytokine mRNA expression, and eosinophil recruitment in bronchoalveolar lavage after allergen inhalation challenge in patients with atopic asthma. *J Allergy Clin Immunol,* 92**,** 313-24.

ROCK, J. R., ONAITIS, M. W., RAWLINS, E. L., LU, Y., CLARK, C. P., XUE, Y., RANDELL, S. H. & HOGAN, B. L. M. 2009. Basal cells as stem cells of the mouse trachea and human airway epithelium. *Proceedings of the National Academy of Sciences of the United States of America,* 106**,** 12771-12775.

ROOPENIAN, D. C. & AKILESH, S. 2007. FcRn: the neonatal Fc receptor comes of age. *Nature Reviews Immunology,* 7**,** 715.

ROSE, E. B., WHEATLEY, A., LANGLEY, G., GERBER, S. & HAYNES, A. 2018. Respiratory Syncytial Virus Seasonality - United States, 2014-2017. *MMWR Morb Mortal Wkly Rep,* 67**,** 71-76.

ROSENBLUM, H. & AMITAL, H. 2011. Anti-TNF therapy: Safety aspects of taking the risk. *Autoimmunity Reviews,* 10**,** 563-568.

SAMULSKI, R. J. & MUZYCZKA, N. 2014. AAV-Mediated Gene Therapy for Research and Therapeutic Purposes. *Annual Review of Virology,* 1**,** 427-451.

SANDLER, A., GRAY, R., PERRY, M. C., BRAHMER, J., SCHILLER, J. H., DOWLATI, A., LILENBAUM, R. & JOHNSON, D. H. 2006. Paclitaxel-carboplatin alone or with bevacizumab for non-small-cell lung cancer. *N Engl J Med,* 355**,** 2542-50.

SANMARTI, R., INCIARTE-MUNDO, J., ESTRADA-ALARCON, P., GARCIA-MANRIQUE, M., NARVAEZ, J., RODRIGUEZ-MORENO, J., GOMEZ-CENTENO, A., PASCAL, M. & YAGUE, J. 2015. Towards optimal cut-off trough levels of adalimumab and etanercept for a good therapeutic response in rheumatoid arthritis. Results of the INMUNOREMAR study. *Annals of the Rheumatic Diseases,* 74.

SAUNDERS, K. O., WANG, L., JOYCE, M. G., YANG, Z. Y., BALAZS, A. B., CHENG, C., KO, S. Y., KONG, W. P., RUDICELL, R. S., GEORGIEV, I. S., DUAN, L., FOULDS, K. E., DONALDSON, M., XU, L., SCHMIDT, S. D., TODD, J. P., BALTIMORE, D., ROEDERER, M., HAASE, A. T., KWONG, P. D., RAO, S. S., MASCOLA, J. R. & NABEL, G. J. 2015. Broadly Neutralizing Human Immunodeficiency Virus Type 1 Antibody Gene Transfer Protects Nonhuman Primates from Mucosal Simian-Human Immunodeficiency Virus Infection. *J Virol,* 89**,** 8334-45.

SAXNE, T., PALLADINO, M. A., JR., HEINEGARD, D., TALAL, N. & WOLLHEIM, F. A. 1988. Detection of tumor necrosis factor alpha but not tumor necrosis factor beta in rheumatoid arthritis synovial fluid and serum. *Arthritis Rheum,* 31**,** 1041-5.

SCHABERT, V. F., WATSON, C., JOSEPH, G. J., IVERSEN, P., BURUDPAKDEE, C. & HARRISON, D. J. 2013. Costs of tumor necrosis factor blockers per treated patient using real-world drug data in a managed care population. *J Manag Care Pharm,* 19**,** 621-30.

SCHAUER, U., HOFFJAN, S., BITTSCHEIDT, J., KÖCHLING, A., HEMMIS, S., BONGARTZ, S. & STEPHAN, V. 2002. RSV bronchiolitis and risk of wheeze and allergic sensitisation in the first year of life. *European Respiratory Journal,* 20**,** 1277-1283.

SCHEPENS, B., IBANEZ, L. I., DE BAETS, S., HULTBERG, A., BOGAERT, P., DE BLESER, P., VERVALLE, F., VERRIPS, T., MELERO, J., VANDEVELDE, W., VANLANDSCHOOT, P. & SAELENS, X. 2011. Nanobodies(R) specific for respiratory syncytial virus fusion protein protect against infection by inhibition of fusion. *J Infect Dis,* 204**,** 1692-701.

SCHETT, G. 2007. Cells of the synovium in rheumatoid arthritis. Osteoclasts. *Arthritis Res Ther,* 9**,** 203.

SCHINDELIN, J., ARGANDA-CARRERAS, I., FRISE, E., KAYNIG, V., LONGAIR, M., PIETZSCH, T., PREIBISCH, S., RUEDEN, C., SAALFELD, S., SCHMID, B., TINEVEZ, J.-Y., WHITE, D. J., HARTENSTEIN, V., ELICEIRI, K., TOMANCAK, P. & CARDONA, A. 2012. Fiji: an open-source platform for biological-image analysis. *Nature Methods,* 9**,** 676.

SCHLABACH, M. R., HU, J. K., LI, M. & ELLEDGE, S. J. 2010. Synthetic design of strong promoters. *Proceedings of the National Academy of Sciences,* 107**,** 2538-2543.

SCHLEHOFER, J. R., EHRBAR, M. & ZUR HAUSEN, H. 1986. Vaccinia virus, herpes simplex virus, and carcinogens induce DNA amplification in a human cell line and support replication of a helpervirus dependent parvovirus. *Virology,* 152**,** 110-7.

SCHMITTGEN, T. D. & LIVAK, K. J. 2008. Analyzing real-time PCR data by the comparative C(T) method. *Nat Protoc,* 3**,** 1101-8.

SENIOR, M. 2017. After Glybera's withdrawal, what's next for gene therapy? *Nature Biotechnology,* 35**,** 491.

SHEALY, D. J., CAI, A., STAQUET, K., BAKER, A., LACY, E. R., JOHNS, L., VAFA, O., GUNN, G., 3RD, TAM, S., SAGUE, S., WANG, D., BRIGHAM-BURKE, M., DALMONTE, P., EMMELL, E., PIKOUNIS, B., BUGELSKI, P. J., ZHOU, H., SCALLON, B. J. & GILES-KOMAR, J. 2010. Characterization of golimumab, a human monoclonal antibody specific for human tumor necrosis factor alpha. *MAbs,* 2**,** 428-39.

SHIGETA, S., HINUMA, Y., SUTO, T. & ISHIDA, N. 1968. The cell to cell infection of respiratory syncytial virus in HEp-2 monolayer cultures. *J Gen Virol,* 3**,** 129-31.

SHRIVER, Z., TREVEJO, J. M. & SASISEKHARAN, R. 2015. Antibody-Based Strategies to Prevent and Treat Influenza. *Frontiers in Immunology,* 6**,** 315.

SHUKLA, A. A. & THOMMES, J. 2010. Recent advances in large-scale production of monoclonal antibodies and related proteins. *Trends Biotechnol,* 28**,** 253-61.

SIBER, G. R., LESZCYNSKI, J., PENA-CRUZ, V., FERREN-GARDNER, C., ANDERSON, R., HEMMING, V. G., WALSH, E. E., BURNS, J., MCINTOSH, K., GONIN, R. & ET AL. 1992. Protective activity of a human respiratory syncytial virus immune globulin prepared from donors screened by microneutralization assay. *J Infect Dis,* 165**,** 456-63.

SIEGEL, R., MILLER, D. & JEMAL, A. 2018. Cancer statistics, 2018. *CA: A Cancer Journal for Clinicians,* 68**,** 7-30.

SIMPSON, S. & BURLS, A. 2001. A systematic review of the effectiveness and cost-effectiveness of palivizumab (Synagis) in the prevention of respiratory syncytial virus (RSV) infection in infants at high risk of infection. *A West Midlands Development and Evaluation Service Report.*

SINGH, D., KOLSUM, U., BRIGHTLING, C. E., LOCANTORE, N., AGUSTI, A., TAL-SINGER, R. & INVESTIGATORS, E. 2014. Eosinophilic inflammation in COPD: prevalence and clinical characteristics. *Eur Respir J,* 44**,** 1697-700.

SINN, P. L., ARIAS, A. C., BROGDEN, K. A. & MCCRAY, P. B., JR. 2008. Lentivirus vector can be readministered to nasal epithelia without blocking immune responses. *J Virol,* 82**,** 10684-92.

SIVAPALASINGAM, S., CABALLERO-PEREZ, D., HOUGHTON, M., YANG, F., DAVIS, J., GAO, B. & GEBA, G. 2015. Phase 1 Study Evaluating Safety, Tolerability, Pharmacokinetics and Immunogenicity of REGN2222 in Healthy Adults: A New Human Monoclonal RSV-F Antibody for RSV Prevention. *Open Forum Infectious Diseases,* 2**,** 912-912.

SKARICIC, D., TRAUBE, C., DE, B., JOH, J., BOYER, J., CRYSTAL, R. G. & WORGALL, S. 2008. Genetic delivery of an anti-RSV antibody to protect against pulmonary infection with RSV. *Virology,* 378**,** 79-85.

SMART, K. A., LANCTOT, K. L. & PAES, B. A. 2010. The cost effectiveness of palivizumab: a systematic review of the evidence. *J Med Econ,* 13**,** 453-63.

SPALDING, K. L., BHARDWAJ, R. D., BUCHHOLZ, B. A., DRUID, H. & FRISÉN, J. 2005. Retrospective Birth Dating of Cells in Humans. *Cell,* 122**,** 133-143.

SRIVASTAVA, A., LUSBY, E. W. & BERNS, K. I. 1983. Nucleotide sequence and organization of the adeno-associated virus 2 genome. *J Virol,* 45**,** 555-64.
ST CLAIR, E. W., WAGNER, C. L., FASANMADE, A. A., WANG, B., SCHAIBLE, T., KAVANAUGH, A. & KEYSTONE, E. C. 2002. The relationship of serum infliximab concentrations to clinical improvement in rheumatoid arthritis: results from ATTRACT, a multicenter, randomized, double-blind, placebo-controlled trial. *Arthritis Rheum,* 46**,** 1451-9.
STAPLETON, N. M., EINARSDOTTIR, H. K., STEMERDING, A. M. & VIDARSSON, G. 2015. The multiple facets of FcRn in immunity. *Immunol Rev,* 268**,** 253-68.
STASTNY, P. 1978. Association of the B-cell alloantigen DRw4 with rheumatoid arthritis. *N Engl J Med,* 298**,** 869-71.
STEFF, A.-M., MONROE, J., FRIEDRICH, K., CHANDRAMOULI, S., NGUYEN, T. L.-A., TIAN, S., VANDEPAER, S., TOUSSAINT, J.-F. & CARFI, A. 2017. Pre-fusion RSV F strongly boosts pre-fusion specific neutralizing responses in cattle pre-exposed to bovine RSV. *Nature Communications,* 8**,** 1085.
STEMPNIAK, M., HOSTOMSKA, Z., NODES, B. R. & HOSTOMSKY, Z. 1997. The NS3 proteinase domain of hepatitis C virus is a zinc-containing enzyme. *Journal of Virology,* 71**,** 2881-2886.
SUBRAMANIAN, K. N., WEISMAN, L. E., RHODES, T., ARIAGNO, R., SANCHEZ, P. J., STEICHEN, J., GIVNER, L. B., JENNINGS, T. L., TOP, F. H., JR., CARLIN, D. & CONNOR, E. 1998. Safety, tolerance and pharmacokinetics of a humanized monoclonal antibody to respiratory syncytial virus in premature infants and infants with bronchopulmonary dysplasia. MEDI-493 Study Group. *Pediatr Infect Dis J,* 17**,** 110-5.
SUDA, T. & LIU, D. 2007. Hydrodynamic gene delivery: its principles and applications. *Mol Ther,* 15**,** 2063-9.
SUMMERFORD, C. & SAMULSKI, R. J. 1998. Membrane-associated heparan sulfate proteoglycan is a receptor for adeno-associated virus type 2 virions. *J Virol,* 72**,** 1438-45.
SUROSKY, R. T., URABE, M., GODWIN, S. G., MCQUISTON, S. A., KURTZMAN, G. J., OZAWA, K. & NATSOULIS, G. 1997. Adeno-associated virus Rep proteins target DNA sequences to a unique locus in the human genome. *J Virol,* 71**,** 7951-9.
SYMMONS, D., TURNER, G., WEBB, R., ASTEN, P., BARRETT, E., LUNT, M., SCOTT, D. & SILMAN, A. 2002. The prevalence of rheumatoid arthritis in the United Kingdom: new estimates for a new century. *Rheumatology (Oxford),* 41**,** 793-800.
SZCZEKLIK, W., WAWRZYCKA, K., WŁUDARCZYK, A., SEGA, A., NOWAK, I., SECZYŃSKA, B., FAJFER, I., ZAJĄC, K., KRÓLIKOWSKI, W. & KÓZKA, M. 2013. *Complications in patients treated with plasmapheresis in the intensive care unit.* 45.
TAN, I., NG, C. H., LIM, L. & LEUNG, T. 2001. Phosphorylation of a novel myosin binding subunit of protein phosphatase 1 reveals a conserved mechanism in the regulation of actin cytoskeleton. *J Biol Chem,* 276**,** 21209-16.
TAN, T. K. 2017. *Development of viral vectors for passive immunisation against influenza.* University of Oxford.
TARANEJOO, S., LIU, J., VERMA, P. & HOURIGAN, K. 2015. A review of the developments of characteristics of PEI derivatives for gene delivery applications. *Journal of Applied Polymer Science,* 132**,** n/a-n/a.
TAYLOR, G. 2017. Animal models of respiratory syncytial virus infection. *Vaccine,* 35**,** 469-480.
TAYLOR, G., STOTT, E. J., BEW, M., FERNIE, B. F., COTE, P. J., COLLINS, A. P., HUGHES, M. & JEBBETT, J. 1984. Monoclonal antibodies protect against respiratory syncytial virus infection in mice. *Immunology,* 52**,** 137-42.
TAYYARI, F., MARCHANT, D., MORAES, T. J., DUAN, W. M., MASTRANGELO, P. & HEGELE, R. G. 2011. Identification of nucleolin as a cellular receptor for human respiratory syncytial virus. *Nature Medicine,* 17**,** 1132-U140.

TENG, M. N. & COLLINS, P. L. 1998. Identification of the respiratory syncytial virus proteins required for formation and passage of helper-dependent infectious particles. *J Virol,* 72**,** 5707-16.
TERVO, D. G., HWANG, B. Y., VISWANATHAN, S., GAJ, T., LAVZIN, M., RITOLA, K. D., LINDO, S., MICHAEL, S., KULESHOVA, E., OJALA, D., HUANG, C. C., GERFEN, C. R., SCHILLER, J., DUDMAN, J. T., HANTMAN, A. W., LOOGER, L. L., SCHAFFER, D. V. & KARPOVA, A. Y. 2016. A Designer AAV Variant Permits Efficient Retrograde Access to Projection Neurons. *Neuron,* 92**,** 372-382.
THOMPSON, W. W., SHAY, D. K., WEINTRAUB, E., BRAMMER, L., COX, N., ANDERSON, L. J. & FUKUDA, K. 2003. Mortality associated with influenza and respiratory syncytial virus in the United States. *JAMA,* 289**,** 179-86.
THOMSON, N. C. & CHAUDHURI, R. 2012. Omalizumab: Clinical Use for the Management of Asthma. *Clinical Medicine Insights. Circulatory, Respiratory and Pulmonary Medicine,* 6**,** 27-40.
THWAITE, R., PAGÈS, G., CHILLÓN, M. & BOSCH, A. 2014. AAVrh.10 immunogenicity in mice and humans. Relevance of antibody cross-reactivity in human gene therapy. *Gene Therapy,* 22**,** 196.
TJELLE, T. E., CORTHAY, A., LUNDE, E., SANDLIE, I., MICHAELSEN, T. E., MATHIESEN, I. & BOGEN, B. 2004. Monoclonal antibodies produced by muscle after plasmid injection and electroporation. *Mol Ther,* 9**,** 328-36.
TRAPANI, I., COLELLA, P., SOMMELLA, A., IODICE, C., CESI, G., DE SIMONE, S., MARROCCO, E., ROSSI, S., GIUNTI, M., PALFI, A., FARRAR, G. J., POLISHCHUK, R. & AURICCHIO, A. 2014. Effective delivery of large genes to the retina by dual AAV vectors. *EMBO Molecular Medicine,* 6**,** 194-211.
TRATSCHIN, J. D., WEST, M. H., SANDBANK, T. & CARTER, B. J. 1984. A human parvovirus, adeno-associated virus, as a eucaryotic vector: transient expression and encapsidation of the procaryotic gene for chloramphenicol acetyltransferase. *Mol Cell Biol,* 4**,** 2072-81.
TUTYKHINA, I. L., SEDOVA, E. S., GRIBOVA, I. Y., IVANOVA, T. I., VASILEV, L. A., RUTOVSKAYA, M. V., LYSENKO, A. A., SHMAROV, M. M., LOGUNOV, D. Y., NARODITSKY, B. S., TILLIB, S. V. & GINTSBURG, A. L. 2013. Passive immunization with a recombinant adenovirus expressing an HA (H5)-specific single-domain antibody protects mice from lethal influenza infection. *Antiviral Res,* 97**,** 318-28.
VAN DER LOO, J. C. M. & WRIGHT, J. F. 2016. Progress and challenges in viral vector manufacturing. *Human Molecular Genetics,* 25**,** R42-R52.
VAN HAASTEREN, J., HYDE, S. C. & GILL, D. R. 2018. Lessons learned from lung and liver in-vivo gene therapy: implications for the future. *Expert Opinion on Biological Therapy,* 18**,** 959-972.
VAN SCHAIK, S. M., ENHORNING, G., VARGAS, I. & WELLIVER, R. C. 1998. Respiratory syncytial virus affects pulmonary function in BALB/c mice. *Journal of Infectious Diseases,* 177**,** 269-276.
VANBOXEL, J. A. & PAGET, S. A. 1975. Predominantly T-Cell Infiltrate in Rheumatoid Synovial Membranes. *New England Journal of Medicine,* 293**,** 517-520.
VARLEY, A. W., GEISZLER, S. M., GAYNOR, R. B. & MUNFORD, R. S. 1997. A two-component expression system that responds to inflammatory stimuli in vivo. *Nat Biotechnol,* 15**,** 1002-6.
VASANTHI, P., NALINI, G. & RAJASEKHAR, G. 2007. Role of tumor necrosis factor-alpha in rheumatoid arthritis: a review. *APLAR Journal of Rheumatology,* 10**,** 270-274.
VENTRE, K. & RANDOLPH, A. G. 2007. Ribavirin for respiratory syncytial virus infection of the lower respiratory tract in infants and young children. *Cochrane Database Syst Rev***,** CD000181.
VERMEIJ, E. A., BROEREN, M. G., BENNINK, M. B., ARNTZ, O. J., GJERTSSON, I., P, L. E. M. V. L., VAN DEN BERG, W. B., KOENDERS, M. I. & VAN DE LOO, F. A. 2014. Disease-regulated local IL-10 gene therapy diminishes synovitis and cartilage proteoglycan depletion in experimental arthritis. *Ann Rheum Dis*.

VIGNA, E., PACCHIANA, G., MAZZONE, M., CHIRIACO, C., FONTANI, L., BASILICO, C., PENNACCHIETTI, S. & COMOGLIO, P. M. 2008. "Active" cancer immunotherapy by anti-Met antibody gene transfer. *Cancer Res,* 68**,** 9176-83.
VISSERS, M., AHOUT, I. M. L., DE JONGE, M. I. & FERWERDA, G. 2016. Mucosal IgG Levels Correlate Better with Respiratory Syncytial Virus Load and Inflammation than Plasma IgG Levels. *Clinical and Vaccine Immunology : CVI,* 23**,** 243-245.
VOGEL, C. L., COBLEIGH, M. A., TRIPATHY, D., GUTHEIL, J. C., HARRIS, L. N., FEHRENBACHER, L., SLAMON, D. J., MURPHY, M., NOVOTNY, W. F., BURCHMORE, M., SHAK, S., STEWART, S. J. & PRESS, M. 2002. Efficacy and Safety of Trastuzumab as a Single Agent in First-Line Treatment of HER2-Overexpressing Metastatic Breast Cancer. *Journal of Clinical Oncology,* 20**,** 719-726.
WAILOO, A. J., BANSBACK, N., BRENNAN, A., MICHAUD, K., NIXON, R. M. & WOLFE, F. 2008. Biologic drugs for rheumatoid arthritis in the Medicare program: a cost-effectiveness analysis. *Arthritis Rheum,* 58**,** 939-46.
WANG, Z., DENG, X., ZOU, W., ENGELHARDT, J. F., YAN, Z. & QIU, J. 2017. Human Bocavirus 1 Is a Novel Helper for Adeno-Associated Virus Replication. *J Virol*.
WANSLEEBEN, C., BOWIE, E., HOTTEN, D. F., YU, Y. R. & HOGAN, B. L. 2014. Age-related changes in the cellular composition and epithelial organization of the mouse trachea. *PLoS One,* 9**,** e93496.
WARE, C. F., CROWE, P. D., VANARSDALE, T. L., ANDREWS, J. L., GRAYSON, M. H., JERZY, R., SMITH, C. A. & GOODWIN, R. G. 1991. Tumor-Necrosis-Factor (Tnf) Receptor Expression in Lymphocytes-T - Differential Regulation of the Type-I Tnf Receptor during Activation of Resting and Effector T-Cells. *Journal of Immunology,* 147**,** 4229-4238.
WATANABE, M., BOYER, J. L. & CRYSTAL, R. G. 2009. Genetic Delivery of Bevacizumab to Suppress Vascular Endothelial Growth Factor-Induced High-Permeability Pulmonary Edema. *Human Gene Therapy,* 20**,** 598-610.
WEINBLATT, M. E., KREMER, J. M., BANKHURST, A. D., BULPITT, K. J., FLEISCHMANN, R. M., FOX, R. I., JACKSON, C. G., LANGE, M. & BURGE, D. J. 1999. A trial of etanercept, a recombinant tumor necrosis factor receptor : Fc fusion protein, in patients with rheumatoid arthritis receiving methotrexate. *New England Journal of Medicine,* 340**,** 253-259.
WILLIAMS, R. O., FELDMANN, M. & MAINI, R. N. 1992. Anti-tumor necrosis factor ameliorates joint disease in murine collagen-induced arthritis. *Proc Natl Acad Sci U S A,* 89**,** 9784-8.
WOLBINK, G. J., VOSKUYL, A. E., LEMS, W. F., DE GROOT, E., NURMOHAMED, M. T., TAK, P. P., DIJKMANS, B. A. C. & AARDEN, L. 2005. Relationship between serum trough infliximab levels, pretreatment C reactive protein levels, and clinical response to infliximab treatment in patients with rheumatoid arthritis. *Annals of the Rheumatic Diseases,* 64**,** 704-707.
WOLK, B., SANSONNO, D., KRAUSSLICH, H. G., DAMMACCO, F., RICE, C. M., BLUM, H. E. & MORADPOUR, D. 2000. Subcellular localization, stability, and trans-cleavage competence of the hepatitis C virus NS3-NS4A complex expressed in tetracycline-regulated cell lines. *J Virol,* 74**,** 2293-304.
WOOLEY, P. H., DUTCHER, J., WIDMER, M. B. & GILLIS, S. 1993. Influence of a recombinant human soluble tumor necrosis factor receptor FC fusion protein on type II collagen-induced arthritis in mice. *J Immunol,* 151**,** 6602-7.
WOZNIAK, K., URBANOWSKA, E. & SNARSKI, E. 2015. [Plasmapheresis in haematology]. *Wiad Lek,* 68**,** 173-8.
WU, H., PFARR, D. S., JOHNSON, S., BREWAH, Y. A., WOODS, R. M., PATEL, N. K., WHITE, W. I., YOUNG, J. F. & KIENER, P. A. 2007. Development of motavizumab, an ultra-potent antibody for the prevention of respiratory syncytial virus infection in the upper and lower respiratory tract. *Journal of Molecular Biology,* 368**,** 652-665.
WU, N. H., YANG, W., BEINEKE, A., DIJKMAN, R., MATROSOVICH, M., BAUMGARTNER, W., THIEL, V., VALENTIN-WEIGAND, P., MENG, F. & HERRLER,

G. 2016. The differentiated airway epithelium infected by influenza viruses maintains the barrier function despite a dramatic loss of ciliated cells. *Sci Rep,* 6**,** 39668.
WU, P., DUPONT, W. D., GRIFFIN, M. R., CARROLL, K. N., MITCHEL, E. F., GEBRETSADIK, T. & HARTERT, T. V. 2008. Evidence of a causal role of winter virus infection during infancy in early childhood asthma. *Am J Respir Crit Care Med,* 178**,** 1123-9.
WU, Z., YANG, H. & COLOSI, P. 2010. Effect of genome size on AAV vector packaging. *Mol Ther,* 18**,** 80-6.
XENARIOU, S., GRIESENBACH, U., LIANG, H. D., ZHU, J., FARLEY, R., SOMERTON, L., SINGH, C., JEFFERY, P. K., FERRARI, S., SCHEULE, R. K., CHENG, S. H., GEDDES, D. M., BLOMLEY, M. & ALTON, E. W. F. W. 2007. Use of ultrasound to enhance nonviral lung gene transfer in vivo. *Gene Therapy,* 14**,** 768.
XIAO, W., CHIRMULE, N., BERTA, S. C., MCCULLOUGH, B., GAO, G. & WILSON, J. M. 1999. Gene Therapy Vectors Based on Adeno-Associated Virus Type 1. *Journal of Virology,* 73**,** 3994-4003.
XIAO, X., LI, J. & SAMULSKI, R. J. 1998. Production of high-titer recombinant adeno-associated virus vectors in the absence of helper adenovirus. *J Virol,* 72**,** 2224-32.
YALKINOGLU, A. Ö., HEILBRONN, R., BÜRKLE, A., SCHLEHOFER, J. R. & ZUR HAUSEN, H. 1988. DNA Amplification of Adeno-associated Virus as a Response to Cellular Genotoxic Stress. *Cancer Research,* 48**,** 3123-3129.
YANG, L. B., LINDHOLM, K., KONISHI, Y., LI, R. & SHEN, Y. 2002. Target depletion of distinct tumor necrosis factor receptor subtypes reveals hippocampal neuron death and survival through different signal transduction pathways. *Journal of Neuroscience,* 22**,** 3025-3032.
YAZICI, Y., SHI, N. & JOHN, A. 2008. Utilization of biologic agents in rheumatoid arthritis in the United States: analysis of prescribing patterns in 16,752 newly diagnosed patients and patients new to biologic therapy. *Bull NYU Hosp Jt Dis,* 66**,** 77-85.
YI, H., KIM, Y., KIM, J., JUNG, H., RIM, Y. A., JUNG, S. M., PARK, S. H. & JU, J. H. 2014. A new strategy to deliver synthetic protein drugs: self-reproducible biologics using minicircles. *Sci Rep,* 4**,** 5961.
YLÄ-HERTTUALA, S. 2012. Endgame: Glybera Finally Recommended for Approval as the First Gene Therapy Drug in the European Union. *Molecular Therapy,* 20**,** 1831-1832.
YOUNG, J. 2002. Development of a potent respiratory syncytial virus-specific monoclonal antibody for the prevention of serious lower respiratory tract disease in infants. *Respir Med,* 96 Suppl B**,** S31-5.
ZHAO, X., SINGH, M., MALASHKEVICH, V. N. & KIM, P. S. 2000. Structural characterization of the human respiratory syncytial virus fusion protein core. *Proceedings of the National Academy of Sciences of the United States of America,* 97**,** 14172-14177.
ZHU, Q., MCLELLAN, J. S., KALLEWAARD, N. L., ULBRANDT, N. D., PALASZYNSKI, S., ZHANG, J., MOLDT, B., KHAN, A., SVABEK, C., MCAULIFFE, J. M., WRAPP, D., PATEL, N. K., COOK, K. E., RICHTER, B. W. M., RYAN, P. C., YUAN, A. Q. & SUZICH, J. A. 2017. A highly potent extended half-life antibody as a potential RSV vaccine surrogate for all infants. *Science Translational Medicine,* 9.
ZINCARELLI, C., SOLTYS, S., RENGO, G. & RABINOWITZ, J. E. 2008. Analysis of AAV Serotypes 1–9 Mediated Gene Expression and Tropism in Mice After Systemic Injection. *Molecular Therapy,* 16**,** 1073-1080.
ZUFFEREY, R., NAGY, D., MANDEL, R. J., NALDINI, L. & TRONO, D. 1997. Multiply attenuated lentiviral vector achieves efficient gene delivery in vivo. *Nat Biotechnol,* 15**,** 871-5.

Appendix

Amino acid sequences of the biologics used in this thesis

Protein	Chain	Sequence
Palivizumab	Heavy	QVTLRESGPALWKPTOTLTLTCTFSGFSLSTSGMSVGWIRQPPGKA LEWLADIWWDDKKDYNPSLKSRLTISKDTSKNQVVLKVTNMDPADTA TYYCARSMITNWYFDWWGAGTTVTVSSASTKGPSVFPLAPSSKSTS GGTAALGCLVKDYFPEPVTVSWNSGALTSGVHTFPAVLQSSGLYSL SSWWTVPSSSLGTOTYICNVNHKPSNTKVDKRVEPKSCDKTHTCPP CPAPELLGGPSWFLFPPKPKDTLMISRTPEVTCVVVDVSHEDPEVKF NWYWDGVEVHNAKTKPREEQYNSTYRVNSWLWLHQDWLNGKEYK CKVSNKALPAPIEKTISKAKGOPREPOWYTLPPSREEMTKNOWSLTC LVKGFYPSDIAVEWESNGOPENNYKTTPPVLDSDGSFFLYSKLTVDK SRWQQGNWFSCSVMHEALHNHYTOKSLSLSPG
	Light	DIQMTQSPSTLSASVGDRVTITCKCOLSWGYMHWYOQKPGKAPKLL IYDTSKLASGVPSRFSGSGSGTEFTLTISSLQPDDFATYYCFQGSGY PFTFGGGTKLEIKRTVAAPSVFIFPPSDEQLKSGTASVWCLLNNFYPR EAKWOWKVDNALQSGNSQESVTEQDSKDSTYSLSSTLTLSKADYEK HKWYACEVTHQGLSSPWTKSFNRGEC
Infliximab	Heavy	LATMATGSRTSLLLAFGLLCLPWLQEGSAEVKLEESGGGLVQPGGS MKLSCVASGFIFSNHWMNWVRQSPEKGLEWVAEIRSKSINSATHYA ESVKGRFTISRDDSKSAVYLQMTDLRTEDTGVYYCSRNYYGSTYDY WGQGTTLTVSSASTKGPSVFPLAPSSKSTSGGTAALGCLVKDYFPE PVTVSWNSGALTSGVHTFPAVLQSSGLYSLSSVVTVPSSSLGTQTYI CNVNHKPSNTKVDKKVEPKSCDKTHTCPPCPAPELLGGPSVFLFPP KPKDTLMISRTPEVTCVVVDVSHEDPEVKFNWYVDGVEVHNAKTKP REEQYNSTYRVVSVLTVLHQDWLNGKEYKCKVSNKALPAPIEKTISK AKGQPREPQVYTLPPSRDELTKNQVSLTCLVKGFYPSDIAVEWESN GQPENNYKTTPPVLDSDGSFFLYSKLTVDKSRWQQGNVFSCSVMH EALHNHYTQKSLSLSPG
	Light	MATGSRTSLLLAFGLLCLPWLQEGSADILLTQSPAILSVSPGERVSFS CRASQFVGSSIHWYQQRTNGSPRLLIKYASESMSGIPSRFSGSGSG TDFTLSINTVESEDIADYYCQQSHSWPFTFGSGTNLEVKRTVAAPSV FIFPPSDEQLKSGTASVVCLLNNFYPREAKVQWKVDNALQSGNSQE SVTEQDSKDSTYSLSSTLTLSKADYEKHKVYACEVTHQGLSSPVTKS FNRGEC
Etanercept	N/A	LATMATGSRTSLLLAFGLLCLPWLQEGSALPAQVAFTPYAPEPGSTC RLREYYDQTAQMCCSKCSPGQHAKVFCTKTSDTVCDSCEDSTYTQL WNWVPECLSCGSRCSSDQVETQACTREQNRICTCRPGWYCALSKQ EGCRLCAPLRKCRPGFGVARPGTETSDVVCKPCAPGTFSNTTSSTDI CRPHQICNVVAIPGNASMDAVCTSTSPTRSMAPGAVHLPQPVSTRS QHTQPTPEPSTAPSTSFLLPMGPSPPAEGSTGDEPKSCDKTHTCPP CPAPELLGGPSVFLFPPKPKDTLMISRTPEVTCVVVDVSHEDPEVKF NWYVDGVEVHNAKTKPREEQYNSTYRVVSVLTVLHQDWLNGKEYK CKVSNKALPAPIEKTISKAKGQPREPQVYTLPPSREEMTKNQVSLTCL VKGFYPSDIAVEWESNGQPENNYKTTPPVLDSDGSFFLYSKLTVDKS RWQQGNVFSCSVMHEALHNHYTQKSLSLSPGK